High spatial resolution heat flow mapping in South Australia; implications for the nature of the South Australian Heat Flow Anomaly and geothermal and mineral resource exploration

by

Chris Matthews, BSc (hons)

Thesis submitted for the degree of Doctor of Philosophy

at

School of Geosciences
Monash University
Melbourne, Australia

September 2014

Copyright Notices

Notice 1

Notice 2

Measuring geothermal gradients from groundwater observation well, Mount Gambier

Geothermal exploration well Gollum #1, Central Flinders Ranges between Parachilna and Ediacara

Table of Contents

Summary

Geothermal exploration activity in Australia over the last decade has highlighted the poor surface heat flow data coverage in this country. While data coverage remains poor, a previous attempt to characterise the heat flow field of South Australia (Neumann et al. 2000) described an "anomalous heat flow zone" in central South Australia. This region was not previously delineated by high spatial resolution heat flow data, but the work published here demonstrates that the "zone" described as the South Australian Heat Flow Anomaly (SAHFA; Neumann et al., 2000), is a region where anomalously high heat flow values are interspersed with low values, and there is significant lateral variation in surface heat flow over scales of tens of kilometres. This thesis addresses the following questions:

- Is the SAHFA, as shown in Cull (1982) and defined by Neumann et al. (2000), a zone of blanket or even dominant high heat flow?
- What is the true nature of the SAHFA when considered on a 10km lateral scale?
- What are the possible reasons for the surface heat flow pattern in southeastern South Australia?

The heat flow field is a fundamental parameter for characterizing the tectonic setting of a geological terrane because the magnitude of surface heat flow, Q_s, can have a strong influence on the mechanical or rheological behaviour of crustal rocks. The distribution of Q_s is also directly relevant to resource exploration, in that it is related directly to the distribution of heat producing elements (HPEs). These control the prospectivity for high geothermal gradients and geothermal energy, as well as potentially the locations of elevated concentrations of uranium. Closely spaced surface heat flow data clearly highlights the location of the Olympic Dam ore body, and would probably have aided previous explorers in the discovery of Prominent Hill.

Surface heat flow mapping in southeastern South Australia revealed a surface heat flow distribution as complex and varied as the geology of the region itself. Two studies in that region demonstrated that, while there is slightly higher than average surface heat flow around some of the volcanic centres in the Newer Volcanics Province, heterogeneous basement heat production is a more likely explanation than remnant magmatic heat for the overall distribution of surface heat flow.

A study was conducted to test the hypothesis that the Torrens Hinge Zone in South Australia was likely to be a region of high average geothermal gradients and thus prospective for geothermal energy. A heat flow drilling program designed to test the idea returned results that validated this hypothesis.

General Declaration

In accordance with Monash University Doctorate Regulation 17/ Doctor of Philosophy and Master of Philosophy (MPhil) regulations the following declarations are made:

I hereby declare that this thesis contains no material which has been accepted for the award of any other degree or diploma at any university or equivalent institution and that, to the best of my knowledge and belief, this thesis contains no material previously published or written by another person, except where due reference is made in the text of the thesis.

This thesis includes three original papers published in peer-reviewed journals and one original paper published in a non-peer-reviewed journal. The ideas, development and writing up of all the papers in the thesis were the principal responsibility of myself, the candidate, working within the School of Geosciences under the supervision of Professor Louis Moresi and Dr Graeme Beardsmore.

The inclusion of co-authors reflects the fact that the work came from active collaboration between researchers and acknowledges input into team-based research.

In the case of chapters 3, 4, 5, and 6, my contribution to the work involved the following:

Thesis chapter	Publication title	Publication status	Nature, extent of candidate's contribution
3	Heat flow: a uranium exploration and modelling tool?	Published in the MESA Journal, edition 41, April 2006	Main research, interpretation and preparation of manuscript (70%)
4	New heat flow data from south-eastern South Australia	Published in *Exploration Geophysics* (peer-reviewed journal) Volume 38 p1–10, 2007	Main research, field work, data processing, interpretation and preparation of manuscript (80%)
5	Geothermal energy prospectivity of the Torrens Hinge Zone: evidence from new heat flow data	Published in *Exploration Geophysics* (peer-reviewed journal) Volume 40 p288–300, 2009	Main research, field work, data processing, interpretation and preparation of manuscript (100%)
6	Heat flow data from the southeast of South Australia: distribution and implications for the relationship between current heat flow and the Newer Volcanics Province	Accepted for publication in *Exploration Geophysics* (peer-reviewed journal)	Main research, field work, data processing, interpretation and preparation of manuscript (70%)

I have not renumbered sections (including figure captions) of submitted or published papers in order to generate a consistent presentation within the thesis.

Signed: _____ Date:_____

Acknowledgements

The journey to complete this body of work has been long and eventful, and has not been possible without the support and assistance of several people.

First and foremost I must acknowledge Dr Graeme Beardsmore. He was my mentor from the very start, and he and I have shared a long journey that began with the question of whether heat flow measurements could give some insight into the thermal state of the crust around the volcanoes of Mount Gambier. Very quickly this evolved into the question of whether the western Otway Basin might be prospective for geothermal energy, which in turn led to a foray into the then nascent hot rocks sector. Many of the ideas had their roots in work done over many years by Professor Jim Cull.

Along the way the work benefitted from another champion of the geothermal potential in Australia, Professor Mike Sandiford, who provided me with great assistance and support. My understanding of the thermal structure and neotectonics of south eastern Australia came largely from his work.

My understanding of the geology of the Flinders Ranges and Torrens Hinge Zone stemmed from the great knowledge gained from "Adelaidean legends" Wolfgang Preiss and Jim Gehling.

The work involved numerous data collection and measurement campaigns, and it could not have proceeded without the great assistance of government personnel such as Jeff Lawson, George McKenzie, Dave Cockshell and Tony Hill in the South Australian Government. Magnificent work in measurement, modelling and collection of data was done by Alex Musson, Andrew Alesci, Christine Sealing, Big Jim Driscoll, the brilliant Bruce Godsmark, Nicky Pollington and Lyndon Parham. Without them none of this would have been possible.

Much of the work was integral in the expansion of the hot rocks industry in Australia from remote locations right into the national Heartlands. I acknowledge here some of the people in that corporate space who helped me along the way, including Roger Massey-Greene, Dennis Gee, John Canaris and Kerry Parker.

Finally, I would like to dedicate this PhD to my late Mum, who sadly passed away before I completed. I know she would have loved to have seen me graduate, but hopefully she is watching from somewhere. Wherever you may be now Mum, this one's for you.

Chapter 1

Introduction

This thesis presents a study into the nature of the surface heat flow across a region of South Australia loosely defined by longitudes 138^{o}E and 141^{o}E. The current surface heat flow of the study regions, and the insights into the geological evolution of those regions that this data can provide, are of considerable importance to science, society and the energy industry.

Surface heat flow provides insight into the thermal structure of the lithosphere and also the geochemical make up of the crust, giving important parameters for understanding continental evolution – especially because many geological processes are temperature-dependent (e.g. Neumann et al 2000). Because the value of surface heat flow (Q_s) represents the combined flow of thermal energy from two sources: heat flowing from the mantle of the earth (reduced heat flow q_r), and heat generated in the crust by the decay of radioactive isotopes of elements such as U, Th and K (q_c; see equation 1 below), surface heat flow measurements (provided they are not locally influenced by transient effects) can tell scientists about the rate of mantle heat flow as well as the abundance and variable distribution of heat producing elements in the crust (McLaren et al 2003).

$$Q_s = q_r + q_c \qquad (1)$$

The magnitude of surface heat flow at any point in a given Heat Flow Province (HFP; Roy *et al*. 1968), where by definition the magnitude of the mantle component of heat flow q_r is broadly uniform, relates directly to two key factors:

a) The concentration of Heat Producing Elements (HPEs) through the vertical sequence of crustal rocks (McLaren *et al.* 2003), and

b) Local lateral variations in thermal conductivity in the top 10km of the crust.

Of particular importance to the understanding of the tectonothermal evolution of Australia is the fact that the mechanical strength of rocks is temperature-dependent. 'Hot' (and therefore weak) lithosphere responds to even relatively small stresses and undergoes deformation, while 'cold' (and therefore strong) lithosphere withstands greater stresses before undergoing deformation (Sandiford et al 2003). The temperature of the Moho provides a useful proxy for lithospheric strength. Moho temperature is controlled strongly by q_r, q_c, crustal thickness and the thermal conductivity structure of the lithosphere in a given area. As stated in Sandiford et al (2003), there are large regional variations in both q_c and the effective thickness of heat producing crust. McLaren et al (2003) also pointed out, however, that the *horizontal* length scale of a crustal heat source strongly influences the degree to which Equation 1 represents a one-dimensional problem. In other words, the accuracy with which we can predict q_r, and draw conclusions about the thermal state of the crust from individual heat flow measurements depends on lateral variability of heat production in the crust.

The importance to society comes from several areas, not least of which is the need to understand the patterns of seismicity and volcanic hazard that might be experienced. As described in Sandiford et al (2003), the temperature of the Moho provides a useful proxy for lithospheric strength, which in turn influences seismicity. It is therefore important to

understand the distribution of crustal temperature in the region so that scientists can better understand the seismicity.

The Newer Volcanics Province (NVP) of western Victoria and southeast South Australia is an enigmatic zone of eruption centres in an intraplate setting. There are approximately 400 separate volcanic vents between Millicent in South Australia and Melbourne, and their ages range from around 7 Ma to just 4,500 years. Understanding the surface heat flow in this region is something that society has great interest in due to the fact that this volcanic region is dormant, and the nature of the volcanic hazard is not well understood.

Surface heat flow is also an important control on geothermal energy prospectivity (the search for higher than average geothermal gradients). Southeast South Australia has contained geothermal exploration acreage since 2004 (see Chapters 4 and 6), and the region continues to hold significant interest for the geothermal energy sector. The Torrens Hinge Zone (see Chapter 5) has contained geothermal exploration acreage since 2006.

Surface heat flow provides insight into the thermal history of sedimentary basins that have hydrocarbon accumulations. The data allow thermal history to be reconstructed and regional estimates of thermal hydrocarbon maturation to be made. Heat flow can help explorers to understand and model advective flow from faults and map basin-wide diagenesis patterns for structural and primary permeability in reservoirs (e.g. Beardsmore & Cull, 2001).

Basin formation through lithospheric extension induces shallowing and therefore cooling of the Moho. It also reduces the thickness of heat production layers, which further reduces the temperature of the Moho. The result of this is that the reduced temperature strengthens the lithosphere beneath megasedimentary basins such as on continental margins where rifting has occurred, and focuses continental crust deformation at the margins of these basins (Sandiford et al 2003), or in intracontinental regions where the crust is hotter.

Half or more of continental surface heat flow in the Central Australian Heat Flow Province (CAHFP; McLaren et al 2003) is generated in the crust (McLaren et al 2003), so the regional distribution and magnitude of q_c exerts a strong influence on the ongoing evolution of the Australian continent.

Heat flow data are therefore of considerable importance to science and society. Neumann et al (2000) noted that while global surface heat flow datasets and averages have been studied extensively, the continent of Australia has very poor data coverage in comparison to, say, North America, Europe and Africa. In spite of the importance of surface heat flow data, previously only a handful of high spatial resolution surface heat flow studies have been published in Australia (e.g. Houseman et al 1989; Beardsmore 2005; Torrens Energy 2008).

The South Australian Heat Flow Anomaly (SAHFA), defined by Neumann et al (2000), is a region bounded loosely by lines of longitude in the central to eastern part of the state of South Australia. The SAHFA was defined based on a small number of widely spaced surface heat flow values (see Chapter 2). The work described in this thesis aimed to conduct a number of

high spatial resolution surface heat flow studies to determine the lateral variability of surface heat flow within the SAHFA.

The published papers included in this thesis present new surface heat flow data from two distinctly different geological terranes within the SAHFA:

1. Torrens Hinge Zone, a transition region between the eastern margin of the Archaean to Mesoproterozoic Gawler Craton Olympic Domain and the western edge of the Adelaide Rift Complex (Figure 1)
2. Southern Murray Basin to western Otway Basin, a region with a complex tectonothermal history that spans from the Neoproterozoic to the Holocene (Figure 2).

The papers present heat flow mapped in each of the study areas to a spatial resolution sufficient to delineate variations in surface heat flow on a lateral scale of tens of kilometres, comparable with crustal thickness.

This thesis presents three high spatial resolution heat flow studies published by Matthews & Beardsmore (2007), Matthews (2009) and Matthews et al (2013), as well as a discussion paper on the use of heat flow as a tool for iron oxide copper gold uranium (IOCGU) exploration (Matthews and Beardsmore, 2006). It draws conclusions about the practicality and value of high spatial resolution heat flow surveys, and presents a new perspective on the nature of the SAHFA.

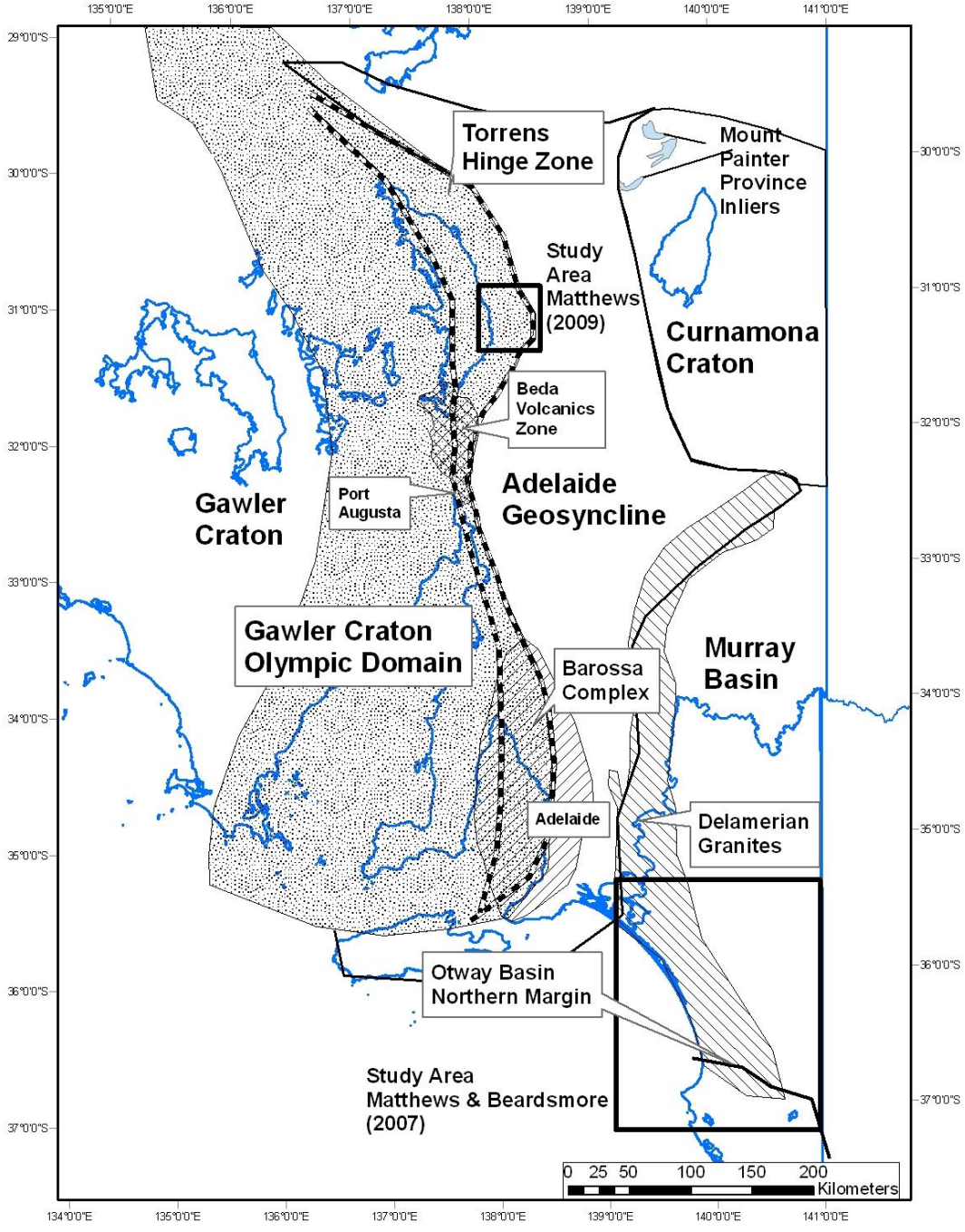

Figure 1 – Study area for Matthews (2009) in the Torrens Hinge Zone of South Australia.

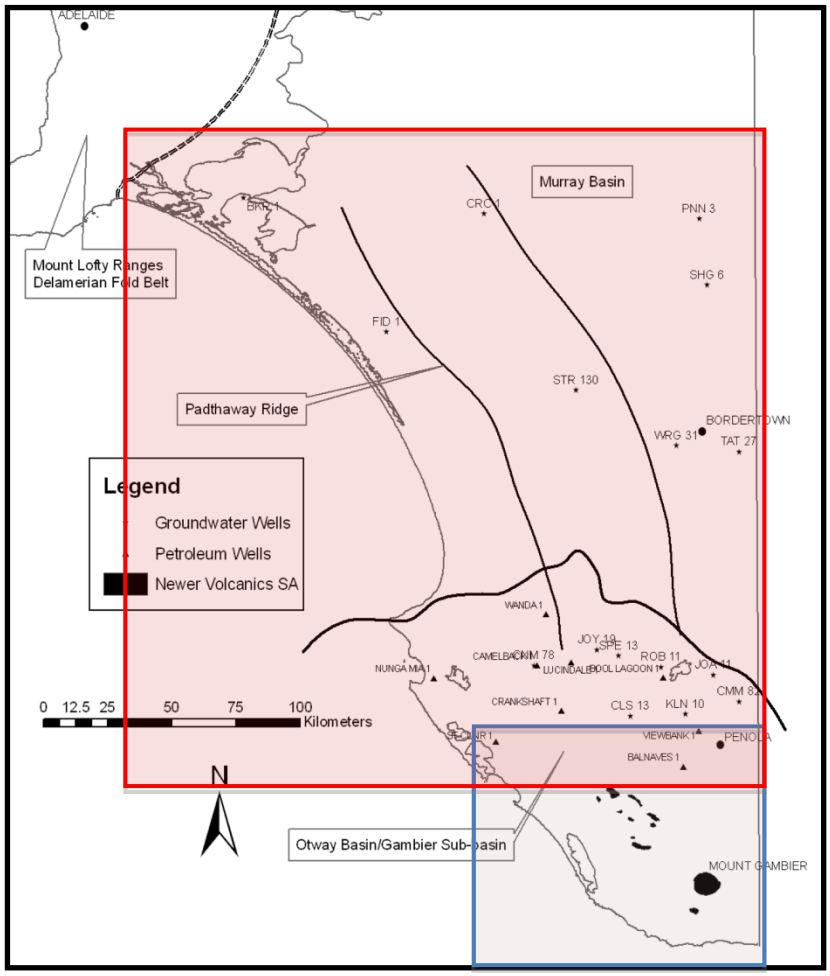

Figure 2 – Study areas in southeast South Australia for Matthews & Beardsmore (2007) in red and Matthews et al (2013) in blue.

References

Beardsmore, G. R., and Cull, J. P., 2001, Crustal heat flow; a guide to measurement and modelling: Cambridge University Press.

Beardsmore, G.R., 2005, Thermal modelling of the hot dry rock geothermal resource beneath GEL99 in the Cooper Basin, Proceedings World Geothermal Congress, Antalya, Turkey, 24-29 April, 2005.

Houseman**,** G.A., Cull, J.P. Muir, P.M. and Paterson, H.L., 1989, Geothermal signatures and uranium ore deposits on the Stuart Shelf of South Australia, Geophysics, 54 (2), p. 158–170.

McLaren, S., Sandiford, M., Hand, M., Neumann, N., Wyborn, L., & Bastrakova, I., 2003, The hot southern continent, heat flow and heat production in Australian Proterozoic terranes: Geological Society of Australia. Special Publication, 22, p. 151–161.

Matthews, C. G., and Beardsmore, G. R., 2006, Heat flow: A uranium exploration and modelling tool? MESA Journal 41 Primary Industries & Resources South Australia, 2006, p. 8–10.

Matthews, C. G., and Beardsmore, G. R., 2007, New heat flow data from southeastern South Australia: Exploration Geophysics, 38, p. 260–269.

Matthews, C. G., 2009, Geothermal energy prospectivity of the Torrens Hinge Zone: evidence from new heat flow data: Exploration Geophysics, 40, p. 288–300.

Matthews, C. G., Beardsmore, G. R., Driscoll, J., Pollington, N., 2013, Heat flow data from the southeast of South Australia: distribution and implications for the relationship between current heat flow and the Newer Volcanics Province, Exploration Geophysics, 44 (2), p. 133–144.

Neumann, N., Sandiford, M., and Foden, J., 2000, Regional geochemistry and continental heat flow; implications for the origin of the South Australian heat flow anomaly, Earth and Planetary Science Letters, 183, p. 107–120.

Roy, R. F., Blackwell, D. D., and Birch, F., 1968, Heat generation of plutonic rocks and continental heat-flow provinces: Earth and Planetary Science Letters, 5, p. 1–12.

Sandiford, M., Frederiksen, S. & Braun, J., 2003, The long-term thermal consequences of rifting; implications for basin reactivation, Basin Research, 15 (1), p. 23-43.

Torrens Energy Limited, 2008, 780 000 PJ Inferred Resource, Parachilna Project, South Australia. ASX Announcement 20 August *2008*. Available online at: http://www.asx.com.au/asxpdf/20080820/pdf/31bsp0dcmt4sw0.pdf (first accessed 21 August 2008.)

Chapter 2

Literature Reviews:

Part 1

The South Australian Heat Flow Anomaly

Part 2

The geology of southeast South Australia

Part 3

The Torrens Hinge Zone and Central Flinders Ranges

2.1 Part 1: The 'Central Australian Heat Flow Province' and the 'South Australian Heat Flow Anomaly'

2.1.1 The Central Australian Heat Flow Province

Based on very sparse surface heat flow (Q_s) data, the first attempts to characterise the regional variability of heat flux through the Australian continent were made in the late 1970s and early 1980s (e.g. Sass & Lachenbruch, 1979; Cull, 1982). These authors divided Australia into three major regions that basically matched broad geological age: a western, dominantly Archaean Province with average Q_s of around 40 mW/m^2; an eastern, dominantly Phanerozoic Province with average Q_s around 72 mW/m^2; and a Central, dominantly Proterozoic Province (McLaren et al 2003).

Globally, the average Q_s in a Proterozoic aged region is around 50 mW/m^2 (Pollack et al 1993), but in the Proterozoic Province of Australia the average Q_s is over 80 mW/m^2 (McLaren et al 2003). There are numerous published values of surface heat flow from this zone that are well above both normal continental and global average Proterozoic heat flow values. These anomalous values are generally attributed to an unusual enrichment of much of the Australian Proterozoic crust in heat-producing elements such as U, Th and K (e.g. McLaren et al 2003).

Roy et al (1968) defined a heat flow province as a region of exposed basement having a common mantle contribution of heat flow (q_r), broadly uniform tectonothermal history, and a characteristic heat production depth scale. On that basis, McLaren et al (2003) defined the Proterozoic region of Australia as the 'Central Australian Heat Flow Province' (CAHFP), and their analysis of data available at the time supported this naming. For further discussion of this see Chapter 5.

2.1.2 The South Australian Heat Flow Anomaly

The 'South Australian Heat Flow Anomaly' (SAHFA), defined by Neumann et al (2000), is a region defined loosely by lines of longitude in the central to eastern part of the state of South Australia (Neumann et al 2000; Figure 1). At the time of that publication there were fewer than 30 published surface heat flow values for the whole of South Australia, with eight of these published by Houseman et al (1989) from a relatively small area around Olympic Dam (see Chapters 4 and 5). The sparse nature of this dataset enabled only the most basic understanding of the SA heat flow regime. The study published by Houseman et al (1989)

represented the only heat flow study in Australia with a spatial resolution on the order of tens of kilometres at the time of publication of Neumann et al (2000).

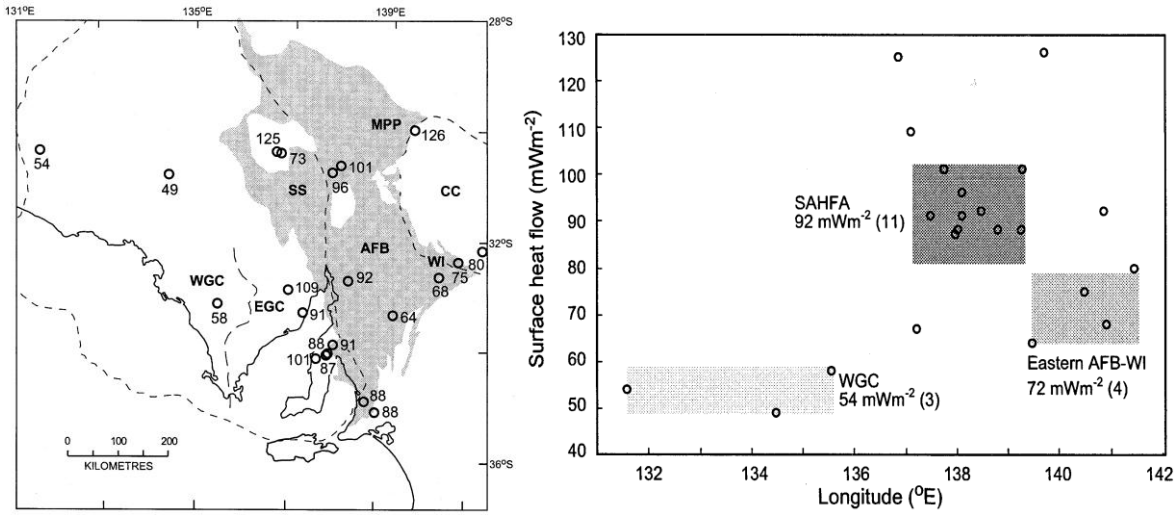

Figure 1. Left: The South Australian surface heat flow data set as it existed at the time of publication of Neumann et al (2000). Right: Surface heat flow estimates as a function of longitude across South Australia. Both figures from Neumann et al (2000).

The Proterozoic aged geological features that are thought to contribute to crustal heat production within the SAHFA include high heat producing rocks of the Hiltaba Suite, Gawler Range Volcanics and Barossa Complex (Gawler Craton Olympic Domain; Figure 2), the Mount Painter Province Inliers and greater Curnamona Craton (Figure 2). The average heat generation of these rock units ranges from 2.9 to 16.1 $\mu W/m^3$ (Neumann et al 2000; McLaren et al 2003).

The published estimates of heat flow used to define the SAHFA were derived almost exclusively from mineral exploration drillholes, and Cull (1982) described the integrity of many of these values as 'questionable'. Moreover, mineral exploration holes generally target local geochemical or geophysical anomalies, so whether estimates of heat flow from these holes are representative of regional surface heat flow is debatable.

Neumann et al (2000) examined whether any transient effects could have affected the heat flow values used to define the SAHFA. They discussed recent tectonism, current magmatic activity and advection associated with groundwater movement in sedimentary basins. While they ruled out current magmatism and basin-related groundwater advection, they considered that proximal neotectonic activity might have influenced some values such as those around

Arkaroola in the Northern Flinders Ranges Mount Painter Province.

Neumann et al (2000) also discussed whether abnormally high mantle heat flow could contribute to the high values observed in the SAHFA. They referred to Zielhuis and van der Hilst (1996) who showed that teleseismic tomography wave speeds beneath the SAHFA are high. This suggests a relatively cool upper mantle, consistent with high heat flow being restricted to shallower levels. Neumann et al (2000) and McLaren et al (2003) also deduced that the mantle-derived component of surface heat flow in the CAHFP (and the SAHFA) is as low as 20–30 mW/m^2. The bulk of the elevated surface heat flow observed in the Olympic Dam area was most likely generated in the crust.

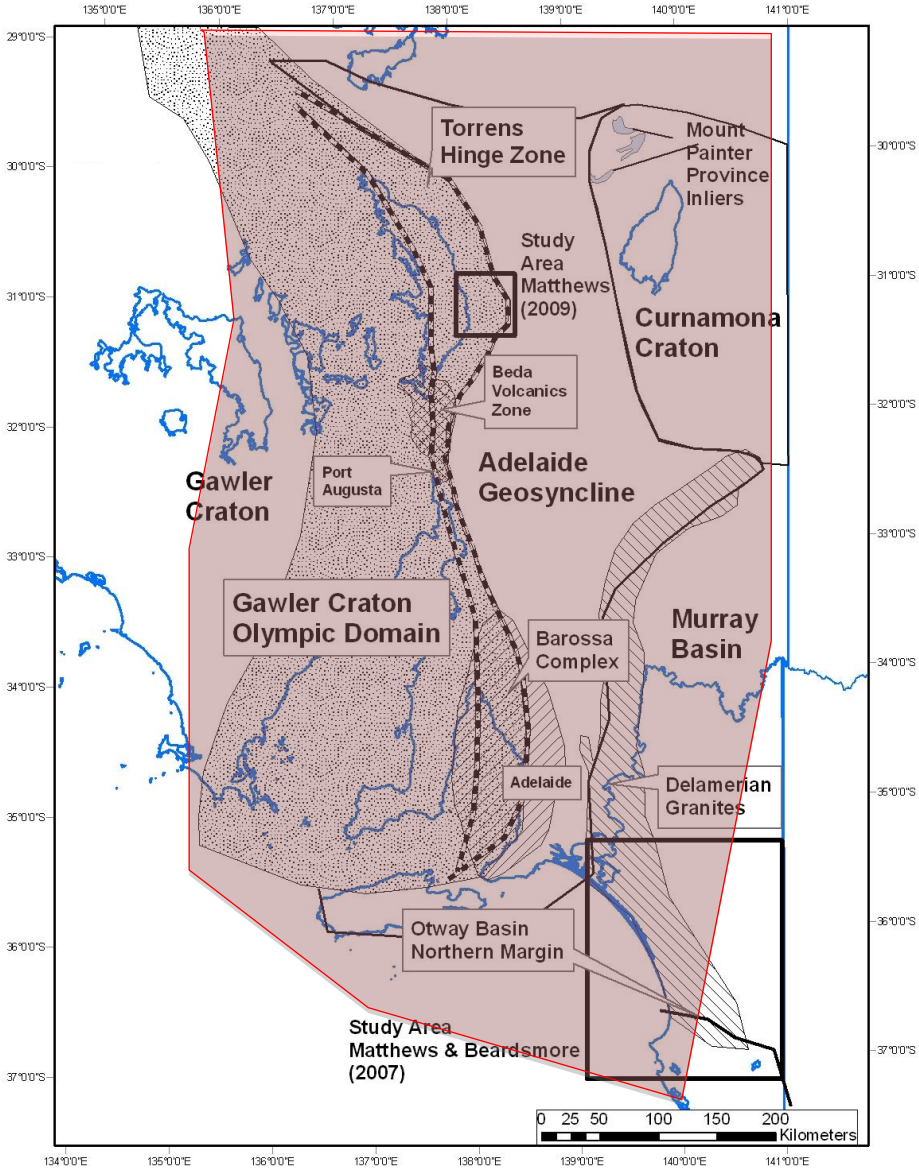

Figure 2. Reproduction of Chapter 1 Figure 1 with the SA Heat Flow Anomaly region shaded in red.

The Olympic Dam study of Houseman et al (1989) showed that surface heat flow varies by a factor of two over a lateral distance of at most 30 km. The highest values correspond to areas with known high heat production rocks near the surface. Matthews and Beardsmore (2007) published 24 heat flow values from an area of approximately 150 km x 200 km in the south-eastern corner of South Australia (Figure 2; also see Chapter 7). The highest heat flow values observed in that study corresponded with the Padthaway Ridge, a shallow crustal geological feature containing Palaeozoic, heat-producing granitoids (see section 2.2.2).

The Mesoproterozoic Hiltaba Suite granitoids generate significant heat in parts of the SAHFA. The Torrens Hinge Zone (THZ, see part 3) contains two additional suites of rocks that are known to be high heat producing; namely the Mesoproterozoic Gawler Range Volcanics, and the Palaeoproterozoic Barossa Complex (Figure 3). See Chapter 5 for more discussion on basement heat production in the SAHFA.

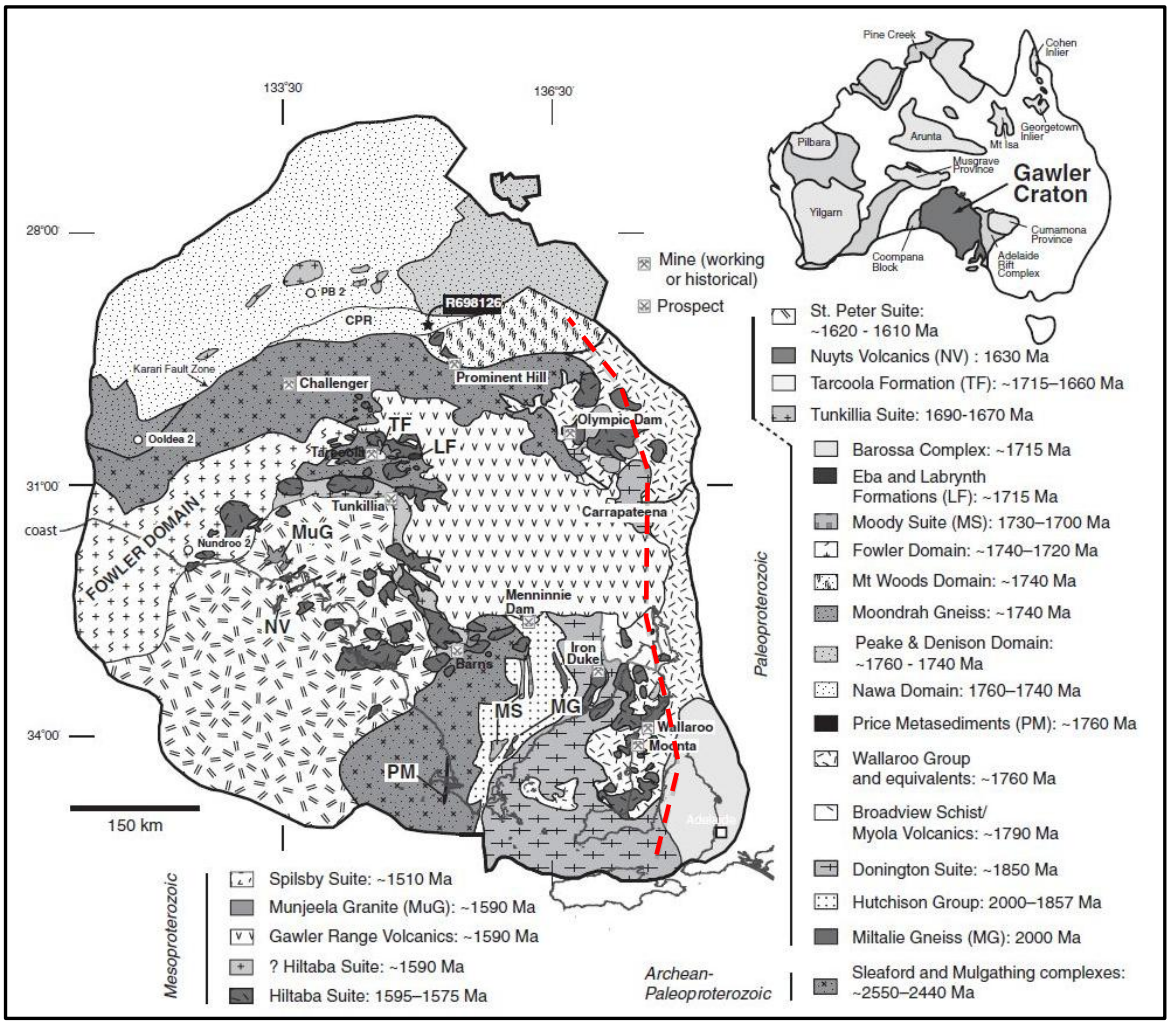

Figure 3. Basement geology distribution in the Gawler Craton (from Hand et al 2007). The approximate western boundary of the Torrens Hinge Zone (discussed in part 3) is marked by the red dashed line.

The significant but likely non-uniform contribution of crustal heat production (Hand et al 2007) has implications when considering the representative nature of the current heat flow dataset for those parts of Australia where there is widely spaced surface heat flow data. It is unlikely that heat flow varies in a smooth fashion between the current heat flow data points, and more likely that there are short wavelength variations related to basement geology.

2.1.3 The consequences of heterogeneous heat production

An uneven spatial distribution of high heat producing elements, and resulting surface heat flow and Moho temperature, could result in heterogeneous lateral lithospheric response to applied stress, and thermal histories of shallow sequences. McLaren et al (2002) showed that it is likely that the peak metamorphism in the Mount Painter Province, which occurred during the Delamerian Orogeny, was due to the burial of high heat producing rocks beneath thick sedimentary cover rather than mantle derived magmatic heat sources. Furthermore, McLaren et al (2002) were able to show that this hot, relatively weak section of the lithosphere experienced uplift and denudation significantly greater than the surrounding geographic regions. They showed that the tectonic stresses related to the Alice Springs Orogeny, which occurred around 100 Ma after the Delamerian Orogeny and was largely focussed in Central Australia, were probably also responsible for the uplift seen in the distal location of the Mount Painter Province. Their conclusion was that tectonic deformation in the Central-Northern Flinders Ranges has been localized around thermally weakened crust. Indeed, they went on to conclude that this thermal effect is still apparent during the current day Sprigg's Orogeny (see part 2).

McLaren et al (2005) stated that, "Radiogenic heat sources give rise to significant lithospheric weakening, and thus the abundance and redistribution of crustal heat sources should have exerted profound control on tectonic activity in areas of high average heat production. This view of tectonic activity in terms of the long-term thermomechanical stability of the crust has proven useful in understanding the distribution of active deformation in modern continental interiors". They stated also that the lithosphere under the CAHFP may be weakened by a factor of 2–3 (at least in parts where high heat production was concentrated) relative to regions with lower crustal heat generation, and would have deformed under milder tectonic stress conditions.

The distribution of current surface heat flow, and the reasons for that distribution, are thus critical controls on ongoing tectonic activity, with implications for seismic hazard, mineral

exploration, geothermal energy exploration, and models of continental evolution. Surface heat flow surveys with lateral resolution of tens of kilometres between stations can help to produce maps at the right scale to investigate such matters.

2.2 Part 2: Southeast South Australia geology introduction

The southeast South Australia study area has a complex and ongoing geological history, including Proterozoic lithospheric mantle; Neoproterozoic to Early Palaeozoic sediment deposition and a subsequent orogenic event with associated igneous activity; Mesozoic rifting and associated basin formation that continued into the Neogene; Late Neogene to Recent compressive tectonics; and finally ongoing Pleistocene–Recent mafic volcanism. The geology of the region is reviewed below, from the oldest to the youngest features.

2.2.1 Lithospheric mantle and basement

Work by several authors in the areas of seismic tomography and geochemical analysis tested hypotheses on the age of the continental lithosphere and the thickness of the crust under the Otway Basin.

Prior to 1996, Morton & Drexel (1995) assumed that the Delamerian Fold Belt (DFB) lay beneath the western Otway Basin, and the Lachlan Fold Belt (LFB) lay beneath the eastern Otway Basin. They thought the age of basement under both the western and eastern Otway Basin was probably Palaeozoic. McBride et al (1996) challenged this Palaeozoic age when geochemical sampling of mantle xenoliths from the Newer Volcanic Province (NVP) of western Victoria and eastern South Australia revealed key features of the basement architecture.

The boundary between the DFB and the LFB is defined as the Moyston Fault Zone (MFZ, Figure 4) and McBride et al (1996) showed it to be a geochemical discontinuity when xenoliths, which provide samples of the sub-continental lithospheric mantle (SCLM), were analysed and indicated Proterozoic SCLM under the DFB and Phanerozoic SCLM under the LFB. Fission Track data published by Foster & Gleadow (1992, 1993) identified distinctly different cooling histories on either side of the MFZ during the Cretaceous (Miller et al 2002).

Graeber et al (2002) further investigated the Otway Basin basement with teleseismic tomography based on seismic wave speed structural analysis. The MFZ has been shown previously to be a seismic discontinuity (Zielhuis & van der Hilst 1996) with high wave speeds west of the MFZ and lower than average speeds east of it. The high wave speeds west

of the MFZ support the hypothesis that the crust is thicker and that the basement to the west of the MFZ is Proterozoic. Graeber et al (2002) also identified a low seismic wave speed zone under the NVP in southern Victoria, which they attributed to a high mantle temperature anomaly.

Finlayson et al (1993) and Finlayson et al (1996) investigated the thickness of the crust in the western Otway Basin. They showed that the Tartwaup Fault Zone (TFZ; discussed below) defines a major crustal thickness discontinuity. Deep seismic imagery shows that the thickness of the crust north of the TFZ is approximately 31 km while south of this zone it is just 25-26 km (Figure 5). Finlayson et al (1998) outlined the crustal architecture in a long transect from the onshore Otway Basin margin to the outer southern edge of the Otway Basin in the deep ocean where Otway Basin sediments overlie oceanic crust. The TFZ was a major focus of early Cretaceous spreading in the Southern Australian Rift System. The late Cretaceous episode that led to the separation of Australia and Antarctica was focused on a line off the current shoreline of southern Australia (Teasdale et al 2002).

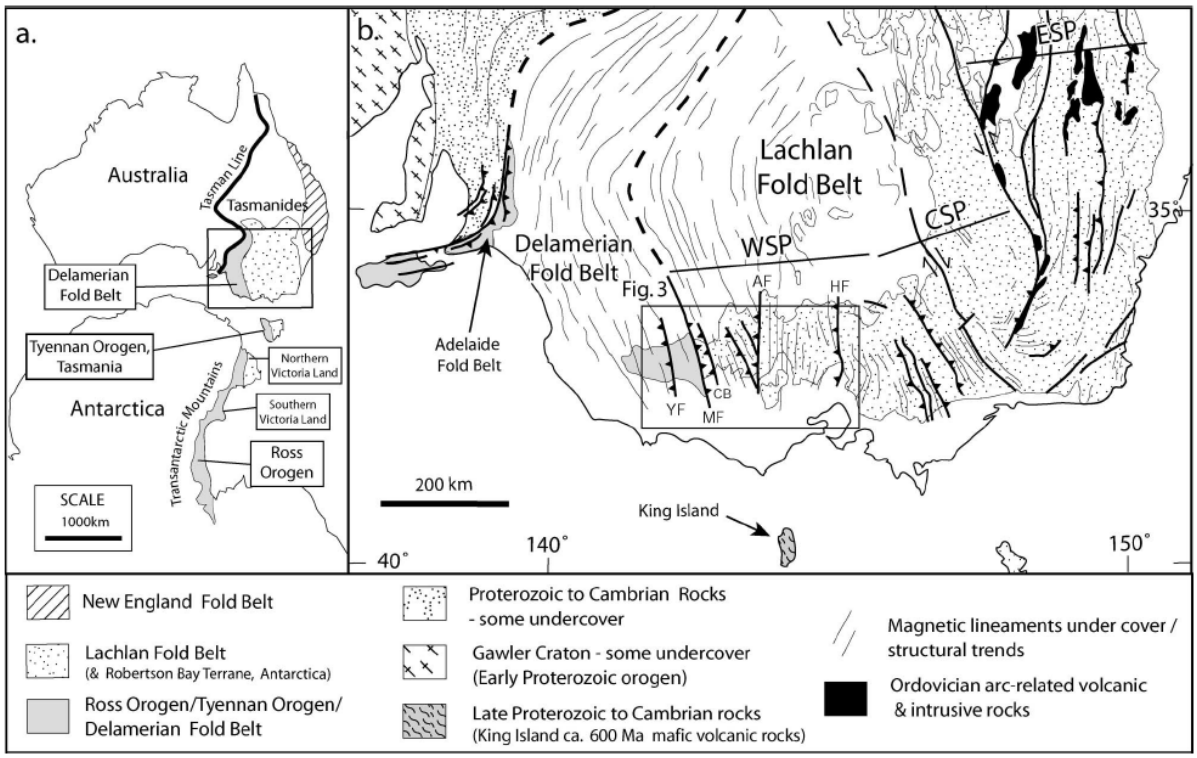

Figure 4 (a) Basement geology of eastern Australia (from Miller et al 2002, modified from Gray & Foster 1998) and relationship to the basement geology of eastern Antarctica including the Ross Orogen, (locations of Antarctica and Australia reflect relative positions at about 110 million years prior to the breakup of eastern Gondwana). (b) Delamerian and Lachlan Fold Belts, southeastern Australia (modified from Gray & Foster 1998). WSP, western subprovince; CSP, central subprovince; ESP, eastern subprovince; YF, Yarramjylup Fault; MF, Moyston Fault Zone; AF, Avoca Fault; HF, Heathcote Fault; CB, Coongee Break.

Mantle xenoliths in the Newer Volcanics Province (NVP) provide representative samples of the SCLM under the DFB and LFB. Lower crust petrology is determined using mainly isotopic and mineralogical data (Sutherland & Hollis 1982). Re-Os data from spinel-peridotite xenoliths from across the NVP have served to redefine the Tasman Line – the Proterozoic/Phanerozoic crustal boundary beneath eastern Australia – to one approximately concordant with the Stawell Zone-Mortlake Discontinuity-Shipwreck Trough line (McBride et al 1996; Handler & Bennett 2001; Miller et al 2002). This line is the approximate DFB-LFB boundary (Figure 6). Seismic data such as presented by Graeber et al (2002) support the Tasman Line location derived from the mantle xenolith studies, and more recently Fishwick & Rawlinson (2012) have added support to this interpretation.

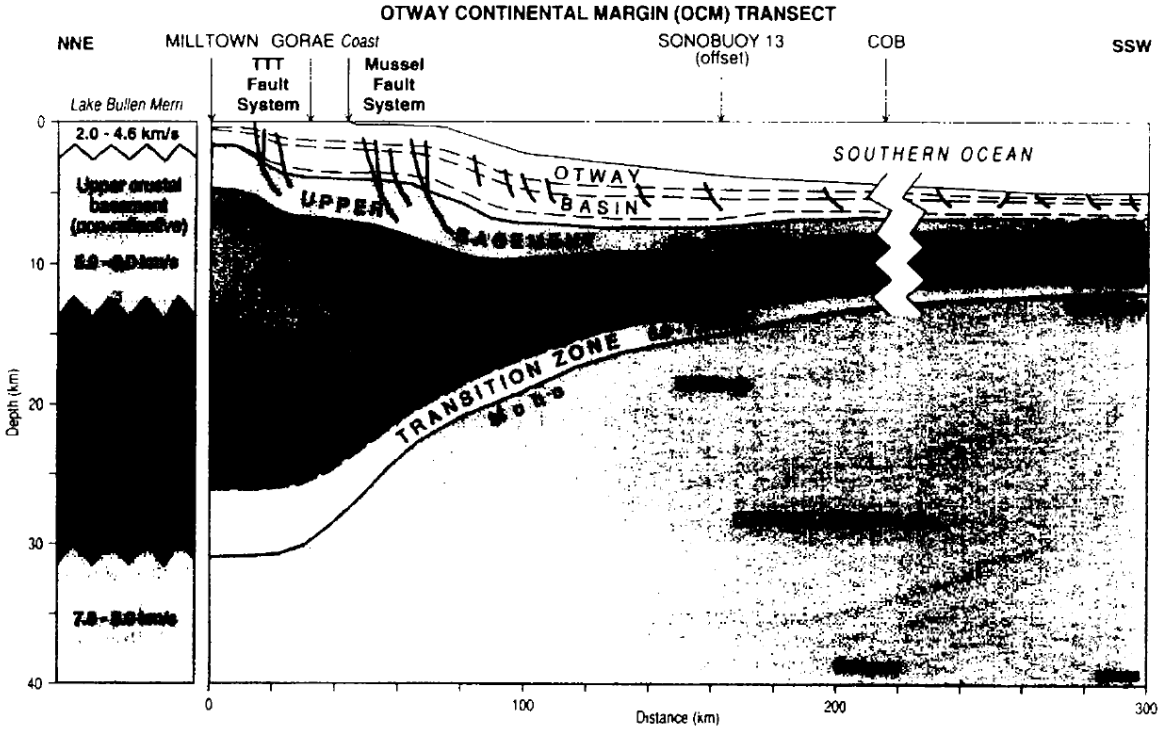

Figure 5. A cross-section of crustal thickness across the southern margin of the Otway Basin. Note that the Tartwaup Fault Zone (part of 'TTT' above) is a zone of significant crustal thinning (from Finlayson *et al.* 1998).

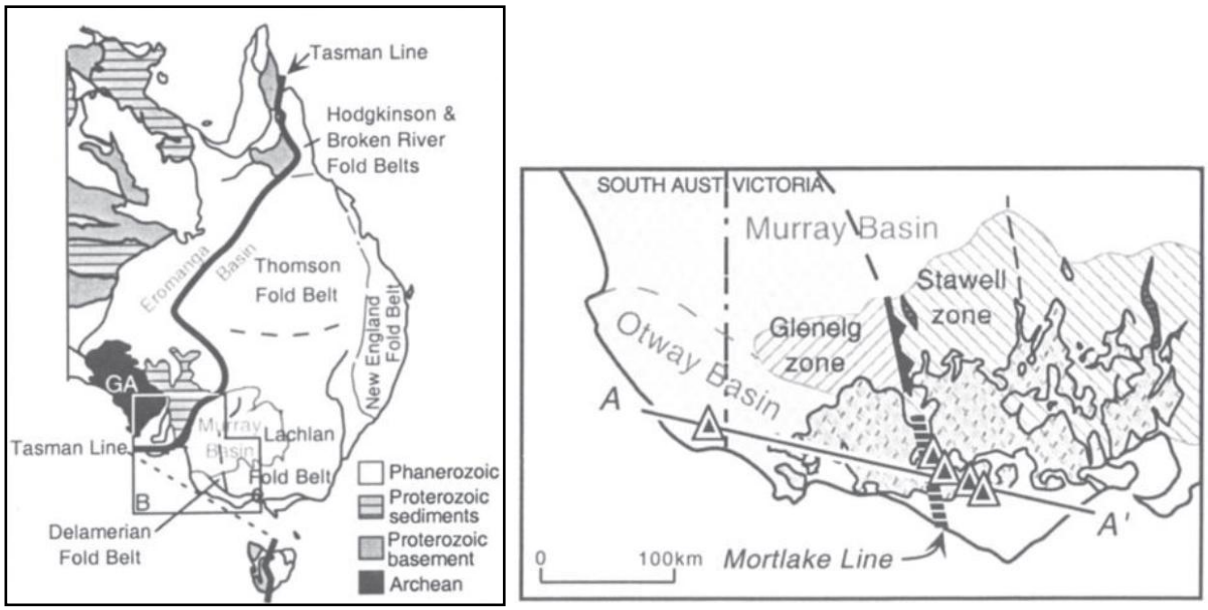

Figure 6. Left: location of the Tasman Line as presented by Handler & Bennett (2001). The Sub-continental Lithospheric Mantle is Proterozoic as far east as the boundary between the Delamerian and Lachlan Fold Belts. Right: the Mortlake Line is the same zone as the Moyston Fault Zone labelled on Figure 1.

2.2.2 Cambro-Ordovician Delamerian Fold Belt

Accepting the location of the Tasman Line as defined in Section 2.2.1, crustal basement to the study area is comprised of Delamerian Fold Belt deposits of sediments and igneous material of Early Cambrian age (Jensen-Schmidt et al 2002). The sediments were deposited during Early Cambrian rifting prior to the Late Cambrian–Early Ordovician orogenic event known as the Delamerian Orogeny (e.g. Jenkins & Sandiford 1992). See section 2.3 below for further description.

Igneous activity during and immediately following the Delamerian Orogeny resulted in the emplacement of mafic to felsic intrusives and extrusives (Foden et al 2002; Jensen-Schmidt et al 2002). The timing of termination of the Delamerian Orogeny was around 485 Ma, and the change is marked by a change in granite composition from syn-tectonic granitoids to post-tectonic suites (Foden et al 2002). See section 2.3 below for further discussion on the Delamerian Orogeny.

One key granite suite lies within the study area in the lower southeast SA – the Padthaway Ridge (Figure 7), described as a series of granitic and rhyolitic rocks forming a roughly linear basement high (Turner et al 1992). The granites and volcanics do not contain metamorphic fabrics and thus post-date the Delamerian Orogeny (Turner et al 1992). Figure 8 shows the

known outcrop occurrences of the Padthaway Ridge igneous rocks.

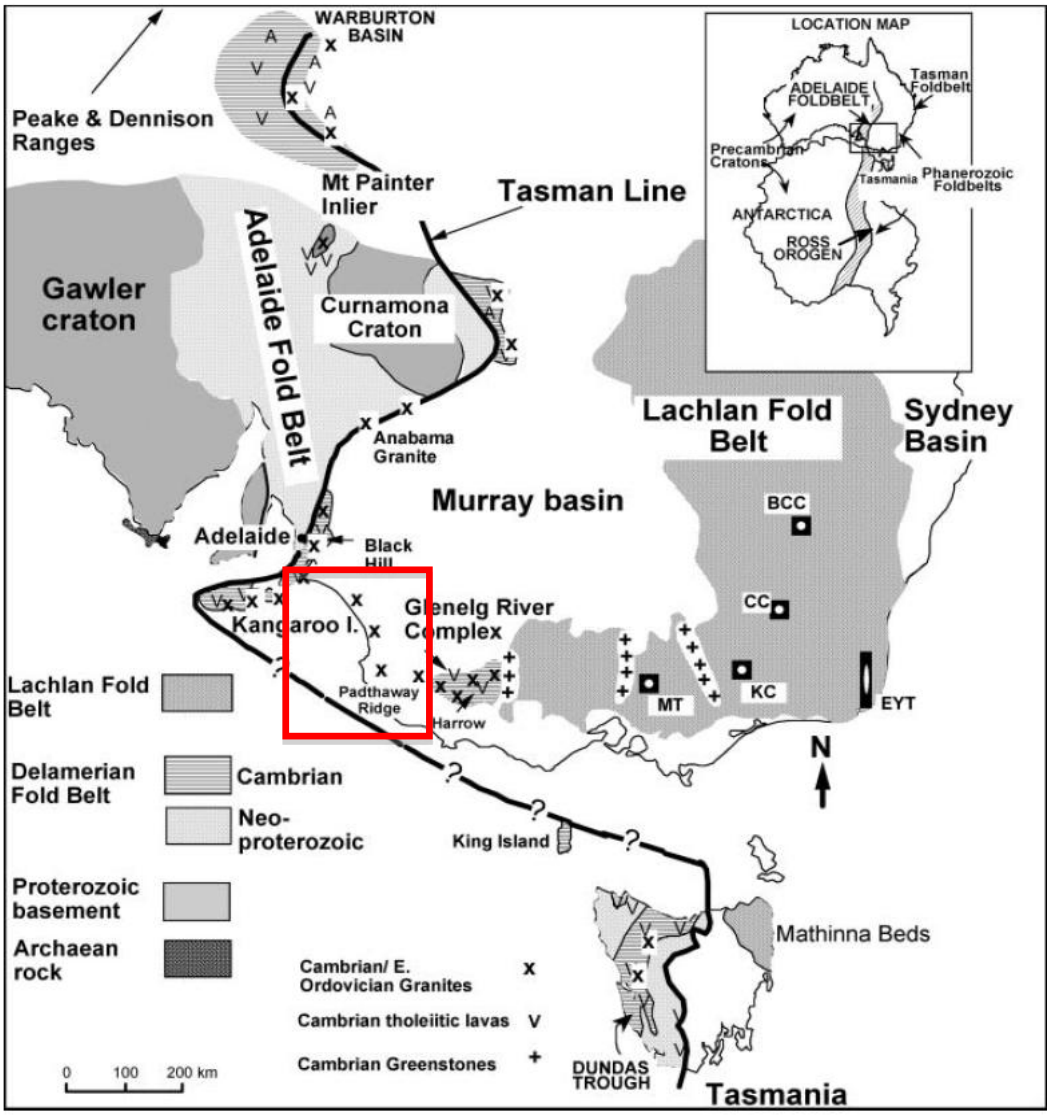

Figure 7. Ordovician and older geology of southeastern Australia from Foden et al (2002). The Padthaway Ridge Cambro-Ordovician granites lie within the southeast South Australia study area (red square).

2.2.3 Mesozoic–Tertiary Rifting

The Otway Basin developed as part of the Bassian rift between Australia and Antarctica. The first stage of basin formation was in the Late Jurassic to Early Cretaceous. During this time thermal doming was followed by extension and the "initial fracturing" episode (Boult 2002; O'Brien et al 1994; Miller et al 2002). Deep lacustrine sediments and volcanism characterise the Casterton Formation lithologies from this time (Figure 9).

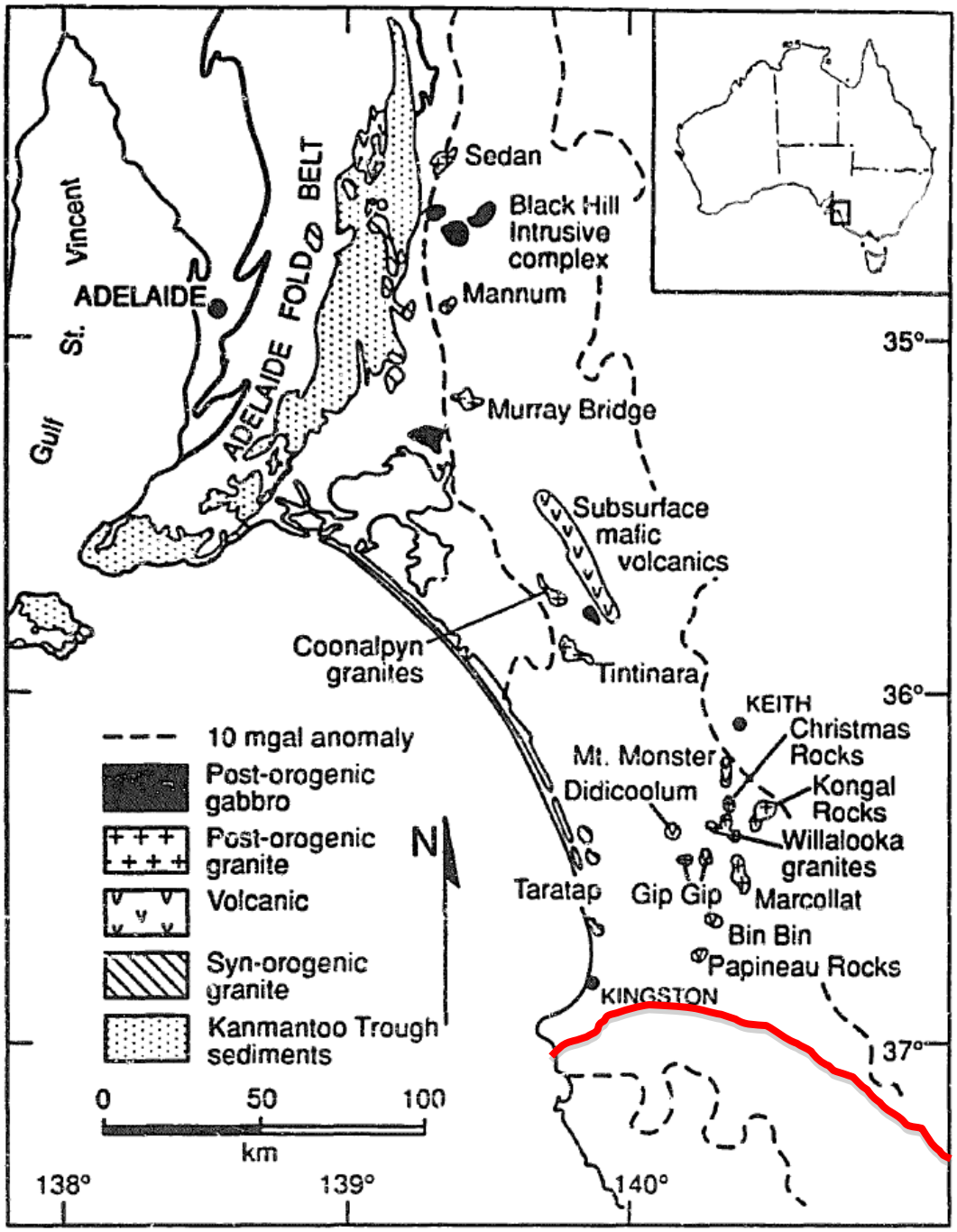

Figure 8. Basement geology of the Padthaway Ridge region from Turner et al (1992). The dotted line marks the edge of a gravity anomaly that is the likely extent of the basement rocks. Note also the overlap between the southern edge of the Ridge and the northern margin of the Otway Basin (red line).

The orientation of extension was NW-SE, with extension half-grabens developing into today's Torquay Sub-basin and the Robe and Saint Clair Troughs and transtensional half-grabens in the Penola Trough (Figure 10; O'Brien et al 1994). Extension and sedimentation occurred at this time in the Otway Basin along with the Torquay Sub-basin, the Gippsland and Bass Basins (Teasdale et al 2002; Miller et al 2002).

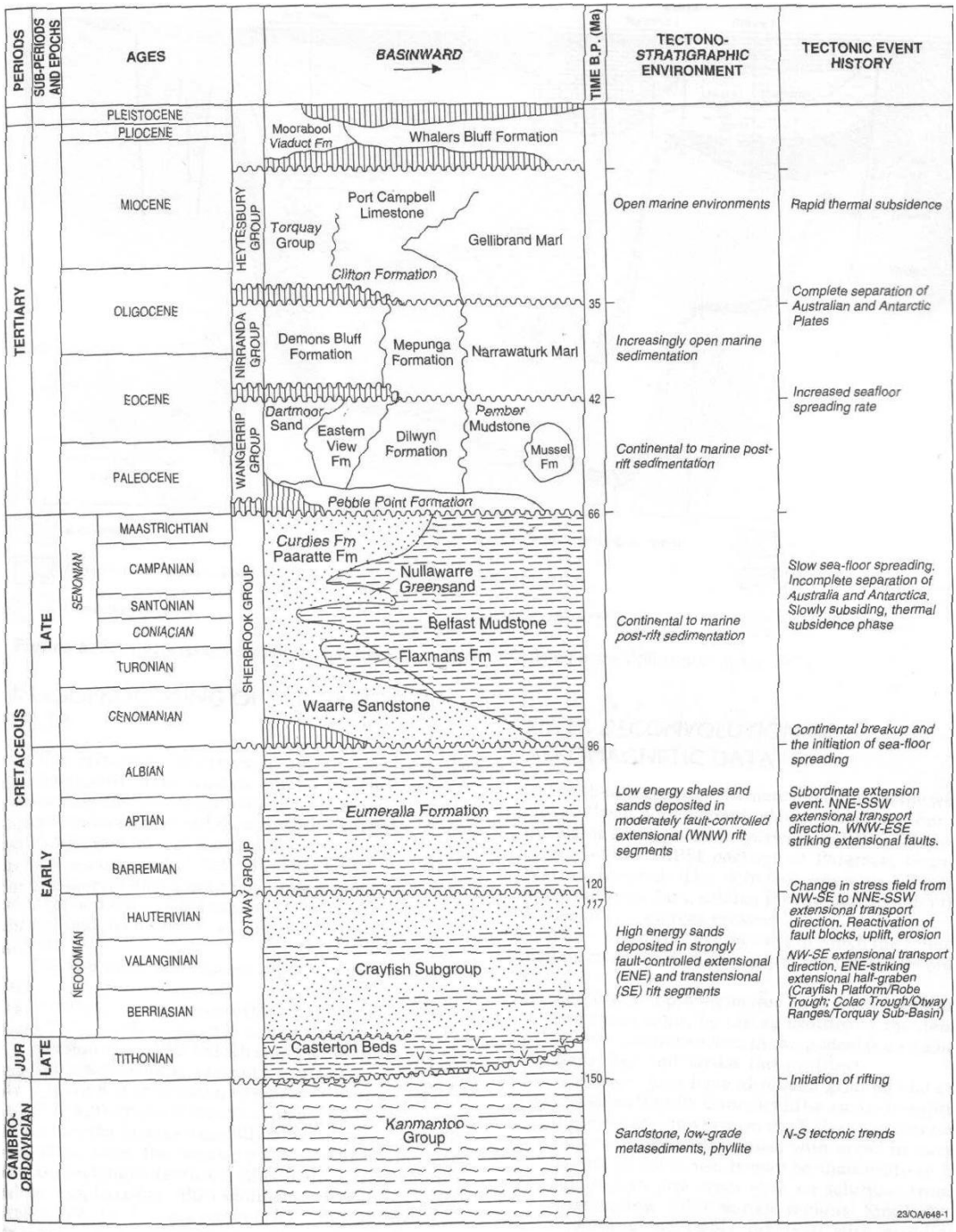

Figure 9. Stratigraphic column for the evolution of the Otway Basin including tectonic events (from O'Brien *et al* 1994).

Miller et al (2002) attributed a difference between the structural trends of the western and eastern Otway Basin at this time to the partitioning of strain along the Stawell Zone, which is the boundary between the Delamerian Fold Belt and the Lachlan Fold Belt. O'Brien et al (1994) earlier attributed the change in structural trend to different responses (either extensional

or transtensional) to sinistral wrenching in various parts of the Otway Basin.

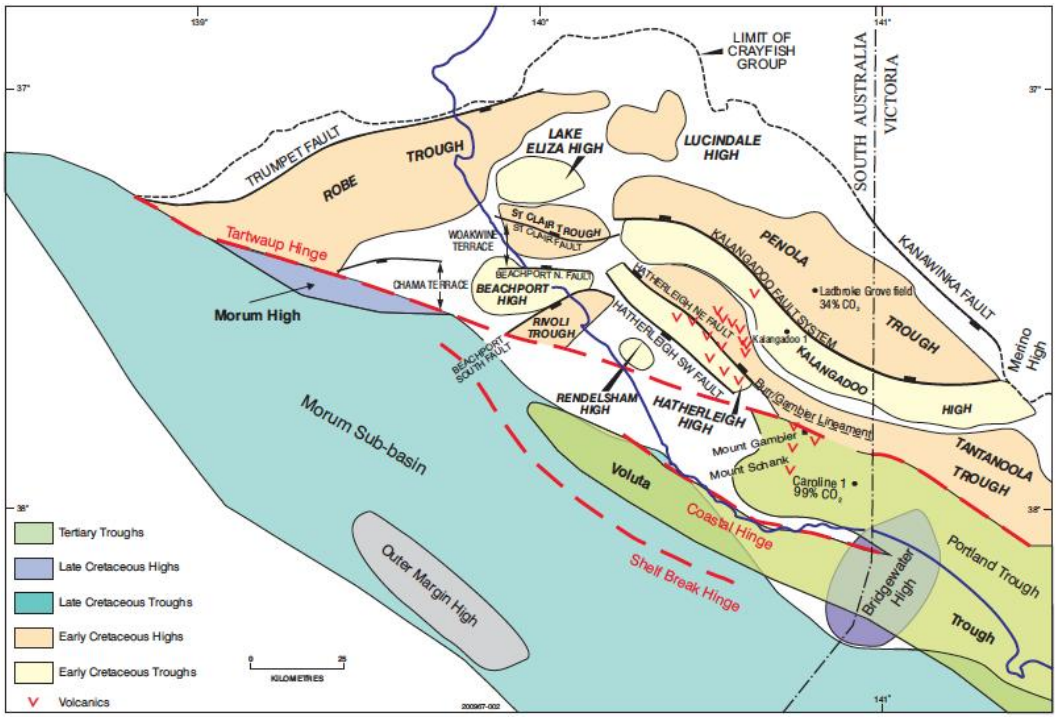

Figure 10. Structural elements of the Western Otway Basin in South Australia. (from Jensen-Schmidt et al 2002).

A Late Jurassic to Early Cretaceous event (150–120 Ma) saw the establishment of the Tartwaup Fault Zone (TFZ) as a major focus of tectonic activity. The TFZ can be considered part of a continuous line that includes the Mussel, Timboon and Sorrell Fault Zones (Figure 11). Much of the intracontinental rift fracturing was localised in this zone (Teasdale et al 2002).

Sediments associated with this period are part of the Crayfish Subgroup. The thickest intersections of the Crayfish Subgroup from petroleum exploration are in the Penola and Robe Troughs (Figure 10) with, for example, 4700 m in the onshore Robe Trough (O'Brien et al 1994). The Crayfish Subgroup has not been intersected by drilling south of the TFZ, a fact that probably reflects drill depth deficiency rather than a lack of those sediments in the area. The thickness of the Otway Group, including the Eumeralla Formation, increases greatly south of the TFZ to the point where seismic and drillhole data concerning the base of the Early Cretaceous are inconclusive in this area.

The Late Early Cretaceous (around 117 Ma) was a time of post-rift sag in the Otway, Gippsland and Bass Basins and is marked stratigraphically in the Otway Basin by sediments from low energy floodplain environments and volcanogenic detrital material of the Eumeralla

Formation (Figure 9, Morton & Drexel 1995). At this time, also, the extensional transport direction changed from NW–SE to NNE–SSW, the continental break-up orientation (O'Brien et al 1994).

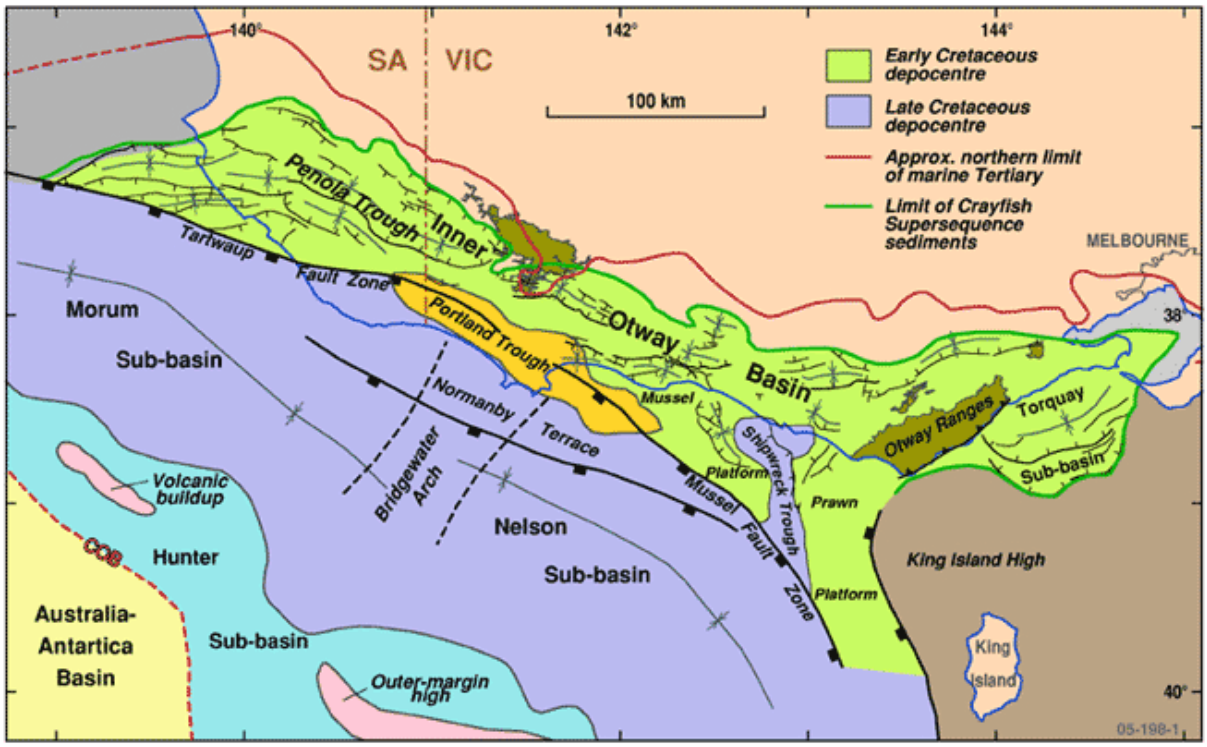

Figure 11. Location and structural map for the Otway basin (from Geoscience Australia, 2012)

The Mid-Cretaceous (Albian, 100–95 Ma) was a time of uplift and erosion in the Otway Basin. This time period saw the initial stage of sea floor spreading (O'Brien et al 1994). No sediments have been identified from this time but U-Th/He fission track analyses provide insight into the thermal and tectonic history. The data suggest different thermal histories for the western and eastern Otway Basin in the Mid-Cretaceous (House et al 2000). Prior to 95 Ma, the burial histories of the two regions appear similar, but after 95 Ma they diverge, with continuous burial and heating in the west and significant structural inversion and uplift in the east (House et al 2000). There have been up to three denudation events in the eastern Otway Basin, with the first in the Mid-Cretaceous, while over the same time period only minor denudation has occurred in the west, mostly on basin margins and basement highs (House et al 2000).

True continental rifting between Australia and Antarctica began and the southern Australian passive continental margin developed during the early Late Cretaceous. Major extension and subsidence occurred south of the Tartwaup Fault Zone, including rapid subsidence in the

Voluta Trough (Morton & Drexel 1995). The major stratigraphic units of this time are part of the Sherbrook Group. North of the TFZ the Sherbrook Group is relatively thin compared to south of the TFZ where the group is at least 5 km thick (Morton & Drexel 1995). Perincek & Cockshell (1995) described reactivation of Early Cretaceous faults, major movement along the TFZ and a significant basin deepening in the western Otway Basin.

Following the Late Cretaceous rifting, subsidence continued through the Palaeocene and into the Eocene (65–44 Ma). The Wangerrip and Nirranda Groups were deposited during this time. The continental margin was subsiding slowly and a mid-ocean ridge was beginning to develop close to the Otway margin (O'Brien et al 1994). During the period 44–35 Ma, sea floor spreading rapidly increased in the Southern Ocean and the Otway margin subsided, leading to an increase in sedimentation rate. The marine origin of the Narrawaturk Marl in the Nirranda Group reflects this change (O'Brien et al 1994).

2.2.4 Neogene–Recent Orogenic Activity

Sandiford (eg. 2003a; 2003b) reviewed the neotectonics of southeast Australia, revisiting and reviving observations made in South Australia by Sprigg (e.g. 1945, 1946, 1952). Southeast Australia is currently in a reverse fault stress regime (e.g. Denham et al 1981; Perincek & Cockshell 1995; Dickinson et al 2002; Sandiford 2003a) that replaced a previous strike-slip regime between 12 and 5 Ma. The reorientation of stress has been attributed to changes in activity on the Australian-Pacific Plate boundary in the vicinity of the South Island of New Zealand (Sandiford 2003a), and on the northern margin of the Australian plate (e.g. Woodhead et al 2010).

The current maximum compressive stress direction in southeast Australia is E–W to NW–SE (Denham et al 1981; Coblentz et al 1995; Hillis et al 1999; Dickinson et al 2002; Sandiford 2003b). Pre-existing extensional structures have been reactivated in the reverse sense as compressive stresses propagated across the Indo-Australian Plate (Dickinson et al 2002; Sandiford 2003a). Several active faults in the Mount Lofty, Otway and Strzelecki Ranges, and the Saint Vincent Basin, are responding to the current stress field.

Stratigraphic data presented by Dickinson et al (2002) and Sandiford (2003b) showed two recent periods of uplift—one in the latest Miocene and another in the Late Pliocene–Recent. Sandiford (2003a) collectively named these events the 'Sprigg's Orogeny' in honour of the pioneering studies by Reg Sprigg in South Australia and Victoria. In the southeast South

Australia study area there has been 40–90 m of uplift in the last million years (Murray-Wallace et al 1998). Evidence for earlier, Late Miocene uplift exists in the form of angular erosional unconformities between folded and reverse faulted Miocene strata and overlying Pliocene sediments in several basins, including the Otway Basin. Sedimentological evidence supports the stratigraphic observations with a change in facies type between Miocene cool water carbonates and overlying Pliocene siliciclastic sediments. Uplifted Pliocene coastal strandlines in the Otway Ranges provide constraints on the timing of Plio-Pleistocene uplift in that area. Sandiford (2003b) showed that significant uplift in the Otway Ranges occurred between 1 and 2 Ma.

Murray-Wallace and others built on the work of Sprigg (e.g. 1952, 1959) in the Coorong to Mount Gambier Coastal Plain region of South Australia. This area contains spectacularly preserved records of Quaternary climate and sea level change (Murray-Wallace et al 1998), which can be used to outline a Late Neogene tectonic history of the region. A complete record of sea level highstands dating back to around 900 ka exists in the form of a series of barrier shoreline deposits of the Bridgewater Formation (eg. Sprigg 1959; Huntley et al 1993; Murray-Wallace et al 1998; Murray-Wallace 2002). There are between 10 and 13 separate barrier dune systems (Sprigg 1952; Murray-Wallace et al 1998) forming a pattern of sub-parallel dune 'ranges' that coalesce to the NW and SE (Figure 12). Sea level highstands have differed by no more than nine vertical metres in the last 900 ka (Murray-Wallace 2002), and this enables geologists to quantify the epeirogenic uplift in southeast South Australia over the same time period.

The rates of epeirogenic uplift vary significantly across the Coastal Plain. For example, there has been virtually no uplift in the Salt Creek area (top left corner of Figure 12) during the Quaternary, compared to a rate of 0.07 m/ka near Robe and up to 0.13 m/ka near Mount Gambier (Murray-Wallace 2002). The lack of uplift in the Salt Creek area explains why the dunes coalesce there—each dune was deposited immediately adjacent to the previous one.

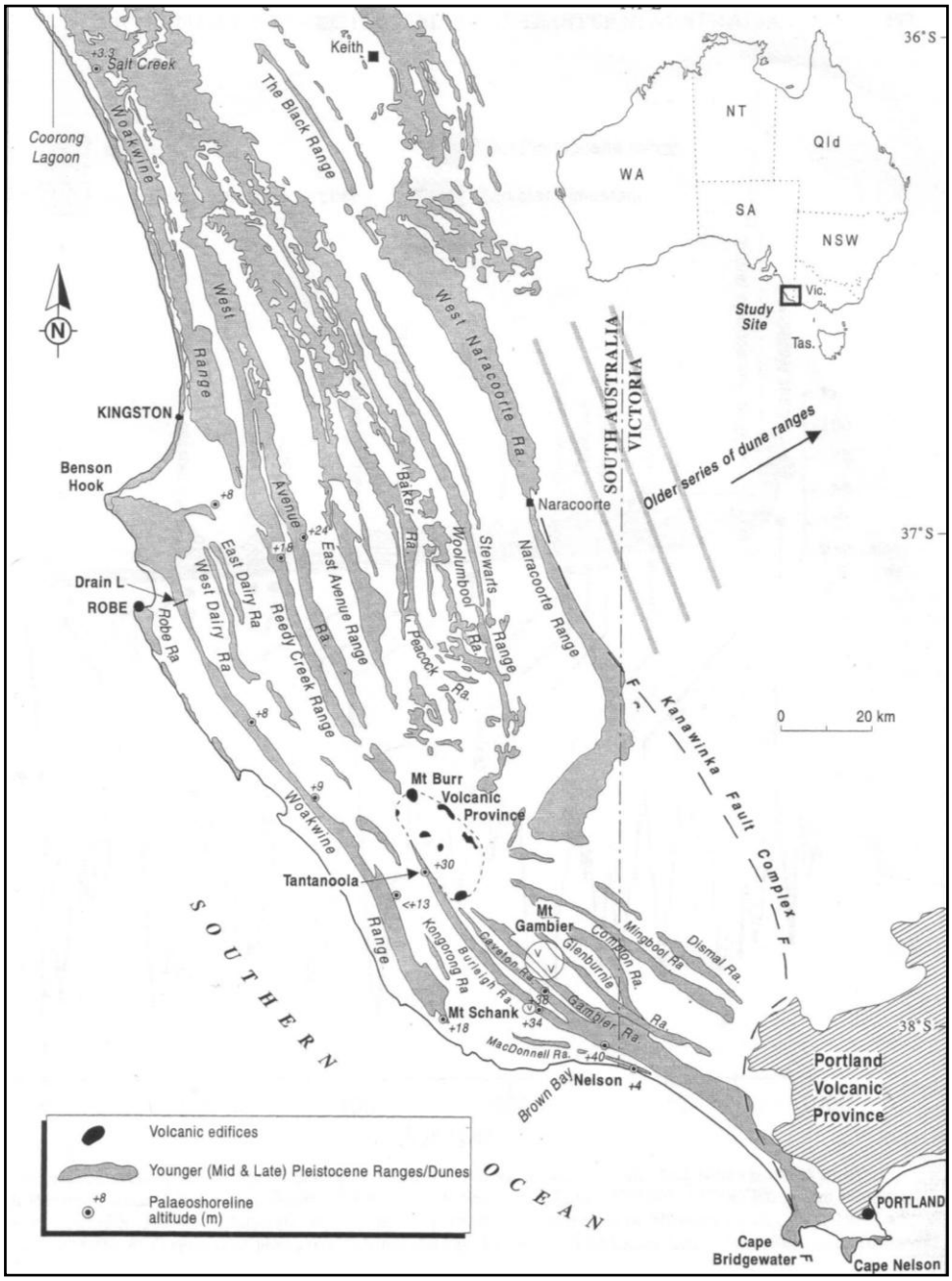

Figure 12. The Coorong to Mount Gambier Coastal Plain. Pleistocene barrier dunes are shown with present altitudes (from Murray-Wallace 2002).

There are, broadly speaking, two proposed mechanisms for the Late Neogene evolution of South Australia's southeast. The first mechanism invokes uplift related to volcanism. Murray-Wallace et al (1998) showed that the Tertiary Gambier Limestone (which would have been sub-horizontal at time of deposition) is elevated in a 'dome' structure spatially correlated with the Mt Burr Volcanics (Figure 13). Sprigg (1952) had previously recognised this 'dome' and concluded that it must have been in place prior to the deposition of the Naracoorte Range dunes around 900 ka.

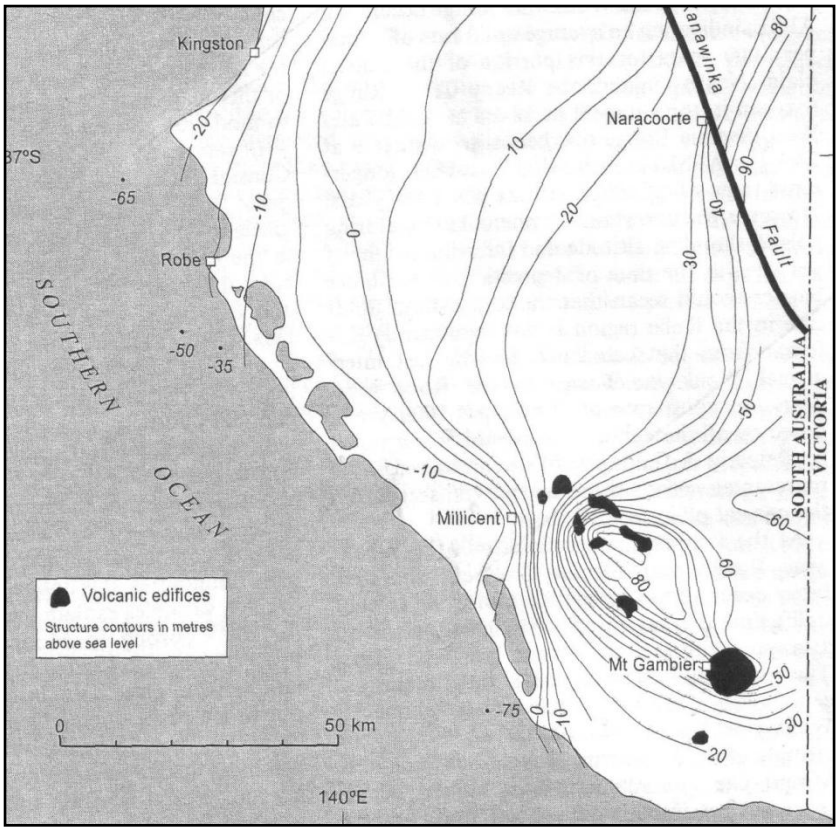

Figure 13. Subcrop map of the surface of the Gambier Limestone in the southeast of South Australia. Maximum elevation spatially corresponds to the Newer Volcanics centres (from Murray-Wallace et al 1998).

Spatial correlation between the dome and volcanics suggests that the uplift may be thermal in nature. Doming and warping associated with volcanism is seen elsewhere in the NVP (Joyce 2000) and provides a simple and logical explanation for the existence of elevated topography. Joyce (2000) used pre-volcanic palaeo-drainage patterns from the NVP of the Central Highlands in Victoria to argue that a doming event clearly preceded volcanism in that case.

The second proposed mechanism relates to compressive stress and upwarping. Sprigg (1952) produced graphic depictions of current elevation along the Pleistocene barrier dunes (Figure 14c), which clearly show a relative difference in uplift rates along strike. Sprigg called the uplift the 'Mount Gambier Upwarp' or 'Arch' (Sprigg 1952) and noted that its 'fold axis' trends NE (Figure 15), almost perpendicular to the current maximum compressive stress direction. Sandiford (2003b) presented topographic profiles along Pliocene strandlines, running approximately parallel to the Pleistocene lines, and showed a similar pattern and degree of elevation (Figure 14a/b). Sprigg's 'Mount Gambier Upwarp' may therefore reflect regional deformation affecting at least the Otway and Murray Basin Regions.

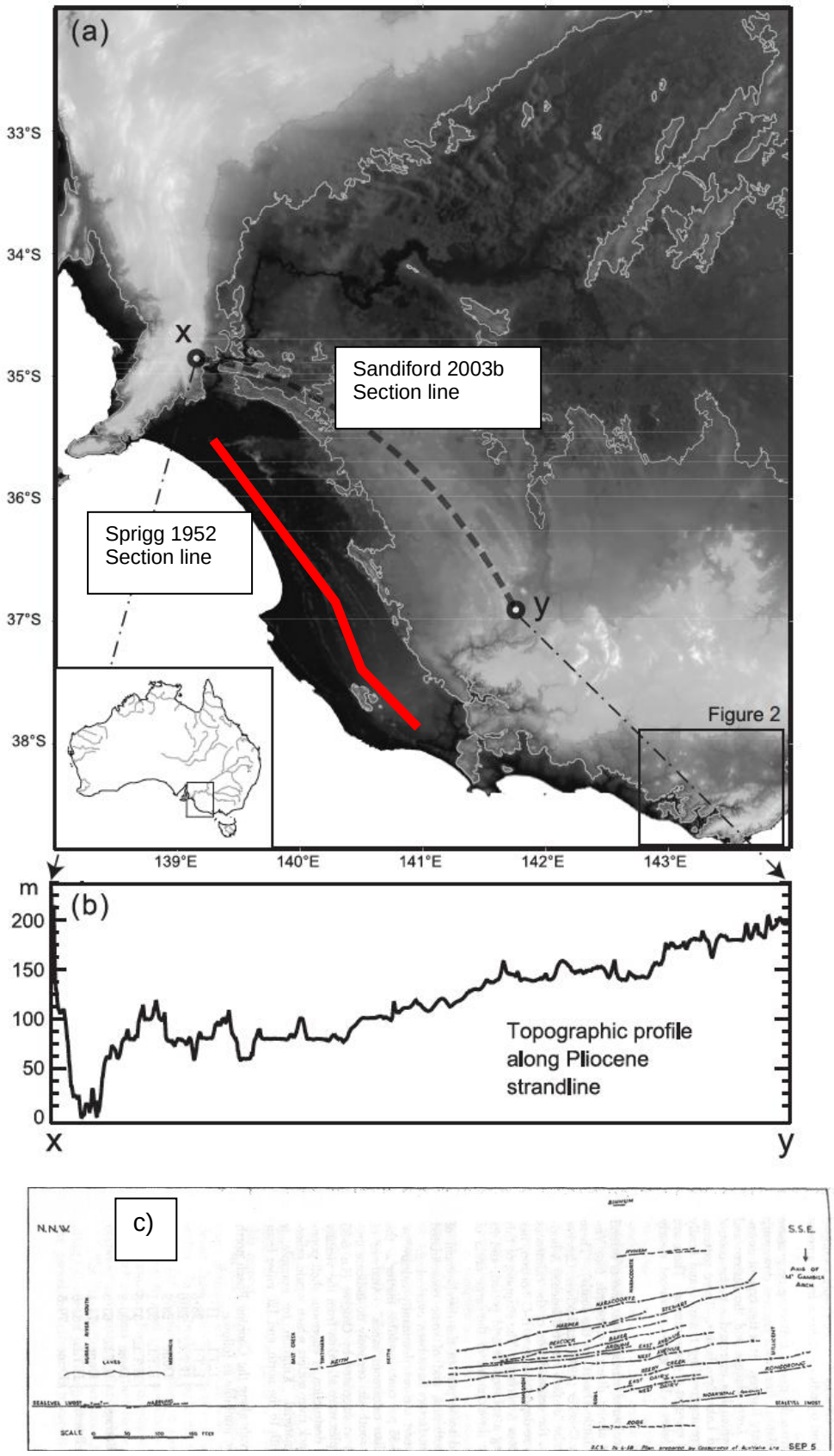

Figure 14. Topographic elevations along (a/b) Pliocene strandlines (from Sandiford 2003b) and (c) Pleistocene strandlines (from Sprigg 1952). Note the correlation between the degree/distribution of uplift.

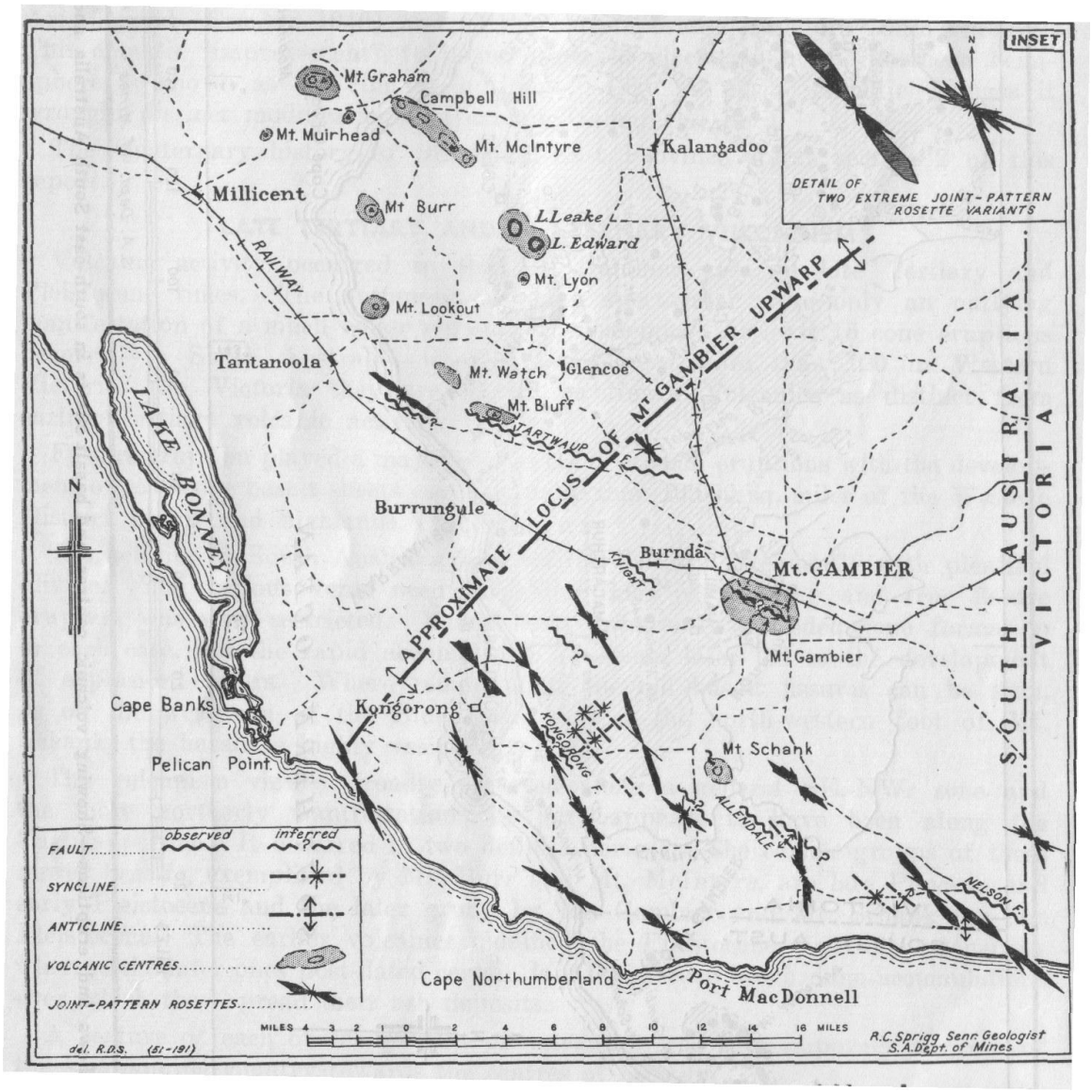

Figure 15. Tectonic map of the Lower South East of South Australia showing faults and fold axes (from Sprigg 1952). The fold axis of the 'Mount Gambier Upwarp' trends almost perpendicular to the current maximum compressive stress direction.

As stated earlier, the rates of neotectonic uplift vary significantly across the Coorong to Mount Gambier Coastal Plain. For example, there has been up to 38 m of uplift around the Mount Gambier and Mount Schank areas, but only four metres of uplift just a few kilometres away at Nelson on the South Australia – Victoria border (Figure 12).

The Early Pleistocene Coomandook Formation, a shallow marine and beach deposit, underlies the entire coastal plain and pre-dates the Middle-Late Pleistocene Bridgewater Formation. It outcrops in two places on the Coorong to Mount Gambier Coastal Plain—in the Tartwaup Fault Zone at Tantanoola and a more extensive exposure east of Mount Gambier. The larger

exposure sits at between 40 and 60 metres above sea level. This inlier of Early Pleistocene sediments appears to place a maximum time constraint on the most recent reverse movement on the Tartwaup Fault and on the uplifting of the 'Mount Gambier Upwarp'. If the Coomandook Formation was deposited at sea level or in a shallow marine environment by the Early Middle Pleistocene (around 1 Ma), then the area has been uplifted by at least 40 to 60 metres since 1 Ma, possibly more if erosion is taken into account. The Tartwaup Fault has also been activated in the reverse sense since that time.

In summary, the Western Otway Basin has experienced significant neotectonic activity over the last million years. Uplift began after approximately 1 Ma, with significant topography in the vicinity of the South Australian Newer Volcanics by around 600 ka. The elevations of the Bridgewater Formation Dunes (Figure 12) indicate that epeirogenic uplift has been more or less continuous between the time of the Naracoorte Ranges (approximately 900 ka) and at least the time of the Woakwine Ranges (approximately 120 ka). Uplift has been spatially non-uniform, with the greatest degree of uplift in the Lower South East near Mount Gambier.

2.2.5 Pleistocene–Recent mafic volcanism – the Newer Volcanics Province

The Newer Volcanics Province (NVP) of western Victoria and southeast South Australia is a 15,000 km^2, 450 km long east–west zone of eruption centres in an intraplate setting. There are approximately 400 separate volcanic vents broadly classified into two groups: the Central Volcanoes and the Lava Fields (Johnson et al 1989). Their distribution stretches from a line extending almost due north of Melbourne to the western end of the Mount Burr Range in southeast South Australia, and can be grouped into three regions: the Central Highlands Province and Western Plains in Victoria, and the South Australian Mount Gambier Zone (Figure 16; van Otterloo 2011). The NVP straddles the Moyston Fault Zone, the inferred boundary between the DFB and the LFB, with a majority of the volcanic vents (approximately 250) lying to the east.

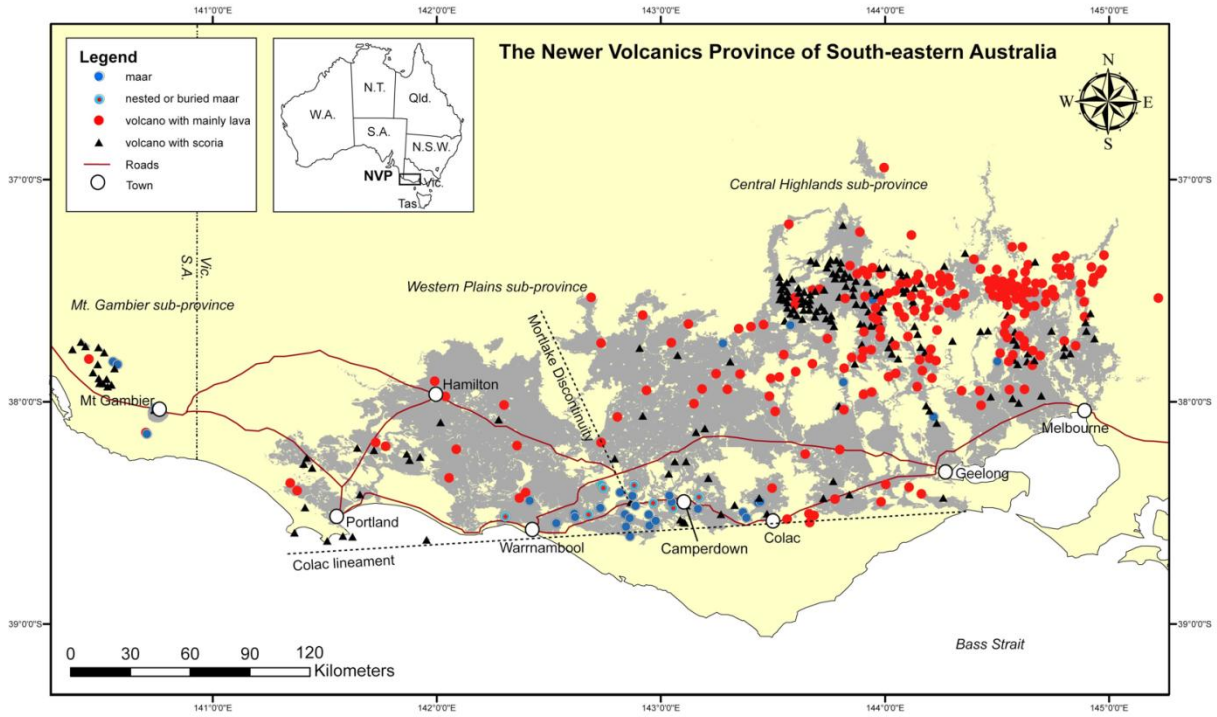

Figure 16. Volcano type and distribution in the NVP (from van Otterloo 2011).

Broadly speaking, the Central Volcanoes classify as cinder cones, tuff cones, tuff rings and maars, with scoria and/or lava (Cas 1989). Phreatomagmatic interaction led to maar formation in several eruption centres, primarily in the Otway Basin. The Lava Field volcanoes in the western NVP are derived from a "diffuse dyke and pipe swarm up to 100 km across" (Cas 1989). Explosive scoria cones overprint many of the lava flows, and several flows have well-preserved lava tunnels and/or lava canals (Cas 1989).

The origin and mechanism for formation of the NVP are unclear. Globally, intraplate eruptions are documented in four general settings: Rift Zones, Basin and Range, mantle hotspot and uplifted flanks of rifted continental margins (Johnson et al 1989). The rise of magma through the crust usually requires a tensional stress regime such as arc, back-arc or transtensional zones. The distribution of volcanic centres in the NVP appears to be controlled in part by crustal weaknesses (Cas 1989; Perincek & Cockshell 1995). A spatial correlation exists between volcanism and the major faults of the Otway Basin; Mount Gambier, the Mount Burr Volcanics, Cape Bridgewater, Portland, Tower Hill, Mount Napier and several other volcanoes are located in the TFZ and the Kanawinka Fault Zone, where the current WNW maximum compressive stress has resulted in NNW-NW trending strike-slip transtension (Perincek & Cockshell 1995). Johnson & Wellman (1989) suggested 'leaky transform faults' as a possible mechanism for the opening of fractures in the crust that may

have led to volcanism.

McBride et al (2001) used Osmium isotope data to show that two distinct families of lavas were extruded in the NVP, one of which has chemistry consistent with an Ocean Island Basalt (OIB)-type mantle plume source. A lack of crustal material in the eastern NVP magmas led Wellman (1989) to conclude the magma rose rapidly through the crust. In contrast, McBride et al (2001) concluded that the Lava Field or 'Plains Series' lavas might have some degree of crustal contamination.

Graeber et al (2002) interpreted a prominent low seismic wave speed anomaly under the eastern NVP from teleseismic tomography data, geographically correlating with the highest spatial density of eruption centres. They proposed that the anomaly corresponds to relatively hot mantle.

Vogel & Keays (1997) concluded from rare earth element and platinum group element data that all of the NVP magmas are derived from partial melting of either a subducted eclogitized ocean slab or a basalt-melt enriched SCLM. They also compared the NVP chemistry to OIB over a mantle plume. They did not support a mantle plume hypothesis, however, due to the lack of a clear N-S younging of the NVP Lava Fields volcanoes. East-under-west subduction characterises the western LFB (Collins & Vernon 1992) and therefore it is possible that the SCLM under the NVP contains subducted oceanic lithosphere.

The NVP has zones of high CO_2 accumulation. The CO_2 has an isotopic signature indicative of mantle origin (Sheard 1990; Cartwright et al 2002).

The theory for the formation of the NVP that is arguably most consistent with the available evidence at this stage is thermal stimulation of a stressed lower crust by one or more mantle hotspots (Sutherland 1981; Cas 1989). Sutherland (1981) first argued the case for a hotspot, citing a strong linear correlation between latitude and age for the NVP central volcano or cones activity. The Coral Sea Anomaly off the coast of Queensland is interpreted to represent a migrating hotspot trace younging to the south, and its trace has been projected to correspond spatially with the youngest volcanoes of the NVP at the present time (Sutherland 1981). Future volcanic activity is predicted in or off the coast of southeastern Australia on this basis.

2.2.6 The South Australian NVP

There are eighteen (18) large-scale NVP vent locations in South Australia. Most of them are in the Mount Burr Range area northwest of Mount Gambier (Figure 14), with the remainder at

Mounts Gambier and Schank. A possible submarine or subterranean volcanic centre is postulated to exist off the coast in the Beachport area (Sprigg 1959). The reported ages of the South Australian NVP volcanoes range from 20,000 – 1,000,000 years for the Mount Burr Volcanics, and Holocene for Mount Gambier and Mount Schank (Sheard & Nicholls 1989). Age estimates for the latter two eruption centres include 4,930–18,100 years for Mount Schank (Smith & Prescott 1987), 5–38 ka for Valley Lake at Mount Gambier (Barton & McElhinny 1981), and 4–8 ka at Mount Gambier (Blackburn et al 1982). Leaney et al (1995) presented carbon and oxygen isotope data extracted from sediment core from the Blue Lake and concluded that the age of Mount Gambier is at least 28 ka. This conclusion was challenged by Murray-Wallace et al (1998) who proposed that the sediment core tested by Leaney et al (1995) may have been contaminated to a significant extent by older, ^{14}C-depleted material such as the surrounding Gambier Limestone. If upper ages are taken for Mounts Gambier and Schank then they can be considered contemporary in age to the 'younger' events of the Mount Burr Volcanics.

Sprigg's (1959) postulation of submarine volcanic activity near Beachport is of interest. Hard rock, submarine ridges extend offshore perpendicular to the coastline down the continental slope from the locations of epicentres of recent earthquakes. These ridges are 15–30 km long and constitute the only outcrop in that area of seafloor. Sprigg proposed that they could be submarine lava flows from very recent (50–100 years) events. O'Brien et al (1994) presented aeromagnetic data showing a distinct signature of exposed volcanics in South Australia, and also proposed a buried occurrence near Beachport.

2.2.7 Southeast South Australia geology summary

The geology of southeast South Australia has had a complex geological history. The area has a sub-continental lithospheric mantle of Proterozoic age, basement crustal geology of Palaeozoic metamorphosed sediments (Delamerian Fold Belt) and syn- and post-tectonic magmatic bodies (Padthaway Ridge), overlain by Jurassic to Tertiary basin sediments of the Gambier Sub-basin and Murray Basin. This history resulted in heterogeneous zones of heat production, and a likely redistribution of heat due to lateral thermal conductivity contrasts (refer to Chapter 6). The Neogene to Quaternary saw the onset of compressive neotectonics and enigmatic basaltic volcanism.

The current surface heat flow regime is therefore of considerable interest in light of the region's geological past. It could help discriminate between the relative thermal influences of

a number of geological factors. The Neogene–Recent volcanic and neotectonic events might be expected to have a thermal signature; the granites of the Padthaway Ridge may contribute significant heat flow to the crust; and the lateral thermal conductivity contrasts in the region related to Palaeozoic or Mesozoic tectonic events may be conducting heat towards the Otway Basin margin.

2.3 Part 3: The Torrens Hinge Zone and Central Flinders Ranges

2.3.1 The Torrens Hinge Zone

The Torrens Hinge Zone defines the western edge of a tectonic rift zone that formed during the breakup of the Rodinia Supercontinent, beginning around 830 Ma (Preiss 2010). Spatially it lies immediately east of the Archaean to Mesoproterozoic Gawler Craton (Hand et al 2007), which at the time of rifting was the easternmost extent of the Australian continent (e.g. Preiss 2000; 2010).

In terms of broad spatial divisions, the rift sedimentary sequences can be divided into three parts (Figure 17):

1. A western part comprised of rift-related sediments overlying the Gawler Craton in a platform setting, known as the Stuart Shelf;
2. An eastern region - the rift complex-proper, with a thick (up to 18 km) sedimentary package that records a complex history of tectonic rift and sag events spanning temporally from 830 Ma to 500 Ma with at least five successive rift cycles (Preiss, 2000). The broad rift zone is known collectively as the Adelaide Geosyncline (Preiss, 2000).
3. The transition between the Stuart Shelf and the Adelaide Geosyncline, known as the Torrens Hinge Zone.

The Neoproterozoic portion of the geological time period during which these sediments were deposited is locally known as the Adelaidean Period (Mawson & Sprigg 1950), and the rift cycles are broadly allocated to five chronostratigraphic units, named from oldest to youngest: Willouran, Torrensian, Sturtian, Marinoan and Cambrian (Figure 18). The Willouran and Torrensian units include associated igneous events, while the Sturtian and Marinoan units record glaciation events. The latest subgroup of the Marinoan unit, known as the Pound Subgroup, includes the Ediacara Member, which contains the earliest known metazoan

fossils. This time period has hence been proclaimed as the Ediacaran Period (Preiss 2010; Knoll et al 2006).

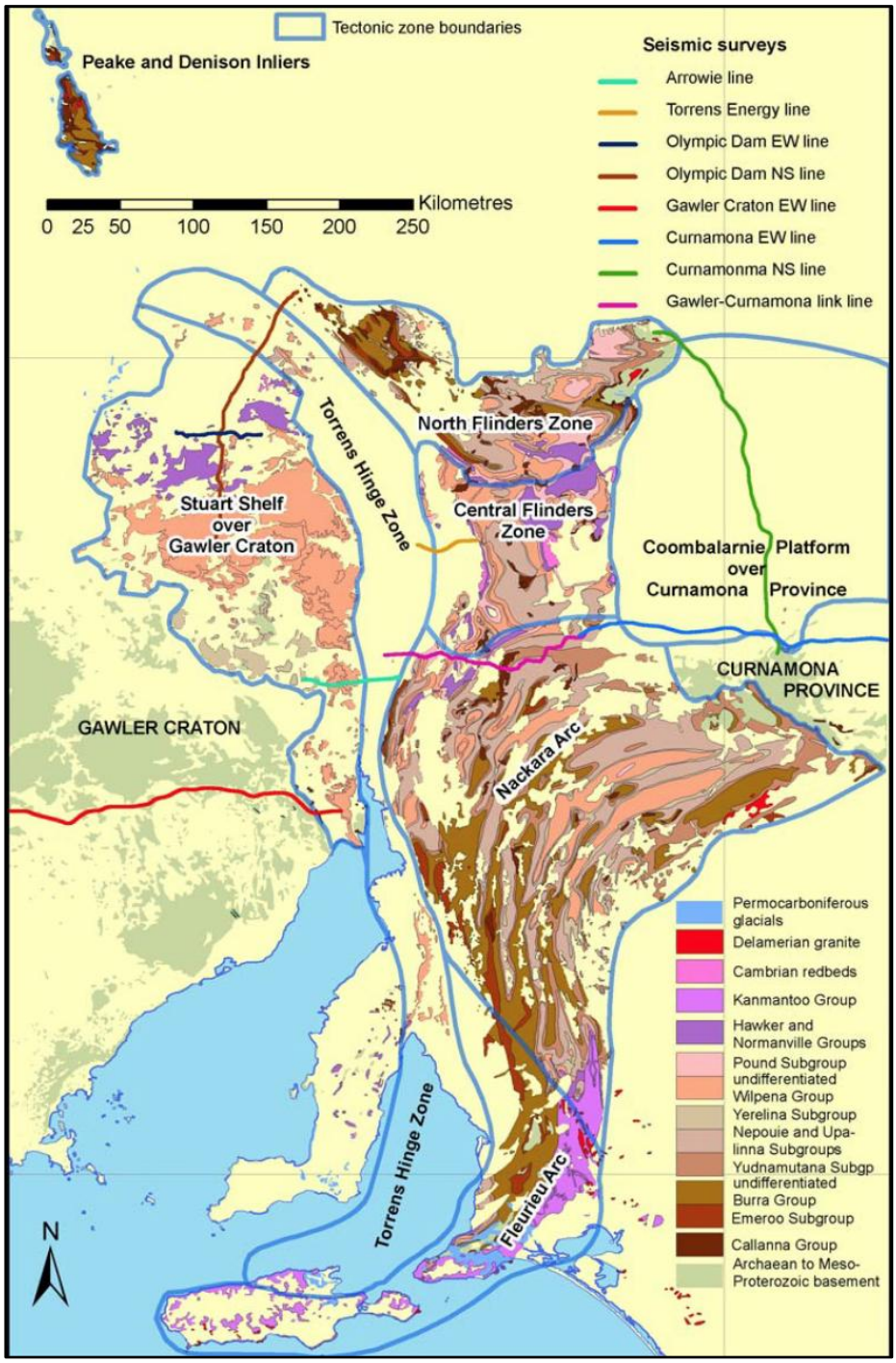

Figure 17. Proterozoic to Palaeozoic geology of the Stuart Shelf, Torrens Hinge Zone and Adelaide Geosyncline showing tectonic zones of the Delamerian Orogen (from Preiss, 2010).

The Cambro-Ordovician Delamerian Orogeny variably deformed the sediments of the Torrens Hinge Zone and Adelaide Geosyncline (e.g. Preiss 2000). The latter now forms part of the broader Delamerian Fold Belt (DFB). Four major tectonic zones of the DFB are recognized

within the Adelaide Geosyncline (Figure 17). In order of greatest to least deformation intensity, they are the Fleurieu Arc, the Nackara Arc, the North Flinders Zone, and the Central Flinders Zone. Geophysical data suggest that the basement to the sediment package is shallowest beneath the Central Flinders Zone (Preiss 2010).

Chronostratigraphic units		Lithostratigraphic units, Flinders Ranges					Major events	Estimated Ages
		Supergroup	*Group*	*Subgroup*	*Selected Formations*	*Member*		
?mid-Cambrian		Moralana	Lake Frome				Redbeds	
Early Cambrian			Unnamed		Wirrealpa		marine limestone	
					Billy Creek		redbeds, tuffs	~510 Ma
			Hawker		Wilkawillina		archaeocyathan reefs	
					Parachilna		worm-burrows	
Marinoan	Ediacaran	Heysen	Wilpena	Pound	Rawnsley		thick sand sheet	
						Ediacara	metazoan fossils	
					Bonney		Redbeds	
				unnamed	Wonoka		submarine canyons	
					Bunyeroo		bolide impact layer	
				Sandison	ABC Range		transgression-regression	
					Brachina			
					Nuccaleena			
			Umberatana	Yerelina	Elatina		Glaciation	?635 Ma
								or 580 Ma
				Upalinna	Angepena		basin-margin redbeds	
Sturtian				Nepouie	Balcanoona		ooids, microbial reefs	
					Tapley Hill	Tindelpina	transgression-regression	~650 Ma
				Yudnamutana	Wilyerpa		deglaciation, rifting	~660 Ma
					Appila/Pualco		glaciation, rifting	
							major unconformity	
Torrensian		Warrina	Burra	Belair			Sag basin, deltas	
				Bungarider			Sag basin, deltas, deep-water dolomite	
				Mundallio	Skillogalee		paralic dolomite, magnesite	
						Kooringa	Burra Cu, felsic magma	~790 Ma
				Emeroo			major rifting, clastics minor mafic volcanism	
Willouran			Callanna	Curdimurka			major rifting, clastics, carbonates, evaporites	
							minor mafic and	
					Rook		felsic volcanism	~800 Ma
				Arkaroola	Wooltana		mafic volcanism	827±6 Ma
					Wywyana		sag basin	
					Paralana			

Figure 18. Stratigraphic column for the sedimentary sequences of the Adelaide Geosyncline. Key formations and major events are shown (from Preiss 2010).

The competent nature of the proximal Gawler Craton basement may have protected the THZ region from significant deformation during the Delamerian Orogeny. Thus, while the Adelaide Geosyncline is now a moderately to intensely deformed package within the DFB, the THZ remains a "meridional belt of gentle folding" (Preiss 2000). The THZ is estimated to hold between 2500m and 7000m thickness of sediments (de Vries et al 2006), underlain by Mesoproterozoic Gawler Craton in the north (Ferris et al 2002) and by the Palaeoproterozoic Barossa Complex in the south (e.g. Preiss 1993).

2.3.2 Controls on Adelaidean Rifting

The sediment thickness in the Adelaide Geosyncline is highly variable, with preferential depocentres located in various locations throughout the successive rift cycles. The locations and timing of these depocentres are summarised in Preiss (2000). Deposition in the Willouran, Torrensian and Sturtian time periods (Figure 18) was spatially controlled by extensional activation along largely pre-existing basement fault structures. Some of these structures, such as the Paralana Fault, remained active throughout the Adelaidean time period, while others shifted location in later time periods or were initially activated during those times (Preiss 2000). Figure 19 is a reproduction of the map of basement-controlled extensional tectonics during the Torrensian time period from Preiss (2000).

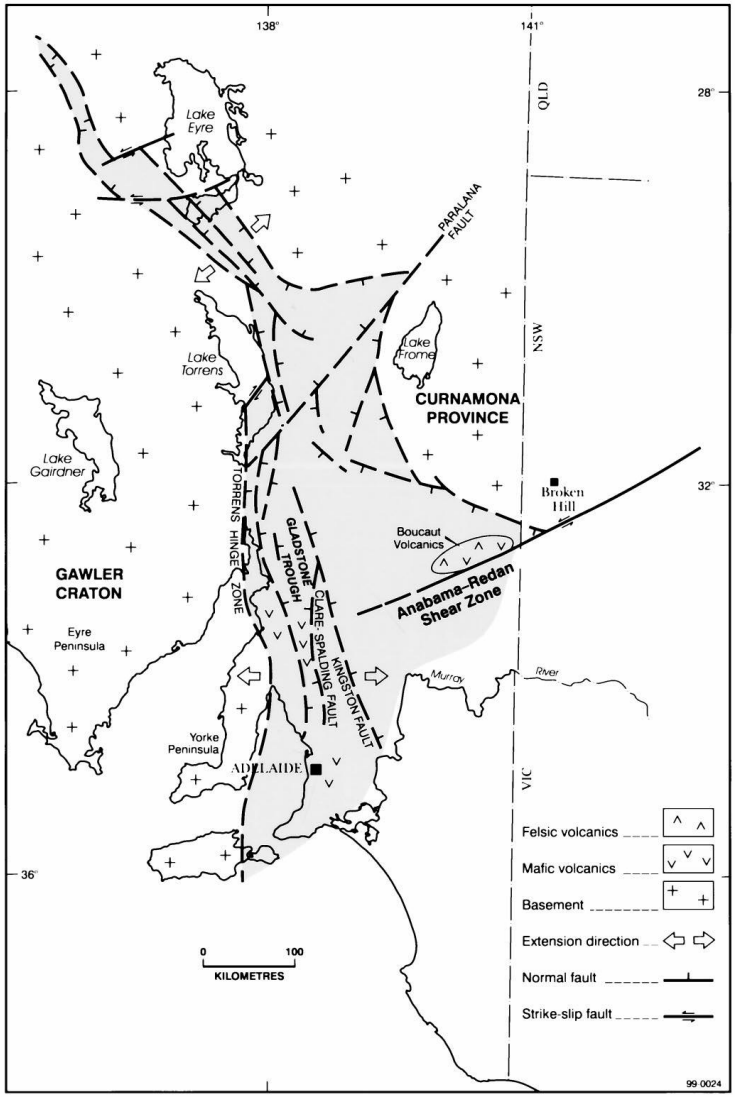

Figure 19. Basement-controlled extensional tectonics of the Torrensian time period (see Figure 18 for age relationship) in the Adelaide Geosyncline (from Preiss 2000).

Preiss (2000) used a range of approaches to map the locations and timing of the rifts in the Neoproterozoic. These included mapping faults from the Delamerian Orogeny that that were reactivations of Neoproterozoic basement rift structures, mapping thickness variations in Adelaidean sediments, mapping onlap relationships between units, and mapping diapir distributions, which indicated thick early stage evaporitic sediment localities.

Paul et al (1999) investigated structural controls on deformation in the Central to North Flinders Zones (Figure 17), and demonstrated that the boundaries of these zones have been, and still are controlled by the Paralana Fault to the east and the Norwest Fault in the west (Figure 20). These faults controlled deposition in the Neoproterozoic, the locations of contractual deformation from the Delamerian to present day Sprigg's Orogeny (Paul et al 1999).

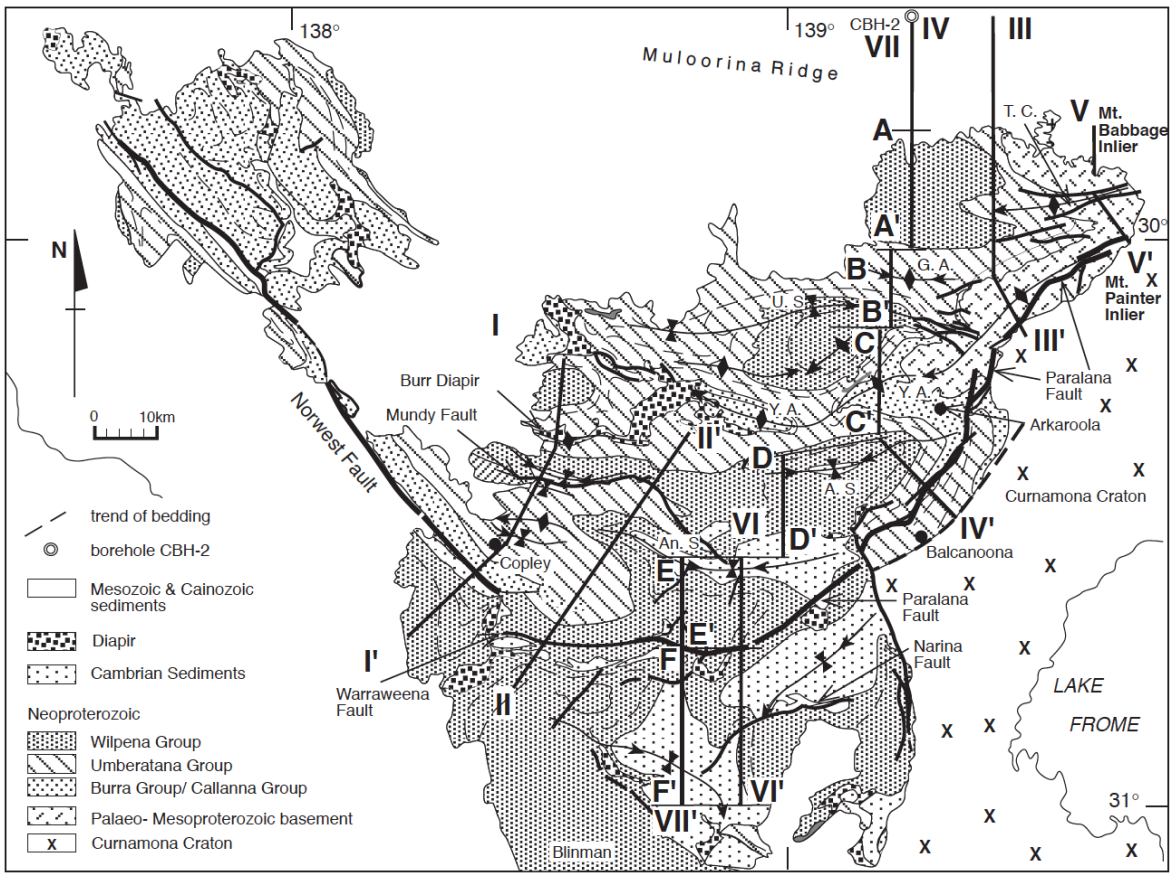

Figure 20. Structural map of the Northern Flinders Zone from Paul et al (1999). Note that the Norwest and Paralana Faults are long-lived faults that were active in the earliest stages of the Neoproterozoic rifting (e.g. Figure 19; Preiss 2000)

Paul et al (1999) also pointed out that the greatest deformation in the Northern Flinders Zone,

resulting in basin inversion uplift so extreme that it removed all sediment cover and exposed basement rocks, occurred in the zone of highest recorded heat flow. They concluded that "High heat flow in the northern Flinders Ranges suggests that the structural style not only reflects the pre-Delamerian basin architecture but is also a consequence of the reactivation of thermally perturbed, weakened basement." This conclusion, also reached by McLaren and others, is discussed in greater detail in section 2.1.3 above. This correlation of high heat flow, basin depocentres and long-lived basement fault reactivation is supported by new data from the western side of the Central-Northern Flinders Zone presented in this thesis (see Chapter 5, Matthews 2009).

In summary, pre-existing faulting and thermal weakening from anomalous heat production and high heat flow have served over a long period of time to shape the formation of the tectonic framework of the central part of South Australia.

References

Barton, C. E. & McElhinny, M. W., 1981, A 10,000 yr geomagnetic secular variation record from three Australian maars, Geophysical Journal of the Royal Astronomical Society, 67 (2), p. 465-485.

Beardsmore, G.R., 2005, Thermal modelling of the hot dry rock geothermal resource beneath GEL99 in the Cooper Basin: Proceedings World Geothermal Congress, Antalya, Turkey, 24-29 April, 2005.

Beardsmore, G. R., and Cull, J. P., 2001, Crustal heat flow; a guide to measurement and modelling: Cambridge University Press.

Boult, P. J., 2002, Summary and introduction In: Boult, P.J. and Hibburt, J.E. (Eds), The petroleum geology of South Australia, Vol. 1: Otway Basin. 2nd edn. South Australia. Department of Primary Industries and Resources. Petroleum Geology of South Australia Series, Vol. 1, ch. 1.

Cartwright, I. (Monash University, Hydrogeology and Environment Research Group, Clayton, Victoria, Australia), Weaver, T., Tweed, S., Ahearne, D., Cooper, M., Czapnik, K. & Tranter, J., 2002, Stable isotope geochemistry of cold CO (sub 2) -bearing mineral spring waters, Daylesford, Victoria, Australia; sources of gas and water and links with waning volcanism, Chemical Geology, 185 (1-2), p. 71-91.

Cas, R. A. F. (Co-ordinator), 1989, 'Physical Volcanology' in Johnson, R.W., Knutson, J. & Taylor, S.R., (eds) (1989), Intraplate volcanism in eastern Australia and New Zealand: Cambridge, England, Cambridge University press, p 55–87.

Coblentz, D. D., Sandiford, M., Richardson, R. M., Zhou, S. & Hillis, R., 1995, The origins of the intraplate stress field in continental Australia, Earth and Planetary Science Letters, 133 (3-4), p. 299-309.

Collins, W. J. & Vernon, R. H., 1992, Palaeozoic arc growth, deformation and migration across the Lachlan fold belt, southeastern Australia in Fergusson, C. L. & Glen, R. A. (eds), The Palaeozoic eastern margin of Gondwanaland; tectonics of the Lachlan fold belt, southeastern Australia and related orogens, Tectonophysics, 214 (1-4), p. 381-400.

Cull, J. P., 1982, An appraisal of Australian heat-flow data, BMR Journal of Australian Geology and Geophysics, 7, p. 11–21.

de Vries, S., Fry, N., and Pryer, L., 2006, OZ SEEBASE Proterozoic Basins Study, Report to Geoscience Australia by FrOG Tech Pty Ltd.

Denham, D., Weekes, J. & Krayshek, C., 1981, Earthquake evidence for compressive stress in the Southeast Australian crust, Journal of the Geological Society of Australia, 28 (3-4), p. 323-332.

Dickinson, J. A., Wallace, M. W., Holdgate, G. R., Gallagher, S. J. & Thomas, L., 2002, Origin and timing of the Miocene-Pliocene unconformity in Southeast Australia, Journal of Sedimentary Research, 72 (2), p. 288-303.

Ferris, G. M., Schwarz, M. P., and Heithersay, P., 2002, The Geological Framework, Distribution and Controls of Fe-Oxide Cu-Au Mineralisation in the Gawler Craton, South Australia. Part I – Geological and Tectonic Framework, In Porter, T.M. ed., 2002 – Hydrothermal Iron Oxide Copper- Gold & Related Deposits: A Global Perspective, volume 2; PGC Publishing, Adelaide.

Finlayson, D. M., Owen, A., Johnstone, D. & Wake-Dyster, K. D., 1993, Moho and petrologic crust-mantle boundary coincide under southeastern Australia, Geology (Boulder), 21 (8), p. 707-710.

Finlayson, D. M., Johnstone, D. W., Owen, A. J. & Wake-Dyster, K. D., 1996, Deep seismic images and the tectonic framework of early rifting in the Otway Basin, Australian southern

margin in White, Don J. (editor), Ansorge, Joerg (editor), Bodoky, Tamas J. (editor), Hajnal, Zoltan (editor), Seismic reflection probing of the continents and their margins, Tectonophysics, 264 (1-4), p. 137-152.

Finlayson, D. M., Collins, C. D. N., Lukaszyk, I. & Chudyk, E. C., 1998, A transect across Australia's southern margin in the Otway Basin region; crustal architecture and the nature of rifting from wide-angle seismic profiling in Klemperer, Simon L. (editor), Mooney, Walter D. (editor), Deep seismic profiling of the continents; II, A global survey, Tectonophysics, 288 (1-4), p. 177-189.

Fishwick, S. & Rawlinson, N., 2012, 3-D structure of the Australian lithosphere from evolving seismic datasets, Australian Journal of Earth Sciences: An International Geoscience Journal of the Geological Society of Australia, 59 (6), 809-826.

Foden, J. D., Elburg, M. A., Turner, S. P., and Sandiford, M., 2002, Granite production in the Delamerian Orogen, South Australia, Journal of the Geological Society 159, p. 557–575.

Foster, D. A. & Gleadow, A. J. W., 1992, Reactivated tectonic boundaries and implications for the reconstruction of southeastern Australia and northern Victoria Land, Antarctica, Geology (Boulder), 20 (3), p. 267-270.

Foster, D. A. & Gleadow, A. J., 1993, The architecture of Gondwana rifting in southeastern Australia; evidence from apatite fission track thermochronology in Findlay, R. H., Unrug, R., Banks, M. R., Veevers, J. J. (eds), Assembly, evolution and dispersal; proceedings of the Gondwana eight symposium, International Gondwana Symposium, 8, p. 597-603.

Geoscience Australia, 2012, "Otway Basin," www.ga.gov.au/oceans/sa_Otway.jsp. Accessed August 20 2012.

Graeber, F. M., Houseman, G. A., Greenhalgh & S. A., 2002, Regional teleseismic tomography and the western Lachlan Oregon and the Newer volcanic province, Southeast Australia, Geophysical Journal International, 149 (2), p. 249-266.

Gray, D.R., and Foster, D.A., 1998, Character and kinematics of faults within the turbidite-dominated Lachlan Orogen: implications for the tectonic evolution of eastern Australia: Journal of Structural Geology, 20, 1691-1720

Hand, M., Reid, A. and Jagodzinski, E., 2007, Tectonic framework and evolution of the Gawler

Craton, South Australia, Economic Geology , 102 , p. 1377-1395.

Handler, M. R. & Bennett, V. C., 2001, Constraining continental structure by integrating Os isotopic ages of lithospheric mantle with geophysical and crustal data; an example from southeastern Australia, Tectonics, 20 (2), p. 177-188.

Hillis, R. R., Enever, J. R. & Reynolds, S. D., 1999, In situ stress field of eastern Australia, Australian Journal of Earth Sciences, 46 (5), p. 813-825.

House, M. A., Kohn, B. P., Farley, K. A. & Raza, A., 2000, (U-Th)/He thermochronometry in southeastern Australia; confirmation of laboratory diffusion experiments and insights into the Cenozoic thermal history of the Otway Basin Anonymous, Fission track 2000; 9th international conference on fission track dating and thermochronology, Abstracts - Geological Society of Australia, 58, p. 169-171.

Houseman**,** G.A., Cull, J.P. Muir, P.M. and Paterson, H.L., 1989, Geothermal signatures and uranium ore deposits on the Stuart Shelf of South Australia: *Geophysics*, 54 (2), 158–170.

Huntley, D. J., Hutton, J. T. & Prescott, J. R., 1993, The stranded beach-dune sequence of South-east South Australia; a test of thermoluminescence dating, 0-800 ka, Quaternary Science Reviews, 12 (1), p. 1-20.

Jenkins, R. J. F. & Sandiford, M., 1992, Observations on the tectonic evolution of the southern Adelaide Fold Belt: *Tectonophysics*, 214, 27-36

Jensen-Schmidt, B., Cockshell, C. D. & Boult, P. J., 2002, *Structural and tectonic setting* In: Boult, P.J. and Hibburt, J.E. (Eds), *The petroleum geology of South Australia, Vol. 1: Otway Basin. 2nd edn*. South Australia. Department of Primary Industries and Resources. Petroleum Geology of South Australia Series, Vol. 1, ch. 5.

Johnson, R.W., Knutson, J. & Taylor, S.R. (eds), 1989, Intraplate volcanism in eastern Australia and New Zealand: Cambridge, England, Cambridge University press, 408 p.

Johnson, R. W. & Wellman, P. (Co-ordinators), 1989, 'Framework for Volcanism' in Johnson, R.W., Knutson, J. & Taylor, S.R., (eds). (1989), Intraplate volcanism in eastern Australia and New Zealand: Cambridge, England, Cambridge University press, p. 1–53.

Joyce, B., 2000, 'Volcanic activity in the Quaternary of Victoria, Australia.' <http://wwwrses.anu.edu.au/envgeo/AQUADATA/AQUA/meetings/Bowlerfest/Joyce.html> (accessed 10 February 2004).

Knoll, A. H., Walter, M. R., Narbonne, G. M., and Christie-Blick, N., 2006, The Ediacaran Period: A new addition to the geologic time scale, Lethaia , 39 , p. 13–30.

Leaney, F. W. J., Allison, G. B., Dighton, J. C. & Trumbore, S., 1995, The age and hydrological history of Blue Lake, South Australia, Palaeogeography, Palaeoclimatology, Palaeoecology, 118 (1-2), p. 111-130.

Matthews, C. G., 2009, Geothermal energy prospectivity of the Torrens Hinge Zone: evidence from new heat flow data: *Exploration Geophysics*, 40, 288–300.

Matthews, C. G., and Beardsmore, G. R., 2007, New heat flow data from southeastern South Australia: *Exploration Geophysics*, **38**, 260–269.

Mawson, D., and Sprigg, R. C., 1950, Subdivision of the Adelaide System, Australian Journal of Science, 13, p. 69–72.

McBride, J. S., Lambert, D. D., Greig, A. & Nicholls, I. A., 1996, Multistage evolution of Australian subcontinental mantle; Re-Os isotopic constraints from Victorian mantle xenoliths, Geology (Boulder), 24 (7), p. 631-634.

McBride, J. S., Lambert, D. D., Nicholls, I. A. & Price, R. C., 2001, Osmium isotopic evidence for crust-mantle interaction in the genesis of continental intraplate basalts from the Newer Volcanics Province, southeastern Australia, Journal of Petrology, 42 (6), p. 1197-1218.

McLaren, S., Dunlap, W. J., Sandiford, M. & McDougall, I., 2002, Thermochronology of high heat producing crust at Mount Painter, South Australia: implications for tectonic reactivation of continental interiors, Tectonics, 21(4), doi:10.1029/2000TC001275.

McLaren, S., Sandiford, M., Hand, M., Neumann, N., Wyborn, L., and Bastrakova, I., 2003, The hot southern continent, heat flow and heat production in Australian Proterozoic terranes, Geological Society of Australia, Special Publication, 22, p. 151–161.

McLaren, S., Sandiford, M. & Powell, R., 2005, Contrasting styles of Proterozoic crustal evolution: A hot-plate tectonic model for Australian terranes, Geology 33, p. 673-676.

Miller, J. McL., Norvick, M. S. & Wilson, C. J. L., 2002, Basement controls on rifting and the associated formation of ocean transform faults; Cretaceous continental extension of the southern margin of Australia, Tectonophysics, 359 (1-2), p. 131-155.

Morton, J.G.G. & Drexel, J.F. (eds), 1995, Petroleum geology of South Australia. Petroleum Division, SA Dept. of Mines and Energy, Vol 1. Otway Basin, p. 211.

Murray-Wallace, C. V., Belperio, A. P. & Cann, J. H., 1998, Quaternary neotectonism and intra-plate volcanism; the Coorong to Mount Gambier coastal plain, southeastern Australia; a review Stewart, I. S. & Vita-Finzi, C. (eds), Coastal tectonics, Geological Society Special Publications, 146, p. 255-267.

Murray-Wallace, C.V., 2002, Pleistocene coastal stratigraphy, sea-level highstands and neotectonism of the southern Australian passive continental margin - a review. Journal of Quaternary Science 17, 469-489.

Neumann, N., Sandiford, M., and Foden, J., 2000, Regional geochemistry and continental heat flow; implications for the origin of the South Australian heat flow anomaly, Earth and Planetary Science Letters, 183, p. 107–120.

O'Brien, G. W., Reeves, C. V., Milligan, P. R., Morse, M. P., Alexander, E. M., Willcox, J. B., Yunxuan, Z., Finlayson, D. M., & Brodie, R. C., 1994, New ideas on the rifting history and structural architecture of the Western Otway Basin: Evidence from the integration of aeromagnetic, gravity and seismic data, APEA Journal 34, p. 529-54.

Paul, E., Flottmann, T., Sandiford, M., 1999, Structural geometry and controls on basement-involved deformation in the northern Flinders Ranges, Adelaide Fold Belt, South Australia, Australian J. Earth Sci. 46 (3), p. 343–354.

Perincek, D. & Cockshell, C. D., 1995, The Otway Basin; Early Cretaceous rifting to Neogene inversion Anonymous, Australian Petroleum Exploration Association conference, The APEA Journal, 35, Part 1, p. 451-466.

Pollack, H.N., Hurter, S.J. and Johnson, J.R., 1993. Heat flow from the Earth's interior: analysis of the global data set. Reviews of Geophysics, 31(3), p.267–280.

Preiss, W. V., 1993, Basement inliers of the Mount Lofty Ranges, In Drexel J. F. Preiss W. V. and Parker A. J, eds., The Geology of South Australia, Geological Survey of South Australia Bulletin 54, p. 51–105.

Preiss, W. V., 2000, The Adelaide Geosyncline of South Australia and its significance in Neoproterozoic continental reconstruction, Precambrian Research, 100, p. 21–63.

Preiss, W. V., 2010, Geology of the Neoproterozoic to Cambrian Adelaide Geosyncline and Cambrian Delamerian Orogeny, in Korsch, R.J., and Kositcin, N., editors, 2010. South

Australian Seismic and MT Workshop 2010. Geoscience Australia, Record, 2010/10, p. 34-41.

Roy, R. F., Blackwell, D. D., and Birch, F., 1968, Heat generation of plutonic rocks and continental heat-flow provinces: Earth and Planetary Science Letters, 5, p. 1–12.

Sandiford, M., 2003a, Neotectonics of SE Australia and the origin of the intraplate stress field in Skilbeck, C. G. & Hubble, T. C. T. (eds), Understanding Planet Earth; searching for a sustainable future; abstracts of the 15th Australian geological convention, Abstracts - Geological Society of Australia, 59, p. 435.

Sandiford, M., 2003b, Geomorphic constraints on the late Neogene tectonics of the Otway Range, Victoria, Australian Journal of Earth Sciences, 50 (1), p. 69-80.

Sandiford, M., Frederiksen, S. & Braun, J., 2003, The long-term thermal consequences of rifting; implications for basin reactivation, Basin Research, 15 (1), p. 23-43.

Sass, J. H., and Lachenbruch, A. H., 1979, Thermal regime of the Australian Continental Crust. In M.W. McElhinny ed., The Earth: its origin, structure and evolution. Academic Press, London.

Sheard, M. J., 1990, A guide to Quaternary volcanoes in the lower south-east of South Australia, Mines and Energy Review - South Australia, 157, p. 40-50.

Sheard, M. J. & Nicholls, I. A., 1989, 'Mount Gambier sub-province' in Johnson, R.W., Knutson, J. Taylor, S.R., (eds). (1989), Intraplate volcanism in eastern Australia and New Zealand: Cambridge, England, Cambridge University press, p 142.

Smith, B. W. & Prescott, J. R., 1987, Thermoluminescence dating of the eruption at Mt. Schank, South Australia, Australian Journal of Earth Sciences, 34 (3), p. 335-342.

Sprigg, R. C., 1945, Some aspects of the geomorphology of the Mount Lofty ranges, Transactions of the Royal Society of South Australia, 69, Part 2, p. 277-302.

Sprigg, R. C., 1946, Reconnaissance geological survey of portion of the western escarpment of the Mount Lofty ranges, Transactions of the Royal Society of South Australia, 70, Part 2, p. 313-347.

Sprigg, R. C., 1952, The geology of the South-East Province, South Australia, with special reference to Quaternary coast-line migrations and modern beach developments, Bulletin - Geological Survey of South Australia, 29, p. 120.

Sprigg, R. C., 1959, Presumed submarine volcanic activity near Beachport, south-east South Australia, Transactions of the Royal Society of South Australia, 82, p. 195-203.

Sutherland, F. L., 1981, Migration in relation to possible tectonic and regional controls in eastern Australian volcanism, Journal of Volcanology and Geothermal Research, 9 (2-3), p. 181-213.

Sutherland, F. L. & Hollis, J. D., 1982, Mantle-lower crust petrology from inclusions in basaltic rocks in eastern Australia; an outline in Brousse, R. & Lameyre, J. (eds), Magmatology, Journal of Volcanology and Geothermal Research, 14 (1-2), p. 1-29.

Teasdale, J., Pryer, L., Stuart-Smith, P., Romine, K., Loutit, T., Etheridge, M., Shi, Z., Foss, C., Vizy, J. Henley & P. Kyan, D., 2002, 'Otway and Sorrell Basins SEEBASE Project. SRK Consulting (CD ROM).

Torrens Energy Limited, 2008, 780 000 PJ Inferred Resource, Parachilna Project, South Australia. *ASX Announcement 20 August 2008*. Available online at: http://www.asx.com.au/asxpdf/20080820/pdf/31bsp0dcmt4sw0.pdf (first accessed 21 August 2008.)

Turner, S. P., Foden, J. D., and Morrison, R., 1992, Derivation of A-type magma by fractionation of basaltic magma and an example from the Padthaway Ridge, South Australia, Lithos 28, p. 151–179.

van Otterloo, J., 2011, "Newer Volcanics Map," http://vhub.org/resources/845. Accessed May 25 2012.

Vogel, D. C. & Keays, R. R., 1997, The petrogenesis and platinum-group element geochemistry of the Newer Volcanic Province, Victoria, Australia, Chemical Geology, 136 (3-4), p. 181-204.

Wellman, P., 1989, 'Upper Mantle, Crust and Geophysical Volcanology of Eastern Australia' in Johnson, R.W., Knutson, J. & Taylor, S.R., (eds). (1989), Intraplate volcanism in eastern Australia and New Zealand: Cambridge, England, Cambridge University press, p 29–37.

Woodhead, J., Hergt, J., Sandiford, M., & Johnson, W., 2010 The big crunch: Physical and chemical expressions of arc/continent collision in the Western Bismarck arc, Journal of Volcanology and Geothermal Research 190, p. 11–24.

Zielhuis, A. & van der Hilst, R. D., 1996, Upper-mantle shear velocity beneath eastern

Australia from inversion of waveforms from SKIPPY portable arrays, Geophysical Journal International, 127 (1), p. 1-16.

Chapter 3

Heat flow as a mineral exploration tool

A key influence on the magnitude of surface heat flow is the distribution of Heat Producing Elements (HPEs) in the crustal rocks (e.g. McLaren *et al.* 2003). It follows that high spatial resolution surface heat flow mapping can serve as a tool for locating elevated HPE concentrations in the upper crust.

Houseman et al (1989) published surface heat flow data in the Roxby Downs region of South Australia, an area hosting several known IOCG-U (iron oxide copper gold-uranium) deposits, including Australia's largest discovered uranium orebody at Olympic Dam. The data clearly shows a large surface heat flow anomaly corresponding to the Olympic Dam orebody.

Modelling of another IOCG-U orebody – the Prominent Hill deposit close to Olympic Dam – shows that it is likely that there is a surface heat flow anomaly associated with this mineral occurrence. Several companies previously held the exploration license for the Prominent Hill area, but walked away from the tenement following unsuccessful drilling campaigns where no economic mineralization was found. The measurement of surface heat flow, had it been done, would probably have (indirectly) indicated the presence of a proximal heat producing body, and thus the IOCG-U mineralisation that was discovered just 250m away from previous drilling by subsequent explorers.

Matthews & Beardsmore published the following discussion paper in MESA Journal 41 in 2006.

In summary, closely spaced surface heat flow data clearly highlights the location of the Olympic Dam ore body, and would probably have aided previous explorers in the discovery of Prominent Hill.

By being able to detect elevated concentrations of heat producing elements relative to surrounding rocks, anomalies caused by economic mineralization may be found. This points to the value of surface heat flow mapping as a tool for project scale IOCG-U exploration.

Declaration for Thesis Chapter 3

Declaration by candidate

In the case of Chapter 3, the nature and extent of my contribution to the work was the following:

Nature of contribution: Main research, interpretation and preparation of manuscript
Extent of contribution (%): 70%

The following co-authors contributed to the work.

Name:	**Dr Graeme Beardsmore**
Nature of contribution:	**Data processing, modelling**

Candidate's Signature

Date

Declaration by co-authors

The undersigned hereby certify that:

(1) the above declaration correctly reflects the nature and extent of the candidate's contribution to this work, and the nature of the contribution of each of the co-authors.
(2) they meet the criteria for authorship in that they have participated in the conception, execution, or interpretation, of at least that part of the publication in their field of expertise;
(3) they take public responsibility for their part of the publication, except for the responsible author who accepts overall responsibility for the publication;
(4) there are no other authors of the publication according to these criteria;
(5) potential conflicts of interest have been disclosed to (a) granting bodies, (b) the editor or publisher of journals or other publications, and (c) the head of the responsible academic unit; and
(6) the original data are stored at the following location(s) and will be held for at least five years from the date indicated below:

Location(s) **South Yarra, Victoria**

[Please note that the location(s) must be institutional in nature, and should be indicated here as a department, centre or institute, with specific campus identification where relevant.]

Signature 1 

Date **17 May 2013**

Heat flow: a uranium exploration and modelling tool?

Chris G Matthews[1, 2] and Graham R Beardsmore[2, 3]

1 PACE Program, PIRSA 2 School of Geosciences, Monash University 3 Hot Dry Rocks Pty Ltd

Introduction

Heat flow measurements published by Houseman et al. (1989) around the Olympic Dam Mine include six values that form a profile across the Olympic Domain — a NW-trending structure that contains the Olympic Dam Cu–U–Au–Ag–REE orebody, Prominent Hill Cu–U–Au deposit and the recent Carrapateena FeO–Cu–Au discovery (Fig. 1). The heat flow profile shown in Figure 2 demonstrates that there are heat flow anomalies associated with both the enormous Olympic Dam orebody and the satellite Acropolis Cu–U–Au prospect.

Heat flow varies by almost a factor of two across the area with the two highest values associated with Olympic Dam (125 mW/m²) and Acropolis (101 mW/m²). Heat flow drops markedly away from these two points, suggesting that it may correspond to uranium levels in the crust.

Surface heat flow (Q_s) represents the combined flow of thermal energy from two sources: heat flowing from the mantle of the earth (reduced heat flow, q_r), and heat actively generated in the crust by radiogenic elements such as U, Th and K (q_c). Stated simply:

Equation 1 $$Q_s = q_r + q_c$$

The global average heat flow on the continents is around 65 mWm^{-2} (e.g. Pollack et al., 1993), with variations that reflect the age of crustal rocks. The central part of Australia, essentially defined by the existence of Proterozoic crustal rocks, is known as the Central Australian Heat Flow Province (CAHFP; e.g. McLaren et al., 2003), and previously the Central Shield Heat Flow Province (Sass and Lachenbruch, 1979). In this zone, there are numerous published values of heat flow that are well above normal continental heat flow values. These anomalous values are generally attributed to the unusual enrichment of the Australian Proterozoic crust in heat-producing elements such as U, Th and K (McLaren et al., 2003).

It is estimated that the mantle-derived component of heat flow (q_r) in the eastern

Figure 1 *Location of the heat flow profile across the Olympic Dam area. Coloured dots show data points from Houseman et al. (1989), with heat flow values in mWm^{-2}.*

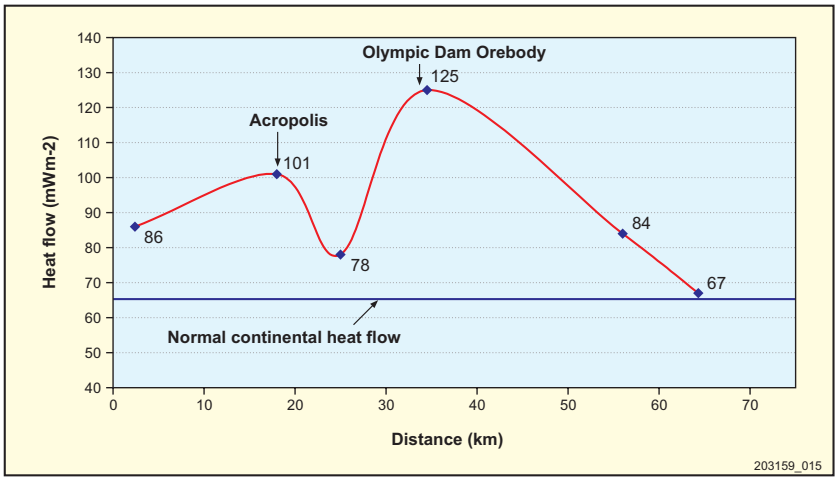

Figure 2 *Heat flow profile across the Acropolis prospect and Olympic Dam deposit, illustrating elevated heat flow values associated with the deposits.*

Gawler Craton is as low as 20–30 mWm^{-2} (Neumann et al., 2000). Therefore, the bulk of the thermal anomalies in the Olympic Dam area must be due to the crustal component (q_c) of heat flow. This has implications for the so-called South Australian Heat Flow Anomaly (SAHFA; Neumann et al., 2000), and also for the possible use of heat flow data as a uranium exploration tool.

The South Australian heat flow data set

There are only 30 heat flow data published for the whole of South Australia with, in many cases, hundreds of kilometres between points (Fig. 3). The data have been derived almost exclusively from mineral exploration drillholes and many of them are of questionable integrity (Cull, 1982). The SAHFA (Neumann et al., 2000) is a poorly constrained region defined loosely by lines of longitude in the central to eastern part of the state, encompassing most of the elevated heat flow values reported for South Australia, as well as a number of low values. The Olympic Dam example illustrates that the SAHFA may be little different to the previously proposed heat flow province, a region where any number of individual heat flow anomalies may be found. The concept is consistent with the idea that the Australian Proterozoic crust has a common value of q_r, and broadly similar tectonothermal history and heat production depth scale (Roy et al., 1968). Infill data to a much greater resolution than currently exists is desperately needed.

Heat flow as a uranium exploration and modelling tool

Although there are heat flow anomalies associated with the Olympic Dam and Acropolis bodies, the data spacing is insufficient to resolve the true wavelength and amplitude of the anomalies. However, the expected shape and amplitude of a heat flow anomaly due to a buried heat source in a conductive medium can be investigated using numerical models. Take, for example, a body with the approximate dimensions of the Prominent Hill deposit to the NW of Olympic Dam. The deposit can be modelled as a rectangular prism of ore 1000 m long in the E–W direction, around 200–300 m wide, and 700 m vertical thickness (Oxiana, 2005). The top of the body is around 150 m below the surface. Assuming typical but conservative radiogenic isotopic abundances for such a body (100 ppm U, 50 ppm Th, 1.7% K_2O), average heat generation is likely to be on the order of 60 µW/m³ throughout the body. A simple model of the effect of such a buried heat source on surface heat flow is shown in plan view in Figure 4, and in profile in Figure 5.

Heat flow anomalies on the order of 2–3 mW/m² can be resolved with precise thermal conductivity and thermal gradient measurements. The model results shown above imply that the thermal anomaly due to a deposit of dimensions similar to Prominent Hill should be detectable at least 250 m beyond the north and south flanks of the mineralised zone, and perhaps as far as 350 m away. The model also shows clearly that surface heat flow increases to a maximum immediately above the ore body.

Typically in iron oxide – copper–gold exploration ventures, gravity and/or magnetic geophysical targets are drilled. On many occasions these holes intersect basement that is altered, but not mineralised. Under these circumstances, with no direct evidence of mineralisation, companies may make the decision to 'walk away' from the prospects. Figure 5 shows that barren holes as far as 350 m away from the Prominent Hill deposit may yield heat flow data that indicate the existence of a nearby radiogenic heat source. Equally importantly, heat flow measurements in barren holes may reveal no thermal anomaly and thus justify the abandonment of a prospect.

Vertical heat flow, **Q**, at depth, z, in a borehole may be calculated from two independent parameters:

Equation 2 $\quad Q_z = \lambda_z \times \beta_z$

where λ_z = thermal conductivity of the rocks at depth z, and

β_z = thermal gradient at depth z

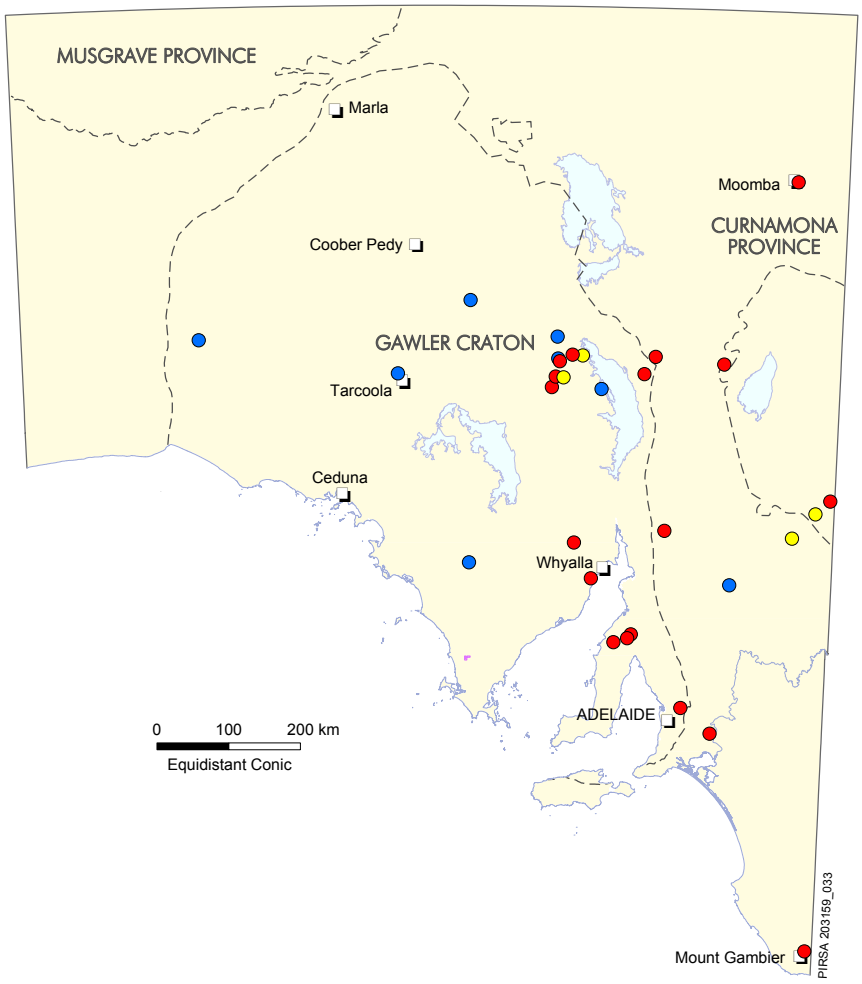

Figure 3 *South Australia's heat flow data set (data from Cull, 1982; Houseman et al., 1989; Beardsmore, 2005). Blue = ≤65 mW/m², yellow = 66–80 mW/m², red = >80 mW/m². Note the apparent heat flow anomaly down the centre of the state, as well as the large areas with no data.*

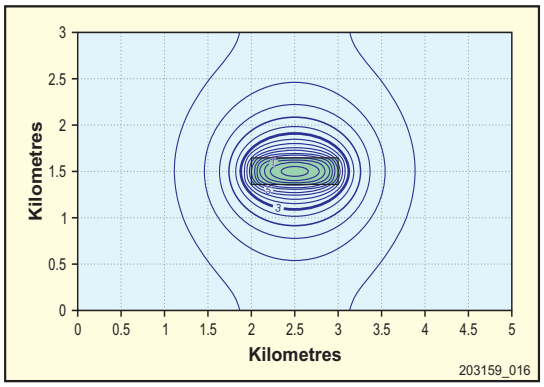

Figure 4 *Modelled surface heat flow anomaly (mW/m²) due to a 60 µW/m³ heat source buried in a thermally conductive medium. The dimensions of the source approximate those of Prominent Hill, as detailed in the text. Contour interval = 0.5 mW/m².*

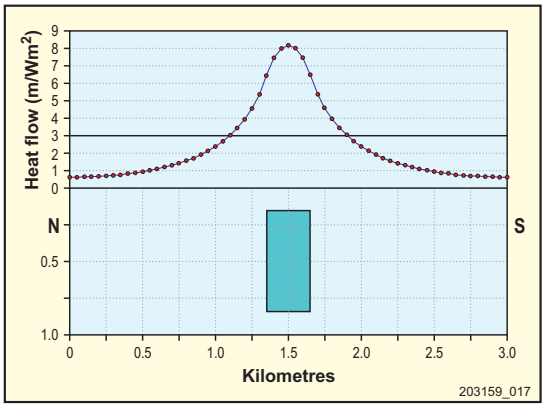

Figure 5 *N–S profile across the surface heat flow anomaly shown in Figure 4. Model cells are 50 × 50 m.*

Thermal conductivity is best measured in a laboratory using fresh core. Application of Equation 2 requires a conductivity measurement over an interval of constant thermal gradient. However, the exact intervals of constant gradient are not known until a temperature log is measured, so ideally the hole should be fully cored. At the very least, substantial sections of continuous core are required.

Thermal gradient is derived from a temperature log, ideally measured to a precision of 0.001 °C at least several weeks after drilling to ensure the hole has regained thermal equilibrium with the surrounding rocks. This may require that the hole be cased to ensure it remains open long enough to measure temperature. Preferably the hole should contain standing water, but a usable log of lesser quality can be obtained from an air-filled hole. The temperature log is used to identify and quantify sections of constant thermal gradient, which are then correlated with thermal conductivity data from the same interval.

We propose that heat flow measurements may be of great use for uranium exploration in a number of ways:

1 To determine whether or not a barren hole may be close to a radiogenic heat source (this requires that 'background' heat flow be known)

2 Heat flow measurements from a number of holes spaced over several hundred metres may reveal a heat flow gradient or 'vector' pointing towards a nearby ore body.

3 The magnitude and shape of a heat flow anomaly observed across an ore body could be modelled to estimate the depth, extent and grade of mineralisation if the base of the body is not known.

4 Old holes and prospects can be reappraised if the holes remain open and core is available.

Note that 'background' heat flow is not uniform in the South Australian crust. The presence or absence of two key basement granite suites — the high heat producing Mesoproterozoic Hiltaba Suite or the relatively low heat producing Palaeoproterozoic Donington Suite — will influence the background heat production and therefore heat flow levels.

Conclusion

Surface heat flow is not constant across South Australia. Rather, it varies across relatively short wavelengths due to active heat sources buried in the shallow crust. This makes heat flow a potential exploration tool for ore bodies, with the ability to *directly detect uranium mineralisation.*

A fully cored and thermally logged borehole can yield valuable information about the thermal regime in the vicinity of the hole. This, in turn, can be related to the likelihood of significant quantities of radiogenic material existing nearby. A series of such boreholes can be used to constrain 3D thermal models of the crust. In addition, a reappraisal of existing holes that did not intersect mineralisation may reveal thermal anomalies suggesting nearby active heat sources.

The eastern Gawler Craton contains several known mineral prospects that could be test sites for heat flow based uranium exploration. These include Marathon South, Titan, Mount Gunson and Carrapateena in the Olympic Domain. In addition, there are large uranium provinces in the Northern Territory, Queensland and Western Australia that are considered to be potentially suitable for this exploration method.

Would the story of the discovery of Prominent Hill in the Olympic Domain have been different if heat flow had been measured in a hole that missed the ore body by just 250 m?

References

Beardsmore, G.R., 2005. Thermal modelling of the hot dry rock geothermal resource beneath GEL 99 in the Cooper Basin. *In: World Geothermal Congress, Antalya, Turkey, 24–29 April, 2005. Proceedings,*

Cull, J.P., 1982. An appraisal of Australian heat-flow data. *BMR Journal of Australian Geology and Geophysics,* 7(1),11-21.

Houseman, G.A., Cull, J.P., Muir, P.M. and Paterson, H.L., 1989. Geothermal signatures and uranium ore deposits on the Stuart Shelf of South Australia. *Geophysics,* 54(2):158-170.

McLaren, S., Sandiford, M., Hand, M., Neumann, N., Wyborn, L. and Bastrakova, I., 2003. The hot southern continent; heat flow and heat production in Australian Proterozoic terranes. *In:* Hills, R.R. and Mueller, R.D. (Eds), Evolution and dynamics of the Australian Plate. *Geological Society of America. Special Paper,* 372:157-167.

Neumann, N., Sandiford, M. and Foden, J., 2000. Regional geochemistry and continental heat flow; implications for the origin of the South Australian heat flow anomaly. *Earth and Planetary Science Letters,* 183(1/2):107-120.

Oxiana Ltd, 2005. Oxiana moves Prominent Hill to full feasibility study, media release, 23 August. Oxiana Ltd, viewed 1/5/2006, <www.oxiana.com.au>.

Pollack, H.N., Hurter, S.J. and Johnson, J.R., 1993. Heat flow from the Earth's interior: analysis of the global data set. *Reviews of Geophysics*, 31(3):267-280.

Roy, R.F, Blackwell, D.D. and Birch, F., 1968. Heat generation of plutonic rocks and continental heat flow provinces. *Earth and Planetary Science Letters,* 5:1-12.

Sass, J.H. and Lachenbruch, A.H., 1979. Thermal regime of the Australian continental crust. *In:* McElhinny, M.W. (Ed.), *The Earth—its origin, structure and evolution.* London American Press, London, pp. 301-351.

For further information contact Chris Matthews, phone +61 8 8278 9497, email <cgmat1@student.monash.edu>.

Chapters 4-6

Heat flow estimates from the South Australian Heat Flow Anomaly

Chapters 4, 5 and 6 are published papers reporting the outcomes of high spatial resolution heat flow studies from three areas within the SA Heat Flow Anomaly. The three studies reveal surface heat flow distributions as complex and varied as the geology of the regions themselves.

All three papers include discussions on the methodology used to collect data and estimate heat flow, and the sources of uncertainty, including specific discussions on the variability of thermal conductivity values within relevant formations. In particular, the need for conductivity measurements from as many randomly selected core samples as possible from each formation is identified. Generally, thermal conductivity estimates are a greater source of error than thermal gradient measurements due to the reliable nature of thermal gradient measurements from water bores and bottom hole temperature estimates (see below).

The thermal conductivity measurements from the Gambier Limestone – the key formation for heat flow estimates from water bores in Chapters 4 and 6 – varied mainly due to two factors: the variable porosity of the limestone and the occurrence of the higher thermal conductivity minerals dolomite and chert in some parts of the formation.

Thermal conductivity values from formations covered within Chapter 5 show generally less variability than the Gambier Limestone, due mainly to the greater age of the sediments from the Torrens Hinge Zone and the general lack of porosity in the formations.

The reliability of estimated bottom hole temperatures (BHT) from petroleum wells – corrected using standard methods such as the Horner Plot (Lachenbruch & Brewer, 1959) or directly measured during drill stem tests (DST), repeat formation tests (RFT), cased hole tests (CHT), or production logging tests (PLT) of formation fluids (Beardsmore & Cull, 2001; see Chapters 4 and 6 for further discussions) – was tested by comparison between coincident water bore and petroleum wells. Two of the petroleum wells in the study area for Chapter 6 were converted into groundwater observation wells after drilling. This enabled a comparison between heat flow estimated from petroleum and groundwater wells at the same location. The comparison (below) shows reasonable agreement between the two values at each of the two locations. The comparison supports the viability of using relatively shallow water wells to calculate heat flow values, but also suggests that BHT estimates from petroleum wells are compatible with direct measurements from shallow water bores.

Well Names Petroleum/Water	Heat flow from petroleum well (mW/m^2)	Heat flow from water well (mW/m^2)
Kentgrove 1/MAC 57	74 ± 16.3	73 ± 8.6
Burrungule 1/BEN 13	65 ± 3.3	60 ± 7.1

All three of the studies assume that the thermal regimes are dominantly conductive. The bases for this assumption in each of the areas are discussed in the relevant Chapters. Despite the southeast of South Australia being a region where advection is a possibility – due particularly to either lateral groundwater flow in shallow aquifers or active hydrothermal flow due to recent volcanism – no direct evidence was found for such activity.

While the 10-15 km spacing of heat flow estimates in the study areas may not be close enough to detect anomalous shallow crustal heat production the size of ore bodies, it will pick up lithosphere-scale anomalies that extend to depths and widths greater than 10 km.

Heat flow data published by Matthews & Beardsmore (2007; Chapter 4) were collected in a region of South Australia that spans between the southern Murray Basin and the northern margin of the Otway Basin. The paper shows that surface heat flow magnitude is non-uniform and highly variable over relatively short lateral distances. Chapter 7 of this thesis shows modelling attempts that seek to explain why heat flow data exhibit such variation in this region. The new heat flow values in this paper range between 42 and 123 mW/m^2. A 40 km x 15 km zone of elevated heat flow is identified along the northern margin of the Otway or Gambier Sub-basin. This may correspond to the occurrence of Delamerian granitoid units of the Padthaway Ridge (see Chapters 2 and 7).

Heat flow data published by Matthews (2009; Chapter 5) were collected in the Torrens Hinge Zone (THZ), a region of South Australia that marks the transition between the eastern margin of the Archaean to Mesoproterozoic Gawler Craton Olympic Domain and the western edge of the Adelaide Rift Complex.

Matthews et al (2013; Chapter 6) added 34 new surface heat flow data points to those published by Matthews & Beardsmore (2007) in the southeastern corner of South Australia (Chapter 4).

All three of the study areas fall entirely within the bounds of the Central Australian heat Flow Province as defined by McLaren et al (2003), and the South Australian Heat Flow Anomaly of Neumann et al (2000). The detailed distribution of surface heat flow in the areas had not previously been examined, and each area contained only a few widely spaced surface heat flow estimates. The studies presented in the papers tested the concept that the SAHFA is a zone of blanket high heat flow.

The tectonothermal history and resulting current thermal state of the southern Murray and western Otway Basins (Chapter 4) have been influenced by several events that spanned a time period from the Proterozoic to Recent. These events included the creation of Proterozoic sub-continental lithospheric mantle, Palaeozoic deformation and associated granite emplacement, Mesozoic-Palaeogene rifting between Australia and Antarctica, Neogene-recent ongoing compressive tectonic activity, and (in the Otway basin) Pliocene-Recent ongoing basaltic volcanism.

The study area for Chapter 5 is also geologically complex. It sits on the eastern margin of the Archaean to Mesoproterozoic Gawler Craton, itself being the eastern edge of the Gondwana Supercontinent. Section 2.3.1 of this thesis described the geological framework and history of the Torrens Hinge Zone (THZ), which includes its cratonic beginnings with accumulations of high heat producing elements, a major rifting event in the Neoproterozoic, a major orogenic event in the early Palaeozoic, and now the Spriggs Orogeny in the Tertiary-Recent (Section 2.2.4).

Geological and conductive heat flow principles implied that the THZ is likely to be a region of high average geothermal gradients and thus prospective for Engineered Geothermal Systems (EGS). A heat flow drilling program designed to test the idea returned results that validated this hypothesis (Chapter 5).

The study area of Chapter 6 contained just one previously published surface heat flow value (92 mW/m^2; Cull 1982) located close to the volcanic centres near Mount Gambier. The results of the study in this thesis are very significant for interpreting the broader tectonic evolution and current thermal state of the region, in particular investigating whether the Newer Volcanics Province (NVP) of eastern Australia has an associated surface heat flow signature. This is discussed further in Chapter 7.

There are 18 volcanic vent locations in southeast South Australia. Most of them are in the Mount Burr Range area west of Mount Gambier, with the remainder at Mounts Gambier and Schank. The reported ages of the South Australian NVP volcanoes range from 20,000 – 1,000,000 years for the Mount Burr Volcanics (Sheard and Nicholls, 1989), and Holocene for Mount Gambier and Mount Schank.

The study presented in the Chapter 6 revealed that, while there is slightly higher than average surface heat flow around some of the volcanic centres, heterogeneous basement heat production is a more likely explanation than remnant magmatic heat for the overall distribution of surface heat flow. There are no observed heat flow anomalies greater than 10 mW/m^2 associated with the NVP, and the distribution of heat flow in southeast South Australia is most simply explained by non-volcanic phenomena. Such a result is consistent with heat flow analyses around hot spot volcanism in other parts of the world (Stein & Von Herzen 2007).

The high spatial resolution of the three heat flow studies gives comfort to the notion that the heat flow anomalies observed are not due to heterogeneous mantle (reduced) heat flow. The anomalies observed can be explained in large part by the role of lateral variations in crustal heat production and thermal conductivity contrast.

The paper in Chapter 4 was published in *Exploration Geophysics* in 2007, Chapter 5 was published in *Exploration Geophysics* in 2009, and Chapter 6 was published in *Exploration Geophysics* in 2013.

References

Cull, J. P., 1982, An appraisal of Australian heat-flow data, BMR Journal of Australian Geology and Geophysics, 7, p. 11–21.

Matthews, C. G., and Beardsmore, G. R., 2007, New heat flow data from southeastern South Australia, Exploration Geophysics, **38**, p. 260–269.

Matthews, C. G., 2009, Geothermal energy prospectivity of the Torrens Hinge Zone: evidence from new heat flow data, Exploration Geophysics, 40, p. 288–300.

Matthews, C. G., Beardsmore, G. R., Driscoll, J. and Pollington, N., 2013, Heat flow data from the southeast of South Australia: distribution and implications for the relationship between current heat flow and the Newer Volcanics Province, Exploration Geophysics, 44 (2), p. 133–144.

McLaren, S., Sandiford, M., Hand, M., Neumann, N., Wyborn, L., and Bastrakova, I., 2003, The hot southern continent, heat flow and heat production in Australian Proterozoic terranes, Geological Society of Australia, Special Publication, 22, p. 151–161.

Neumann, N., Sandiford, M., and Foden, J., 2000, Regional geochemistry and continental heat flow; implications for the origin of the South Australian heat flow anomaly, Earth and Planetary Science Letters, 183, p. 107–120.

Sheard, M. J. & Nicholls, I. A., 1989, 'Mount Gambier sub-province' in Johnson, R.W., Knutson, J. Taylor, S.R., (eds). (1989), Intraplate volcanism in eastern Australia and New Zealand: Cambridge, England, Cambridge University press, p 142.

Stein, C. A. & Von Herzen, R. P., 2007, Potential effects of hydrothermal circulation and magmatism on heatflow at hotspot swells, The Geological Society of America, Special paper 430, 2007.

Declaration for Thesis Chapter 4

Declaration by candidate

In the case of Chapter 4, the nature and extent of my contribution to the work was the following:

Nature of contribution: Main research, data collection and processing, interpretation and preparation of manuscript
Extent of contribution (%): 80%

The following co-authors contributed to the work.

Name: **Dr Graeme Beardsmore**
Nature of contribution: **Data processing, modelling**

Candidate's Signature

Date

Declaration by co-authors

The undersigned hereby certify that:

(1) the above declaration correctly reflects the nature and extent of the candidate's contribution to this work, and the nature of the contribution of each of the co-authors.
(2) they meet the criteria for authorship in that they have participated in the conception, execution, or interpretation, of at least that part of the publication in their field of expertise;
(3) they take public responsibility for their part of the publication, except for the responsible author who accepts overall responsibility for the publication;
(4) there are no other authors of the publication according to these criteria;
(5) potential conflicts of interest have been disclosed to (a) granting bodies, (b) the editor or publisher of journals or other publications, and (c) the head of the responsible academic unit; and
(6) the original data are stored at the following location(s) and will be held for at least five years from the date indicated below:

Location(s) **South Yarra, Victoria**

[Please note that the location(s) must be institutional in nature, and should be indicated here as a department, centre or institute, with specific campus identification where relevant.]

Signature 1 

Date **17 May 2013**

CSIRO PUBLISHING
www.publish.csiro.au/journals/eg *Exploration Geophysics*, 2007, **38**, 260–269

New heat flow data from south-eastern South Australia*

Chris Matthews[1,3] Graeme Beardsmore[1,2]

[1]School of Geosciences, Monash University, VIC 3800, Australia.
[2]Hot Dry Rocks Pty Ltd, PO Box 871, South Yarra, VIC 3141, Australia.
[3]Corresponding author. Email: chris.matthews@torrensenergy.com

Abstract. Heat flow has been measured in south-east South Australia at a spatial resolution greater than previously available. The study area contains the Southern Murray Basin, Padthaway Ridge, and Western Otway Basin. An extensive network of groundwater observation wells across the study area was used, along with several petroleum wells in the Otway Basin, to measure thermal gradients and calculate 24 new heat flow values.

Geothermal gradients were either measured directly using a cable, winch, and thermistor in cased or open holes with standing water, or by estimating average geothermal gradients from petroleum well completion temperature data. Thermal conductivity values were measured directly on existing core samples using a divided bar apparatus.

A map constructed from the measured values reveals a heat flow dataset that is non-uniform and variable over relatively short distances. Measured heat flow values range between 42 and 123 mW/m^2. In particular, a 40 km long, 15 km wide zone of elevated heat flow is identified along the northern margin of the Otway or Gambier Sub-basin that may correspond to the occurrence of Delamerian granitoids units of the Padthaway Ridge. High-resolution surface heat flow mapping provides valuable data for further research into the tectonothermal evolution of south-east Australia.

Key words: Australia, heat flow, thermal gradient, thermal conductivity, Murray Basin, Otway Basin, Delamerian Fold Belt, Padthaway Ridge, Newer Volcanics Province.

Introduction

The state of South Australia, with an area of almost one million square kilometres, has a total of just 30 published heat flow data points (Figure 1). Temperature distribution within the Earth's crust is a 'potential field', equivalent in many ways to gravity or magnetism. As with gravity anomalies, the amplitude and wavelength of surface heat flow anomalies are directly related to the magnitude and depth of the heat source causing the anomaly. An intra-crustal heat source produces a surface heat flow anomaly with a wavelength the same order of magnitude as the depth of burial. It follows that heat flow data spaced hundreds of kilometres apart are not able to delineate crustal heat sources. In fact, heat flow data should be collected at a maximum spacing of ~10–15 km if crustal heat sources are to be detected.

The aim of this research project has been to measure surface heat flow values across the south-eastern corner of South Australia, an area with a complex tectonothermal history. The small number of existing heat flow data in the region is indicative of the resolution of this dataset across the state. Prior to this study, only one published heat flow data point existed, in the far south of the region near the volcanic centre of Mount Gambier (Figure 1).

The study area has undergone several stages of geological activity, including the following events (Figure 2)

a) The existence of Proterozoic Sub-continental Lithospheric Mantle (McBride et al., 1996)
b) The complex tectonic and magmatic event history of the Delamerian Orogeny during the Cambrian–Ordovician (e.g. Jenkins and Sandiford, 1992)
c) Post-Delamerian emplacement of variably heat producing A-type granitoids, including the Padthaway Ridge granites (Turner et al., 1992)
d) Mesozoic to Palaeogene rifting between Australia and Antarctica, creating the Otway Basin, including the Gambier Sub-basin (e.g. O'Brien et al., 1994; Boult and Hibburt, 2002)
e) Development of the Palaeozoic to Neogene intracratonic, overlapping Murray, Berri and Nadda Basins (Rogers et al., 1995)
f) Miocene–Recent ongoing compressive neotectonic activity with associated uplift (Sandiford, 2003)
g) Pleistocene–Recent, ongoing, basaltic volcanism (Sheard, 1990)

Basement geology is dominated by metamorphosed sediments (Delamerian Fold Belt) and syn- and post-tectonic magmatic bodies (Padthaway Ridge). The basement is overlain by Jurassic to Tertiary basin sediments of the Gambier Sub-basin and Murray Basin. The Neogene to Quaternary has seen the onset of compressive neotectonics and basaltic volcanism. The current surface heat flow regime is therefore of considerable interest in light of the complex geological history. For example, do the recent volcanic and neotectonic events have a thermal signature? Do the high heat producing A-type granites contribute significant heat flow to the crust? Is there a detectable change in thermal conditions across the margin of the Otway Basin that may be related to Palaeozoic or Mesozoic tectonic events?

Current status of the SA heat flow dataset

Currently the heat flow dataset for South Australia is represented by 30 data points spread widely across the state (Figure 1). The

*Presented at the Australian Earth Science Convention, July 2006.

 10.1071/EG07028 0812-3985/07/040260

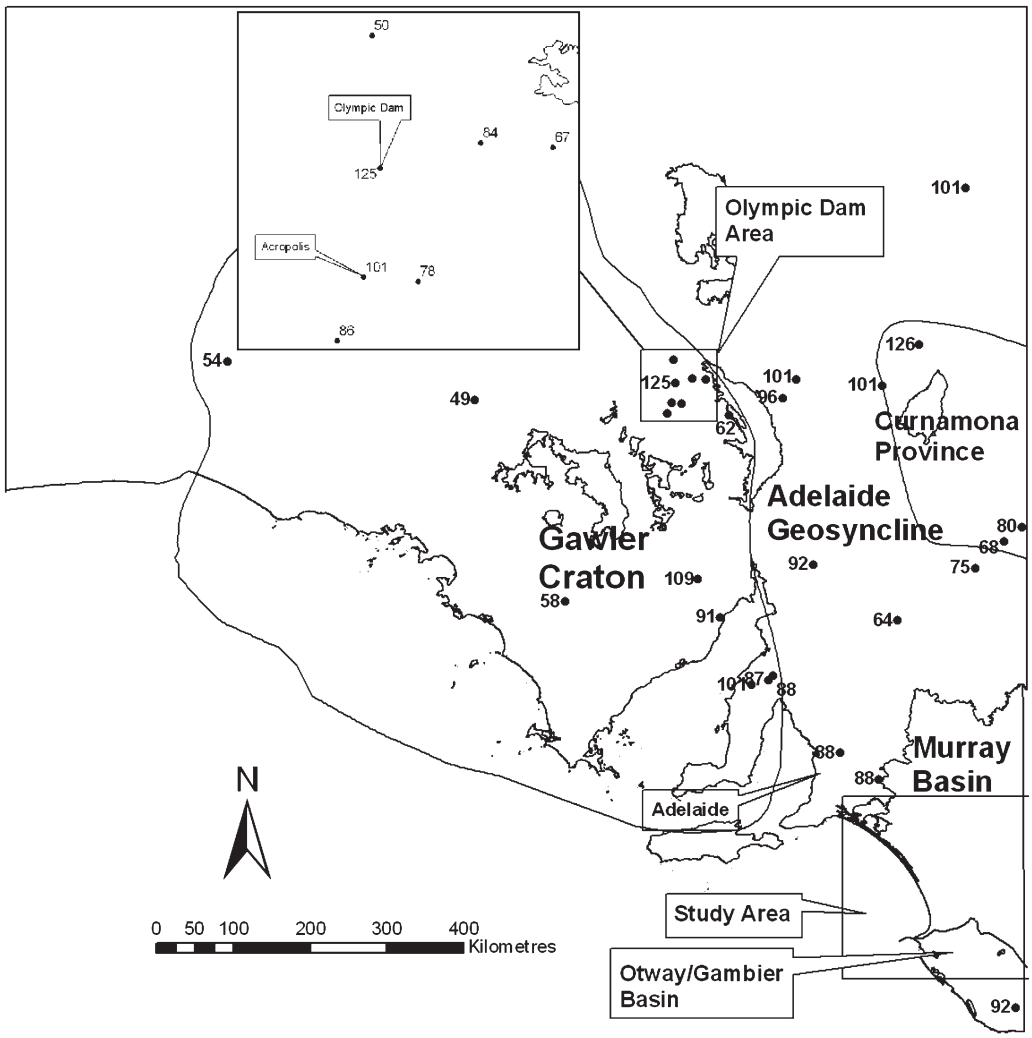

Fig. 1. The current status of the South Australian heat flow dataset (data from Cull, 1982; Houseman et al., 1989; and Beardsmore, 2005) superimposed on the major geological elements of the State. The study area is outlined, containing no previous data. The enlargement of the Olympic Dam area shows the large variation in surface heat flow corresponding to uranium anomalies in basement rocks.

current dataset enables only the most basic understanding of the SA heat flow regime, and requires sweeping assumptions to be made about the nature of the heat flow between data points. The data have been derived almost exclusively from mineral exploration drillholes and the integrity of many values has been described as 'questionable' (Cull, 1982). Mineral drillholes commonly target geological or geophysical anomalies, so in many cases heat flow data may be from basement that is thermally anomalous.

A large number of drillholes exist in the Olympic Dam area. Houseman et al. (1989) made heat flow measurements in several holes in the area, not all of which were over ore bodies (Figure 1). The dataset revealed that heat flow is variable by a factor of more than two in the Olympic Dam area, and that the highest values correspond to the locations of the Olympic Dam and Acropolis ore bodies, which represent intracrustal radiogenic heat sources. It is estimated that crustal heat production in the Eastern Gawler Craton, the setting for the Olympic Dam deposit, accounts for at least 75% of the observed surface heat flow (Neumann et al., 2000). This significant contribution of crustal heat production has implications when considering the representative nature of the current heat flow dataset. It is unlikely that heat flow varies in a gradual fashion between the current heat flow data points, but more likely that there will be short wavelength variations depending on basement geology. There is a need for higher resolution heat flow data to resolve crustal-scale features.

Heat flow fundamentals

Heat flows through the Earth mainly by conduction and advection. Conduction is the movement of energy through solid surfaces by the transfer of kinetic energy between particles (e.g. Beardsmore and Cull, 2001). Advection involves the mass transport of heat associated with the physical motion of materials and includes the process of convection, one of the key driving mechanisms of tectonics. Conduction is assumed to be the dominant mode of heat transport in the crust, while convection dominates in the mantle. The magnitude of vertical conductive heat flow, Q_0, at the Earth's surface can be calculated (e.g. Beardsmore and Cull, 2001):

$$Q_0 = \lambda_z \beta_z + \sum A, \qquad (1)$$

where λ_z = thermal conductivity ($W.m^{-1}.K^{-1}$) at depth z, a physical property of the rocks; β_z = vertical geothermal gradient ($K.m^{-1}$) at depth z, the rate of change in temperature per metre depth; $\sum A$ = total rate of internal heat generation ($W.m^{-3}$) between the surface and depth z, heat produced inside the system. Average conductive heat flow is calculated from measurements

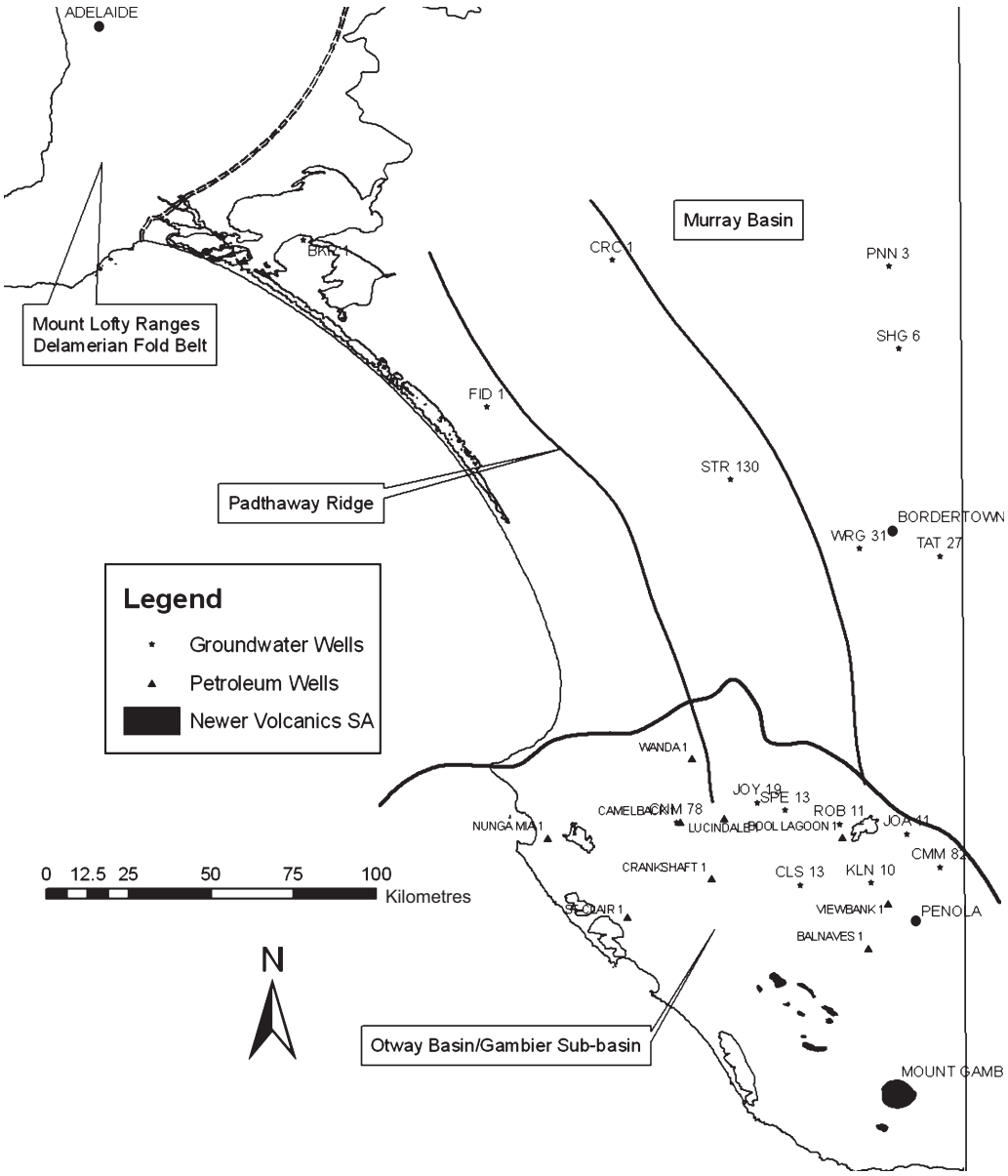

Fig. 2. The tectonic framework of the study area with locations of data collection points located. Basement geology is dominated by Cambro-Ordovician orogenesis of Neoproterozoic sediments (Delamerian Fold Belt), as well as the syn- and post-tectonic magmatism (Padthaway Ridge). This basement is overlain by Jurassic to Tertiary basin sediments of the Gambier Sub-basin and Murray Basin. The Neogene to Quaternary has seen the onset of compressive neotectonics and enigmatic basaltic volcanism. Note the higher density of groundwater wells in the Gambier Sub-basin. There are no petroleum wells with useful temperature data in the Murray Basin.

of λ_z and β_z over several intervals within a borehole, or over one interval by assuming negligible $\sum A$.

The combined thermal conductivity of adjacent formations depends on the configuration of the formations with respect to the flow of heat (e.g. Beardsmore and Cull, 2001). If two formations are flat-lying and heat is flowing vertically (the usual case), the combined thermal conductivity is the harmonic mean of the two. If, however, heat is flowing parallel to the boundary between two formations, the combined thermal conductivity is arithmetic mean of the two. Generally, the average thermal conductivity of a column of rock is determined from the harmonic mean of the conductivities of the individual formations.

Data collection and heat flow calculations

New heat flow values in this study are derived from data collected from a series of groundwater observation bores and petroleum exploration wells (Figure 2). In making our measurements, we assumed that the study area is in a purely conductive thermal regime. Future work may show this assumption to be flawed, but at present we believe it reasonable. Although there are proximal volcanic centres with activity possibly as recent as 5000 years ago (Sheard, 1990), there is no evidence of active hydrothermal convection systems associated with them. Harder to discount is the possibility of a thermal disturbance due to water flowing through shallow aquifers. Many of the boreholes we examined were drilled to monitor ground water, and so terminated in aquifers. These aquifers could affect the local thermal gradient if they have a significant vertical component of fluid flow close to the borehole. For example, rapid rise of fluid up a fault conduit and into a horizontal aquifer could raise the thermal gradient above the aquifer relative to below. Our interpretations of the observed thermal gradients assume that this does not occur anywhere in the study region.

The standing water level and salinity of groundwater aquifers in south-east South Australia are regularly monitored through a network of bores called 'Obswells'. These cased and capped boreholes remain undisturbed between quarterly salinity and level readings. We utilised this network to measure geothermal gradients to a maximum depth of 270 m. Geological and geophysical data enabled us to determine lithological variation in each hole. The area is also prospective for petroleum, and several deeper exploration boreholes have been drilled. We extracted stratigraphic and temperature data from the well completion reports of these bores.

Thermal gradient is the rate of change in temperature with depth, so a gradient measurement inherently requires a minimum of two temperature measurements at different depths. We first collected a temperature log (e.g. Figure 3) from within each water bore by measuring temperature at discrete depth intervals (1–2 m) from the surface to the bottom of the hole. Temperatures were measured to a precision of ±0.001°C and an absolute accuracy of ±0.01°C using a thermistor probe on the end of 1000 m of cable, calibrated between 15 and 55°C. Depth was determined to within ± 0.02 m using a mechanical trip meter on the borehole collar. As illustrated in Figure 4, the geothermal gradients vary with lithology. Heat flow remains constant across a geological boundary (a requirement of the law of conservation of energy) so according to equation 1 there is an inverse relationship between geothermal gradient and thermal conductivity. Where a rock is less conductive there is a higher geothermal gradient, and vice versa. The product of the two variables should be consistent between discrete lithostratigraphic units.

For nine petroleum wells in the study area, equilibrium bottom hole temperatures (eBHT) were estimated from data in well completion reports. This was achieved through Horner Plot correction (Lachenbruch and Brewer, 1959) of measured BHTs (e.g. Figure 5) and temperatures collected during drill stem tests (DST) of formation fluids (Beardsmore and Cull, 2001). An average geothermal gradient was determined for each drillhole using eBHT and the average surface temperature (from Bureau of Meteorology website: www.bom.gov.au).

The thermal conductivity of a rock is a complex function of the properties of its constituent grains and pore fluids. Typical pore fluids are about an order of magnitude less conductive than typical mineral grains, so porosity has a dominant effect on the conductivity of the whole rock (e.g. Beardsmore and Cull, 2001). Geological formations with relatively homogenous mineralogy and porosity have relatively constant thermal conductivity.

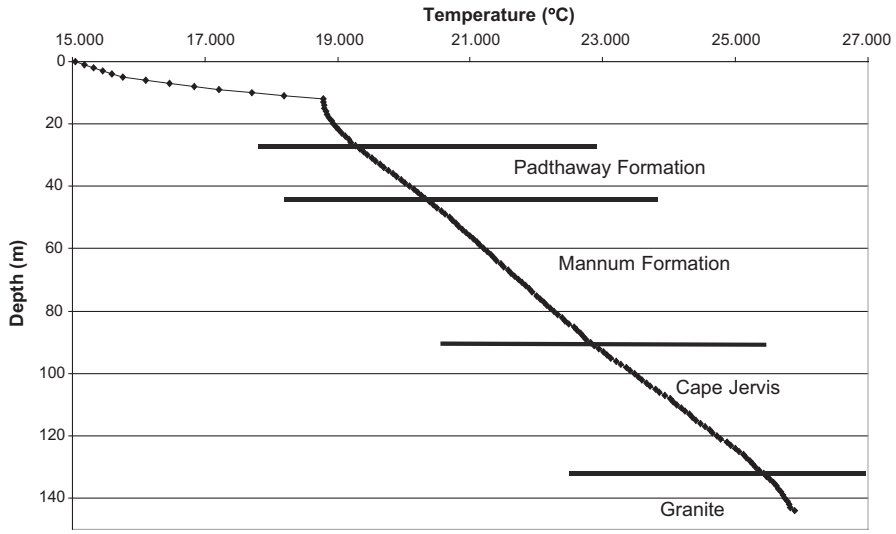

Fig. 3. The measured geothermal gradient from groundwater well BKR 1 (see Figure 2 for location). There is a distinct change in gradient as the profile passes between strata.

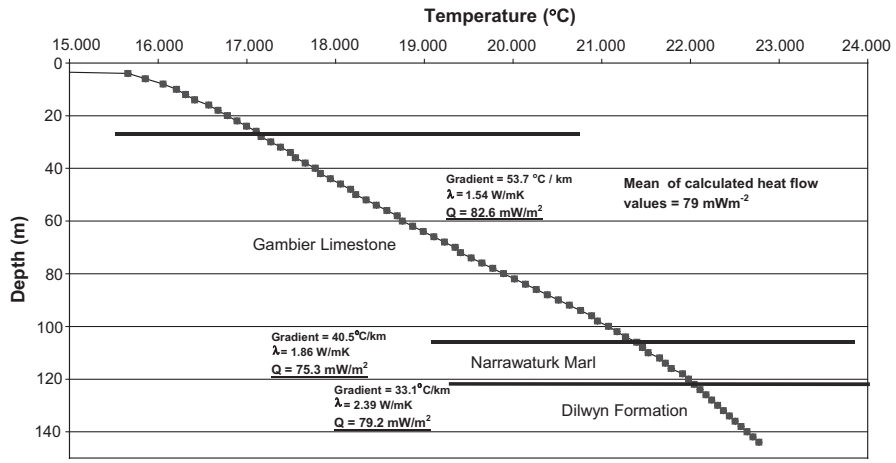

Fig. 4. Temperatures measured in groundwater well JOY 19 (see Figure 2 for location). There is strong agreement between estimated heat flow values, and the arithmetic mean of these estimates has been used to arrive at the final value for heat flow.

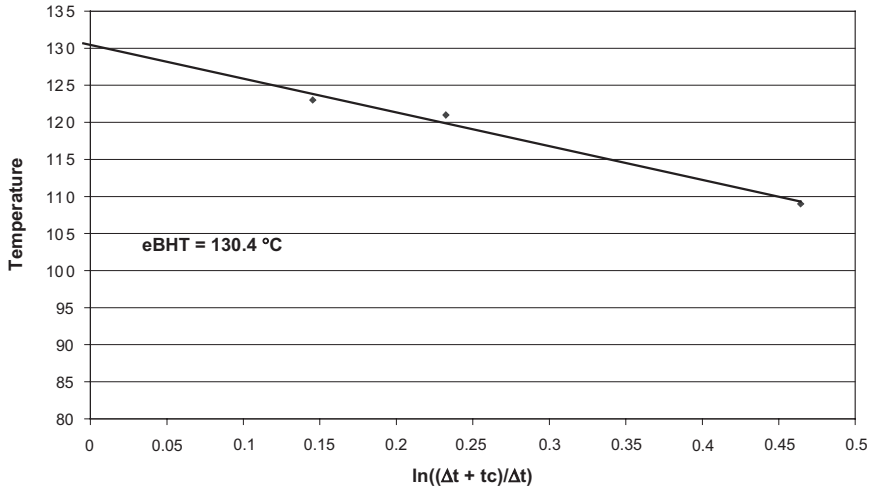

Fig. 5. Horner Plot from petroleum well St Clair 1 (see Figure 2 for location). Uncorrected bottom hole temperatures are used to estimate the true bottom hole temperature (eBHT).

However, thermal conductivity might vary markedly within formations displaying significant heterogeneity in porosity or mineralogy.

Our aim was to characterise the bulk thermal conductivity of each geological formation encountered in our study. Ideally, in order to achieve this goal, thermal conductivity should be measured on several random samples from each formation sufficient to derive a statistical mean and variance for the natural range of values. Three samples might be sufficient for a homogenous formation, whereas a much larger number may be required for heterogeneous formations.

In practice, it is difficult to access sufficient quantities of core material to fully characterise all formations. Core of specific formations is often very limited, or available from only one or two boreholes. In many cases, no core is available at all. Thermal conductivity can still be measured on available core, and the results statistically treated to derive mean values and variances, but these variances do not take into account uncertainties arising from possible lateral or vertical facies variation. This is a limitation on all heat flow measurements that rely on thermal conductivity measurements from previously collected core, and needs to be kept in mind when reviewing the results of this study.

For consolidated material such as core samples or hand specimens, the use of a divided bar apparatus is the best method for measuring λ. This involves the application of a constant thermal gradient across a sample of unknown thermal conductivity in series with materials of known thermal conductivity. Heat flow is measured across the known material and used to determine the conductivity of the test sample.

We measured the thermal conductivity of core samples from 14 formations, and the results are presented in Table 1. The thermal conductivity value is typically the dominant source of uncertainty in calculating heat flow, with a much higher level of confidence in the measured thermal gradients. Thermal conductivity results from some geological formations have a large statistical variance (Table 1). This translates into lower confidence, or larger uncertainties, in heat flow estimates derived from these values. In particular, the various units of the Gambier Limestone, and lithological variations within those units, show a range of thermal conductivities. Achieving confidence in the values for the Murray Basin sediments was also difficult due to large lateral facies variation across the Basin and the small number of available core samples.

Table 1. Thermal conductivity values measured using a divided bar apparatus in most cases the measurements were repeated three times, with final figures taken from the harmonic mean of measured values. A full summary of thermal conductivity measurements is in the appendix.

Rock Unit	λ_{av} (W/mK)	+/−
Newer Volcanics Vesicular lava	1.66	±0.04
Newer Volcanics Vesicular lava	1.50	±0.03
Gambier Limestone Green Point Member Unit 1	1.52	±0.03
Gambier Limestone Green Point Member Unit 1	2.08	±0.04
Gambier Limestone Green Point Member Unit 1	2.18	±0.04
Gambier Limestone Green Point Member Unit 2	1.25	±0.02
Gambier Limestone Green Point Member Unit 2	1.43	±0.03
Gambier Limestone Green Point Member Unit 2	1.20	±0.02
Gambier Limestone Green Point Member Unit 3	1.15	±0.02
Gambier Limestone Green Point Member Unit 3	1.24	±0.02
Gambier Limestone Green Point Member Unit 4	1.62	±0.02
Gambier Limestone Green Point Member Unit 4	1.49	±0.03
Gambier Limestone Green Point Member Unit 4	1.52	±0.02
Gambier Limestone Camelback Member	1.51	±0.03
Gambier Limestone Camelback Member	1.46	±0.03
Gambier Limestone Camelback Member	2.39	±0.04
Gambier Limestone Greenways Member	2.10	±0.04
Gambier Limestone Greenways Member	1.53	±0.03
Gambier Limestone Greenways Member	1.65	±0.03
Gambier Limestone Greenways Member	1.83	±0.03
Dilwyn Formation Clay	1.08	±0.03
Dilwyn Formation Clay	1.28	±0.03
Dilwyn Formation Clay	1.22	±0.03
Dilwyn Formation Sandstone	2.39	±0.15
Mannum Formation Limestone	1.43	±0.03
Mannum Formation Limestone	1.33	±0.03
Narrawaturk Marl	1.86	±0.12
Buccleuch Formation	1.08	±0.03
Buccleuch Formation	1.93	±0.04
Geera Clay	0.85	±0.02
Ettrick Formation	0.68	±0.01
Delamerian Granite	2.89	±0.06
Delamerian Granodiorite	2.95	±0.04
Delamerian Granite	2.79	±0.06
Delamerian Granite	2.84	±0.06
Kanmantoo Schist	2.95	±0.06
Kanmantoo Schist	3.37	±0.08

For the groundwater observation bores, heat flow was estimated for each stratigraphic layer. In most bores this resulted in two or three independent estimates of heat flow (e.g. Figure 4).

Where estimated values of heat flow agreed closely, a mean value was calculated for the bore. Where values were dissimilar, heat flow values were assigned based on the conductivity intervals with the highest confidence.

For the petroleum wells, laboratory conductivity values were assigned based on stratigraphic profiles in well completion reports. Heat flow was calculated from the average geothermal gradient and harmonic mean thermal conductivity.

Results

In total, nine petroleum well and 15 groundwater observation wells were analysed, and a total of 24 new heat flow data points were derived for South Australia (Table 2, Figure 6). These new data increase the size of the entire South Australian dataset from 30 to 54 points. The uncertainties in the heat flow estimates presented in Table 2 depend on the uncertainty of the thermal conductivity. Where heat flow was derived from gradient and conductivity from a single formation, the percentage uncertainty in the heat flow value is the same as for the thermal conductivity value. When more than one formation is averaged (when heat flow estimates from different formations fall within one standard deviation of each other), the uncertainty in the heat flow value is the arithmetic mean percentage uncertainty divided by the square root of the number of formations used.

Discussion and conclusions

The relatively high spatial resolution of the new heat flow data reveal a zone of high heat flow that appears to correspond approximately with the margin of the Gambier Sub-basin. Heat flow is low to medium elsewhere in the study area, with one high measurement close to the eastern margin of the Mount Lofty Ranges (Figure 6).

Table 2a. A summary of all measured heat flow values from this study.

Table 2a summarises the heat flow measurements from water wells. The uncertainty in single heat flow estimates was calculated from the uncertainty in the average thermal conductivity of the lithologies in each drillhole, while where more than one estimate was made the uncertainty is the standard deviation of the estimates.

Hole ID	Basin	Hole Depth	Interval (from–to)	λ (W/mK)	Thermal gradient (°C/km)	Q_s estimate	Final Q_s	+/−
CLS 13	Gambier	270	40–170	1.54	43.2	66.5	**58**	12
			232–270	1.80	27.6	49.7		
CMM 82	Gambier	130	70–94	1.19	56.0	66.7	**65**	3
			94–130	2.39	26.4	63.1		
JOA 11	Gambier	130	40–78	1.54	36.6	56.4	**58**	2
			78–130	1.80	33.0	59.3		
JOY 19	Gambier	144	26–106	1.54	53.7	82.6	**79**	4
			106–122	1.86	40.5	75.3		
			122–144	2.39	33.1	79.2		
KLN 10	Gambier	214	40–132	1.54	40.6	62.5	**62**	1
			158–232	1.80	34.4	61.9		
ROB 11	Gambier	136	20–114	1.54	63.3	97.5	**98**	22
SPE 13	Gambier	148	40–114	1.54	61.0	94.0	**87**	6
			114–130	1.86	45.6	84.7		
			136–148	2.39	34.2	81.7		
BKR 1	Murray	144	37–86	1.38	55.7	76.9	**89**	17
			135–144	2.87	35.3	101.4		
CRC 1	Murray	121	85–93	1.08	62.9	67.9	**68**	1
FID 1	Murray	122	43–71	1.38	53.9	74.4	**75**	12
			71–84	1.08	69.8	75.4		
PNN 3	Murray	104	74–104	1.38	46.1	63.6	**64**	3
SHG 6	Murray	220	100–173	1.38	53.1	73.3	**73**	3
STR 130	Murray	101	53–92	1.38	30.4	41.9	**42**	2
TAT 27	Murray	170	61–110	1.38	56.7	78.2	**79**	1
			130–144	1.93	41.4	80.0		
WRG 31	Murray	142	53–73	1.38	49.4	68.17	**68**	3

Table 2b. A summary of heat flow data from petroleum wells.

Hole ID	Basin	Hole Depth	Estimated surface T (°C)	eBHT (°C)	Method	Depth	Total Hole Depth	B_{ave} (°C/km)	λ_{ave} (W/mK)	Q_s	+/−
Lucindale-1	Gambier	748	16.0	61.67	DST	748	979.6	61.1	2.01	**123**	10
Balnaves-1	Gambier	2874	16.0	115.88	Horner	2874	2874	33.9	1.97	**69**	6
Viewbank-1	Gambier	2510	16.0	100.4	Horner	2510	2510	33.6	2.12	**72**	6
Crankshaft-1	Gambier	2535	15.5	98.8	DST	2494	2535	33.4	2.11	**70**	6
St Clair-1	Gambier	3284	16.0	130.45	Horner	3284	3284	34.8	2.05	**77**	6
Nunga Mia-1	Gambier	2648	16.0	103.8	Horner	2648	2648	33.2	1.92	**64**	5
Bool Lagoon-1	Gambier	810	16.5	50.3	Horner	810	810	41.7	2.09	**88**	7
Camelback-1	Gambier	1783	16.0	89	Horner	1783	1783	40.9	2.41	**99**	9
Wanda-1	Gambier	678	16.0	45.7	Horner	678	678	43.8	2.25	**99**	8

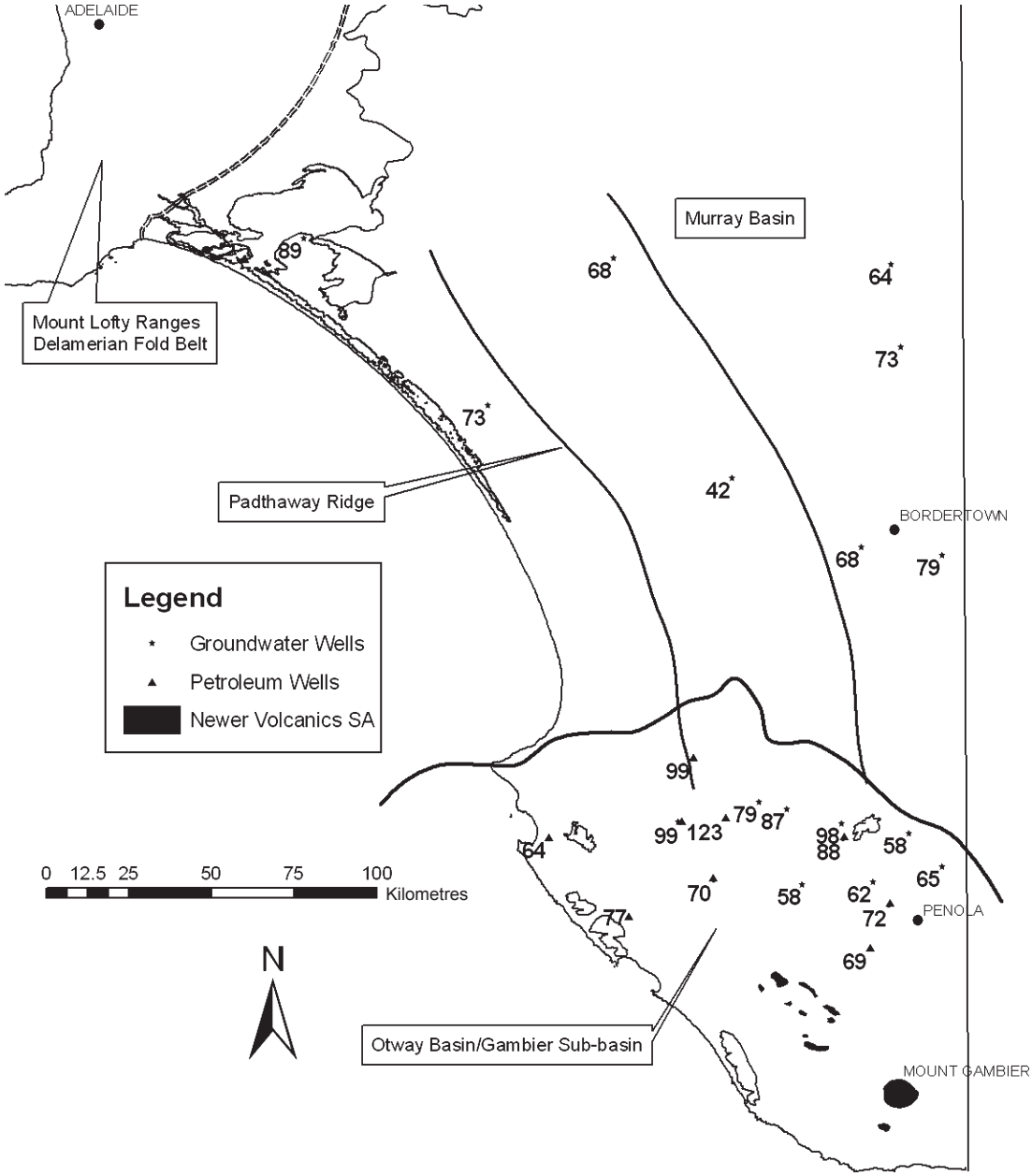

Fig. 6. The map of heat flow values measured in this study. Values are in mW/m^2. There appears to be a zone of high heat flow corresponding to the northern margin of the Gambier Sub-basin. A single high value was measured at the eastern margin of the Delamerian Fold Belt. Note: Uncertainty values are not displayed on the map but are listed in Table 2.

Heat flow values between 60 and 70 mW/m^2 are to be expected for crust of Proterozoic age and this tectonic history (e.g. Jessop, 1990). Several of the new heat flow values are far higher than this, especially in a zone ~40 km long (east–west) and 10–15 km wide (north–south) at the northern margin of the Otway Basin. This could be due to a combination of factors. First, heat would be naturally refracted away from the insulating sedimentary package of the Otway Basin (e.g. Sandiford et al., 2003). Second, Delamerian Orogeny, post-tectonic, A-type granitoids outcrop and subcrop in the Padthaway Ridge (Figure 2), an arbitrary region loosely defined by the existence of outcropping Delamerian Orogeny post-tectonic granitoids. Using data published by Foden et al., (2002) and Turner et al., (1992), we calculated that these granites produce radiogenic heat at rates between 2.3 and 10.5 μW/m^3, with an average of 5.5 μW/m^3, and should therefore contribute a significant crustal component to surface heat flow, perhaps as much as 50 mW/m^2 (e.g. McLaren et al., 2003). The wavelength of the observed high heat flow zone, diminishing to background levels within 10 km to the south, is consistent with a heat source at a maximum depth of 10 km.

The Otway and Murray Basins contain several areas under geothermal exploration licence (GEL), and these new heat flow values may aid explorers in their efforts to find high temperature resources. In a conductive regime, heat flow remains constant with depth (ignoring internal heat production), allowing reliable temperature estimates for considerable depths below accessible boreholes.

We have demonstrated that new heat flow data can be collected within South Australia utilising existing resources. Our simple exercise has increased the size and geographical range of the South Australian heat flow dataset and revealed heat flow patterns on a finer scale than previously recognised. In particular we observe variation in heat flow on the order of

100% over wavelengths of 20 km or less. These variations can only be attributed to heat sources within the middle to upper crust. The nature of these anomalies remains speculative at present. Possible causes include a mid to upper crustal high heat generating granite pluton; elevated conductive basement rocks refracting heat preferentially through a restricted geographic area; a cooling magmatic intrusion associated with the Newer Volcanic Province; deep-seated upwelling fluid.

With boreholes and core samples available over much of Australia, there is great potential to significantly build on the current heat flow dataset using the methods outlined in this paper. Heat flow studies of this kind may reveal geothermal energy targets, delineate IOCG uranium-rich ore bodies, provide extra information about the structure and composition of the mid to upper crust, and continue to build the Australian heat flow database.

Acknowledgments

Special thanks are given to those who have helped in the data collection and analysis for this paper. In particular, Jeff Lawson and George MacKenzie are thanked for their help in accessing suitable groundwater wells. The assistance of M. Sandiford and J. Cull with their helpful insights is appreciated as well.

References

Beardsmore, G. R., 2005, Thermal modelling of the hot dry rock geothermal resource beneath GEL99 in the Cooper Basin. *Proceedings World Geothermal Congress, Antalya, Turkey, 24–29 April, 2005*.

Beardsmore, G. R., and Cull, J. P., 2001, Crustal heat flow; a guide to measurement and modelling, Cambridge University Press.

Boult, P. J., and Hibburt, J. E., (eds) 2002, The Petroleum Geology of South Australia. Vol. 1, The Otway Basin, 2nd Edition. *South Australia, Department of Primary Industries and Resources, Petroleum Geology of South Australia Series, Vol. 1*.

Cull, J. P., 1982, An appraisal of Australian heat-flow data: *BMR Journal of Australian Geology and Geophysics* **7**, 11–21.

Foden, J. D., Elburg, M. A., Turner, S. P., and Sandiford, M., 2002, Granite production in the Delamerian Orogen, South Australia: *Journal of the Geological Society* **159**, 557–575.

Houseman, G. A., Cull, J. P., Muir, P. M., and Paterson, H. L., 1989, Geothermal signatures and uranium ore deposits on the Stuart Shelf of South Australia: *Geophysics* **54**, 158–170. doi: 10.1190/1.1442640

Jenkins, R. J. F., and Sandiford, M., 1992, Observations on the tectonic evolution of the Southern Adelaide Fold Belt: *Tectonophysics* **214**, 27–36. doi: 10.1016/0040-1951(92)90188-C

Jessop, A. M., 1990, *Developments in Solid Earth Geophysics*, Vol. 17, *Thermal Geophysics*. Elsevier.

Lachenbruch, A. H., and Brewer, M. C., 1959, Dissipation of the temperature effect of drilling a well in Arctic Alaska. *United States Geological Survey Bulletin*, 1083-C, 73–109.

McBride, J. S., Lambert, D. D., Greig, A., and Nicholls, I. A., 1996, Multistage evolution of Australian subcontinental mantle; Re-Os isotopic constraints from Victorian mantle xenoliths: *Geology (Boulder)* **24**, 631–634. doi: 10.1130/0091-7613(1996)024<0631:MEOASM>2.3.CO;2

McLaren, S., Sandiford, M., Hand, M., Neumann, N., Wyborn, L., and Bastrakova, I., 2003, The hot southern continent, heat flow and heat production in Australian Proterozoic terranes: *Geological Society of Australia, Special Publication* **22**, 151–161.

Neumann, N., Sandiford, M., and Foden, J., 2000, Regional geochemistry and continental heat flow: implications for the origin of the South Australian heat flow anomaly: *Earth and Planetary Science Letters* **183**, 107–120. doi: 10.1016/S0012-821X(00)00268-5

O'Brien, G. W., Reeves, C. V., Milligan, P. R., Morse, M. P., Alexander, E. M., Willcox, J. B., Yunxuan, Z., Finlayson, D. M., and Brodie, R. C., 1994, New ideas on the rifting history and structural architecture of the western Otway Basin: evidence from the integration of aeromagnetic, gravity and seismic data: *APEA Journal* **34**, 529–555.

Rogers, P. A., Lindsay, J. M., Alley, N. F., Barnett, S. R., Lablack, K. L., and Kwitco, G., 1995, Murray Basin. In J. F., Drexel, and W. V., Preiss (eds). The Geology of South Australia. Vol. 2, The Phanerozoic. *South Australia Geological Survey*, Bulletin 54.

Sandiford, M., 2003, Neotectonics of SE Australia and the origin of the intraplate stress field in Skilbeck, C. G., Hubble, C. T., Thomas (eds). *Understanding Planet Earth; searching for a sustainable future; abstracts of the 15th Australian geological convention, Abstracts – Geological Society of Australia*.

Sandiford, M., Frederiksen, S., and Braun, J., 2003, The long-term thermal consequences of rifting: implications for basin reactivation: *Basin Research* **15**, 23–43. doi: 10.1046/j.1365-2117.2003.00196.x

Sheard, M. J., 1990, A guide to Quaternary volcanoes in the lower south-east of South Australia: *Mines and Energy Review – South Australia*, **157**, 40–50.

Turner, S. P., Foden, J. D., and Morrison, R., 1992, Derivation of A-type magma by fractionation of basaltic magma and an example from the Padthaway Ridge, South Australia: *Lithos* **28**, 151–179. doi: 10.1016/0024-4937(92)90029-X

Manuscript received 10 May 2006; accepted 4 October 2007.

Appendix

Detailed tables of thermal conductivity sampling and the raw data used in Horner Plot corrections to estimate bottom hole temperatures.

Table 1. A detailed summary of thermal conductivity samples and measurements undertaken in this study. The measurement methods and error calculations are discussed in the text.

Bore	Sample No.	Depth (m)	Diameter	Δx(mm)	λ_o(W/mK)	+/–	λ_t	+/-	λ_{av}	+/-	Formation	Lithology
RR66	01A		60	11.35	1.66	± 0.04	1.66	± 0.04	**1.66**	**± 0.04**	Vesicular lava	Basalt
RR66	02A		60	20.02	1.47	± 0.04	1.47	± 0.04	**1.50**	**± 0.03**	Vesicular lava	Basalt
	02B			16.43	1.54	± 0.04	1.54	± 0.04				
RR66	03A	57.2	59.5	26.70	1.50	± 0.04	1.53	± 0.04	**1.52**	**± 0.03**	Green Point Member Unit 1	Limestone/Marl
	03B			19.70	1.48	± 0.04	1.50	± 0.04				
RR66	04A	63.3	60	16.27	2.08	± 0.05	2.08	± 0.05	**2.08**	**± 0.04**	Green Point Member Unit 1	Limestone/Marl
	04B			14.97	2.09	± 0.05	2.09	± 0.05				
RR66	05A	73.7	57.6	18.48	1.14	± 0.03	1.24	± 0.03	**1.25**	**± 0.02**	Green Point Member Unit 2	Limestone/Marl
	05B		57.1	19.82	1.15	± 0.03	1.27	± 0.03				
RR66	06A	83.5	60	26.00	1.18	± 0.03	1.18	± 0.03	**1.15**	**± 0.02**	Green Point Member Unit 3	Limestone/Marl
	06B			19.37	1.13	± 0.03	1.13	± 0.03				
RR66	07A	87.5	53.9	27.70	1.46	± 0.04	1.84	± 0.05	**1.62**	**± 0.02**	Green Point member Unit 4	Limestone/Marl
	07B			31.75	1.32	± 0.03	1.63	± 0.04				
	07C			24.98	1.20	± 0.03	1.44	± 0.04				
RR66	08A	108.0	60	23.80	1.54	± 0.04	1.54	± 0.04	**1.49**	**± 0.03**	Green Point Member Unit 4	Limestone/Marl
	08B			17.90	1.44	± 0.04	1.44	± 0.04				
RR66	09A	111.3	60	39.53	1.54	± 0.04	1.54	± 0.04	**1.52**	**± 0.02**	Green Point member Unit 4	Limestone/Marl
	09B			22.79	1.51	± 0.04	1.51	± 0.04				
	09C			32.84	1.52	± 0.04	1.52	± 0.04				
RR66	10A	122.3	60	24.60	1.49	± 0.04	1.49	± 0.04	**1.51**	**± 0.03**	Camelback Member	Limestone/Dolomitic Limestone
	10B			19.30	1.54	± 0.04	1.54	± 0.04				
RR66	11A	177.1	60	25.20	2.20	± 0.06	2.20	± 0.06	**2.10**	**± 0.04**	Greenways Member	Limestone/Marl
	11B			17.00	2.00	± 0.05	2.00	± 0.05				
RR66	12A	177.3	59.5	24.50	1.54	± 0.04	1.57	± 0.04	**1.53**	**± 0.03**	Greenways Member	Limestone/Marl
	12B			21.30	1.48	± 0.04	1.50	± 0.04				
RR66	13A	192.1	60						**1.08**	**± 0.03**	Dilwyn Formation	Clay
	13B				1.08	± 0.03	1.08	± 0.03				
RR65	14A	35.5	60	28.07	2.18	± 0.05	2.18	± 0.05	**2.18**	**± 0.04**	Green Point Member Unit 1	Limestone/Marl
	14B			19.34	2.19	± 0.05	2.19	± 0.05				
RR65	15A	73.1	60	26.40	1.45	± 0.04	1.45	± 0.04	**1.43**	**± 0.03**	Green Point Member Unit 2	Limestone/Marl
	15B			19.60	1.42	± 0.04	1.42	± 0.04				
RR65	16A	84.2	59	22.10	1.17	± 0.03	1.21	± 0.03	**1.20**	**± 0.02**	Green Point Member Unit 2	Limestone/Marl
	16B			16.70	1.15	± 0.03	1.19	± 0.03				
RR65	17A	122.2	59	24.20	1.19	± 0.03	1.23	± 0.03	**1.24**	**± 0.02**	Green Point Member Unit 3	Limestone/Marl
	17B			16.80	1.20	± 0.03	1.24	± 0.03				
RR65	18A	163.0	60	26.00	1.44	± 0.04	1.44	± 0.04	**1.46**	**± 0.03**	Camelback Member	Limestone/Dolomitic Limestone
	18B			21.45	1.48	± 0.04	1.48	± 0.04				
RR65	19A	168.5	60	24.65	2.35	± 0.06	2.35	± 0.06	**2.39**	**± 0.04**	Camelback Member	Limestone/Dolomitic Limestone
	19B			25.41	2.43	± 0.06	2.43	± 0.06				
RR65	20A	178.0	60	26.40	1.68	± 0.04	1.68	± 0.04	**1.65**	**± 0.03**	Greenways Member	Limestone/Marl
	20B			19.50	1.62	± 0.04	1.62	± 0.04				
RR65	21A	187.9	60	24.10	1.79	± 0.04	1.79	± 0.04	**1.83**	**± 0.03**	Greenways Member	Limestone/Marl
	21B			20.30	1.87	± 0.05	1.87	± 0.05				
RR65	22A	235.2	60						**1.28**	**± 0.03**	Dilwyn Formation	Clay
	22B			21.20	1.28	± 0.03	1.28	± 0.03				
RR65	23A	236.1	60	22.20	1.22	± 0.03	1.22	± 0.03	**1.22**	**± 0.03**	Dilwyn Formation	Clay
	23B											
LD3	24A	157.1	36.9	17.87	2.74	± 0.10	2.74	± 0.10	**2.79**	**± 0.06**	Delamerian granite	Granite
	24B			20.74	2.80	± 0.10	2.80	± 0.10				
	24C			24.82	2.84	± 0.10	2.84	± 0.10				
LD3	25A	161.0	36.9	19.85	2.91	± 0.10	2.91	± 0.10	**2.84**	**± 0.06**	Delamerian granite	Granite
	25B			15.02	2.81	± 0.10	2.81	± 0.10				
	25C			23.26	2.79	± 0.10	2.79	± 0.10				
BHC1	30A	185.5	44.2	26.91	1.30	± 0.05	1.50	± 0.05	**1.43**	**± 0.03**	Mannum Formation	Limestone
	30B			19.24	1.20	± 0.04	1.39	± 0.05				
	30C			17.51	1.21	± 0.04	1.40	± 0.05				
BHC1	31A	198.7	44.6	23.90	1.20	± 0.04	1.33	± 0.05	**1.33**	**± 0.03**	Mannum Formation Limestone	Limestone
	31B			21.32	1.14	± 0.04	1.30	± 0.05				
	31C			27.69	1.17	± 0.04	1.37	± 0.05				
BHC1	33A	218.4	42	25.95	0.57	± 0.02	0.73	± 0.03	**0.68**	**± 0.01**	Ettrick Formation	Clay
	33B			20.20	0.51	± 0.02	0.66	± 0.02				
	33C			24.83	0.52	± 0.02	0.67	± 0.03				
Oakvale 1	37A	36.1	53	20.18	0.66	± 0.02	0.85	± 0.03	**0.85**	**± 0.02**	Geera Clay	Clay
COONALPYN DOWNS 1	39A	64.4	47.6	17.85	0.95	± 0.03	0.95	± 0.03	**1.08**	**± 0.03**	Buccleuch Formation(?)	Clay
	39B			28.58	1.25	± 0.04	1.25	± 0.04				
WYN1	41A	148.0	47.6	22.09	1.96	± 0.07	1.96	± 0.07	**1.93**	**± 0.04**	Buccleuch Formation(?)	Silty Clay
	41B			18.38	1.94	± 0.07	1.94	± 0.07				
	41C			21.19	1.90	± 0.07	1.90	± 0.07				
KIN4	42A	86.3	47.6	18.18	2.87	± 0.10	2.87	± 0.10	**2.95**	**± 0.06**	Kanmantoo Schist	Schist
	42B			22.15	3.01	± 0.11	3.01	± 0.11				
	42C			12.21	2.97	± 0.10	2.97	± 0.10				
MBT6	43A	254.5	47.6	24.76	2.85	± 0.10	2.85	± 0.10	**2.89**	**± 0.06**	Delamerian granite	Granite
	43B			20.35	2.75	± 0.10	2.75	± 0.10				
	43C			23.57	3.08	± 0.11	3.08	± 0.10				
MTR1	45A	85.9	47.6	26.22	3.41	± 0.12	3.41	± 0.12	**3.37**	**± 0.08**	Kanmantoo Schist	Scist
	45B			22.03	3.34	± 0.12	3.34	± 0.12				
PADD32	46A	84.1	50.62	21.21	2.09	± 0.05	2.94	± 0.07	**2.95**	**± 0.04**	Granodiorite	Granodiorite
	46B			25.61	2.04	± 0.05	2.87	± 0.07				
	46C			22.71	2.18	± 0.05	3.06	± 0.07				

Table 2. The raw data for the Horner Plots that were ued to calculate the corrected bottom hole temperature for selected petroleum wells.

Hole ID	Measured BHT (°C)	Time Since Circulation Ceased (hrs)	Estimated true BHT from Horner Plot (°C)
Balnaves 1	103	12.5	
	104	21.33	
	110	29.5	**113.3**
Viewbank 1	87.8	7.5	
	93.3	16.5	
	95.5	29	
	98.9	35.8	**100.4**
St Clair 1	109	7.75	
	121	17.5	
	123	29.25	**130.4**
Nunga Mia 1	87.8	8.3	
	96.7	20.4	
	100	41.3	**103.8**
Bool Lagoon 1	44.4	3	
	47.2	6.25	
	47.8	8.25	**50.3**
Camelback 1	74.4	10.7	
	77.2	14.5	
	80	18.5	
	82.2	24.2	**89.0**
Wanda 1	42	10	
	43	14	**45.7**

CSIRO PUBLISHING
www.publish.csiro.au/journals/eg *Exploration Geophysics*, 2009, **40**, 288–300

Geothermal energy prospectivity of the Torrens Hinge Zone: evidence from new heat flow data

Chris Matthews

Torrens Energy Ltd, 12 Eton Road, Keswick, SA 5035, Australia and School of Geosciences, Monash University, Vic. 3800, Australia. Email: [redacted]

Abstract. The Torrens Hinge Zone is a long but narrow (up to 40 km wide) geological transition zone between the relatively stable Eastern Gawler Craton 'Olympic Domain' to the west, and the sedimentary basin known as the Adelaide Geosyncline to the east. The author hypothesised from first principles that the Torrens Hinge Zone should be prospective for high geothermal gradients due to the likely presence of high heat flow and insulating cover rocks. A method to test this hypothesis was devised, which involved the determination of surface heat flow on a pattern grid using purpose-drilled wells, precision temperature logging and detailed thermal conductivity measurements. The results of this structured test have validated the hypothesis, with heat flow values over 90 mW/m^2 recorded in five of six wells drilled. With several kilometres thickness of moderate conductivity sediments overlying the crystalline basement in this region, predicted temperature at 5000 m ranges between 200 and 300°C.

Key words: Adelaide Geosyncline, Australia, Curnamona Craton, Delamerian Fold Belt, Engineered Geothermal Systems, Gawler Craton, Heat Flow, Thermal Conductivity, Thermal Gradient, Torrens Hinge Zone.

Introduction

The geothermal energy industry in Australia is a relatively young entity. Utilisation of geothermal resources to date has been restricted to low enthalpy direct uses and very small-scale electricity generation. The most advanced development activity is in the central Australian Cooper Basin (Chopra, 2005; Figure 1). Work completed in this region has highlighted the opportunity for large-scale electricity generation from deep, high enthalpy Engineered Geothermal Systems (EGS; Geodynamics Limited, 2009), while several southern Australian sedimentary basins such as the Otway and Gippsland Basins (Figure 1) are now being explored for lower enthalpy, but more conventional, Hot Sedimentary Aquifer (HSA) geothermal resources. Both subsectors have been inferred to contain enormous quantities of stored heat (e.g. Torrens Energy Limited, 2008; Panax Geothermal Limited, 2009).

For an area to be prospective for geothermal power generation there must exist high average geothermal gradients to create high temperatures at depths over a significant area which can be economically drilled. In addition to this the heat must be able to be economically exploited. This requires the existence of suitable reservoir rocks with either high natural porosity and permeability, or the conditions that allow permeability to be artificially enhanced by reservoir engineering. Economics are also driven by location and the cost of bringing the power to market competitively. Geothermal resources are not transportable in the way that fossil fuels are, making it desirable that resources be located proximal to a market. The remote location with respect to the existing national electricity grid is a significant economic obstacle to large-scale development in the Cooper Basin high enthalpy EGS subsector. There is a strong economic incentive to locate EGS resources closer to the transmission system in southern Australia. In summary, the following criteria are optimal for a resource to be viable for economic geothermal power generation:

1. High average geothermal gradient,
2. Suitable reservoir conditions, or the ability to economically engineer them, and
3. A proximal market for the generated power.

The surface heat flow and broad thermal conductivity structure (and thus the temperature field) of most of Australia is poorly understood at this stage. Preliminary estimates (e.g. Cull, 1982; Cull and Conley, 1983; Somerville et al., 1994; Chopra and Holgate, 2005) provided broad approximations of the Australian continent temperature field, but suffered from a sparse geographic distribution of heat flow and thermal conductivity data. Over most of the continent, conductivity data in the case of the earlier studies, and geothermal gradient or bottom hole temperature data in the latter work, are not available at sufficient spatial resolution to allow temperature modelling to a high degree of confidence.

Heat flow

Heat flows through the Earth mainly by conduction and advection. Conduction is the movement of energy through solid surfaces by the transfer of kinetic energy between particles (e.g. Beardsmore and Cull, 2001). Advection involves the mass transport of heat associated with the physical motion of materials and includes the process of convection in the mantle. Conduction is assumed to be the dominant mode of heat transport in the crust, while convection dominates in the mantle.

In practice, average vertical conductive heat flow, Q_0, at the Earth's surface can be calculated (e.g. Beardsmore and Cull, 2001):

$$Q_0 = \lambda_z \beta_z + \Sigma A, \quad (1)$$

where λ_z = thermal conductivity (W/mK) at depth z, a physical property of the rocks; β_z = vertical geothermal gradient (K/m) at

 10.1071/EG09022 0812-3985/09/030288

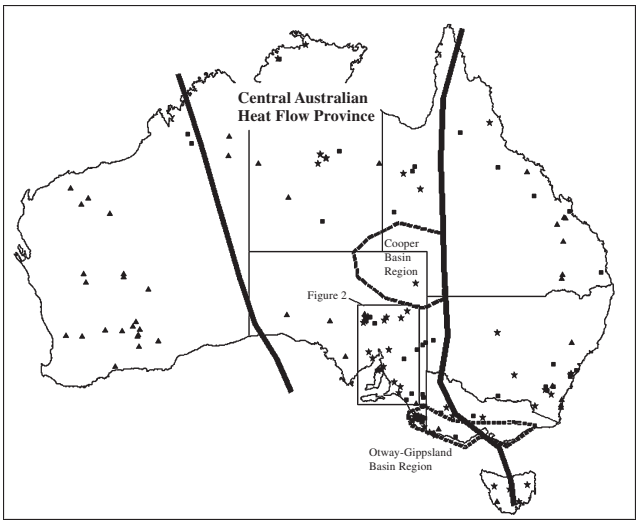

Fig. 1. Australian Heat flow data, compiled from Cull (1982), Houseman et al. (1989) and Matthews and Beardsmore (2007). The Central Australian Heat Flow Province is marked by solid lines, and the EGS province of the Cooper Basin region plus the HSA province of the Otway Gippsland Basin region are outlined with dashed lines. Key to heat flow data points: triangles: $\leq$60 mW/m^2; squares: 61–80 mW/m^2; stars: >80 mW/m^2.

depth z, the rate of change in temperature per metre depth; ΣA = additional heat added between the surface and depth z, heat produced inside the system. Average conductive heat flow is calculated from measurements of λ_z and β_z over several intervals within a borehole, or over one interval by assuming negligible ΣA.

Surface heat flow (Q_s) represents the combined flow of thermal energy from two sources: heat flowing from the mantle of the earth (reduced heat flow, q_r), and heat actively generated in the crust by the decay of radioactive elements such as U, Th and K (q_c). Stated simply:

$$Q_s = q_r + q_c. \quad (2)$$

The Central Australian heat flow province and the South Australian heat flow anomaly

The global average surface heat flow on the continents is around 65 mW/m^2 (e.g. Pollack et al., 1993), with values typically decreasing with increasing age of basement crustal rocks. The central part of Australia, essentially defined by the existence of Proterozoic crustal rocks, is known as the Central Australian Heat Flow Province (CAHFP; e.g. McLaren et al., 2003, figure 1), and previously the Central Shield Heat Flow Province (Sass and Lachenbruch, 1979). In this zone, there are numerous published values of surface heat flow that are well above both normal continental and global average Proterozoic Terrane heat flow values. These anomalous values are generally attributed to the unusual enrichment of much of the Australian Proterozoic crust in the main heat-producing elements such as U, Th and K (e.g. McLaren et al., 2003).

The South Australian Heat Flow Anomaly (SAHFA; Neumann et al., 2000) is a region defined loosely by lines of longitude in the central to eastern part of the state of South Australia, encompassing reported elevated heat flow values, but also several low values, as is shown in two higher resolution studies (see below).

Before 1989 there were less than 30 published surface heat flow values for the whole of South Australia with, in many cases, hundreds of kilometres between adjacent points (Matthews and Beardsmore, 2007). This dataset enabled only the most basic understanding of the SA heat flow regime, and required sweeping assumptions to be made about the nature of the heat flow distribution between data points. The data were derived almost exclusively from mineral exploration drillholes and the integrity of many values has been described as 'questionable' (Cull, 1982). Two subsequent studies by Houseman et al. (1989) and Matthews and Beardsmore (2007) collected vertical heat flow data to a much greater spatial resolution in parts of the SAHFA.

Houseman et al. (1989) revealed that surface heat flow is variable by a factor of more than two in the Olympic Dam area, and that the highest values correspond to the locations of the Olympic Dam and Acropolis ore bodies, which represent shallow crustal radioactive heat sources (Figure 2). It is estimated that the mantle-derived component of vertical heat flow (q_r) in the eastern Gawler Craton 'Olympic Domain' (Figure 2; Ferris et al. 2002), is as low as 20–30 mW/m^2 (Neumann et al., 2000). Therefore, the bulk of the surface heat flow anomalies in the Olympic Dam area must be due to the crustal component (q_c) of heat flow.

Matthews and Beardsmore (2007) published 24 heat flow values from an area in the south-eastern corner of South Australia. A similar spread of results was obtained to that of the Olympic Dam study, with heat flow varying by a factor of three over the region. Furthermore, the Padthaway Ridge, a shallow crustal geological feature containing Palaeozoic heat producing granitoids – corresponds to the zone of highest heat flow.

The Olympic Dam and eastern South Australia examples illustrate that the SAHFA is not a zone of consistently high 'blanket' heat flow, and that it may be little different to the previously proposed CAHFP. The concept is consistent with the idea that the Proterozoic CAHFP crust has a common value of q_r, with broadly similar tectonothermal history and heat production depth scale (Roy et al., 1968).

The heat-producing Proterozoic geological terranes in the SAHFA are dominated in the centre and west by the Hiltaba Suite, Gawler Range Volcanics and Barossa Complex (Eastern Gawler Craton; Figure 2) and in the east by the Mount Painter Province Inliers and greater Curnamona Craton (Figure 2). These rock units range in heat production from 2.9 to 16.1 μW/m^3 (Neumann et al., 2000; McLaren et al., 2003).

This significant contribution of crustal heat production has implications when considering the representative nature of the current heat flow dataset for those parts of Australia where there is widely spaced surface heat flow data. It is unlikely that heat flow varies in a smooth fashion between the current heat flow data points, and more likely that there will be short wavelength variations depending on basement geology.

Regional setting

The Study Area is located within the Torrens Hinge Zone (THZ) at the western boundary of the Central Flinders Zone (Figure 3), wholly on the PARACHILNA 1 : 250 000 map sheet in South Australia. The area was first systematically mapped by Dalgarno and Johnson (1966) and updated by Reid and Preiss (1999).

Preiss (2005) described the THZ as a 'zone of syn-sedimentary faulting and flexuring which separates the Gawler Craton [in the west]. . . from the rifted basins of the Adelaide Geosyncline to the east.'

Preiss (2000) described the Adelaide Geosyncline (AG) as 'a deeply subsident Neoproterozoic to Middle Cambrian basin complex. . .with a record of at least five major successive rift cycles.' The Neoproterozoic portion of the geological time

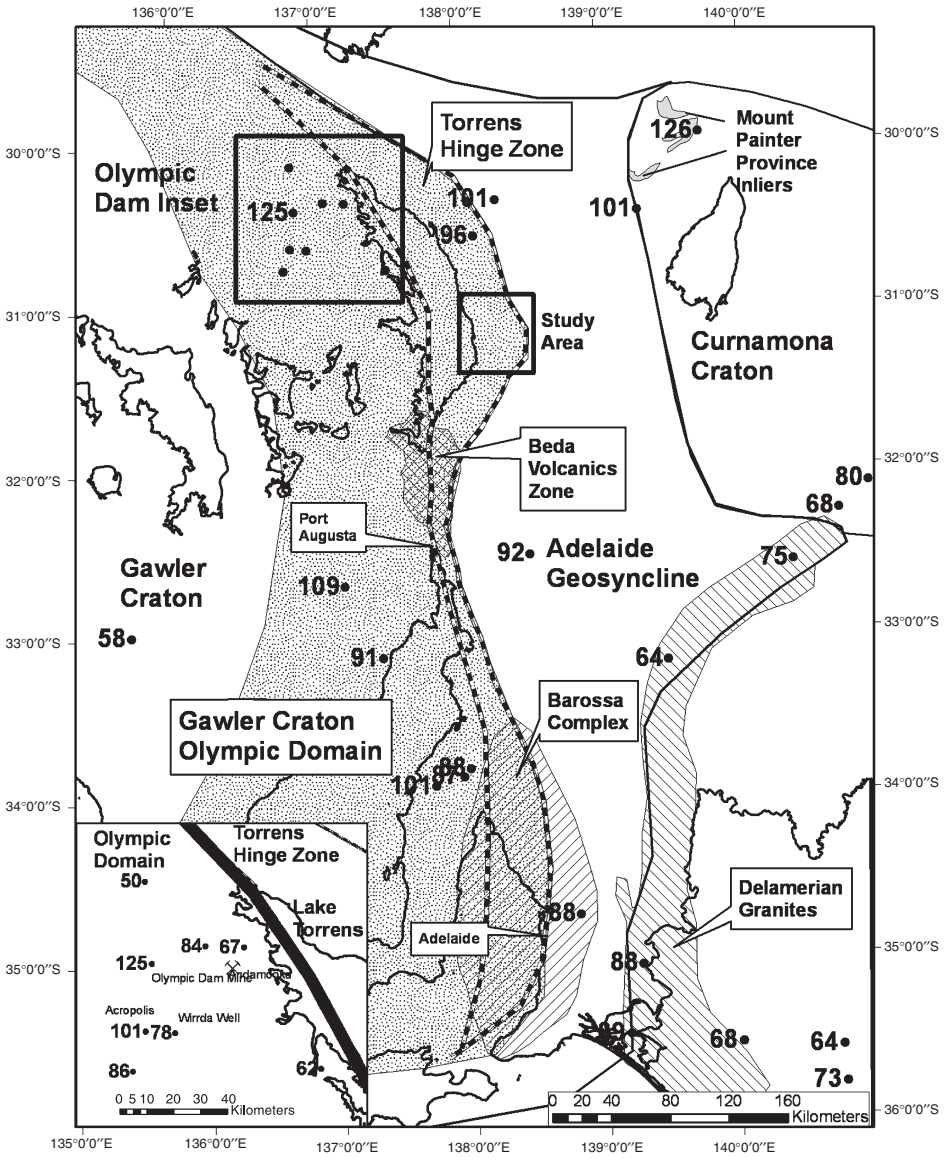

Fig. 2. Key geological elements of central South Australia. The Torrens Hinge Zone is a narrow elongate transition zone between the Eastern Gawler Craton and the Adelaide Geosyncline, and is also intersected by the Neoproterozoic Beda Volcanics and the Palaeoproterozoic Barossa Complex. Heat Flow values are too widely spaced to gauge the true nature of the SA Heat Flow Anomaly. The inset shows values measured by Houseman et al. (1989).

period during which these sediments were deposited is locally known as the Adelaidean Period (Mawson and Sprigg, 1950), and the rift cycles are broadly allocated to five sub-periods, named from oldest to youngest: Willouran, Torrensian, Sturtian, Marinoan and Cambrian (Table 1, stratigraphic column).

The THZ is essentially a region of overlap between the Gawler Craton and Adelaide Geosyncline (Figure 2). Over most of the THZ, the Adelaidean and Cambrian sedimentary sequences are underlain at depths between 2500 and 7000 m (de Vries et al., 2006) by The Mesoproterozoic Gawler Craton Olympic Domain (Ferris et al., 2002). In the south, the Palaeoproterozoic Barossa Complex (e.g. Preiss, 1993) also underlies the THZ.

To the east in the Adelaide Geosyncline proper, the sediments have been variably deformed by the Cambro-Ordovician Delamerian Orogeny (e.g. Preiss, 2000); with that region now part of the Delamerian Fold Belt (DFB). It is considered by the author that the competent nature of the Olympic Domain basement may have protected the THZ region from the full effects of the Delamerian Orogeny. Thus, while the Adelaide Geosyncline is now within the DFB, the THZ remains a 'meridional belt of gentle folding' (Preiss, 2000).

Close to Port Augusta the earliest rifting phase of the Adelaide Geosyncline is marked by the extrusion of the mafic Beda Volcanics at around 827 Ma (Preiss, 2000). This area is here termed the Beda Volcanics Zone (BVZ; Figure 2). The thickness of the Beda Volcanics in the THZ to the north of Port Augusta is estimated to be up to 1500 m (Dalgarno and Johnson, 1966).

Basement heat production estimates

As discussed above, parts of the SAHFA contain significant basement heat production from the Mesoproterozoic Hiltaba Suite granitoids. However, the THZ also contains two additional high heat producing geological occurrences, namely

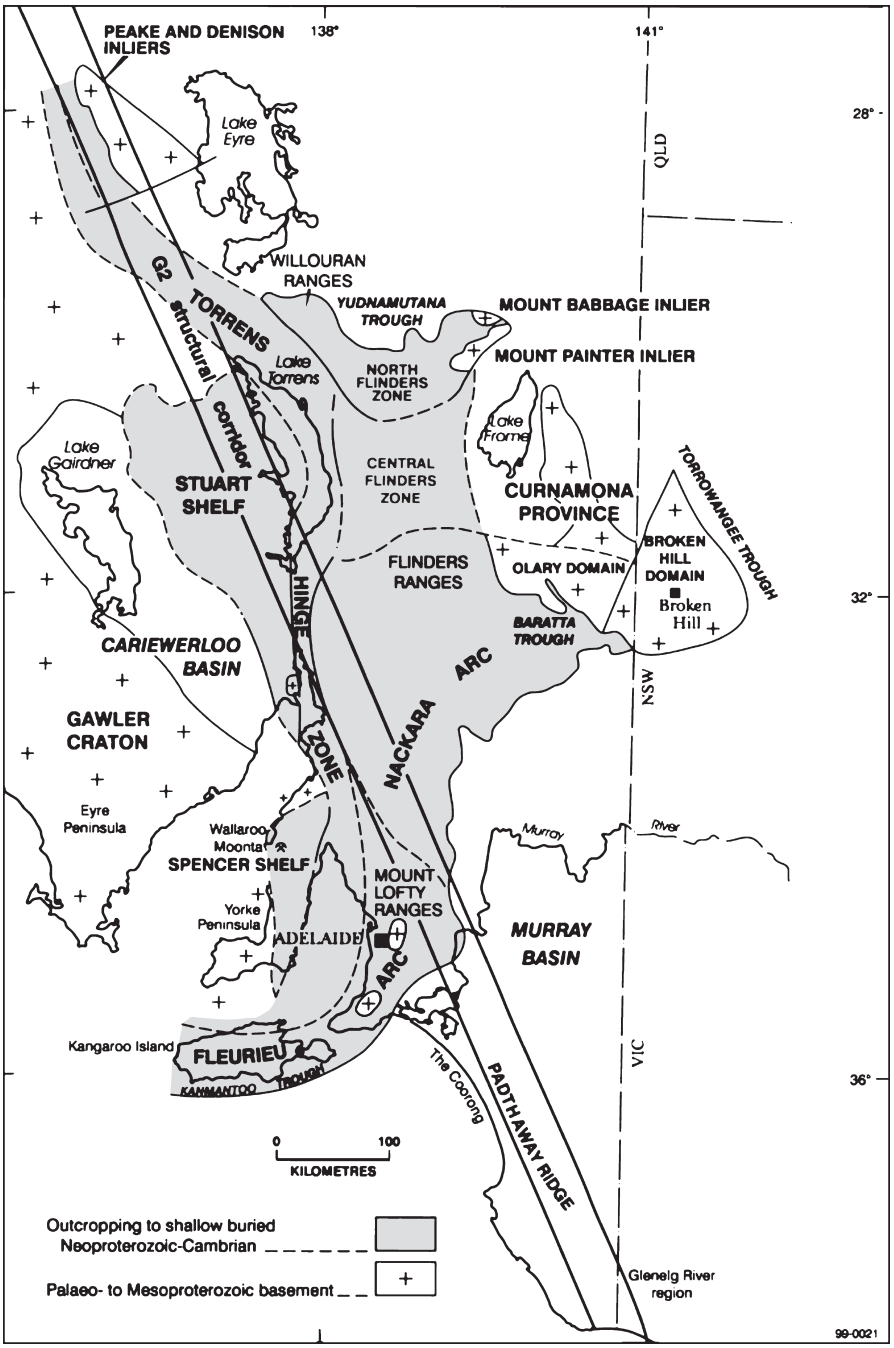

Fig. 3. The distribution in central to eastern South Australia of the Adelaide Geosyncline, Torrens Hinge Zone, Stuart Shelf (Gawler Craton), and Curnamona Craton. After Preiss (2000).

the Mesoproterozoic Gawler Range Volcanics, and the Palaeoproterozoic Barossa Complex.

The Gawler Range Volcanics (GRV) are felsic volcanic units (rhyolite, rhyodacite and dacite), and are considered to be comagmatic with the Hiltaba Suite granites mentioned above (Allen et al., 2003). The GRV were emplaced in a subaerial, intracontinental setting in the Gawler Craton between 1585 and 1600 Ma (Allen et al., 2003). Geochemical data from Allen et al. (2003) were used to estimate the average heat production of the GRV, with the method of calculating values taken from Beardsmore and Cull (2001). The GRV heat production was calculated to be 4.01 $\mu W/m^3$. This value and the known widespread geographic distribution of both the Hiltaba Suite and GRV indicate that a background of high heat production and therefore high heat flow is likely for many regions of the Olympic Domain.

The Palaeoproterozoic Barossa Complex (BC) forms the basement to Adelaidean and Cambrian cover sequences of the Southern Adelaide Geosyncline (Figure 2), and is exposed in five inliers in the Mt Lofty Ranges, near Adelaide. Rock types of the exposed inliers include quartzo-feldspathic granitic and augen gneisses, albite–actinolite gneiss, aplite, syenite, pegmatite, schist, psammopelite and quartzite (Belousova et al., 2006). Heat production is highly variable in the BC, ranging from 0.48 to 12.19 μWm^{-3} (M. Szpunar, PIRSA 2005, pers. comm.). However, the existence of high heat production in parts of the BC adds further potential heat production to the southern THZ.

Table 1. Generalised stratigraphic column for the Torrens Hinge Zone in South Australia north of Port Augusta (Figure 2).

The majority of the basement heat production in the THZ is likely to come from the Mesoproterozoic Hiltaba Suite granitoids and the Gawler Range Volcanics, with insulating Neoproterozoic sedimentary and mafic volcanic units overlying the basement.

Torrens Hinge Zone General Stratigraphy		
Age	Group	Unit
Pleistocene/Holocene	Pirie-Torrens Basin	Undifferentiated Clays and Gravels
Oligocene-Miocene	Pirie-Torrens Basin	Neuroodla Formation
Eocene	Pirie-Torrens Basin	Cotabena Formation
Middle Cambrian	Lake Frome Group	Pantapinna Formation Balcoracana Formation Moodlatana Formation
Middle Cambrian	Unnamed Group	Wirrealpa Limestone Billy Creek Formation
Early Cambrian	Hawker Group	Wilkawillina Limestone Parachilna Formation
Neoproterozoic (Adelaidean, Late Marinoan)	Wilpena Group Pound Subgroup	Rawnsley Quartzite Bonney Sandstone
Neoproterozoic (Adelaidean, Late Marinoan)	Wilpena Group	Wonoka Formation Bunyeroo Formation
Neoproterozoic (Adelaidean, Late Marinoan)	Wilpena Group Sandison Subgroup	ABC Quartzite (incl. Corraberra Sandstone) Brachina Formation (incl. Tregolana Shale) Nuccaleena Formation
Neoproterozoic (Adelaidean, Early Marinoan)	Umberatana Group Yerelina Subgroup	Elatina Formation/Whyalla Sandstone
Neoproterozoic (Adelaidean, Early Marinoan)	Umberatana Group Upalinna Subgroup	Trezona Formation Wilmington Formation Angepena Formation Etina Formation
Neoproterozoic (Adelaidean, Late Sturtian)	Umberatana Group Nepouie Subgroup	Brighton Limestone Tapley Hill Formation (incl. Woocalla Dolomite Member)
Neoproterozoic (Adelaidean, Early Sturtian)	Umberatana Group Yudnamutana Subgroup	Wilyerpa Formation Appila Tillite Other equivalent Sturtian Glacials
Neoproterozoic (Adelaidean, Late Torrensian)	Burra Group Unnamed Subgroup	Saddleworth Formation
Neoproterozoic (Adelaidean, Middle Torrensian)	Burra Group Mundiallo Subgroup	Skillogalee Dolomite
Neoproterozoic (Adelaidean, Early Torrensian)	Burra Group Emeroo Subgroup	Rhynie Sandstone
Neoproterozoic (Adelaidean, Willouran)		Beda Volcanics Backy Point Formation
Mesoproterozoic Eastern Gawler Craton		Pandurra Formation Gawler Range Volcanics Hiltaba Suite Granitoids
Palaeoproterozoic		Barossa Complex

Central Flinders Zone and study area

Deformation is less intense in the Central Flinders Zone (CFZ; Figure 3) than in the rest of the Adelaide Geosyncline, dominated by open dome-and-basin interference folds, with shortening generally less than 10% (Preiss, 2000). The Zone is situated in the narrowest part of the Adelaide Geosyncline, between the Gawler Craton and Curnamona Craton (Figure 2), and potential field data suggests that there may be a region of shallow basement underlying the CFZ (Reid and Preiss, 1999). The CFZ also displays a lesser degree of metamorphism than the rest of the Geosyncline (Preiss, 2000). Furthermore, the Mount Painter and Mount Babbage Inliers (here termed the Mount Painter Province Inliers; Figure 2) at the western end of the CFZ have a broadly similar geological provenance to the Hiltaba Granite Suite of the Olympic Domain, as well as exceptionally high heat production (e.g. McLaren et al., 2006).

Hypothesis

The Torrens Hinge Zone (THZ; Figure 2) has all the geological elements necessary for economic geothermal

power generation. It is likely to contain areas of high heat flow, low to moderate average thermal conductivity sedimentary or volcanic cover rocks, and a high probability of having suitable crystalline basement EGS reservoir potential due to modelled basement depth. The third criterion, proximity to a market, is met by the existence of the national power grid throughout most of the central and southern THZ region.

Heat flow data are now available to test the hypothesis.

The author designed a test to determine whether the THZ is indeed prospective for high geothermal gradients and EGS geothermal energy across areas with widths greater than 10 km. This test involved three stages:

(a) Collection of thermal conductivity data from existing rock or core samples from the region or from rocks that represented conditions in the region, in order to characterise the thermal conductivity structure of the geological units down to 5000 m depth.
(b) A structured drilling programme, with associated temperature logging conducted after any drilling induced temperature perturbations had subsided, to measure vertical heat flow in the THZ adjacent to the CFZ.
(c) Conductive temperature modelling to predict temperature at depth.

Results

Thermal conductivities from existing rock samples

The thermal conductivity of a rock is a complex function of its mineralogy, layer anisotropy and porosity. Thermal conductivity might vary markedly within formations displaying significant heterogeneity in porosity, mineralogy or structure. The thermal conductivity value is typically the dominant source of uncertainty in calculating heat flow, with a much higher level of confidence in the measured thermal gradients.

One primary aim of the present study was to characterise the bulk thermal conductivity of each geological formation that exists in the THZ. Ideally, in order to achieve this goal, thermal conductivity should be measured on enough random specimens from each formation to derive a statistical mean and variance that reflects the natural range of values. In practice, it is difficult to access sufficient quantities of core material to fully characterise all formations. Core of specific formations is often available from only one or two boreholes, or not available at all. The results of thermal conductivity measurements on available core can be statistically treated to derive mean measured values and variances, but these variances do not take into account uncertainties arising from possible lateral or vertical facies variation. This limitation creates uncertainty in all heat flow measurements that rely on thermal conductivity measurements from previously collected core.

During 2006 and 2007, thermal conductivity specimens were taken from pre-existing core specimens of sedimentary and igneous rocks of the THZ. From each specimen, three samples were taken to ensure the repeatability of the results within each specimen. These samples were water-saturated and analysed using a divided bar apparatus, which involves the application of a constant thermal gradient across a sample of unknown thermal conductivity, in series with materials of known thermal conductivity. Heat flow is measured across the known material and used to determine the conductivity of the test sample. The thermal conductivity of 113 core and three hand specimens were measured from a total of 20 formations of the Adelaide Geosyncline and BVZ, and the results are presented in Table 2. The harmonic mean of the three samples from each specimen was taken as the thermal conductivity for that specimen, to one standard deviation.

Discussion of thermal conductivity in the Torrens Hinge Zone

As stated earlier, the Adelaide Geosyncline is a Neoproterozoic to Cambrian basin complex. Sedimentary units include coarse to fine clastics, diamictites and carbonates (Foden et al., 2001).

Table 2. Summary of thermal conductivity values measured on core specimens taken from historic wells drilled in the Torrens Hinge Zone and Adelaide Geosyncline.

From Musson and Alesci (2007) and Beardsmore (2006). Each specimen was split into three samples, with the recorded value of thermal conductivity for each specimen being the harmonic mean of the three samples. The thermal conductivity value for each formation in the table is the harmonic mean of all specimens, ± one standard deviation.

Unit	Age	Number of Specimens	Lithology	λ_{av} (W/mK)
Balcoracana Formation	Middle Cambrian	4	Siltstone	2.15 ± 0.17
Moodlatana Formation	Middle Cambrian	2	Siltstone	3.02 ± 0.18
Wilkawillina Limestone	Early Cambrian	7	Dolomitic Limestone	4.49 ± 0.26
Wonoka Formation	Late Marinoan	2	Mudstone	2.27 ± 0.05
Bunyeroo Formation	Late Marinoan	2	Mudstone	1.75 ± 1.09
ABC Range Quartzite	Late Marinoan	4	Quartzite	4.75 ± 0.21
Corraberra Sandstone	Late Marinoan	5	Sandstone	3.11 ± 0.67
Tregolana Shale	Late Marinoan	7	Shale	2.33 ± 0.75
Brachina Formation	Late Marinoan	4	Siltstone	2.68 ± 0.33
Whyalla Sandstone	Early Marinoan	5	Sandstone	5.09 ± 0.40
Angepena Formation	Early Marinoan	5	Siltstone	2.50 ± 0.23
Woocalla Dolomite Member	Sturtian	3	Dolomitic Siltstone	3.22 ± 0.08
Tapley Hill Formation	Sturtian	12	Siltstone	2.82 ± 0.33
Sturtian Glacial Unit	Sturtian	8	Diamictite	3.72 ± 0.87
Saddleworth Formation	Torrensian	3	Shale	2.21 ± 0.11
Woolshed Flat Shale	Torrensian	6	Shale	2.20 ± 0.25
Beda Volcanics	Willouran	19	Mafic Volcanics	2.51 ± 0.26
Backy Point Formation	Willouran	5	Siltstone	2.94 ± 0.54
Pandurra Formation	Mesoproterozoic	5	Sandstone	4.27 ± 0.38
Gawler Range Volcanics	Mesoproterozoic	10	Felsic Volcanics	3.04 ± 0.18

Dominantly Proterozoic in age, the sediments of the Adelaide Geosyncline are generally more metamorphosed and less porous than most equivalent Phanerozoic sedimentary units. Furthermore, the majority of the geographic distribution of these units is in the Adelaide Geosyncline proper, and as such the sediments there have undergone significant orogenic deformation and metamorphism during the Palaeozoic. For these reasons, the sediments have generally been assumed to be poor candidates for thermal insulating cover.

Thermal conductivity is anisotropic, that is the value can be different in different directions in a material. The vertical thermal conductivity of a rock can be greatly affected by factors such as the presence of tectonic fabrics or the tilting of bedding planes due to deformation (Clauser and Huenges, 1995; Beardsmore and Cull, 2001).

A simple test of this was conducted via the direct measurement of thermal conductivity on a single water-saturated sample of the Lower Adelaidean Saddleworth Formation. The sample was cut into a cube shape and thermal conductivity was measured at two angles: perpendicular to layering and parallel to layering. The harmonic mean of three samples measured parallel to layering was 4.05 ± 0.17 W/mK (one standard deviation), while perpendicular to the layering the harmonic mean was around half that at 2.20 ± 0.05 W/mK.

Thus the effects of deformation on vertical thermal conductivity can be significant, and this effect very likely reduces the thermal insulating ability of the sediments in the Adelaide Geosyncline region to the east of the THZ due to the effects of the Delamerian Orogeny. As discussed above, however, the THZ was largely shielded from the deformation associated with the Delamerian Orogeny. The average dip of the strata in that zone is likely to be shallower than in the Adelaide Geosyncline, and steep foliations are also likely to be less common, lessening the negative effects of anisotropy on vertical thermal conductivity.

While sedimentary rocks are generally considered the best insulators, mafic volcanics also have low thermal conductivity (Beardsmore and Cull, 2001). Thermal conductivity measurements on Holocene vesicular basalt rocks from South Australia were published by Matthews and Beardsmore (2007), with two values averaging 1.58 W/mK. The Neoproterozoic Beda Volcanics around Port Augusta (Figure 2) are mafic lavas (Preiss, 2000), and have undergone weak metamorphism and alteration. A total of 19 specimens were analysed from core samples of the Beda Volcanics, with the harmonic mean of thermal conductivity being 2.51 ± 0.26 W/mK (Musson and Alesci, 2007). It is likely that the elevated thermal conductivity in these samples relative to their Holocene equivalents is due to alteration and metamorphism plus the removal of most of the original vesicular porosity. However, the harmonic mean of the measures values indicates that the Beda Volcanics are still relatively good insulators.

Structured heat flow measurement programme

As with other potential fields, the amplitude and wavelength of surface heat flow (and thus temperature distribution) are directly related to the magnitude and depth of the heat source. An intra-crustal heat source produces a surface heat flow anomaly with a wavelength in a similar order of magnitude as the depth of burial (e.g. Matthews and Beardsmore, 2006). Due to the current status of the heat flow dataset in Australia, with most values spaced hundreds of kilometres apart, it is impossible to adequately delineate crustal heat flow anomalies.

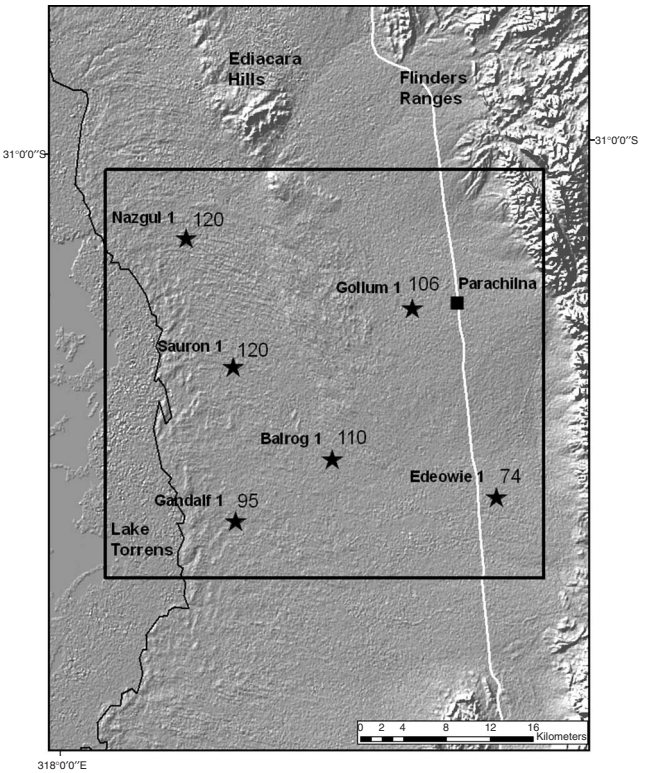

Fig. 4. Heat flow results, in mW/m^2, from the study area (see Figure 2 for location). All values are greater than the global continental average, and five of the six are above the average for the SAHFA (~91 mW/m^2).

The depth to crystalline basement in the THZ is estimated to be between 2.5 and 7 km depth (de Vries et al., 2006). An effective test of the hypothesis therefore required heat flow data to be collected at a maximum spacing of ~10–15 km to allow effective mapping of heat flow distribution and the identification of moderate to large scale heat sources.

A six well heat flow drilling programme was designed in the Parachilna area (Study Area Figure 2). Figure 4 shows the locations of the six wells. One existing well, Edeowie 1, was re-entered, with five additional wells purpose drilled.

Data collection

Cored drillholes

Each well was designed to reach a depth where the rock is competent enough to be fully cored for around 200 m of continuous downhole depth. In the Study Area this involved rotary mud drilling through the mostly unconsolidated Cenozoic clays and sands, found to be between 250 and 400 m deep, followed by diamond coring through the underlying Cambrian shale, limestone, siltstone and sandstone sequences.

Thermal gradient data

A temperature log from within each heat flow well was taken by measuring temperature at discrete depth intervals (0.05 m) from the surface to the bottom of each well. Sufficient time (at least 5 weeks) was allowed following completion of drilling activities to ensure thermal equilibration (Beardsmore and Cull, 2001). Several temperature logs were taken from most wells, and the thermal gradient over a time series was

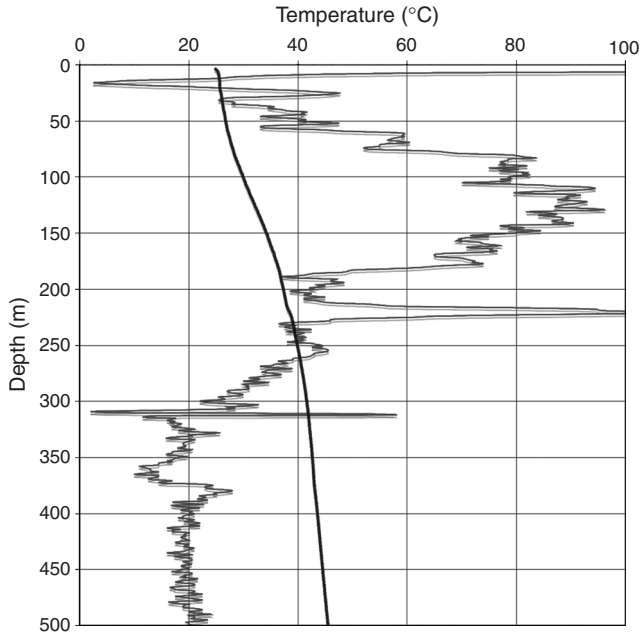

Fig. 5. Temperature profile and thermal gradient data for Balrog 1 (see Figure 4 for location). The boundary between the Tertiary units and underlying Cambrian strata is at 310 m. The Tertiary units are lower conductivity unconsolidated clays, sands and gravels, while the Cambrian rocks intersected in this well were predominantly quartzite and sandstone.

compared to ensure that temperatures had indeed equilibrated. Temperatures were measured to a precision of ±0.001°C and an absolute accuracy of ±0.01°C using truck-mounted logging equipment contracted from the South Australian Government Department of Water Land Biodiversity and Conservation (DWLBC).

As illustrated in the thermal gradient data measured in Balrog 1 (Figure 5), the geothermal gradient varies with lithology. In a purely conductive regime heat flow remains constant across a geological boundary (a requirement of the law of conservation of energy) so according to equation 1 there is an inverse relationship between geothermal gradient and thermal conductivity.

Thermal conductivity data

Five of the six heat flow wells contained at least 200 m of continuous core section. To allow statistically representative thermal conductivity profiles to be established, core specimens were taken every 7 m on average throughout the cored section. Up to three samples were prepared and measured from each specimen using a steady-state divided bar apparatus. The results are presented in Table 3; the reported value of conductivity for each sample was the harmonic mean of the measured sample values from that depth, to one standard deviation.

Heat flow models

Inversion modelling

Average vertical conductive heat flow is the product of average thermal gradient and average thermal conductivity over any given depth interval.

The following methodology was adopted to reach a heat flow determination for each well.

Three assumptions were made. These were that:

1. Each conductivity value is representative of the rocks from which the sample was extracted.
2. The boundary between one conductivity value and the next is the midpoint between measurement points.
3. A dominantly conductive regime exists.

The thermal conductivity profile for each well was then used to model a theoretical temperature profile that would result from a given magnitude of heat flow in a conductive heat flow regime. This theoretical profile was then plotted against the observed temperature log and the magnitude of the heat flow parameter in the model was adjusted until the modelled temperature profile best matched the logged temperatures.

Heat flow results

In total, five purpose-drilled wells and one existing well (Edeowie 1) gave six new heat flow values in the Torrens Hinge Zone spaced 13–15 km apart, providing heat flow coverage for an area ~35 × 35 km in size at a spatial resolution suitable for investigating heat sources in the basement (Figure 4).

The results of the heat flow study are presented in Table 4, and form the major constraint for the hypothesis test. The results of this structured test have validated the hypothesis, with heat flow values over 90 mW/m^2 recorded in five of six wells drilled.

Appendix 1 contains modelled conductive temperature profiles constructed using thermal conductivity measurements from core samples and assigned heat flow regimes, plotted against actual measured temperature profiles for each well.

Discussion

The shallow heat flow drilling programme designed to test the hypothesis proved effective in characterising the surface heat flow in the study area. Some uncertainties were observed in the analysis of the data; in particular that the vertical heat flow values obtained from two of the wells, namely Gandalf and Gollum, showed that there are departures from modelled conductive heat flow values. The two main candidates for the source of these departures are thermal measurements (conductivity and thermal gradient), and lateral heat advection either by flowing groundwater or active local faulting.

It is considered unlikely that the uncertainties stem from potentially unrepresentative thermal conductivity measurements or unequilibrated thermal gradient surveys, because in general the results of the thermal conductivity analysis appeared to be a robust, repeatable and reliable

Table 3. Summary of thermal conductivity values measured on core specimens taken from wells drilled in this study.
Each specimen was split into three samples, with the recorded value of thermal conductivity for each specimen being the harmonic mean of the three samples. The thermal conductivity value written in the table is the harmonic mean of all specimens, ± one standard deviation.

Age	Unit	Method	Number of Specimens	Lithology	λ_{av} (W/mK)
Middle Cambrian	Pantapinna Fm	Divided Bar	56	Sandstone/Quartzite	5.17 ± 0.98
Middle Cambrian	Billy Creek Fm	Divided Bar	39	Shale/Siltstone	2.52 ± 0.38
Early Cambrian	Wilkawillina LS	Divided Bar	19	Limestone	3.78 ± 0.71

Table 4. Surface heat flow measured in wells from this study.

Well	Heat flow (mW/m^2)
Edeowie 1	74 ± 7
Gollum 1	106 ± 2[A]
Sauron 1	120 ± 1
Nazgul 1	120 ± 1
Balrog 1	110 ± 2
Gandalf 1	95 ± 2[B]

[A]Gollum 1 displayed a departure from the conductive heat flow inversion model. While a conductive heat flow of 106 mW/m^2 provides a good fit with observed data (see Appendix 1), the best fit conductive model can be found by applying a heat flow of 80 mW/m^2 in the interval 250–340 m depth, and 111 mW/m^2 in the interval 340–500 m.

[B]Gandalf 1 also displayed a departure from the conductive heat flow inversion model. While a conductive heat flow of 95 mW/m^2 provides a good fit with observed data (see Appendix 1), the best fit conductive model can be found by applying a heat flow of 116 mW/m^2 in the interval 375–433 m depth, and 83 mW/m^2 in the interval 433–545 m.

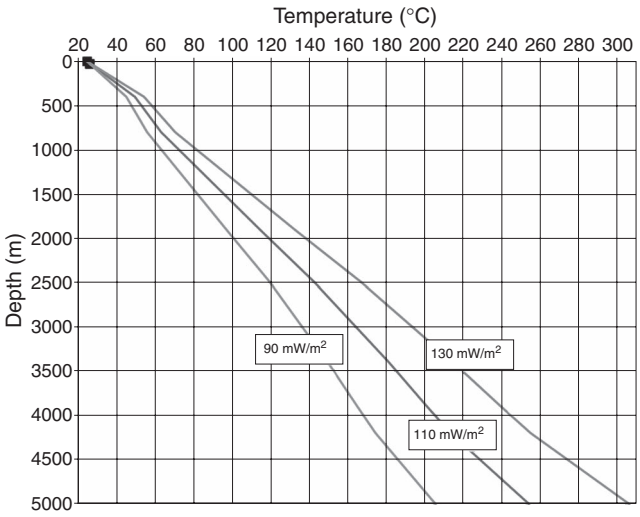

Fig. 6. Temperature modelling for the Parachilna area in the Torrens Hinge Zone. The modelling assumes a thermal conductivity profile derived from available published geological data and the weighted harmonic means of measured or assigned thermal conductivities. Three heat flow values were modelled: 90, 110 and 130 mW/m^2. Five of the six wells drilled in this study returned heat flow values between 95 and 120 mW/m^2. The average measured surface temperature was around 25°C.

Table 5. Parameters used in the 1D modelling of temperature to 5000 m depth beneath the study area. Thermal conductivity groupings have been assigned based on a) measured values on core specimens or assigned textbook values, and b) assumed proportions of each unit in the stratigraphic groupings.

Depths to the tops of each stratigraphic group were based on potential fields modelling and known thicknesses of the formations in nearby outcrops.

Stratigraphic grouping	Thermal conductivity (W/mK)	Top of grouping in modelled profile
Cainozoic	1.80	0
Cambrian	3.50	400
Late Marinoan	2.64	800
Early Marinoan	2.79	1900
Sturtian	3.37	2500
Torrensian	3.82	3400
Willouran	3.80	3900
Basement	3.04	4200

dataset, and thermal gradient data was repeatable over two separate surveys. Therefore, the departures from the conductive heat flow models in Gandalf and Gollum are attributed to modest advection at levels intersected by each of the wells. This effect is not considered to be significant in the overall results of the hypothesis test. There is no evidence that can be seen in this study of large scale deeper advective effects on the thermal regime.

The technique used to test the hypothesis is considered to be robust, and applicable to other geographical regions where there is EGS prospectivity. This technique is being used to map heat flow and EGS potential in other parts of the THZ, and has the potential to be utilised in regions in any part of the world where the thermal structure is dominated by conductive heat flow.

Armed with the data collected in this study, modelling was undertaken to estimate temperature at greater depths. The modelling method is based on the assumption that thermal energy, measured as conductive heat flow, remains relatively constant and predictable with depth, with minimal advection.

Once surface vertical heat flow was established, the temperature at greater depths (4000–5000 m) was predicted by building up a thermal conductivity profile to 5000 m depth. Using the weighted harmonic means of thermal conductivity values measured in this study and assigned textbook values for those units without sampled core, as well as unit thicknesses assigned from available published geological data, a range of temperature profiles was modelled in one dimension using heat flows of 90, 110 and 130 mW/m^2 respectively. The modelling shows a temperature range between 200 and 300°C at 5000 m depth (Figure 6).

Heat refraction laterally due to significant thermal conductivity contrast between adjacent geological units is not considered to be a source of significant uncertainty in this modelling due to the fact that there is no great difference between the thermal conductivity of the majority of the units in the model. Table 5 shows the parameters used in the modelling, including modelled stratigraphic thicknesses and bulk thermal conductivities.

Conclusions

It was hypothesised from geological and conductive heat flow principles that the THZ is likely to be a region of high average geothermal gradients and thus prospective for EGS geothermal energy.

The heat flow drilling programme designed to test the idea returned results that have validated this hypothesis.

The sediments have moderate thermal conductivity, and in the THZ are modelled to be between 2.5 and 7 km in total thickness. With this amount of moderate conductivity sediments overlying the crystalline Eastern Gawler Craton basement, plus its proximity to existing power infrastructure, the THZ is now considered prospective for economic EGS development.

The study area is part of a larger, elongate, geographical region with likely similar overall sedimentary and crystalline basement geometries (Figures 2, 3), and it is thought that the temperature field conditions in the Parachilna area may be repeated elsewhere in the THZ.

Acknowledgements

The author wishes to acknowledge several people. Dr Graeme Beardsmore provided teaching and guidance on the measurement and modelling of thermal gradient, thermal conductivity and heat flow in the study. Alex Musson and Andrew Alesci carried out thermal conductivity measurements on existing rock samples, and Professor Mike Sandiford imparted valuable knowledge on the nature and distribution of heat flow and temperature in Australian

Proterozoic terranes. The helpful reviewers' comments and suggestions provided by Prame Chopra, Doone Wyborn and one anonymous reviewer are greatly appreciated as well. Last but not least, the staff and directors of Torrens Energy Limited (especially John Canaris, Dennis Gee, Christine Sealing and Bruce Godsmark) are thanked for collaborating to facilitate the heat flow study and also allowing the results to be published here.

References

Allen, S. R., Simpson, C. J., McPhie, J., and Daly, S. J., 2003, Stratigraphy, distribution and geochemistry of widespread felsic volcanic units in the Mesoproterozoic Gawler Range Volcanics, South Australia: *Australian Journal of Earth Sciences*, **50**, 97–112. doi: 10.1046/j.1440-0952.2003.00980.x

Beardsmore, G. R., 2006, Thermal conductivity of Adelaide Geosyncline core samples. Unpublished report prepared for Torrens Energy Limited.

Belousova, E. A., Preiss, W. V., Schwarz, M. P., and Griffin, W. L., 2006, Tectonic affinities of the Houghton Inlier, South Australia: U-Pb and Hf isotope data from zircons in modern stream sediments: *Australian Journal of Earth Sciences*, **53**, 971–989. doi: 10.1080/08120090600880875

Beardsmore, G. R., and Cull, J. P., 2001, Crustal heat flow; a guide to measurement and modelling: Cambridge University Press.

Chopra, P. N., 2005, The status of the geothermal industry in Australia, 2000–2005. *Proceedings of the World Geothermal Congress*, Antalya, Turkey 24–29 April 2005.

Chopra, P. N., and Holgate, F., 2005, A GIS analysis of temperature in the Australian Crust. *Proceedings of the World Geothermal Congress*, Antalya, Turkey 24–29 April 2005.

Clauser, C., and Huenges, E., 1995, Thermal Conductivity of Rocks and Minerals. *In* T. J. Ahrens ed., *Rock Physics and Phase Relations – a Handbook of Physical Constants*, AGU Reference Shelf, Vol. 3, 105–126: American Geophysical Union, Washington, D.C.

Cull, J. P., 1982, An appraisal of Australian heat-flow data: *BMR Journal of Australian Geology and Geophysics*, **7**, 11–21.

Cull, J. P., and Conley, D., 1983, Geothermal gradients and heat flow in Australian sedimentary basins: *Bureau of Mineral Resources. Journal of Australian Geology and Geophysics*, **8**, 329–337.

Dalgarno, C. R., and Johnson, J. E., 1966, PARACHILNA map sheet. 1st Edition. South Australia Geological Survey Geological Atlas 1 : 250 000 Series, sheet SH 54–13.

de Vries, S., Fry, N., and Pryer, L., 2006, OZ SEEBASE Proterozoic Basins Study. Report to Geoscience Australia by FrOG Tech Pty Ltd.

Ferris, G. M., Schwarz, M. P., and Heithersay, P., 2002, The Geological Framework, Distribution and Controls of Fe-Oxide Cu-Au Mineralisation in the Gawler Craton, South Australia. Part I – Geological and Tectonic Framework. *In* Porter, T.M. ed., *2002 – Hydrothermal Iron Oxide Copper-Gold & Related Deposits*: *A Global Perspective*, volume 2; PGC Publishing, Adelaide.

Foden, J., Barovich, K., Jane, M., and O'Halloran, G., 2001, Sr-isotopic evidence for Late Neoproterozoic rifting in the Adelaide Geosyncline at 586 Ma: implications for a Cu ore forming fluid flux: *Precambrian Research*, **106**, 291–308. doi: 10.1016/S0301-9268(00)00132-7

Geodynamics Limited, 2009, Stage 1 – Proof of Concept Complete. ASX Announcement 31 March 2009. Available online at: http://www.geodynamics.com.au/IRM/Company/ShowPage.aspx?CPID=1947&EID=33944995&PageName=Proof of Concept Complete (accessed 13 June 2009).

Houseman, G. A., Cull, J. P., Muir, P. M., and Paterson, H. L., 1989, Geothermal signatures and uranium ore deposits on the Stuart Shelf of South Australia: *Geophysics*, **54**, 158–170. doi: 10.1190/1.1442640

McLaren, S., Sandiford, M., Hand, M., Neumann, N., Wyborn, L., and Bastrakova, I., 2003, The hot southern continent, heat flow and heat production in Australian Proterozoic terranes: *Geological Society of Australia. Special Publication*, **22**, 151–161.

McLaren, S., Sandiford, M., Powell, R., Neumann, N., and Woodhead, J., 2006, Palaeozoic intraplate crustal anatexis in the Mount Painter Province, South Australia: timing, thermal budgets and the role of crustal heat production: *Journal of Petrology*, **47**, 2281–2302.

Matthews, C. G., and Beardsmore, G. R., 2006, Heat flow: A uranium exploration and modelling tool? *MESA Journal 41 Primary Industries & Resources South Australia*, 2006, 8–10.

Matthews, C. G., and Beardsmore, G. R., 2007, New heat flow data from south-eastern South Australia: *Exploration Geophysics*, **38**, 260–269. doi: 10.1071/EG07028

Mawson, D., and Sprigg, R. C., 1950, Subdivision of the Adelaide System: *Australian Journal of Science*, **13**, 69–72.

Musson, A., and Alesci, A., 2007, Thermal conductivity, magnetic susceptibility and specific gravity measurements of core samples of the Adelaide 'Geosyncline' cover sequence. Unpublished report prepared for Torrens Energy Limited.

Neumann, N., Sandiford, M., and Foden, J., 2000, Regional geochemistry and continental heat flow; implications for the origin of the South Australian heat flow anomaly: *Earth and Planetary Science Letters*, **183**, 107–120. doi: 10.1016/S0012-821X(00)00268-5

Panax Geothermal Limited 2009 Penola Project – Australia's First Conventional Geothermal "Measured Resource". ASX Announcement 23 February 2009. Available online at: www.asx.com.au/asxpdf/20090223/pdf/31g66z1zrbr2j0.pdf (accessed 24 February 2009).

Pollack, H. N., Hurter, S. J., and Johnson, J. R., 1993, Heat flow from the Earth's interior: Analysis of the global data set: *Reviews of Geophysics*, **31**, 267–280. doi: 10.1029/93RG01249

Preiss, W. V., 1993, Basement inliers of the Mount Lofty Ranges. *In* Drexel J. F. Preiss W. V. and Parker A. J, eds., *The Geology of South Australia, Geological Survey of South Australia Bulletin* **54**, 51–105.

Preiss, W. V., 2000, The Adelaide Geosyncline of South Australia and its significance in Neoproterozoic continental reconstruction: *Precambrian Research*, **100**, 21–63. doi: 10.1016/S0301-9268(99)00068-6

Preiss, W. V., 2005, Mineral Explorers Guide: Primary Industries and Resources South Australia DVD Publication.

Reid, P., and Preiss, W. V., 1999, PARACHILNA map sheet. 2nd Edition. South Australia Geological Survey Geological Atlas 1 : 250 000 Series, sheet SH 54–13.

Roy, R. F., Blackwell, D. D., and Birch, F., 1968, Heat generation of plutonic rocks and continental heat-flow provinces: *Earth and Planetary Science Letters*, **5**, 1–12. doi: 10.1016/S0012-821X(68)80002-0

Somerville, M., Wyborn, D., Chopra, P., Rahman, S., Estrella, D., and van der Muelen, T., 1994, Hot dry rock feasibility study. Energy Research and Development Corporation (ERDC), Report 94/243, Canberra, ACT, Australia.

Sass, J. H., and Lachenbruch, A. H., 1979, Thermal regime of the Australian Continental Crust. *In* M.W. McElhinny ed., *The Earth: its origin, structure and evolution*. Academic Press, London.

Torrens Energy Limited, 2008, 780 000 PJ Inferred Resource, Parachilna Project, South Australia. ASX Announcement 20 August 2008. Available online at: http://www.asx.com.au/asxpdf/20080820/pdf/31bsp0dcmt4sw0.pdf (accessed 20 August 2008).

Manuscript received 21 April 2009; accepted 15 July 2009.

Appendix 1

Modelling of thermal gradient and thermal conductivity data for the purpose of estimating heat flow in the wells from this study.

Modelled versus measured thermal gradient in well Balrog 1. The partitioned line on the left hand graph shows a modelled gradient from a conductive heat flow 110 mW/m^2 and thermal conductivities measured every 7 m, with the solid line being the measured geotherm in the well. The right hand graph shows the full geotherm in the well with the modelled geotherm overlain.

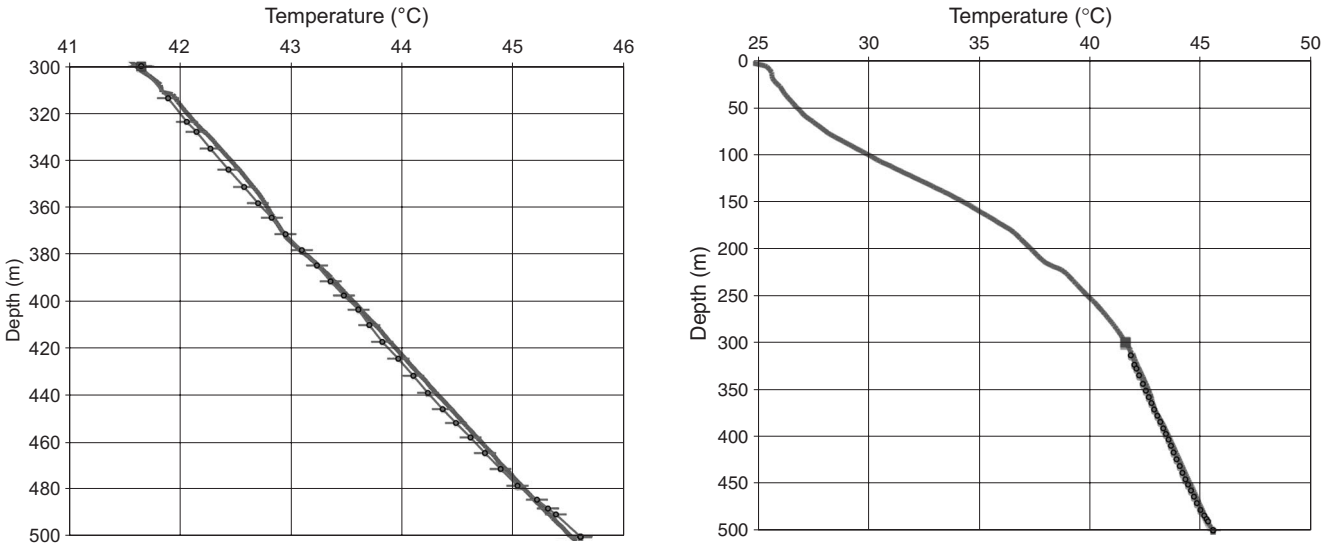

Modelled versus measured thermal gradient in well Gandalf 1. The partitioned line on the right hand graph shows a modelled gradient from a conductive heat flow of 95 mW/m^2 and thermal conductivities measured every 7 m, with the solid line being the measured geotherm in the well. Gandalf 1 displayed a departure from the conductive heat flow inversion model. The best fit conductive model can be found by applying a heat flow of 116 mW/m^2 in the interval 375–433 m depth, and 83 mW/m^2 in the interval 433–545 m. The left hand graph shows the alternative interpretation where heat is added by advection at ~430 m depth.

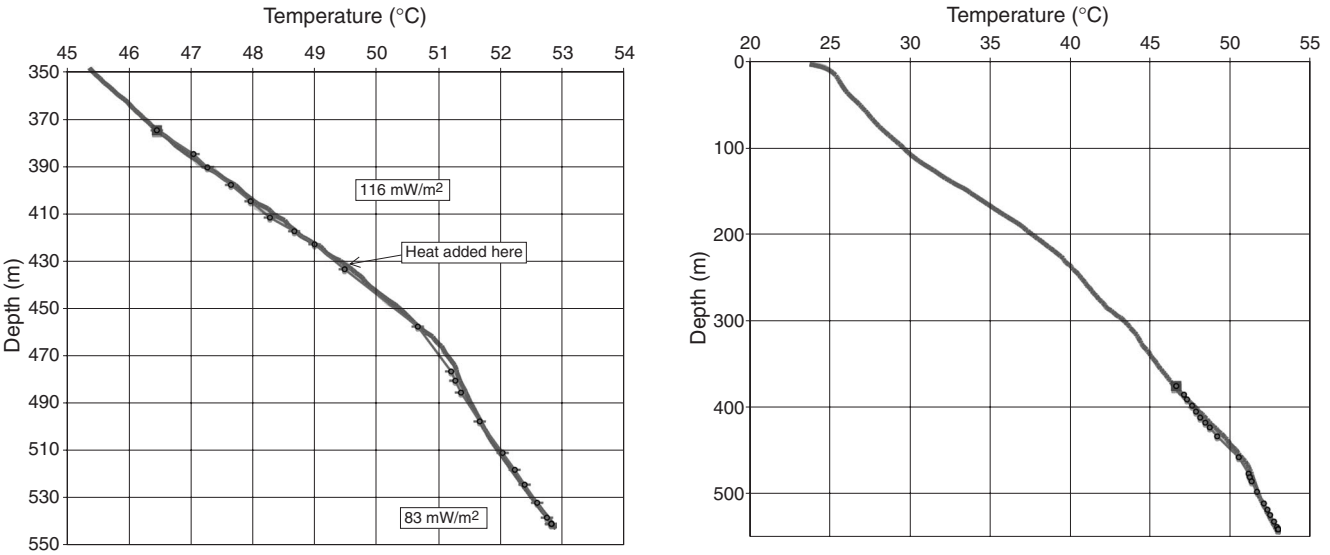

Modelled versus measured thermal gradient in well Edeowie 1. The partitioned line shows a modelled gradient from a conductive heat flow 74 mW/m^2 and thermal conductivities measured on available core samples, with the solid line being the measured geotherm in the well.

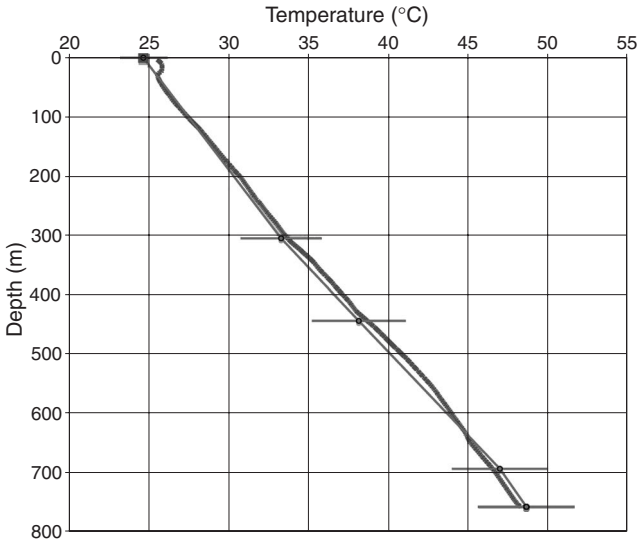

Modelled versus measured thermal gradient in well Nazgul 1. The partitioned line on the left hand graph shows a modelled gradient from a conductive heat flow 120 mW/m^2 and thermal conductivities measured every 7 m, with the solid line being the measured geotherm in the well. The right hand graph shows the full geotherm in the well with the modelled geotherm overlain.

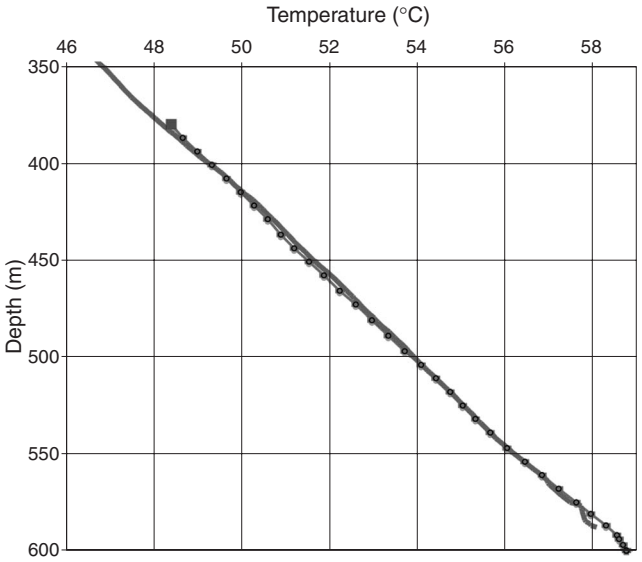

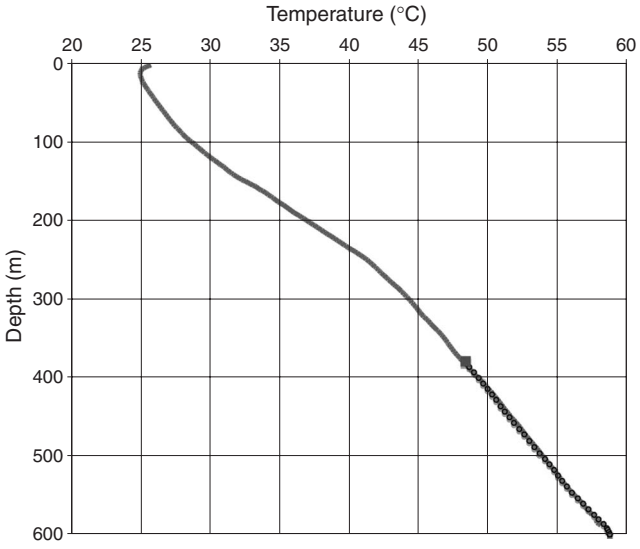

Modelled versus measured thermal gradient in well Sauron 1. The partitioned line shows a modelled gradient from a conductive heat flow 120 mW/m^2 and equivalent modelled thermal conductivity profile as that in Nazgul 1, with the solid line being the measured geotherm in the well.

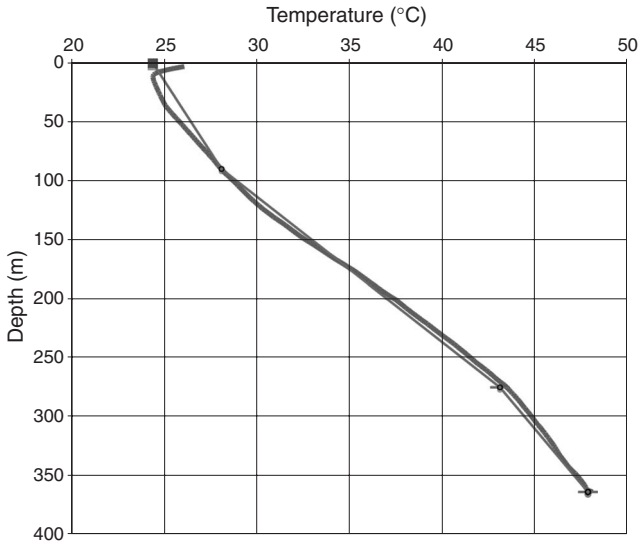

Modelled versus measured thermal gradient in well Gollum 1. The partitioned line on the right hand graph shows a modelled gradient from a conductive heat flow of 106 mW/m^2 and thermal conductivities measured every 7 m, with the solid line being the measured geotherm in the well. Gollum 1 displayed a departure from the conductive heat flow inversion model. The best fit conductive model can be found by applying a heat flow of 80 mW/m^2 in the interval 250–340 m depth, and 111 mW/m^2 in the interval 340–500 m. The left hand graph shows this alternative interpretation where heat is removed by advection at ~340 m depth.

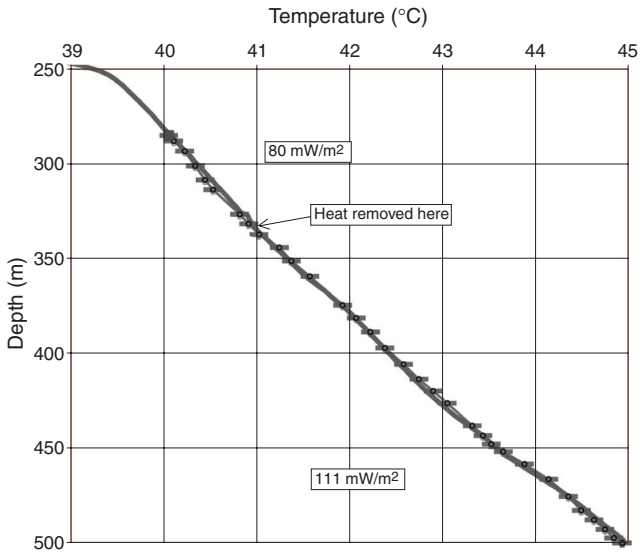

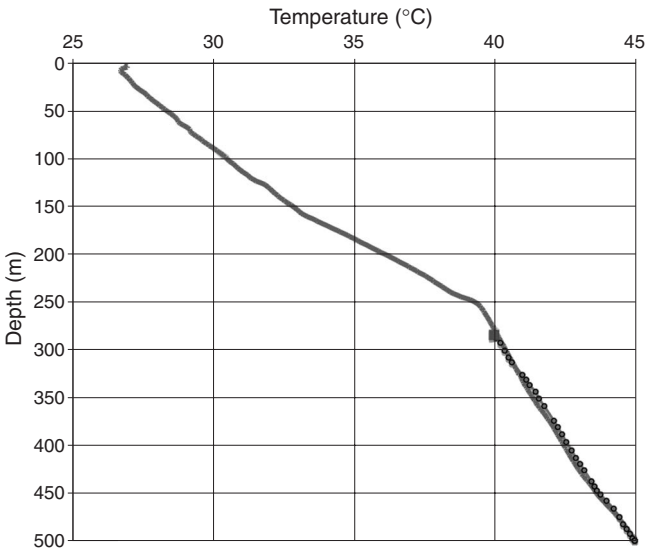

Declaration for Thesis Chapter 6

Declaration by candidate

In the case of Chapter 6, the nature and extent of my contribution to the work was the following:

Nature of contribution: Main research, data collection and processing, interpretation and preparation of manuscript
Extent of contribution (%): 70%

The following co-authors contributed to the work.

Name:	**Dr Graeme Beardsmore**
Nature of contribution:	**Data collection and processing**
Name:	**Jim Driscoll**
Nature of contribution:	**Data processing, modelling**
Name:	**Nicky Pollington**
Nature of contribution:	**Modelling**

Candidate's Signature

Date

Declaration by co-authors

The undersigned hereby certify that:

(1) the above declaration correctly reflects the nature and extent of the candidate's contribution to this work, and the nature of the contribution of each of the co-authors.
(2) they meet the criteria for authorship in that they have participated in the conception, execution, or interpretation, of at least that part of the publication in their field of expertise;
(3) they take public responsibility for their part of the publication, except for the responsible author who accepts overall responsibility for the publication;
(4) there are no other authors of the publication according to these criteria;
(5) potential conflicts of interest have been disclosed to (a) granting bodies, (b) the editor or publisher of journals or other publications, and (c) the head of the responsible academic unit; and
(6) the original data are stored at the following location(s) and will be held for at least five years from the date indicated below:

Location: **Hot Dry Rocks Pty Ltd, South Yarra, Victoria**

Signature 1—Graeme Beardsmore [redacted]

Date 23 April 2013

Signature 2—Jim Driscoll

Date 12 MAY 2013

Signature 3—Nicky Pollington

Date 22/4/2013

CSIRO PUBLISHING

Exploration Geophysics, 2013, **44**, 133–144
http://dx.doi.org/10.1071/EG12052

Heat flow data from the southeast of South Australia: distribution and implications for the relationship between current heat flow and the Newer Volcanics Province

Chris Matthews[1,2,3,4,5] Graeme Beardsmore[4] Jim Driscoll[4] Nicky Pollington[4]

[1]School of Geosciences, Monash University, Clayton, Vic. 3800, Australia.
[2]South Australian Centre for Geothermal Energy Research, The University of Adelaide, Adelaide, SA 5005, Australia.
[3]Panax Geothermal Ltd, Level 2, 139 Frome Street, Adelaide, SA 5000, Australia.
[4]Hot Dry Rocks Pty Ltd, PO Box 251, South Yarra, Vic. 3141, Australia.
[5]Corresponding author. Email: [redacted]

Abstract. This paper presents the results of 34 new heat flow estimates taken in 2004 from 16 water bores and 18 petroleum exploration wells in the western Otway Basin. The average estimated heat flow measured across the study area is 65.6 ± 9.4 mW/m^2, with a range of 42–90 mW/m^2. There are three recognisable sectors within the study area where heat flow is slightly elevated relative to the background levels. These sectors can be broadly classified as Mount Schank (73.5 ± 0.5 mW/m^2), Mount Burr (71.2 ± 7.6 mW/m^2) and Beachport (78.3 ± 10.4 mW/m^2). Thermal conductivity values for each unit involved in heat flow estimation were determined from laboratory measurements on representative core using a divided bar apparatus. Borehole thermal conductivity profiles were then developed in this study by assigning a constant value of conductivity to each geological formation. The process of collecting temperature data involved measuring temperature profiles for 16 water bores using a cable, winch and thermistor, and compiling well completion temperature data from 18 petroleum wells. The precision of temperature data was higher in the water bores (continuous logs) than in the petroleum wells (largely bottom-of-hole temperature estimates). Inversion heat flow modelling suggests heterogeneous heat flow at 6000 m depth, with two zones where vertical heat flow might exceed 90 mW/m^2, and several zones where vertical heat flow might be as low as 40 mW/m^2. Therefore, while slightly higher surface heat flow does coincide with some of the volcanic centres, heterogeneous basement heat production is a more likely explanation, as there are no heat flow anomalies greater than 5–10 mW/m^2 associated with the Pleistocene–Recent Newer Volcanics Province. The distribution of heat flow in south-east South Australia is most simply explained by non-volcanic phenomena.

Key words: Australia, Delamerian Fold Belt, geothermal modelling, heat flow, Newer Volcanics Province, Otway Basin, thermal conductivity, thermal gradient.

Received 20 August 2012, accepted 12 March 2013, published online 22 April 2013

Introduction and aim

This paper presents the results of heat flow estimates taken in 2004 as the first part of a research programme aimed at mapping the distribution of heat flow in south-east South Australia. The heat flow in this region is of considerable interest to science, society and the energy industry. This is a companion paper to Matthews and Beardsmore (2007), which presented the results of heat flow estimates taken in an adjacent part of the south-east of South Australia. Groundwater observation wells across the study area were used, along with petroleum wells in the Otway Basin (Figure 1), to measure thermal gradients and estimate 34 new heat flow values.

The significance to science is due to the complex geological history of the region, with multiple geological events spanning from the Mesoproterozoic to today. One of the most intriguing aspects of the geology is the enigmatic Pleistocene–Recent Newer Volcanics Province (NVP). Understanding the distribution of surface heat flow is a key to understanding how Recent volcanism has influenced the heat flow and temperature of the crust in the NVP.

Surface heat flow is also an important control on geothermal energy prospectivity (the search for higher than average geothermal gradients), and the present Australian heat flow dataset is insufficient to resolve exploration targets at a prospect scale. Only a handful of high spatial resolution studies have been published in Australia (e.g. Houseman et al., 1989; Beardsmore, 2005; Torrens Energy Limited, 2008; Matthews and Beardsmore, 2007; Matthews, 2009). The study area has contained geothermal exploration acreage since 2004, and the region continues to hold significant interest for the geothermal energy sector.

Surface heat flow (Q_s) represents the combined flow of thermal energy from two sources: heat flowing from the mantle of the earth (reduced heat flow q_r), and heat actively generated in the crust by the decay of radioactive isotopes of elements such as U, Th and K (q_c). Stated simply:

$$Q_s = q_r + q_c \quad (1)$$

The aim of this study was to combine the water bore and petroleum well data into a single, consistent dataset of heat flow values. Heat flow is the product of thermal gradient with thermal conductivity (equation 2). The two methods used to estimate heat flow in the study area are described below in *Modelling of heat flow values*.

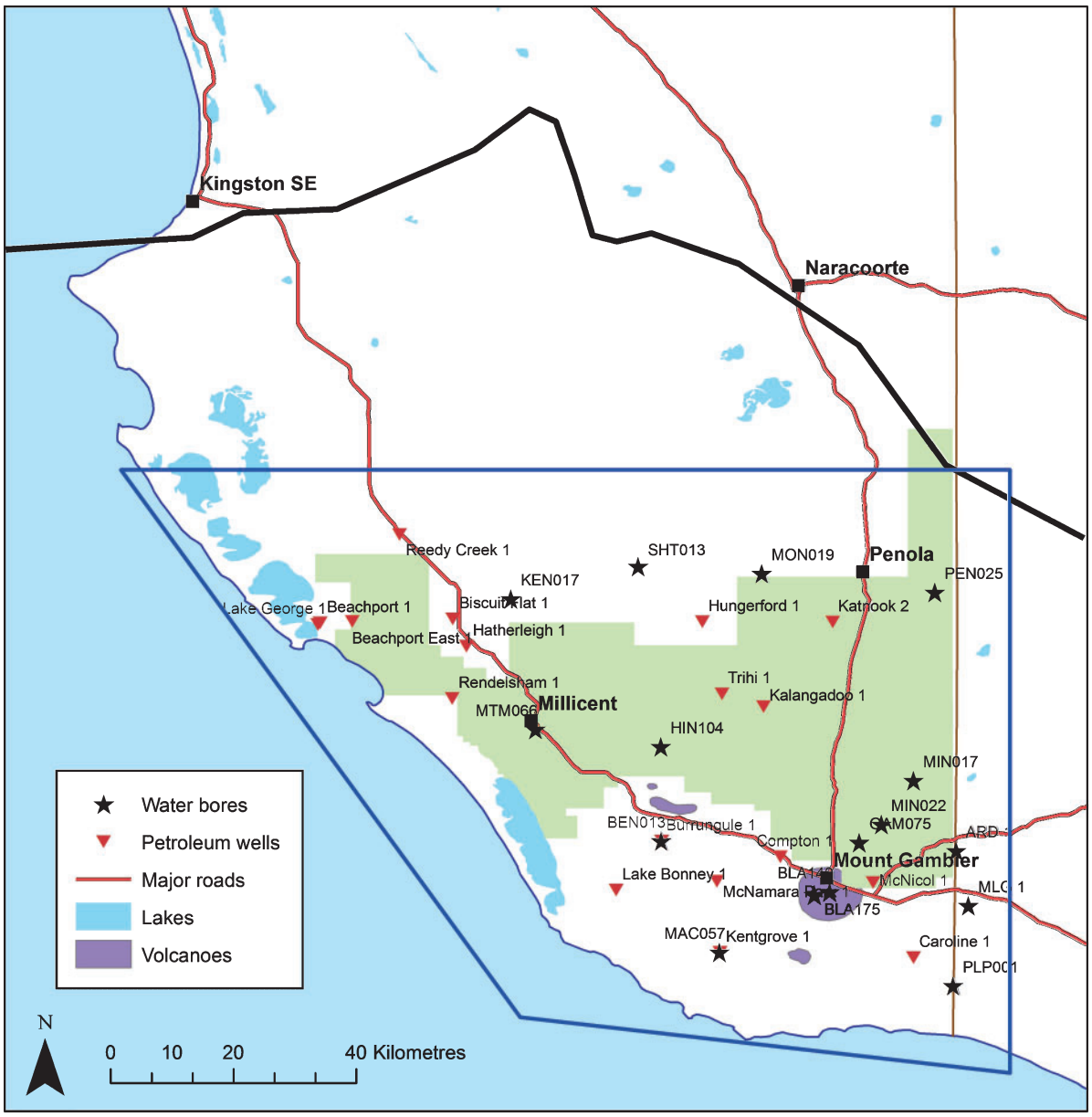

Fig. 1. Southeast South Australia, showing locations and names of all water bores and petroleum wells examined in this study. The black line running just south of Naracoorte and Kingston SE outlines the northern margin of the Otway Basin in South Australia. The study area is outlined in blue, while the area that is the subject of 3D modelling (see *Results*) is shaded in green.

Heat conduction is the movement of energy through solid surfaces by the transfer of kinetic energy between particles (e.g. Beardsmore and Cull, 2001). It is assumed to be the dominant mode of heat transport in the crust, while advection, the mass transport of heat associated with the physical motion of materials, dominates in the mantle. The magnitude of vertical conductive heat flow, Q_s, at the Earth's surface can be calculated (e.g. Beardsmore and Cull, 2001):

$$Q_s = \lambda_z \beta_z + \sum A \qquad (2)$$

where λ_z = thermal conductivity (W/mK) at depth z, a physical property of the rocks; β_z = vertical geothermal gradient (K/m) at depth z, the rate of change in temperature per metre depth; $\lambda_z \beta_z$ = heat flow at depth z (mW/m^2); A = internal heat generation (W/m^3) by the decay of radioactive elements; $\sum A$ = the cumulative rate of heat generated over the interval between the surface and depth z (W/m^2).

Average conductive heat flow over a depth interval is the product of average thermal conductivity and thermal gradient over the same depth interval, commonly the interval defined by a borehole.

Where present, the mass flow of groundwater through rocks can invalidate the assumption of conductive heat flow by carrying heat through advective processes. Such processes can be recognised as anomalies on temperature gradient logs. No such anomalies were observed deeper than the permeable surface limestone units intersected in the top few tens of metres in many boreholes examined in this study. In the absence of any evidence to the contrary beneath this layer, the authors have assumed conductive heat flow dominates the thermal regime of the study area.

Geological framework of the study area

The study area has a complex geological history, including Early Palaeozoic sediment deposition and a subsequent orogenic event

with associated igneous activity; Mesozoic rifting and associated basin formation that continued into the Neogene; Late Neogene to Recent compressive tectonics; and finally ongoing Pleistocene–Recent enigmatic mafic volcanism (Figures 1 and 2). Figures 3 and 4 present the general stratigraphic framework for the region.

Cambro-Ordovician Delamerian Fold Belt

Crustal basement to the study area comprises sediments and volcanic deposits of Cambrian age (Jensen-Schmidt et al., 2002). The sediments were deposited in Early Cambrian rifting before the Late Cambrian–Early Ordovician orogenic event known as the Delamerian Orogeny (e.g. Jenkins and Sandiford, 1992), while igneous activity during and immediately following the Delamerian Orogeny resulted in the emplacement of mafic to felsic intrusives and extrusives (Jensen-Schmidt et al., 2002).

Mesozoic–Tertiary rifting

The Otway Basin developed as part of the Bassian rift between Australia and Antarctica from the Late Jurassic to Late Cretaceous (Figure 2). The 'initial fracturing' episode was in the Late Jurassic to Early Cretaceous, resulting in a series of deep troughs of the Crayfish Group (Figure 4). (Boult, 2002; O'Brien et al., 1994; Miller et al., 2002).

True continental rifting between Australia and Antarctica began, and the southern Australian passive continental margin developed, during the early Late Cretaceous. Major extension and subsidence occurred south of the Tartwaup Fault Zone (TFZ; fig. 2, Geoscience Australia, 2012; Morton and Drexel, 1995). Following the Late Cretaceous rifting, subsidence continued through the Palaeocene and into the Eocene (65–44 Ma). During the period 44–35 Ma, sea floor spreading rapidly increased and the Otway margin subsided, leading to an increase in sedimentation rate (O'Brien et al., 1994).

The Katnook Sandstone, a braided fluvial sandstone, thickens to the north-west, essentially as a sandy facies of the Laira Formation, a lacustrine shale and siltstone with minor meandering fluvial sands. The Pretty Hill Formation is dominantly a sandstone package that occurs in the deepest parts of the troughs. On the extreme northern margin of the Otway Basin, both the Katnook Sandstone and Pretty Hill Formation are absent and the Early Cretaceous Crayfish Group comprises the Laira Formation only.

The Otway Supergroup represents the sediments formed during the late Early Cretaceous. The dominant unit, the Eumeralla Formation, is a meandering fluvial, lacustrine and back-swamp siltstone–shale sequence with some minor coal and sandstone units. It gradually thickens and deepens to the south. The Windermere Sandstone Member is a regionally extensive but thin sand unit that lies at the base of the Eumeralla Formation (O'Brien et al., 1994).

The Late Cretaceous Sherbrook Group is a deltaic wedge that thickens to the south. In the northern part of the basin, where the group is thin, it occurs as coarse sandstone.

The Palaeocene to Eocene Wangerrip Group consists of the Pebble Point Formation, Pember Mudstone and Dilwyn Formation. The Pebble Point Formation is a ferruginous, shoaling-upward, deltaic succession of fine to very coarse-grained, argillaceous sandstone, while the Pember Mudstone consists of micaceous silty claystone and minor fine-grained sandstone (O'Brien et al., 1994). The Dilwyn Formation is a siliciclastic unit, unconsolidated in parts, and is stratified with interbedded sands, gravels, clays and shales. In the Mount Gambier area the Dilwyn Formation is composed of mainly sands and gravels in the northern parts, while containing more clay and shale horizons further to the south (Love et al., 1993).

The Eocene Narrawaturk Marl includes partly glauconitic, grey–brown limestone and marl, silty mudstones, and dolomitic limestone. The Mepunga Formation comprises mixed carbonate

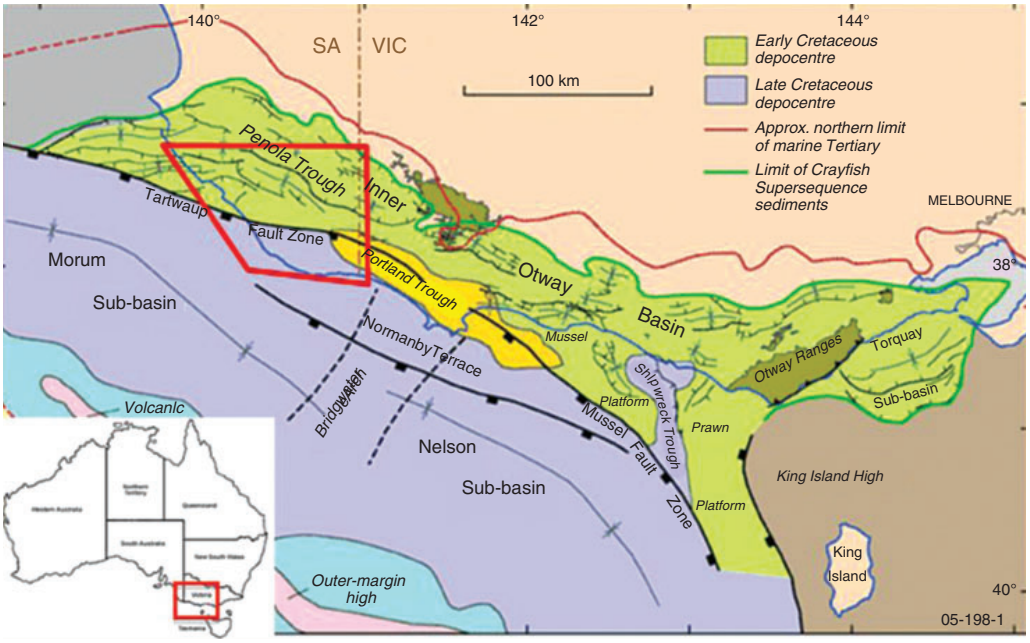

Fig. 2. The Late Jurassic–Cainozoic Otway Basin formed during the Bassian Rift between Australia and Antarctica. The basin formed in two major phases, with the earlier phase manifesting in half-graben trough structures near the northern margin (e.g. the Penola Trough in the study area), known in the above figure as the Inner Otway Basin. The later phase was focussed south of the Tartwaup-Mussel Fault Zone, and was a rifting event that spanned from the Late Cretaceous into the Tertiary, when true continental break up occurred. The Basin has a maximum total sediment thickness of ~13,000 m (Geoscience Australia, 2012). The study area is outlined in red.

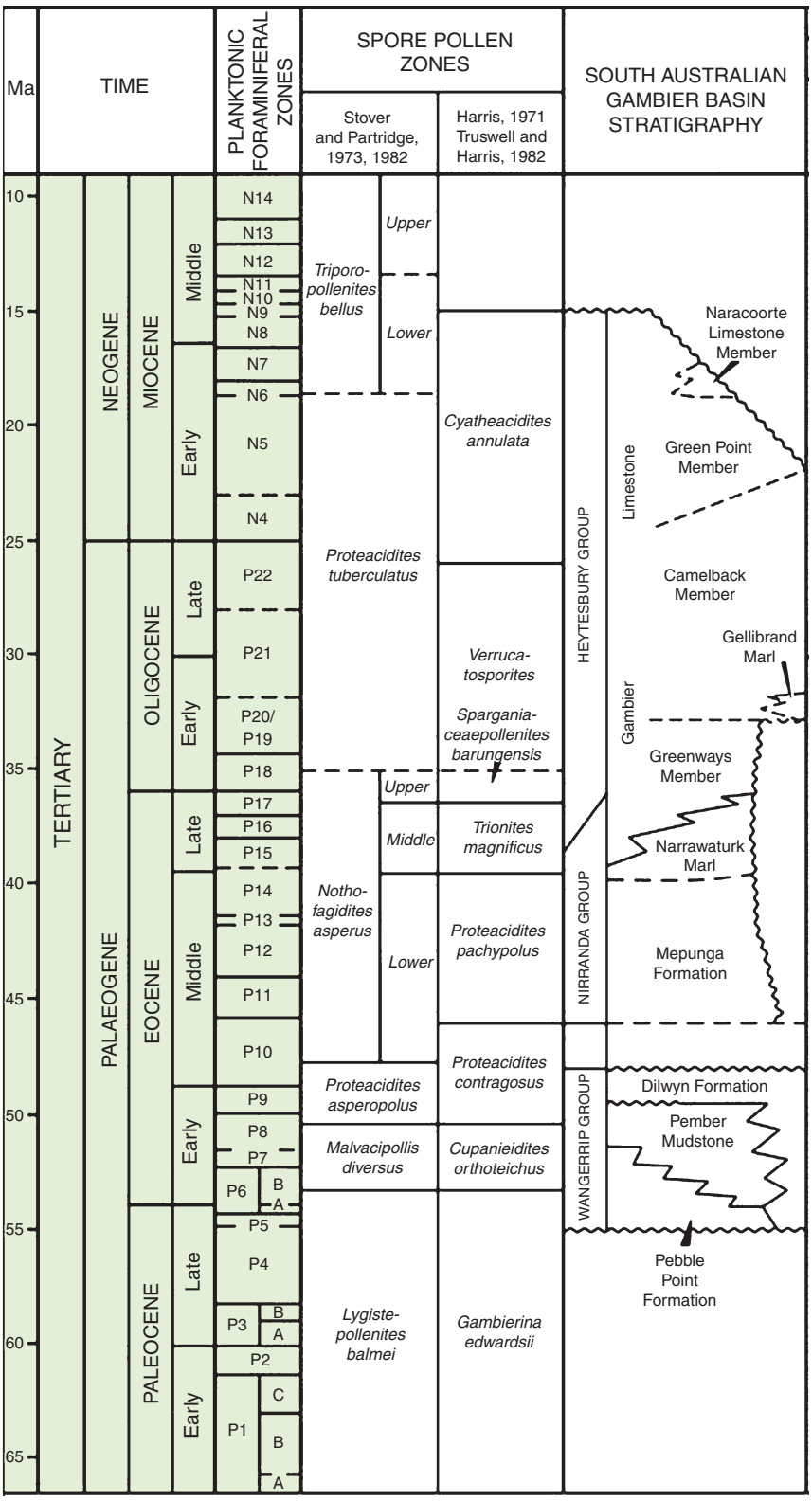

Fig. 3. Lithostratigraphic column of the Gambier sub-Basin (from White (1996)).

and siliciclastic sediments, predominantly sandstone and silty mudstone (Gallagher and Holdgate, 2000).

The Gambier Limestone is subdivided into three parts, and spans in age from Late Eocene to Miocene. The three members are the Greenways, Camelback and Green Point Members (Figure 3). The unit consists of grey to cream, bryozoal limestone, grey to pink dolomite and marl. The thin Compton Conglomerate separates the Greenways from the overlying Camelback Member (Li et al., 2000).

Neogene–Recent orogenic activity

Southeast Australia is currently in a compressive stress regime (e.g. Denham et al., 1981; Perincek and Cockshell, 1995; Dickinson et al., 2002; Sandiford, 2003*a*) that began in the

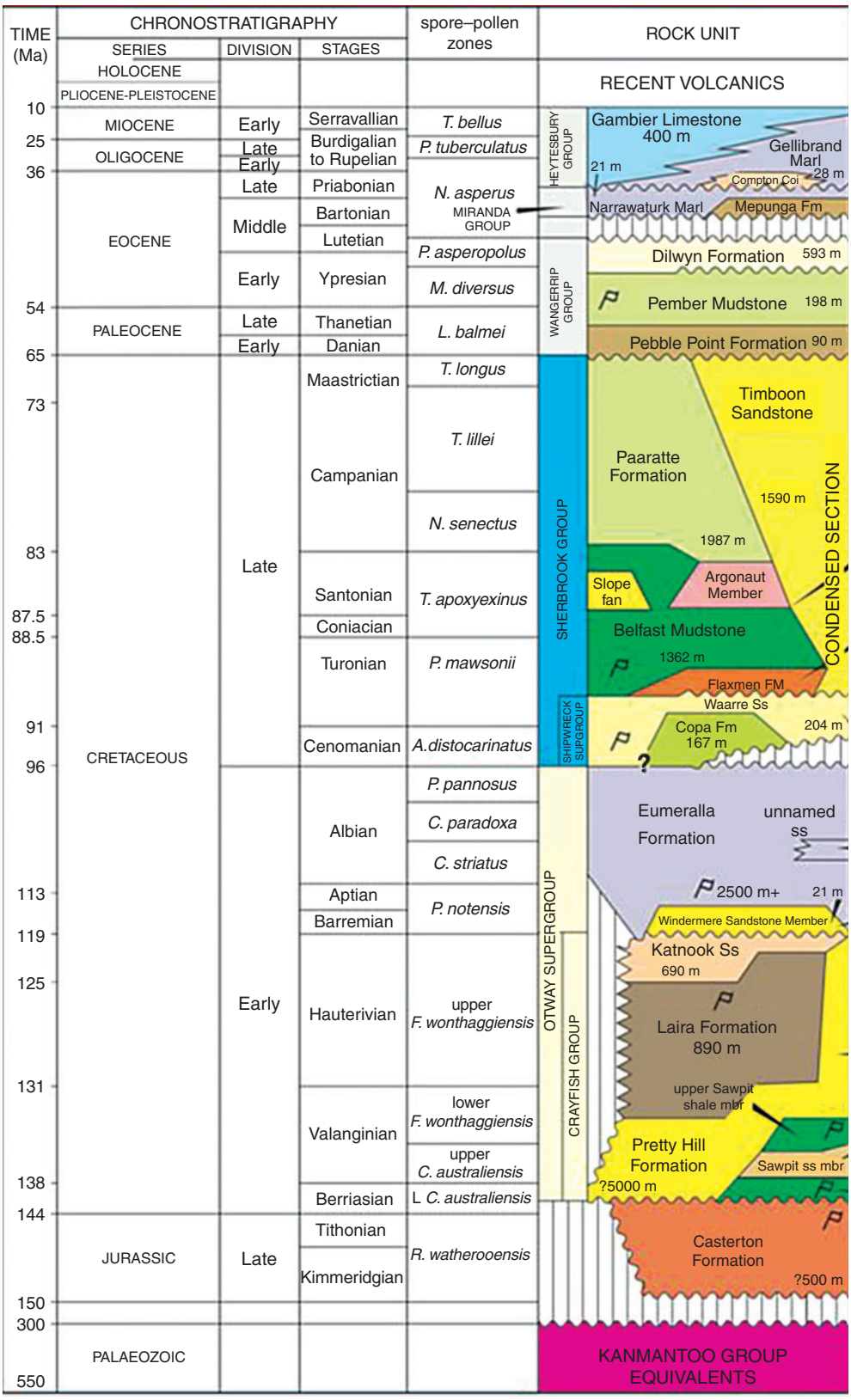

Fig. 4. Stratigraphic column for the Western Otway Basin (from Boult (2002)).

period between 12 and 5 Ma. The compressive stress is generated by orogenic activity on the Australian–Pacific Plate boundary in the vicinity of the South Island of New Zealand (Sandiford, 2003*a*), and on the northern margin of the Australian plate (e.g. Woodhead et al., 2010).

The principal direction of the current compressive stress regime in south-east Australia is approximately E–W to NW–SE (Denham et al., 1981; Coblentz et al., 1995; Hillis et al., 1999; Dickinson et al., 2002; Sandiford, 2003*b*). Pre-existing Bassian Rift extensional structures are being

reactivated in the reverse sense (Dickinson et al., 2002; Sandiford, 2003*a*). In the study area there has been 40–90 m of uplift in the last million years (Murray-Wallace et al., 1998).

Pleistocene–Recent mafic volcanism – the Newer Volcanics Province

The Newer Volcanics Province (NVP) of western Victoria and south-east South Australia is a 15,000 km^2, 450 km long east–west zone of eruption centres. There are ~400 separate volcanic vents identified (Johnson and Wellman, 1989). Their longitudinal distribution is almost identical to the Otway Basin, stretching from a line almost due north of Melbourne to the western end of the Mount Burr Range in south-east South Australia, and can be grouped into three regions: the Central Highlands Province and Western Plains in Victoria, and the South Australian Mount Gambier Zone (Figure 5; van Otterloo, 2011).

The origin and mechanism for formation of the NVP are unclear. The NVP lies in an intraplate setting and the distribution of volcanic centres appears to be controlled in part by crustal weaknesses (Cas, 1989; Perincek and Cockshell, 1995). The theory for the origin of the NVP that best fits the available evidence at this stage is the thermal stimulation of the lower crust by a mantle-derived heat source such as a mantle hotspot (Sutherland, 1981; Cas, 1989).

In the study area there are 18 large-scale vent locations. Most of them are in the Mount Burr Range area west of Mount Gambier (Figures 1 and 5), with the remainder at Mounts Gambier and Schank. A possible submarine or subterranean volcanic centre is postulated to exist off the coast in the western section of the study area (Sprigg, 1959). The reported ages of the South Australian NVP volcanoes range from 20,000–1,000,000 years for the Mount Burr Volcanics (Sheard and Nicholls, 1989), and Holocene for Mount Gambier and Mount Schank.

Methods

Thermal conductivity data

The authors took the approach of assigning a single representative thermal conductivity value to each stratigraphic unit in the study area. The values were all derived from laboratory measurements on core samples using a divided bar apparatus with an accuracy of ±2%. All samples were placed under >95% vacuum for a minimum of three hours. Samples were then submerged in water before returning to atmospheric pressure.

Saturation continued at atmospheric pressure for a minimum of twelve hours, and all samples were left submerged in water until just before conductivity measurement. Thermal conductivity was measured along the long axis of the core. Measurements were conducted at a mean temperature of 25°C (± 2°C). Harmonic mean conductivity and one standard deviation uncertainty were calculated for each specimen (Hot Dry Rocks Pty Ltd, 2012).

For some formations (e.g. the Gambier Limestone), enough samples were measured to gain statistical confidence in the mean value. For other formations, conductivity was assigned according to lithological composition and measurements made on 'pure' lithologies. For example, a formation with 75% shale and 25% sandstone was assigned a weighted average conductivity of measured shale and sandstone values.

Units encountered in water bores

Gambier Limestone and Compton Conglomerate. While several samples were taken from each Member, a lack of detailed geological logging from most wells in the study led to the assignment of a single mean conductivity value to all intervals of the Gambier Limestone in our heat flow modelling. Thermal conductivity was measured on a total of 52 samples from the three members. It was the dominant unit encountered in the water bores, and was therefore the most important unit in the estimation of heat flow in the water bores. The mean (and one standard deviation) thermal conductivity value of 1.50 ± 0.25 W/mK was derived from the individual measurements.

Narrawaturk Marl and Mepunga Formation. For the Narrawaturk Marl a thermal conductivity value of 1.79 ± 0.10 W/mK was derived from six measurements from wells in both the South Australian and Victorian sections of the Otway Basin. For the Mepunga Formation a thermal conductivity value of 2.29 ± 0.24 W/mK was derived from six measurements from wells in both the South Australian and Victorian sections of the Otway Basin.

Dilwyn Formation. The thermal conductivity of the Dilwyn Formation was difficult to measure and estimate, because units within the formation are often unconsolidated and therefore very difficult to sample and accurately measure. A thermal conductivity value of 2.06 ± 0.73 W/mK was estimated based on four measurements conducted on poorly consolidated samples from the South Australian section of the Otway Basin.

Units encountered in petroleum wells

The lithological units (and ages) encountered by petroleum wells assessed in the study included the units described above from the water bores, but also included the remainder of the Wangerrip Group, the Sherbrook Group and the Otway Supergroup of the Otway Basin (Figure 4).

Wangerrip Group. The units of the Wangerrip Group are not well represented in core, and are variable in lithology across the Basin, so a value of 2.42 ± 0.25 W/mK was assigned to the two members of this group based on the assigned value for the Sherbrook Group (discussed below).

Sherbrook Group. Estimating representative thermal conductivity values for the Sherbrook Group posed particular issues since the majority of its formations are laterally variable in lithological composition. We calculated the mean conductivity of all Sherbrook Group samples and used this as a proxy value for the Group at all locations. A universal value of 2.42 ± 0.25 W/mK was derived from the mean and standard deviation of 53 individual measurements on widely spread samples from both the South Australian and Victorian sections of the Otway Basin.

Otway Supergroup. A thermal conductivity value of 1.97 ± 0.11 W/mK was derived for the Eumeralla Formation from 22 individual measurements in wells from both the South Australian and Victorian sections of the Otway Basin. For the Windermere Sandstone Member, a value of 2.60 ± 0.52 W/mK was derived from nine measured values from intra-Eumeralla sand units.

Crayfish Group. For the Pretty Hill Formation, the dominant and key member of the Group, a value of 2.80 ± 0.20 W/mK was derived from 10 measured values from South Australian and Victorian Otway Basin wells. The Katnook Sandstone was assigned the same conductivity value as the Pretty Hill Formation. The Laira Formation was given a value of 2.55 ± 0.20 W/mK based on eight measured values from the Penola Trough (Figure 2).

Basement. For the Cambrian metasedimentary units, a value of 3.44 ± 0.13 W/mK was derived from nine measured values from South Australian wells that encountered basement units. Granite basement was sampled from cored holes in the Padthaway Ridge region on the northern margin of the Otway Basin, and a

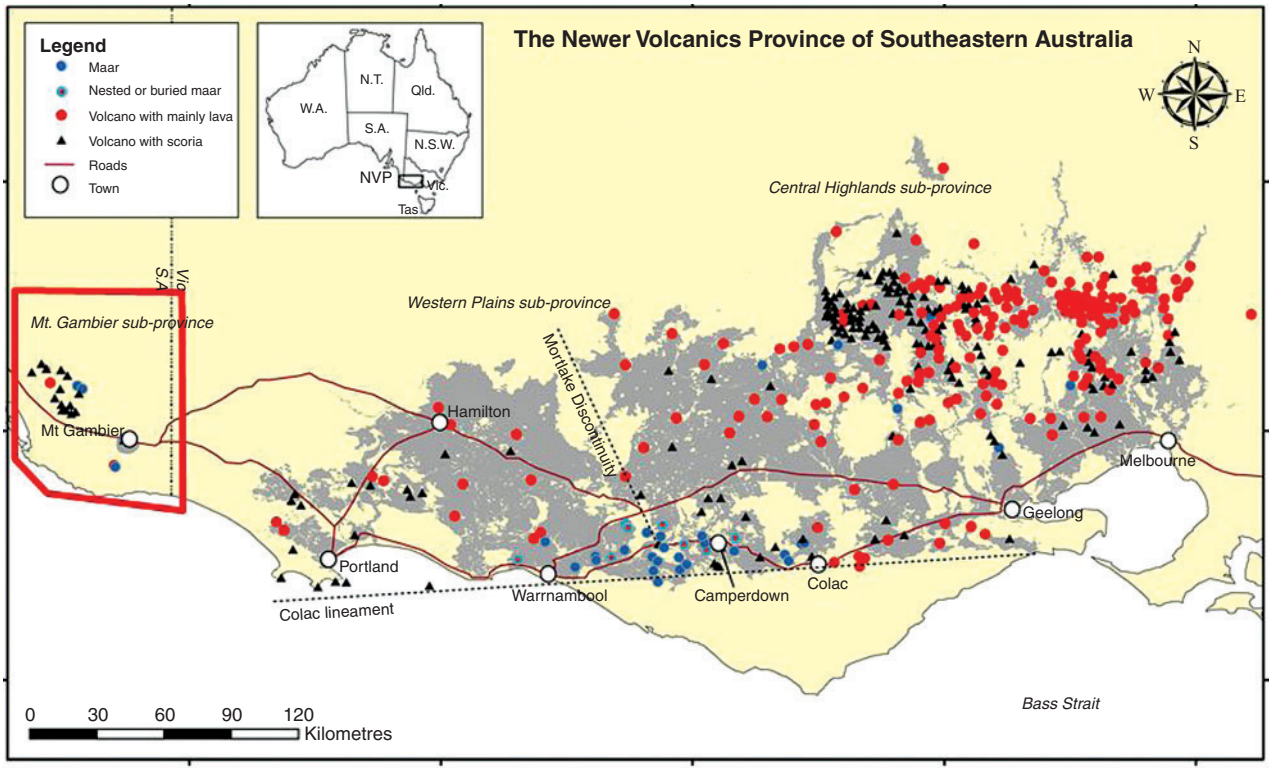

Fig. 5. Volcano type and distribution in the NVP of Victoria and South Australia (after van Otterloo (2011)). The study area is outlined in red at the western end of the map, and contains 18 volcanic occurrences.

mean and standard deviation of 3.06 ± 0.13 W/mK was derived based on four measured values.

Temperature data collection

The process of collecting temperature data involved measuring temperature profiles for 16 water bores using a cable, winch and thermistor, and compiling well completion temperature data from 18 petroleum wells (Figure 1). The precision of temperature data was higher in the water bores (continuous logs) than in the petroleum wells (largely bottom-of-hole temperature estimates).

Temperature from water bores

The standing water level and salinity of groundwater aquifers in south-east South Australia are regularly monitored through a network of bores called 'Obswells'. These cased and capped boreholes remain undisturbed between quarterly salinity and level readings. We utilised this network to measure geothermal gradients to a maximum depth of 450 m below surface.

We first collected a temperature log (e.g. Figure 6) from within each water bore by measuring temperature at discrete depth intervals (1–2 m) from the surface to the bottom of the hole. Temperatures were measured to a precision of ± 0.001°C and an absolute accuracy of ± 0.01°C using a thermistor probe on the end of 1000 m of cable, calibrated between 15 and 55°C. Depth was determined to within 0.02 m using a mechanical trip meter on the borehole collar.

Temperature from petroleum wells

For the petroleum wells in the study area, equilibrium bottom hole temperatures (eBHT) were estimated from data in well completion reports. This was achieved through Horner Plot correction (Lachenbruch and Brewer, 1959) of measured BHTs and temperatures collected during drill stem tests (DST), repeat

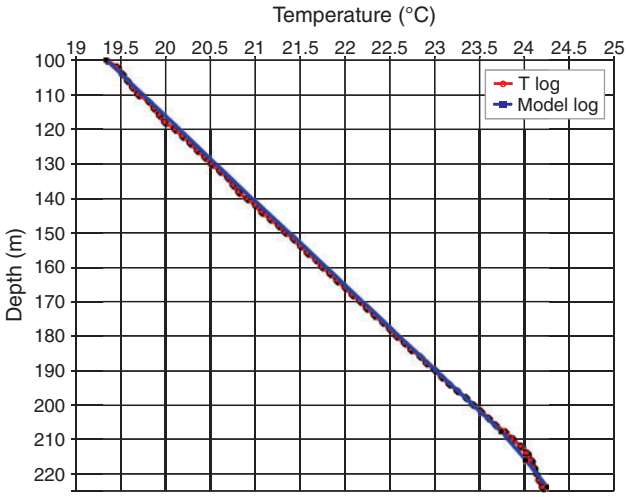

Fig. 6. Heat flow modelling file for water bore KEN 17. The *x*-axis is temperature in °C and the *y*-axis depth in m. The red graduated line represents the precision temperature log, and the clear change in gradient between 215 and 225 m depth reflects the change between the less conductive Narrawaturk Marl and the more conductive underlying Dilwyn Formation. The blue graduated line represents the modelled gradient based on a heat flow of 61 mW/m^2 and thermal conductivity parameters as measured and assigned to recorded borehole stratigraphy. Modelling software used courtesy of Hot Dry Rocks Pty Ltd.

formation tests (RFT), cased hole tests (CHT), or production logging tests (PLT) of formation fluids (Beardsmore and Cull, 2001).

The reliability of heat flow estimates in individual petroleum wells is closely linked to the availability and reliability of down-hole temperature data. The number, type and accuracy of temperature data vary considerably between petroleum wells.

Modelling of heat flow values

Water bores

Major formation descriptions and boundary depths were recorded for the water bores. This allowed modelling of the theoretical thermal gradient within each formation based on a given heat flow and thermal conductivity values assigned as described in *Thermal conductivity data*.

The following methodology was adopted to reach a heat flow determination for each water bore. Three assumptions were made. These were that:

1. Each conductivity value is representative of the rocks from which the sample was extracted under surface pressure and temperature conditions.
2. A dominantly vertical conductive thermal regime exists.
3. Thermal conductivity is a function of temperature but pressure has a negligible effect on conductivity at the modelled depths.

The thermal conductivity profile for each well was then used to model a theoretical temperature profile that would result from a given magnitude of heat flow in a conductive heat flow regime. This theoretical profile was then plotted against the observed temperature log and the magnitude of heat flow in the model was adjusted until the modelled temperature profile best visually matched the logged temperatures. In this way we performed inversion modelling, where we deduced the most likely heat flow that best explained the observations. Figure 6 contains a graphic depiction of the method for estimating heat flow, with one example shown. A visual match of modelled to observed temperatures was sufficient to constrain heat flow estimates to within ±1%. Uncertainties in derived heat flow values were directly related to uncertainties in the assigned thermal conductivity profiles.

Petroleum wells

Only a limited number of temperature data were available from discrete depths for each of the petroleum wells examined in this study. Thermal gradient could not be determined on the scale of individual formations, so an alternative method of estimating heat flow was employed.

Mean surface temperatures for each location were assigned based on data obtained from the Australian Bureau of Meteorology website (www.bom.gov.au).

A one dimensional thermal conductivity profile was derived for each well based on the formation tops reported in each well's Well Completion Report and the thermal conductivities reported in Table 1. A value of heat flow was applied to the model in order to predict a temperature profile through the section. The best estimate of heat flow for the well was that which produced a temperature profile that best fit the available temperature data with a subjective assessment of the reliability of those data. For example, drill stem test temperature data were considered to provide reliable estimates of equilibrium temperature at depth, whereas bottom hole temperatures recorded during wireline logging are prone to underestimate the equilibrium temperature because of the cooling effect of drilling fluid circulation. The uncertainty in the derived heat flow estimate was calculated from the cumulative standard error of the thermal conductivity values, with errors in the temperature data left unquantified (and unquantifiable). Figure 7 shows the graphic depiction of the method employed to estimate heat flow in petroleum well Biscuit Flat 1.

3D inversion modelling

We modelled heat flow and temperature in 3D on a section of the study area. We constrained the modelling using the available or modelled physical parameters of:

- Surface heat flow at discrete well locations as estimated in this study
- Thermal conductivity of formations and Groups as assigned from work in this study
- Heat generation data estimated from measured concentrations of U, Th and K in the various rock units (Turner et al., 1992; Turner et al., 1993)

Table 1. Thermal conductivity (at 25°C) assigned to each formation.

Formation	Lithology	Conductivity (W/mK)	Basis for value
Gambier Limestone	Limestone/ calcarenite/ calcilutite	1.50 ± 0.25	Harmonic mean of 52 measured values
Compton Conglomerate	Sandstone/ conglomerate	2.35 ± 0.47	Analogous Cainozoic conglomerate value used
Narrawaturk Marl	Marl	1.79 ± 0.10	Harmonic mean of 6 measured values
Mepunga Formation	Sandstone/mudstone	2.29 ± 0.24	Harmonic mean of 6 measured values
Dilwyn Formation	Sandstone/mudstone	2.06 ± 0.73	Harmonic mean of 4 measured values
Pember Mudstone	Mudstone	2.42 ± 0.25	Sherbrook Group harmonic mean value used
Pebble Point Formation	Limonitic sandstone	2.42 ± 0.25	Sherbrook Group harmonic mean value used
Sherbrook Group	Mainly sandstone	2.42 ± 0.25	Harmonic mean of 53 measured values
Timboon Sandstone	Sandstone	2.42 ± 0.25	Sherbrook Group harmonic mean value used
Paaratte Formation	Sandstone	2.42 ± 0.25	Sherbrook Group harmonic mean value used
Belfast Mudstone	Mudstone	2.42 ± 0.25	Sherbrook Group harmonic mean value used
Argonaut Delta Member	Sandstone	2.42 ± 0.25	Sherbrook Group harmonic mean value used
Flaxman Formation	Sandstone	2.42 ± 0.25	Sherbrook Group harmonic mean value used
Waarre Sandstone	Sandstone	2.42 ± 0.25	Sherbrook Group harmonic mean value used
Copa Formation	Siltstone	2.42 ± 0.25	Sherbrook Group harmonic mean value used
Eumeralla Formation	Mainly shale	1.97 ± 0.11	Harmonic mean of 22 measured values
Windermere Sandstone Member	Sandstone	2.60 ± 0.52	Harmonic mean of 9 measured values from Eumeralla sands
Katnook Sandstone	Sandstone	2.80 ± 0.56	Pretty Hill Formation value with 20% uncertainty
Laira Formation	Siltstone	2.55 ± 0.20	Harmonic mean of 8 measured values
Pretty Hill Formation	Sandstone	2.80 ± 0.20	Harmonic mean of 10 measured values
Cambrian metasediments	Meta-sediments	3.44 ± 0.13	Harmonic mean of 5 measured values
Cambrian schists	Schists	3.44 ± 0.10	Harmonic mean of 4 measured values
Granite Basement	Granite and granodiorite	3.06 ± 0.13	Harmonic mean of 4 measured values

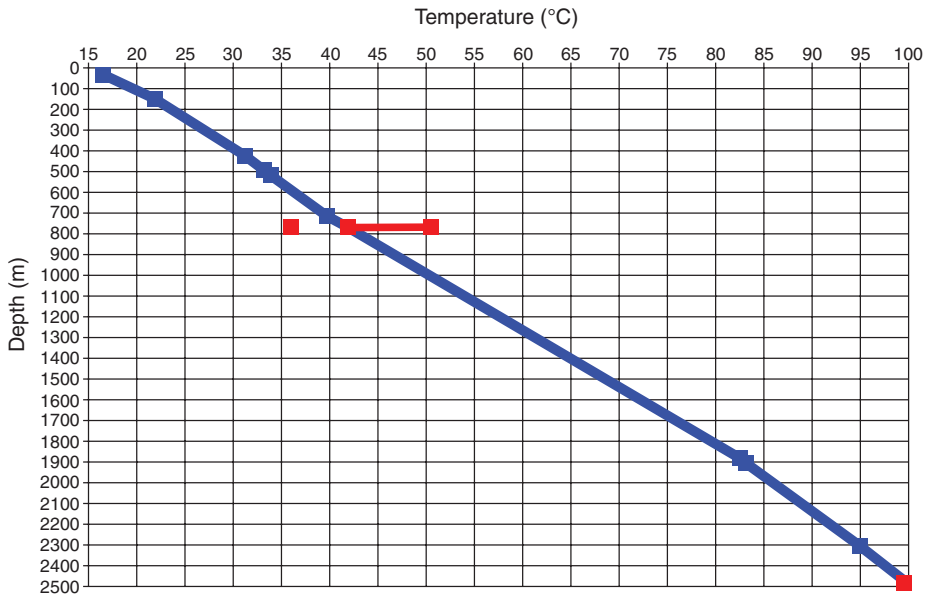

Fig. 7. Heat flow estimate in petroleum well Biscuit Flat 1. Heat flow modelling file for water bore KEN 17. The *x*-axis is temperature in °C and the *y*-axis depth in m. The red markers at 748 m depth indicate one directly measured temperature (36.7°C and a range of possible temperatures (41.8–50.5°C) modelled using the Horner correction. The red marker at 2481 m depth (99.47°C) is a recorded drill stem test. The blue line represents the temperature profile predicted using the conductivity profile of the well (based on reported stratigraphy and assigned thermal conductivity) and an arbitrary value of heat flow, adjusted (to 69 mW/m^2) until the predicted temperature profile best matched the observed temperature data. Modelling software used courtesy of Hot Dry Rocks Pty Ltd.

- A 3D geology 'earth model' created from seismic and drilling data, discretised to an x:y:z cell size of 500 m × 500 m × 70 m.
- Average annual surface temperature from data supplied by the Australian Government Bureau of Meteorology

We then used a proprietary conductive heat flow inversion modelling package called GeoTherm, courtesy of Hot Dry Rocks Pty Ltd, where the software derived the simplest 3D temperature field that explained the observed surface heat flow within the model constraints. GeoTherm begins with a 'guess' at the 3D temperature field, adjusts the thermal conductivity of the formations for *in situ* temperature, then applies a numerical algorithm to 'relax' the temperature field until it obeys the laws of conductive heat flow within and between each cell in the model. Once the model is fully 'relaxed', GeoTherm compares the modelled surface heat flow with the actual observed heat flow at each discrete well location, then distorts the temperature field at the base of the model in a manner dependant on the degree of misfit in each heat flow well location. The process of temperature correction of conductivity, relaxation of the temperature field, comparison of modelled versus observed heat flow at the surface, and distortion of the basal temperature is iteratively repeated until it is manually stopped or achieves a pre-defined 'goodness of fit' of 0.1 mW/m^2 at each well location.

Results

In total, 18 petroleum well and 16 groundwater observation wells were analysed, and a total of 34 new heat flow data points were derived for South Australia (Table 2, Figure 8). The uncertainties for petroleum wells quoted in Table 2 only reflect the quantifiable uncertainty in thermal conductivity values. Heat flow values are also sensitive to uncertainty in temperature data, but it is very difficult to quantify that uncertainty. In general, petroleum temperature data are reliable to ±3−5°C, based on the authors' experience. Uncertainty in thermal gradient, and hence heat flow, is then a function of total well depth. This is not a factor for the estimates of heat flow from water bores, in which temperature data were well constrained.

The distribution of heat flow over the study area appears to be broadly consistent with the tectonic age of the setting. The average heat flow estimated across the study area (± one standard deviation) is 65.6 ± 9.4 mW/m^2 (with a range of 42–90 mW/m^2), which is within the range of expected mean for an area that last experienced a regional thermal event in the Late Cretaceous (Hamza, 1979). This suggests that if a thermal event caused the Newer Volcanics, that event does not presently exert a

Table 2. Summary of results from heat flow modelling. Locations can be found in Figure 1.

Petroleum well	Heat flow (mW/m^2)	Water bore	Heat flow (mW/m^2)
Beachport 1	90 ± 5.7	ARD-1	69 ± 8.0
Beachport East 1	68 ± 4.5	BEN-13	60 ± 7.1
Biscuit Flat 1	70 ± 3.7	BLA-140	52 ± 7.5
Burrungule 1	65 ± 3.3	BLA-175	62 ± 6.1
Caroline 1	64 ± 4.2	GAM-75	71 ± 8.9
Compton 1	59 ± 5.5	HIN-104	75 ± 8.4
Hatherleigh 1	60.5 ± 3.3	KEN-17	61 ± 9.2
Hungerford 1	68 ± 4.9	MAC-57	73 ± 8.6
Kalangadoo 1	61 ± 4.2	MIN-17	64 ± 4.2
Katnook 2	80 ± 3.3	MIN-22	69 ± 6.4
Kentgrove 1	74 ± 16.3	MLG-1	73 ± 10.5
Lake Bonney 1	60 ± 3.3	MON-19	42 ± 6.6
Lake George 1	75 ± 4.1	MTM-66	70 ± 9.6
McNamara Park 1	58 ± 4.9	PEN-25	53 ± 11.3
McNicol 1	63 ± 7.9	PLP-1	57 ± 8.5
Reedy Creek 1	74 ± 3.1	SHT-13	50 ± 8.3
Rendelsham 1	66 ± 3.2		
Trihi 1	77 ± 8.6		

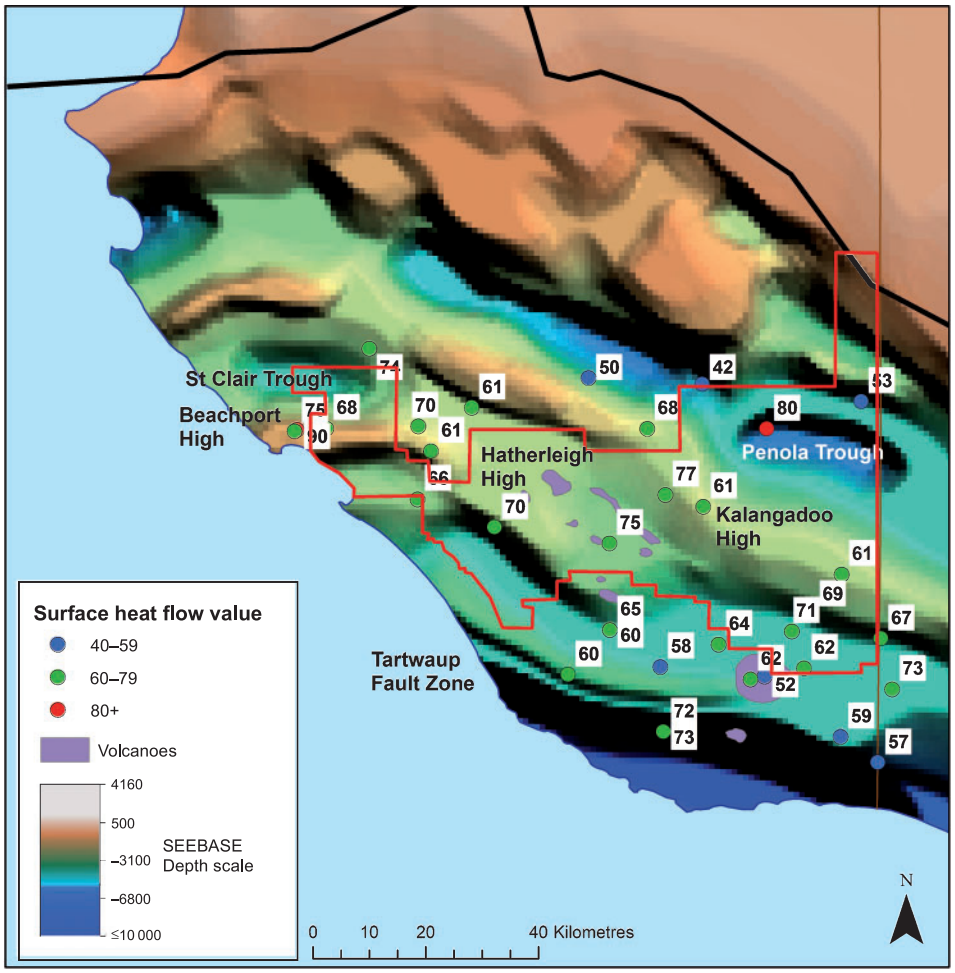

Fig. 8. Heat flow (mW/m^2) results across the study area superimposed on basement structures (image from Jorand et al. (2010)) . There are two recognisable sectors within the study area where heat flow is slightly elevated relative to the background levels, and coincides with areas of known or presumed Recent volcanism. These are located in the vicinity of Mount Schank (73.5 ± 0.5 mW/m^2), and Beachport (78.3 ± 10.4 mW/m^2). Two elevated values occur that are coincident with basement highs. These are located on the Hatherleigh High and Kalangadoo High. Two elevated values are associated with trough structures, in the Penola Trough and St Clair Trough.

regional background thermal influence at the surface. There are, however, two recognisable sectors within the study area where heat flow is slightly elevated relative to the background levels. These sectors coincide with areas of known or presumed Recent volcanism. They can be broadly classified as Mount Schank (Figure 1; 73.5 ± 0.5 mW/m^2), and Beachport (78.3 ± 10.4 mW/m^2).

Two elevated heat flow values occur that are coincident with basement highs (Figure 8). These are water bore HIN 104 (75 ± 8.4 mW/m^2, located on the Hatherleigh High), and petroleum well Trihi 1 (77 ± 8.6 mW/m^2, located on the Kalangadoo High). There are two elevated values located within trough structures: petroleum well Katnook 2 (80 ± 3.3 mW/m^2, located in the Penola Trough), and Reedy Creek 1 (74 ± 3.1 mW/m^2, located in the St Clair Trough).

The heat flow pattern at any depth can be derived from the resultant temperature field of the 3D inversion modelling and the 3D thermal conductivity structure of the model. In this way, we estimated the heat flow pattern at a depth of 6000 m. The results suggest heterogeneous heat flow at 6000 m (below the estimated depth of the deepest troughs, where the rocks are Palaeozoic or older basement), with two zones where vertical heat flow might exceed 90 mW/m^2, and several zones where vertical heat flow might be as low as 40 mW/m^2 (Figure 9*a–d*).

Discussion

The outcomes of this study improve our understanding of the patterns of seismicity and volcanic hazard that might be experienced in this region. The mechanical strength of rocks is temperature dependent and therefore the temperature of the Moho provides a useful proxy for lithospheric strength, a variable controlled strongly by q_r, q_c, crustal thickness and the thermal conductivity structure of the lithosphere in a given area (Sandiford et al., 2003). 'Hot' (and therefore weak) lithosphere responds to even relatively small stresses and undergoes deformation (manifesting as seismicity), while 'cold' (and therefore strong) lithosphere withstands greater stresses before undergoing deformation (Sandiford et al., 2003). The distribution of heat in the region therefore influences seismicity risk.

The pattern of surface heat flow shows a geographical correlation between slightly elevated heat flow and the location of known or surmised volcanic activity related to the Newer Volcanics. However, there are possible explanations for the distribution of elevated heat flow in these areas that do not require remnant heat from magma emplacement. Other possible explanations include heat refraction effects towards basement highs due to lateral thermal conductivity contrasts, and the heterogeneous distribution of buried heat producing granite bodies in the basement to the western Otway Basin.

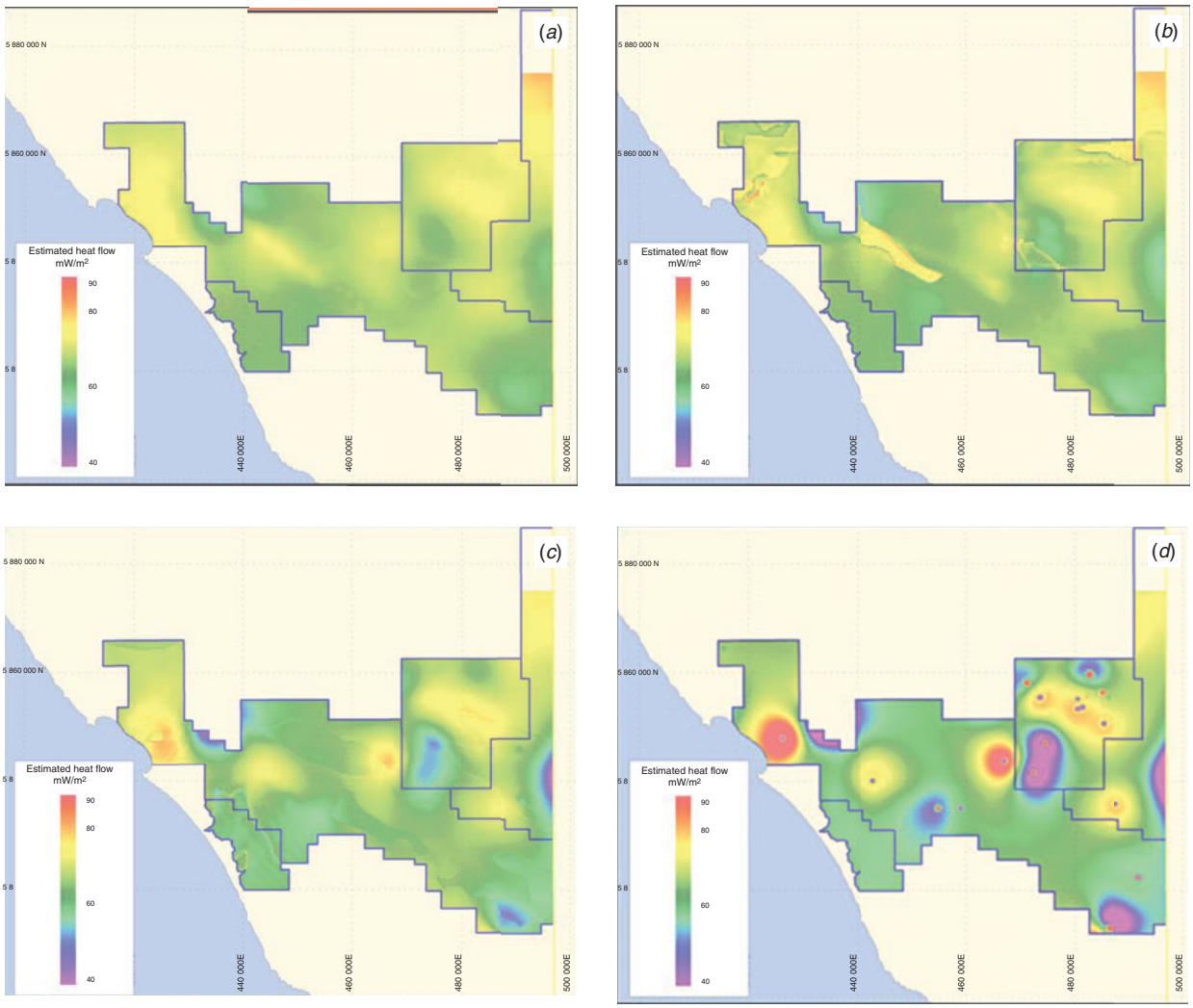

Fig. 9. (*a*) Modelled surface heat flow variation over a portion of the study area. (*b*) Modelled heat flow at 2000 m depth in a portion of the study area as modelled using inversion software. (*c*) Heat flow at 4000 m depth in a portion of the study area as modelled using inversion software. (*d*) Heat flow at 6000 m depth in a portion of the study area as modelled using inversion software.

The basement architecture of the Otway Basin consists of a series of Bassian Rift related troughs between Palaeozoic basement highs. The troughs are filled with sediments, some of which have comparable (e.g. the Pretty Hill Formation), and some lower (e.g. the Eumeralla Formation) thermal conductivity than the basement highs (see Table 1), and as such there is likely to be a complex interplay of heat refraction associated with the lateral thermal conductivity contrasts near the trough boundaries.

Areas of high heat flow in the upper south-east area coincide with basement highs closer to the northern margin of the Otway Basin. Parts of these basement highs are also known to be composed of high heat producing granites (Matthews and Beardsmore, 2007).

There is a geographic correlation between slightly elevated heat flow and the locations of known or surmised Pleistocene–Holocene volcanic activity at Mount Schank and Beachport, but we observed no elevated heat flow around the volcanoes at Mount Gambier. This correlation could suggest a relatively shallow heat source beneath Mount Schank and Beachport.

Another possible explanation is heterogeneous heat production in basement rocks. There are areas of high heat flow in the upper south-east area that coincide with basement rocks of the Padthaway Ridge. The Padthaway Ridge contains sedimentary and igneous rocks, including high heat producing A-type granites (Matthews and Beardsmore, 2007).

Conclusion

Inversion 3D heat flow modelling suggests that heterogeneous heat production in the basement rocks beneath the Otway Basin can explain the observed surface heat flow pattern in the study area. There are no observable significant heat flow anomalies associated with the Pleistocene–Recent Newer Volcanics Province, even though the slightly elevated heat flow does coincide with some of the volcanic centres.

Acknowledgements

Special thanks are given to those who have helped in the data collection and analysis for this paper. In particular, Jeff Lawson and Saad Mustafa in the Mount Gambier Department for Environment, Water and Natural Resources are thanked for allowing access to suitable groundwater wells. The author wishes to acknowledge several people for assistance and guidance in conducting this work. Prof. Mike Sandiford imparted valuable knowledge on the nature and distribution of heat flow and temperature in Australian Proterozoic terranes. Prof. Louis Moresi provided guidance in the understanding of modelling of heat flow and temperature. Last but not least, the staff and directors of Panax Geothermal Limited (especially Kerry Parker and David Jenson) are thanked for making input data

available for the heat flow study, and also allowing the results to be published here.

References

Beardsmore, G. R., 2005, Thermal modelling of the hot dry rock geothermal resource beneath GEL99 in the Cooper Basin: *Proceedings of the World Geothermal Congress, Antalya, Turkey, 24–29 April, 2005*.

Beardsmore, G. R., and Cull, J. P., 2001, *Crustal heat flow: a guide to measurement and modelling*: Cambridge University Press, 324.

Boult, P. J., 2002, Summary and introduction, *in* P. J. Boult, and J. E. Hibburt, eds., *The petroleum geology of South Australia, vol. 1: Otway Basin*, 2nd edition: Department of Primary Industries and Resources (South Australia), Petroleum Geology of South Australia Series, Vol. 1, Ch. 1.

Cas, R. A. F. (Coordinator), 1989, Physical volcanology, *in* R. W. Johnson, J. Knutson, and S. R. Taylor, eds., *Intraplate volcanism in eastern Australia and New Zealand*: Cambridge University Press, 55–87.

Coblentz, D. D., Sandiford, M., Richardson, R. M., Zhou, S., and Hillis, R., 1995, The origins of the intraplate stress field in continental Australia: *Earth and Planetary Science Letters*, **133**, 299–309. doi:10.1016/0012-821X(95)00084-P

Denham, D., Weekes, J., and Krayshek, C., 1981, Earthquake evidence for compressive stress in the Southeast Australian crust: *Journal of the Geological Society of Australia*, **28**, 323–332. doi:10.1080/00167618108729171

Dickinson, J. A., Wallace, M. W., Holdgate, G. R., Gallagher, S. J., and Thomas, L., 2002, Origin and timing of the Miocene-Pliocene unconformity in Southeast Australia: *Journal of Sedimentary Research*, **72**, 288–303. doi:10.1306/082701720288

Gallagher, S. J., and Holdgate, G., 2000, The palaeogeographic and palaeoenvironmental evolution of a Palaeogene mixed carbonate-siliciclastic cool-water succession in the Otway Basin, Southeast Australia: *Palaeogeography, Palaeoclimatology, Palaeoecology*, **156**, 19–50. doi:10.1016/S0031-0182(99)00130-3

Geoscience Australia, 2012, *Otway Basin*. Available at www.ga.gov.au/oceans/sa_Otway.jsp (accessed 20 August 2012).

Hamza, V. M., 1979, Variation of continental mantle heat flow with age: possibility of discriminating between thermal models of the lithosphere: *Pure and Applied Geophysics*, **117**, 65–74.

Hillis, R. R., Enever, J. R., and Reynolds, S. D., 1999, In situ stress field of eastern Australia: *Australian Journal of Earth Sciences*, **46**, 813–825. doi:10.1046/j.1440-0952.1999.00746.x

Hot Dry Rocks Pty Ltd, 2012, Geothermal systems assessment of the Limestone Coast geothermal project, South Australia: Unpublished report for Panax Geothermal Ltd, 206 pp.

Houseman, G. A., Cull, J. P., Muir, P. M., and Paterson, H. L., 1989, Geothermal signatures and uranium ore deposits on the Stuart Shelf of South Australia: *Geophysics*, **54**, 158–170. doi:10.1190/1.1442640

Jenkins, R. J. F., and Sandiford, M., 1992, Observations on the tectonic evolution of the southern Adelaide Fold Belt: *Tectonophysics*, **214**, 27–36. doi:10.1016/0040-1951(92)90188-C

Jensen-Schmidt, B., Cockshell, C. D., and Boult, P. J., 2002, Structural and tectonic setting, *in* P. J. Boult, and J. E. Hibburt, eds., *The petroleum geology of South Australia, vol. 1: Otway Basin,* 2nd edition: Department of Primary Industries and Resources (South Australia), Petroleum Geology of South Australia Series, Vol. 1, Ch. 5.

Johnson, R. W., and Wellman, P. (Coordinators), 1989, Framework for volcanism, *in* R. W. Johnson, J. Knutson, and S. R. Taylor, eds., *Intraplate volcanism in eastern Australia and New Zealand*: Cambridge University Press, 1–53.

Jorand, C., Krassay, A., and Hall, L., 2010, Otway Basin hot sedimentary aquifers and SEEBASE Project: Report to PIRSA-GA-DPI Vic.

Lachenbruch, A. H., and Brewer, M. C., 1959, Dissipation of the temperature effect of drilling a well in Arctic Alaska: *U.S. Geological Survey Bulletin*, **1083-C**, 73–109.

Li, A., McGowran, B., and White, M. R., 2000, Sequences and biofacies packages in the mid-Cenozoic Gambier Limestone, South Australia: reappraisal of foraminiferal evidence: *Australian Journal of Earth Sciences*, **47**, 955–970. doi:10.1046/j.1440-0952.2000.00824.x

Love, A. J., Herczeg, A. L., Armstrong, D., Stadter, F., and Mazor, E., 1993, Groundwater flow regime within the Gambier Embayment of the Otway Basin, Australia: evidence from hydraulics and hydrochemistry: *Journal of Hydrology*, **143**, 297–338. doi:10.1016/0022-1694(93)90197-H

Matthews, C. G., 2009, Geothermal energy prospectivity of the Torrens Hinge Zone: evidence from new heat flow data: *Exploration Geophysics*, **40**, 288–300. doi:10.1071/EG09022

Matthews, C. G., and Beardsmore, G. R., 2007, New heat flow data from southeastern South Australia: *Exploration Geophysics*, **38**, 260–269. doi:10.1071/EG07028

Miller, J. McL., Norvick, M. S., and Wilson, C. J. L., 2002, Basement controls on rifting and the associated formation of ocean transform faults: Cretaceous continental extension of the southern margin of Australia: *Tectonophysics*, **359**, 131–155. doi:10.1016/S0040-1951(02)00508-5

Morton, J. G. G., and Drexel, J. F., eds.,1995, *Petroleum geology of South Australia. Vol. 1 Otway Basin*: Petroleum Division, SA Department of Mines and Energy.

Murray-Wallace, C. V., Belperio, A. P., and Cann, J. H., 1998, Quaternary neotectonism and intra-plate volcanism: the Coorong to Mount Gambier coastal plain, southeastern Australia— a review, *in* I. S. Stewart, and C. Vita-Finzi, eds., *Coastal tectonics*: Geological Society Special Publications, 146, 255–267.

O'Brien, G. W., Reeves, C. V., Milligan, P. R., Morse, M. P., Alexander, E. M., Willcox, J. B., Yunxuan, Z., Finlayson, D. M., and Brodie, R. C., 1994, New ideas on the rifting history and structural architecture of the Western Otway Basin: evidence from the integration of aeromagnetic, gravity and seismic data: *APEA Journal*, **34**, 529–554.

Perincek, D., and Cockshell, C. D., 1995, The Otway Basin: Early Cretaceous rifting to Neogene inversion: *APEA Journal*, **35**, 451–466.

Sandiford, M., 2003*a*, Neotectonics of SE Australia and the origin of the intraplate stress field, *in* C. G. Skilbeck, and T. C. T. Hubble, eds., *Understanding Planet Earth: searching for a sustainable future*: Geological Society of Australia, Abstracts of the 15th Australian Geological Convention, **59**, 435.

Sandiford, M., 2003*b*, Geomorphic constraints on the late Neogene tectonics of the Otway Range, Victoria: *Australian Journal of Earth Sciences*, **50**, 69–80. doi:10.1046/j.1440-0952.2003.00973.x

Sandiford, M., Frederiksen, S., and Braun, J., 2003, The long-term thermal consequences of rifting: implications for basin reactivation: *Basin Research*, **15**, 23–43. doi:10.1046/j.1365-2117.2003.00196.x

Sheard, M. J., and Nicholls, I. A., 1989, Mount Gambier sub-province, *in* R. W. Johnson, J. Knutson, and S. R. Taylor, eds., *Intraplate volcanism in eastern Australia and New Zealand*: Cambridge University Press, 142.

Sprigg, R. C., 1959, Presumed submarine volcanic activity near Beachport, south-east South Australia: *Transactions of the Royal Society of South Australia*, **82**, 195–203.

Sutherland, F. L., 1981, Migration in relation to possible tectonic and regional controls in eastern Australian volcanism: *Journal of Volcanology and Geothermal Research*, **9**, 181–213. doi:10.1016/0377-0273(81)90004-4

Torrens Energy Limited, 2008, 780 000 PJ Inferred Resource, Parachilna Project, South Australia. ASX announcement 20 August 2008. Available at http://www.asx.com.au/asxpdf/20080820/pdf/31bsp0dcmt4sw0.pdf (first accessed 21 August 2008).

Turner, S. P., Foden, J. D., and Morrison, R. S., 1992, Derivation of some A-type magmas by fractionation of basaltic magma: an example from the Padthaway Ridge, South Australia: *Lithos*, **28**, 151–179. doi:10.1016/0024-4937(92)90029-X

Turner, S. P., Foden, J. D., Sandiford, M, and Bruce, D, 1993, Sm-Nd isotopic evidence for the provenance of sediments from the Adelaide Fold Belt and southeastern Australia with implications for episodic crustal addition: *Geochimica et Cosmochimica Acta*, **57**, 1837–1856. doi:10.1016/0016-7037(93)90116-E

van Otterloo, J., 2011, *Newer Volcanics Map*. Available at http://vhub.org/resources/845 (accessed 25 May 2012).

White, M. R., 1996, Subdivision of the Gambier Limestone: *MESA Journal*, **1**, 35–39.

Woodhead, J., Hergt, J., Sandiford, M., and Johnson, W., 2010, The big crunch: physical and chemical expressions of arc/continent collision in the Western Bismarck arc: *Journal of Volcanology and Geothermal Research*, **190**, 11–24. doi:10.1016/j.jvolgeores.2009.03.003

Chapter 7

Modelling the influences on surface heat flow in the western Otway Basin

Modelling the influences on surface heat flow in the western Otway Basin

7.1 Introduction

The aim of this chapter is to examine the possible factors that influence the observed pattern of surface heat flow in the western Otway Basin, and to conclude which factors, and hence which aspects of the geological history of the area, have had the greatest influence on present day surface heat flow. Factors include basement heat generation, heat refraction, heat advection, and remnant magmatic heat.

The western Otway Basin consists of a series of troughs associated with Early Cretaceous rifting and Late Cretaceous sag phase sedimentation. The rifting created a geometry where basement rocks of the Kanmantoo Group (Cambrian) and subsequent Cambro-Ordovician granitoids emplaced during the Delamerian Orogeny sit laterally adjacent to the rift and sag phase basin fill sediments in some locations (Figure 1).

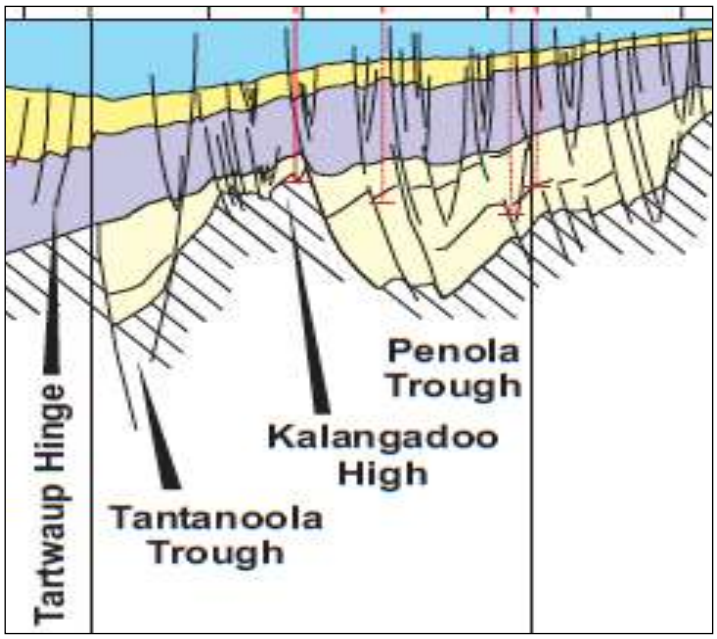

Figure 1: A south–north cross-section through the western Otway Basin north of the Tartwaup Hinge Zone (from Jensen-Schmidt et al 2001). Early Cretaceous rift phase troughs are filled by thick basal Crayfish Group (cream colour) dominated by sandstone and laterally adjacent to basement (white). Overlying Late Cretaceous rift phase Eumeralla Formation (purple) and sag phase Sherbrook Group (yellow) and Heytesbury Group (blue) sediments thicken to the south (left).

The average thermal conductivity of the different rock units can be derived from the previous chapters in this thesis, in particular Chapter 6. The following values represent the most likely values based on the current thermal conductivity dataset:

- Crayfish Group 2.80 W/mK
- Basement 3.50 W/mK
- Eumeralla Formation 1.97 W/mK
- Sherbrook Group 2.42 W/mK

Most significantly, the thermal conductivity of the Crayfish Group shows no significant contrast with the Basement. The later sag phase sediments of the thick Eumeralla Formation and Sherbrook Group are, however, much less conductive than the basement. The geometry of rock units can refract heat flow away from vertical and create lateral heat flow effects, with heat flow preferentially directed towards more conductive rock sequences (Beardsmore & Cull 2001). The mineralogical contrast between the various lithologies in the study area does not affect the thermal regime as much as the geometric arrangement of thermal conductivity and heat production.

As seen in Figure 1, the structural geometry of the Otway Basin in the study area has the potential to bring about heat refraction due to lateral lithology contrasts, but the refractive effects of structural troughs may actually be very small due to the low conductivity contrast between early rift phase and basement rocks. The potential for regional heat refraction towards the northern margin of the Otway Basin in the study area due to the thinning of the relatively insulating sag phase rocks may, however, be a possible explanation for the higher average observed heat flow in that area (figure 2).

A number of geological and geophysical factors affect surface heat flow patterns in a given area. The magnitude of the total conductive flux of heat through the earth's surface is a combination of contributions from two sources, and can be described thus:

$$Q_s = q_r + q_c \qquad (1)$$

Where q_r is the mantle component of heat flow, known as 'reduced heat flow', and q_c is the contribution to surface heat flow from heat generation in the crust. Heat flows approximately vertically through the crust, but a lateral component of heat flow can be induced by lateral conductivity and temperature contrasts due to geological structure and/or active heat sources. As dictated by the second law of thermodynamics, heat flows from hot to cold areas, and if temperatures vary laterally, heat also flows laterally.

The heat equation describes the change in the temperature function over time:

$$\frac{\delta T}{\delta t} - \alpha \left(\frac{\delta^2 T}{\delta x^2} + \frac{\delta^2 T}{\delta y^2} + \frac{\delta^2 T}{\delta z^2}\right) = \mathrm{Q(x,y,z,t)}$$

where:

T = temperature as a function of space (x,y,z) and time (t), and $\delta T/\delta t$ is the rate of change of temperature at a point over time.

α = thermal diffusivity – a quantity dependent on thermal conductivity, density and specific heat capacity.

$\alpha \left(\frac{\delta^2 T}{\delta x^2}\right)$ = the rate of change of heat flow in the x direction. The subsequent two terms are analogous for the y and z directions.

In steady state the function $\delta T/\delta t$ is zero, and the temperature gradients are determined by heat sources and boundary conditions.

If $\delta T/\delta t$ is not equal to zero, then temperatures are changing at a given point over time, and the situation is non-steady state, or transient heat conduction. This can occur when a heat source is introduced into a system, such as a magma injection into the crust from below. In this situation the temperature distribution within a system will change over time towards a new equilibrium with the altered conditions. Once the new equilibrium has been reached, then the time dependent temperature function will again return to zero. In a purely conductive steady state thermal regime, the factors that could influence the distribution and magnitude of surface heat flow and the three dimensional temperature distributions are:

a) Anomalous heat production within the top 10 km of the crust from granitic (or other) bodies;

b) Thermal conductivity contrasts within the geological section that serve to laterally refract heat;

c) Variations in the basal heat flow pattern from variable reduced heat flow q_r;

d) Transient heat sources such as cooling magma bodies;

The heat equation can be solved for arbitrarily complicated geometry. By creating simple models and solutions based on the four factors listed above, we can gain insight into the effects that such factors will have on the surface heat flow pattern.

In this chapter I show that the surface heat flow pattern in the western Otway basin study area is adequately explained by a combination of variable heat production in basement rocks (the major influence) and a minor effect of heat refraction towards the northern margin of the Basin marked by the Padthaway Ridge.

The other two factors listed above – variations in the pattern of reduced heat flow and the presence of transient heat sources – are discussed here but are not considered necessary to explain the observed heat flow estimates.

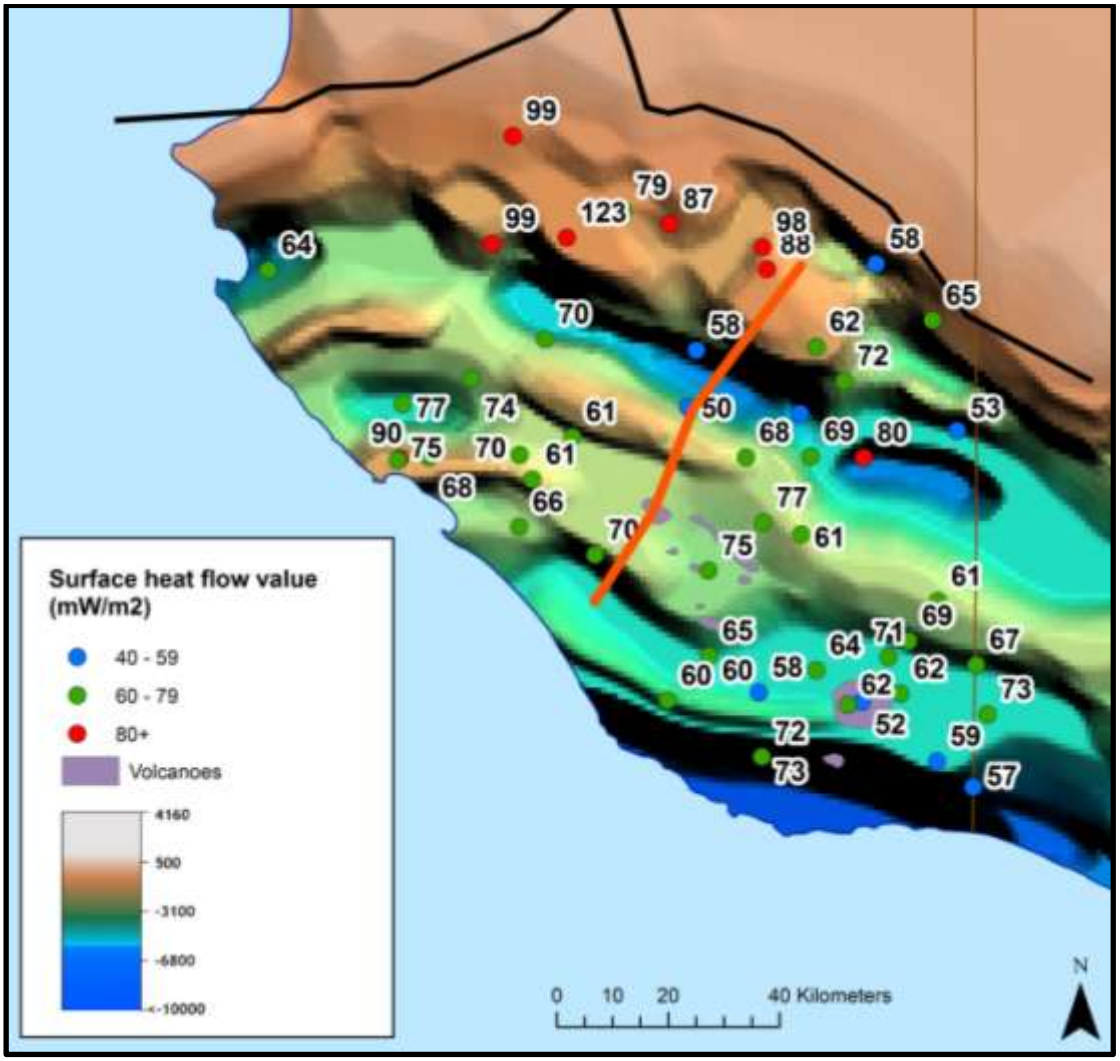

Figure 2: surface heat flow derived from borehole data in the western Otway Basin, superimposed on the basement topography from SEEBASE 2010 (Jorand et al 2010). The orange line shows the location of the cross section in Figure 1.

7.2 Modelling steady state heat flow

When modelling the effect that conductivity contrast and geometry have on the flow of heat and the distribution of temperature, the ideal is to develop analytical solutions to the heat flow equation for different geometries and boundary conditions. Bullard et al (1956) made a model of sinusoidal ridges, Carslaw & Jaeger (1959) created solutions for spherical and ellipsoid shapes, while Lee & Henyey (1974) adapted the previous solutions to ellipsoids and modelled buried cylinders and semi-cylinders.

Another approach is to create numerical algorithms that can be used in finite element modelling. Finite element modelling is a method whereby a large and complex system such as a 3D geological space is broken into small and manageable pieces, each with its own set of spatial coordinates and physical properties. The resolution achievable by a model (gauged by the relative size of the elements in the model) depends on the computing power of the

modelling programme. Once a space has been divided into elements a process such as heat conduction in a solid is mathematically described with differential equations derived from the heat flow equation, and then applied to each element.

To allow modelling to proceed, each element must have a set of initial and boundary conditions. Elements that represent particular geological units in the space can be linked and defined as groups. Another set of initial and boundary conditions must be applied to the full model. These include variations in surface temperature, topography (essentially an additional layer of 'air') as well as local disturbances in surface temperature, and radiogenic heat generation within the model.

The aim of steady state heat flow modelling is to predict the temperature and heat flow of unsampled parts of the 'interior' of a 3D model by matching observations (of temperature or heat flow, for example) at known positions, applying known boundary values and modelling of the interior of the model. One approach to finding a solution is the method of 'relaxation'. Modelling effectively begins with a guess at the steady state temperature distribution within the model. The relaxation algorithm runs to thermally equilibrate each cell in the model relative to its adjacent cells. After doing this for every cell in the model, the model should be closer to full equilibration than the initial guess. The algorithm then repeats the process indefinitely (called 'iteration') until the temperature field 'relaxes' towards a steady state solution. The algorithm stops when the changes between one iteration and the next are small enough to be insignificant. Relaxation is a robust numerical algorithm in that all realistic boundary conditions will result in convergence, although convergence times will vary with the complexity of the model.

As part of this study, I conducted a series of simple numerical modelling exercises to investigate the effect on surface heat flow of heat producing bodies buried at various depths below the surface. I used a modelling software package known as *HeatSeek*, which is based on the relaxation algorithm, and an output generation software called *MapMaker*. Both were developed by Dr Graeme Beardsmore.

HeatSeek employs numerical finite difference methods to solve the 3D conductive heat flow equation over a voxellated model volume. The geological structure within the model volume is approximated as a regular rectangular prismatic 3D grid, with each cell (or voxel) allocated predefined 'rock types'. The overall dimensions of the model are defined by setting the dimensions of the cells, although the total number of cells is limited to 100 in each of the X, Y and Z dimensions. The thermal conductivity and internal heat generation of each cell can be set. The boundary condition of average surface temperature is assumed constant and uniform across the model area. The side boundaries of the model volume are assumed to be perfect insulators, which is to say that zero heat flows through the sides of the model. The base boundary condition of the model can be defined as either constant temperature or constant heat flow (uniform across the model).

Once the boundary conditions and geological structure / rock types are set, Heat Seek employs a relaxation algorithm to converge from an initial temperature distribution (a 1D

solution for heat flow at each X,Y location) to a steady state 3D temperature distribution. The outcome is a discrete value for temperature at every grid node that satisfies all imposed boundary conditions and rock properties (within pre-set precision limits, typically ±0.01°C).

The modelling exercises below are intended to test each of the factors that may influence the surface heat flow patterns observed in the study areas, and then to come up with a model that best fits the observed surface heat flow estimates in the Otway Basin study area.

7.3 Factors that may influence surface heat flow patterns

7.3.1 Anomalous crustal heat production q_c

Observed variations in surface heat flow might be due entirely or partially to lateral variations in crustal heat generation. The basement to the Otway and Murray Basin study areas is comprised of Kanmantoo Group (Cambrian) sediments and volcanics, and/or subsequent Cambro-Ordovician granitoids and extrusives emplaced during and immediately following the Delamerian Orogeny (Jensen-Schmidt et al 2001). The estimated heat production values of these rocks are highly varied, with the Kanmantoo sediments likely to have a heat production less than 1.5 µW/m^3, and the Delamerian granites having estimated heat production values ranging from 1.34–10.57 µW/m^3 (see Appendix 1). The contrast in heat production between basement lithologies means that the crustal contribution to heat flow in the study area is probably not spatially uniform. I carried out a series of modelling exercises to investigate the magnitude and lateral wavelength of possible surface effects from buried anomalous heat sources.

7.3.1.1 Modelling exercise 1 – anomalous heat production: a sphere of radius 500 m with heat production of 10 µW/m^3 buried within a country rock of zero heat production; centre of sphere buried 1000 m or 3000 m below surface; basal heat flow 50 mW/m^2 in both cases. The model size is 5000 m x 5000 m x 5000 m, with the x and y directions divided into cells of 20 and the z direction divided into 50 cells. As described above, the maximum number of cells in any direction is 100.

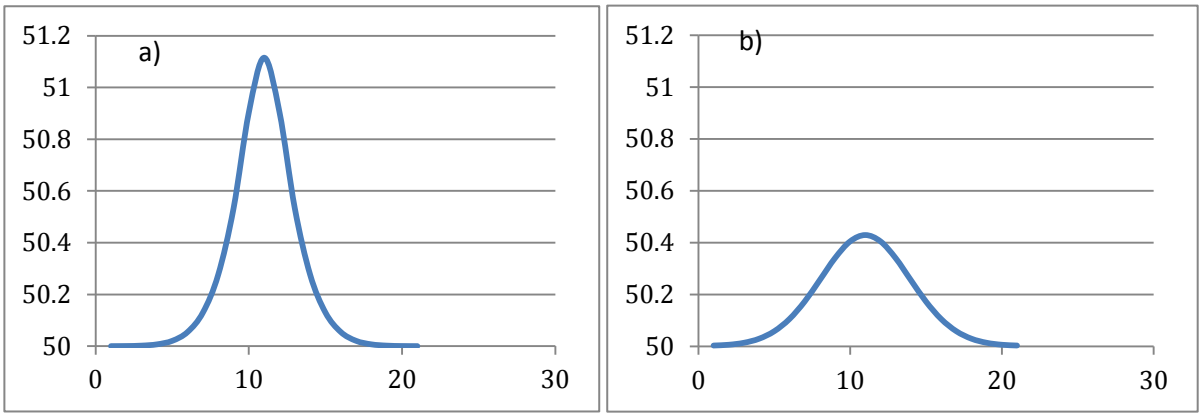

Figure 3: Effect on surface heat flow of a buried sphere of diameter 1000 m and heat production of 10 µW/m^3. The left hand graph (a) shows a surface heat flow anomaly of around 1 mW/m^2 when the top of

the sphere is at 500 m depth, while the right hand side (b) shows the smaller but broader anomaly when the top of the sphere is at 2500 m depth. The horizontal scale is in cell numbers, each one being 250 m.

The results show that the surface heat flow anomaly resulting from such a heat-producing sphere buried at 1000 m would be around 1 mW/m^2 (Figure 3a). When the depth of burial of the same body is increased to 3000 m, the width of the anomaly increases, but the peak magnitude decreases to around 0.4 mW/m^2 (Figure 3b). It follows that the surface heat flow values of up to 123 mW/m^2 seen on the northern margin of the Otway Basin are unlikely to be due solely to small buried bodies with heat production of around 10 µW/m^3.

7.3.1.2 Modelling exercise 2: a long wavelength 2D model with thickening and shallowing basement of moderate heat production, length 100 km, model thickness 10 km, basement heat production a uniform 5 µW/m^3 across the model.

This 'first pass' modelling exercise was aimed at approximating the north-south thermal conductivity structure that might exist beneath the Otway Basin in South Australia (see modelled basin geometry in Figure 1). The first approximation was based on a simple 2D basin cross section model with a uniform basal heat flow of 60 mW/m^2, a basement heat production of 5 µW/m^3 across the model, with a uniform thermal conductivity of 3.5 W/mK, and a cover sequence with no heat production and conductivity of 2.0 W/mK. Regarding the coarseness of this model – 1km cell size – the maximum number of cells in any direction in HeatSeek is 100, so this was the finest possible mesh size for this model. This mesh size is adequate to test the hypothesis in the exercise. It is not possible in HeatSeek to make basal heat flow heterogeneous, and it may be that there will be a higher basal heat flow at the northern margin of the basin (e.g. Sandiford et al 2003), but for the purposes of this basic modelling the uniform basal heat flow demonstrates well the resultant surface heat flow patterns.

Figure 5 shows the modelled surface heat flow under these conditions. The basal heat flow to the model of 60 mW/m^2 is within the expected heat flow range for a geological setting of this age and type (see section 2.1.1). The thermal conductivity values assigned to the basement (3.5 W/mK) and cover (2.0 W/mK) rocks is within the ranges measured during the studies in the Otway Basin region (see Chapters 4 and 6). The basement heat production is also within a feasible range for this region, with measured heat production values of around 2 to 10 µW/m^3 (see Appendix 1). The value of 5 µW/m^3 was also appropriate for this particular model, because using it resulted in a maximum value in the northern end of the model that roughly matches the observed maximum value in the region.

This modelling output roughly matches the *pattern* of surface heat flow observed in the study area (Figure 4), but not the relative magnitudes of surface heat flow. The high surface heat flow in the northern (right hand) end of the model is a result of the thick modelled granitic basement with high cumulative heat production, but the magnitude of heat flow along the southernmost three quarters of the profile from 0–75 km increases steadily from 65 to 90 mW/m^2, inconsistent with the observed heat flow values.

As a first pass using the modelled subsurface geology, the model results suggest that basement depth might be a significant factor controlling the observed distribution of surface heat flow. The second pass modelling is discussed below, and involved altering the parameters to get a better fit with the observed values.

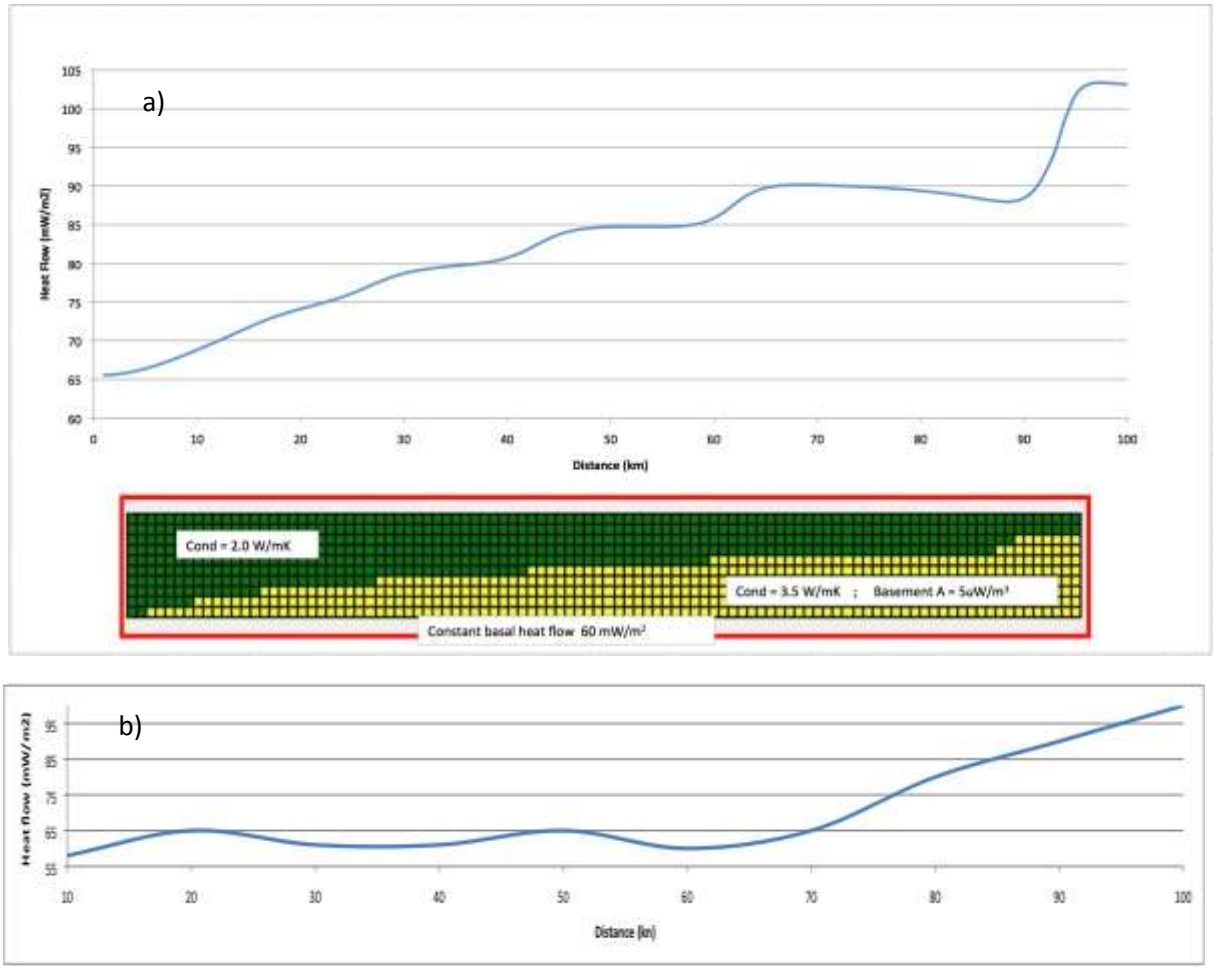

Figure 4: a) Modelling output of a 2D profile approximating the cross section in Figure 1. While the modelled heat flow matches the pattern of the observed surface heat flow (b), the magnitudes do not match between the distances of 0–75 km.

7.3.1.3 Modelling exercise 3: a long wavelength 2D model with thickening and shallowing basement of heat production 2.5 µW/m^3, length 100 km, model thickness 10 km, with approximations of the Penola and Tantanoola Troughs and the high heat producing, granite-rich Padthaway Ridge, and constant basal heat flow of 45 mW/m^2.

This exercise attempted to model the north-south direction thermal conductivity and heat generation structure that might exist beneath the Otway Basin in South Australia based on the basin geometry in Figure 2. The model included: a uniform basal heat flow of 45 mW/m^2; a basement heat production of 2.5 µW/m^3 and thermal conductivity of 3.5 W/mK; a cover sequence with a low heat production of 0.5 µW/m^3 and conductivity of 2.0 W/mK; and the addition of modelled approximations of the Tantanoola and Penola Troughs and Padthaway Ridge. The Troughs contain mostly the Pretty Hill Formation, a dominantly sandstone

formation with moderate conductivity and heat production of (see Figure 5a). It is a fair assumption that the Padthaway Ridge in this region at the northern Otway Basin margin is granite dominated (Turner et al 1992), and has anomalous high heat production of 7 $\mu W/m^3$ (see Appendix 1 for calculated heat production values for the Padthaway Ridge granites). Figure 5a shows the modelled surface heat flow under these conditions.

This model result closely approximates both the observed pattern and magnitude of heat flow in the study area (Figure 5b). The observed broad heat flow pattern is therefore consistent with a simple mechanism of heat refraction and lateral variation in cumulative basement heat generation.

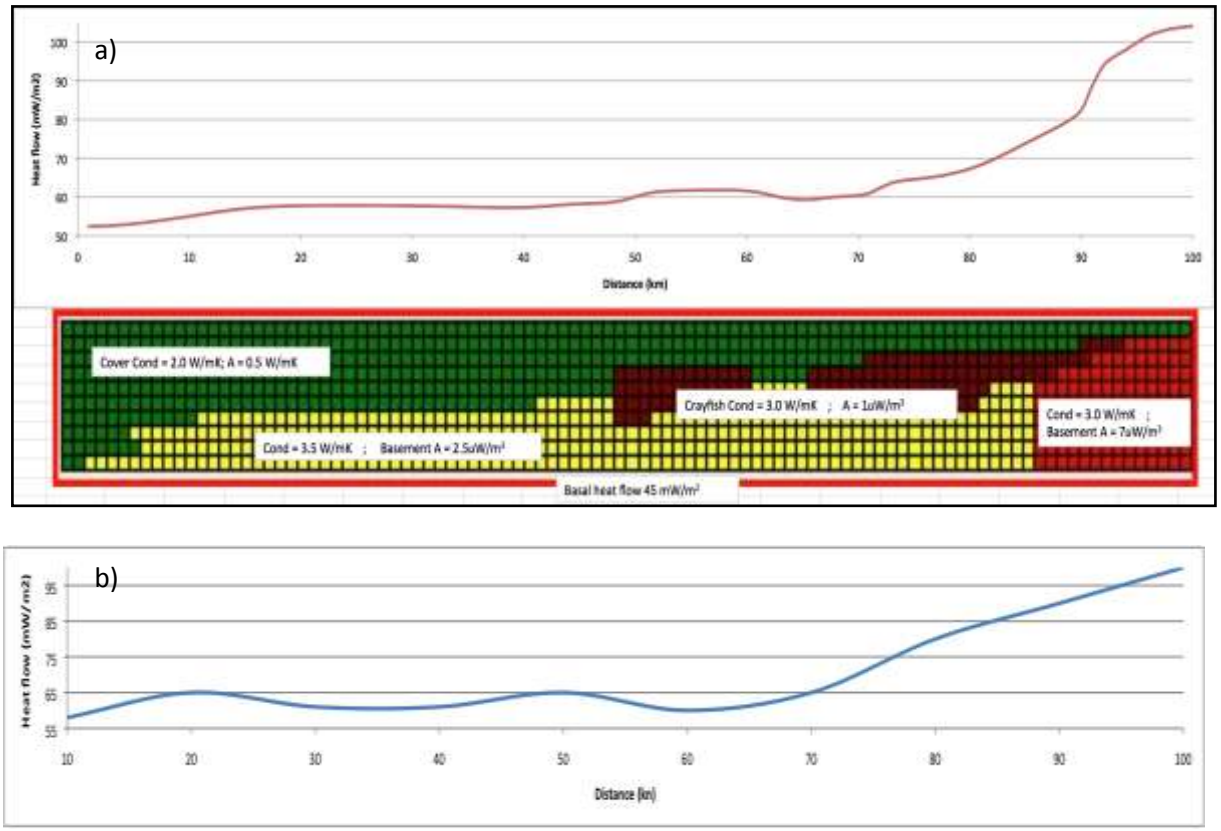

Figure 5: a) Modelling output of a 2D profile approximating the cross section in Figure 1. The reduction of basal heat flow from the previous model, plus the addition of the two early Cretaceous Toughs and the high heat producing Padthaway Ridge produced results that are a close match with b) – the observed surface heat flow trend along the south–north section line in Figure 2.

7.3.2 Heat refraction due to conductivity contrast and geometry

As with other forms of energy such as electricity, heat flows from points of higher to lower 'potential' (in the case of heat flow, temperature) preferentially along paths of least resistance (Beardsmore & Cull 2001). That is, heat flows preferentially through more conductive rocks, which leads to heat refraction away from the vertical if higher and lower conductivity rocks are laterally juxtaposed (e.g. Mildren & Sandiford 1995; Bullard et al 1956; Carslaw & Jaeger 1959; Lee & Henyey 1974).

7.3.2.1 Some previous modelling

Bullard et al (1956), in early attempts to measure and model heat flow on the sea floor devised an equation based on the heat flow equation and a conductivity contrast in an ideal harmonic ridge pattern. This approximation was graphically displayed in Beardsmore & Cull (2001; figure 6). In the modelled scenario, the wavelength of the basement topography was 50 km, amplitude 3 km, basal heat flow was a uniform 100 mW/m^2 and a conductivity contrast of 4 W/mK (basement) versus 2 W/mK (cover) was applied. The analytical result shows the difference between the heat flow above the basement highs and the troughs is more than 18 mW/m^2.

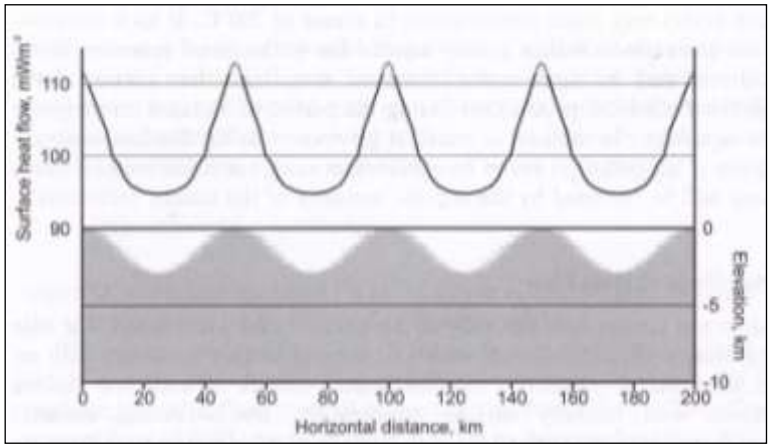

Figure 6: Predicted surface heat flow due to a series of sinusoidal ridges (amplitude 3 km, wavelength 50 km, basement conductivity 4 W/mK, cover conductivity 2 W/mK). Basal heat flow is 100 mW/m^2 and surface T is 0^{o}C (from Beardsmore & Cull 2001 figure 6.4).

The degree of heat refraction and resultant surface heat flow disturbance is a function of conductivity contrast and the geometry of the thermal conductivity distribution, defined by amplitude and wavelength.

Mildren & Sandiford (1995) used a simple model to illustrate the heat refraction effects of lateral conductivity contrast. The 2D model they used is shown in Figure 7. The aim of their modelling was to show the effects of conductivity contrast on lateral temperature distribution. However, temperature distribution by way of isotherms can also show the direction of heat flow, because heat flows perpendicular to isotherms (Beardsmore & Cull 2001). Figure 8 shows how the vertical flow of heat is affected by conductivity contrast.

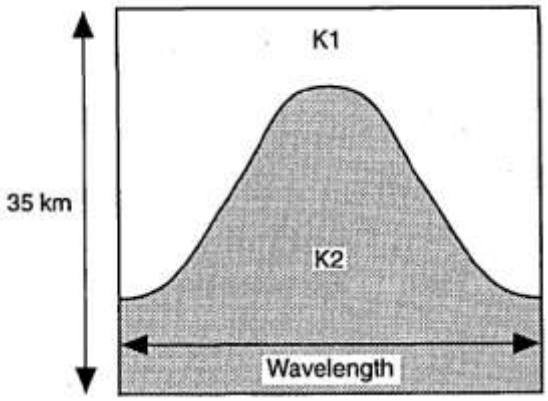

Figure 7: the 2D model used by Mildren & Sandiford (1995) to illustrate the effects of lateral conductivity contrast on temperature distribution.

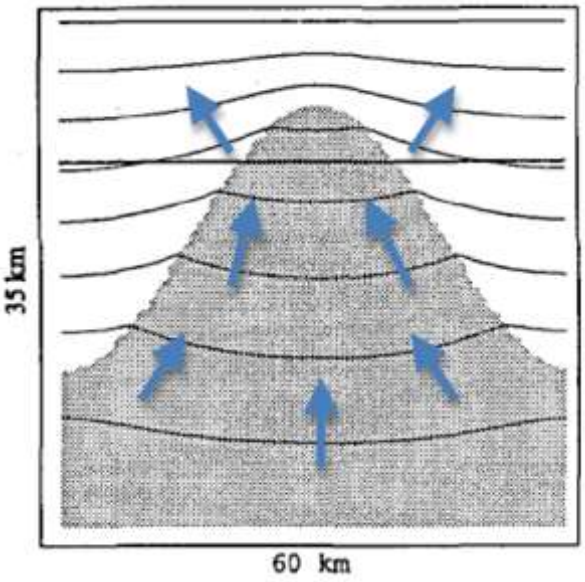

Figure 8: The effects of lateral conductivity contrast on isotherms from Mildren & Sandiford (1995). Arrows indicate direction of heat flow. Grey shade indicates high conductivity basement (k = 3.5 W/mK); white shade indicates low conductivity cover (k = 1.5 W/mK). Note that heat is refracting towards the higher conductivity zone in the basement, but refracting away from it in the adjacent cover rocks. Note also that the greatest distortion from vertical heat flow is at the basement/cover boundary.

7.3.2.2 Modelling exercise 4: a sphere of conductivity 10 W/mK, radius 500 m, buried 2000 m below surface within a country rock of conductivity 2 W/mK.

This exercise modelled the surface heat flow pattern that would result from the burial of a very conductive body within a low conductivity block. The model assumed a uniform basal heat flow of 50 mW/m^2 and no heat production. The model size is 5000 m x 5000 m x 5000 m, with the x and y directions divided into cells of 20 and the z direction divided into 50 cells. As described above, the maximum number of cells in any direction is 100.

The results (Figure 9) show that heat is channelled preferentially through the high conductivity body such that surface heat flow is elevated directly above the body and slightly

reduced in the region around the edges of the body. The maximum magnitude of the predicted surface heat flow anomaly is only about 1.5 mW/m^2.

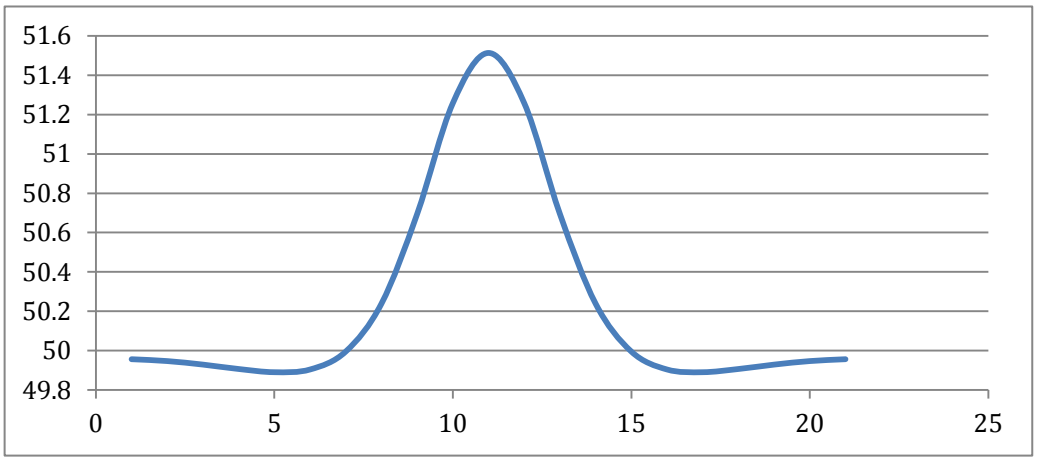

Figure 9: Predicted surface heat flow anomaly due to a sphere of diameter 1000 m and conductivity of 10 W/mK buried 2000 m below the surface in a country rock of conductivity 2 W/mK.

7.3.2.3 Modelling exercise 5: a sphere, conductivity 6 W/mK, radius 500 m, buried 2000 m below surface within a country rock of conductivity 3 W/mK.

This exercise mimicked the model in exercise 4, but reduced the conductivity contrast from 10/2 to 6/3. The model assumed a uniform basal heat flow of 50 mW/m^2 and no heat production. The model size is the same as that from exercise 4.

The results (Figure 10) show a similar pattern of surface heat flow to the previous model, but at much reduced magnitude. The predicted maximum anomaly of about 0.5 mW/m^2 would be below the error limits of detection in most cases.

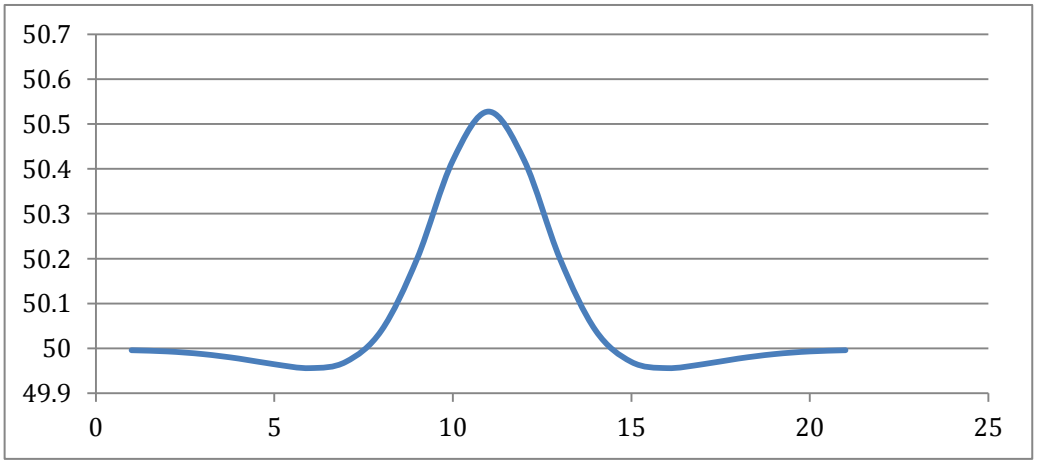

Figure 10: Predicted surface heat flow anomaly due to a sphere of diameter 1000 m and conductivity of 6 W/mK buried 2000 m in a country rock of conductivity 3 W/mK.

7.3.2.4 Modelling exercise 6: a long wavelength 2D model with thickening and shallowing basement, a moderate conductivity contrast (3.5/2), length 100 km, constant basal heat flow 60 mW/m^2.

This exercise aimed to isolate the contribution that heat refraction alone might make to the observed surface heat flow distribution in the western Otway Basin (see modelled basin geometry in figure 1). The model was based on a simple 2D basin cross section model with a uniform basal heat flow of 60 mW/m^2, basement thermal conductivity of 3.5 W/mK, and a cover sequence with a conductivity of 2.0 W/mK. Figure 11 shows the modelled surface heat flow under these conditions.

The results show a pattern of surface heat flow that approximates the observed pattern, but with much lower amplitude. The surface heat flow alters very little along about three quarters of its length (with lateral negative changes in surface heat flow where heat is refracted from one adjacent lateral area to its neighbour coinciding with step-wise changes in basement geology and thus conductivity/depth in the model; see section 7.3.2.1 above for previous modelling on this), and then rises to its greatest value at the northern end where the basement is shallowest. The model shows that the heat refraction effect of the thickening basement/thinning cover could account for an anomaly of just 4 mW/m^2 at the northern end.

It is clear that a large body with significant thermal conductivity contrast is alone not sufficient to explain the observed surface heat flow anomaly of about 50 mW/m^2 in the north of the study area, but that northerly directed thermal refraction may contribute to the overall observed heat flow pattern.

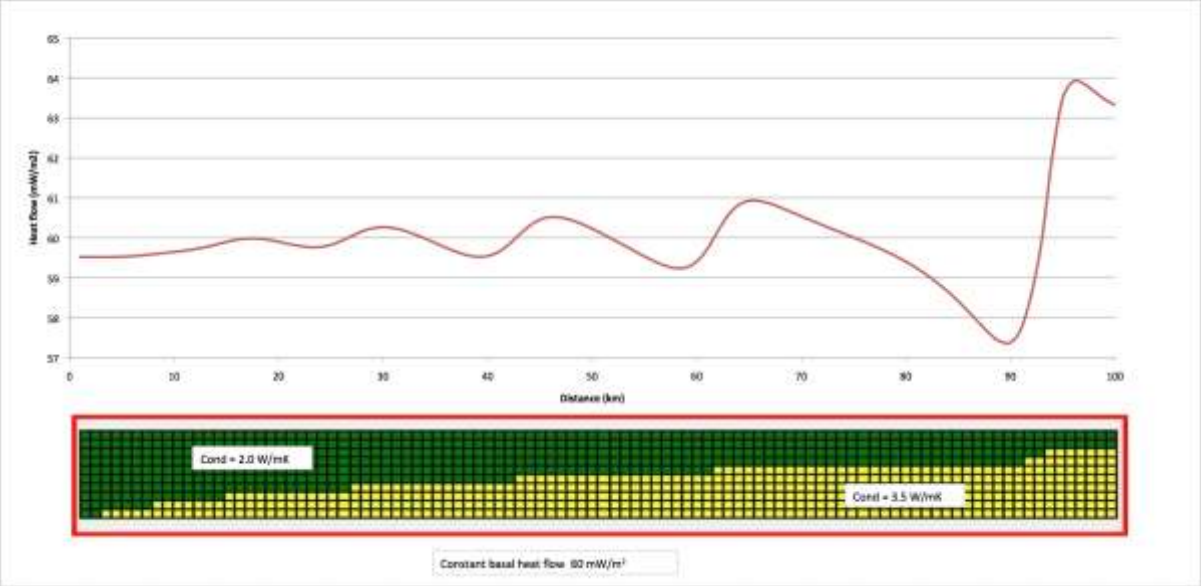

Figure 11: Predicted surface heat flow from a 2D profile approximating the cross section in Figure 1. No heat production has been included, and nor have the geological features of the Penola and Tantanoola Troughs or the Padthaway Ridge. The maximum effect of the thermal conductivity contrast on surface heat flow is just 4 mW/m^2, not enough to explain the observed heat flow variation in the study area.

7.3.3 Variable reduced heat flow in the study area

Observed variations in surface heat flow could be due entirely or partially to variations in the mantle component of heat flow, q_r. Graeber et al (2002) presented the results of a study into lateral variations in compressive seismic wave-speeds from the crust and upper mantle in Western Victoria, a region that includes the eastern Otway Basin and the Newer Volcanics Province (NVP). While the area covered did not include the study area from Chapter 6 in the western Otway Basin, a clear upper mantle low wave-speed anomaly was identified that spatially corresponds to the highest density of the NVP volcanism in the Central Highlands of Victoria (Figure 12). The low wave-speed anomaly is possibly due to elevated temperatures in the upper mantle (an upper mantle 'hotspot'). This would likely result in higher q_r in that area relative to surrounding areas. With Recent volcanism in the lower southeast study area in South Australia, lateral variations in q_r are plausible.

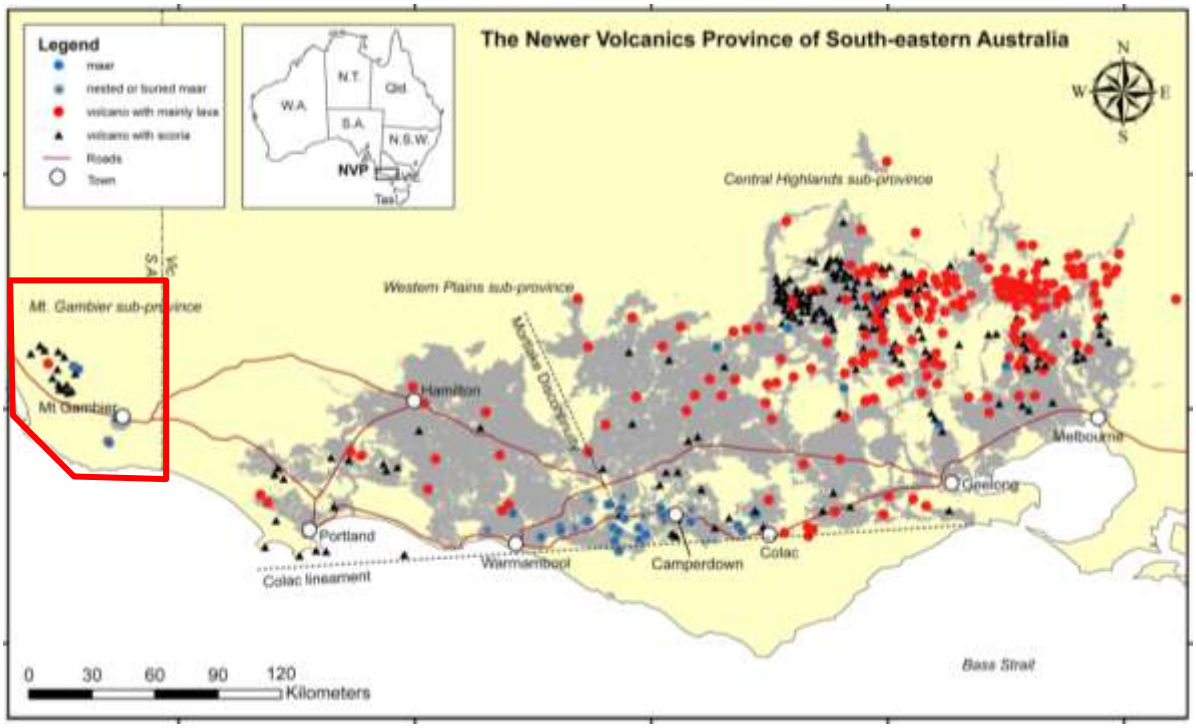

Figure 12: Volcano type and distribution in the NVP of Victoria and South Australia (from van Otterloo 2011). The Chapter 6 study area is outlined in red at the western end of the map, and contains 18 volcanic occurrences.

7.3.4 Transient heat flow effects due to recent magma emplacement

The results of modelling presented above show that the observed surface heat flow distribution within the study area can be broadly explained by lateral variations in thermal conductivity and crustal heat generation. However, local transient heat flow anomalies cannot be totally ruled out because of the prevalence of relatively recent volcanism in the area.

The study area contains a portion of the Newer Volcanics Province (NVP) of southeast Australia (see sections 2.2.5 and 2.2.6). There are 18 large-scale vent locations within the study area. Most of them are in the Mount Burr Range area west of Mount Gambier, with the remainder at Mounts Gambier and Schank (Figures 2, 12 & 13). The reported ages of the

South Australian NVP volcanoes range from 20,000 – 1,000,000 years for the Mount Burr Volcanics (Sheard & Nicholls, 1989), and possibly Holocene for Mount Gambier and Mount Schank.

Van Otterloo et al (2012) divided the South Australian NVP into two sectors: east and west. They associated the sectors with two magmatic suites that rose to the surface rapidly (~10 cm/s) from depths of ~90 km ("western basanites") and ~60 km ("eastern trachybasalts") at temperatures of 1100–1200^{o}C. Such events might have imprinted transient thermal effects on surface heat flow.

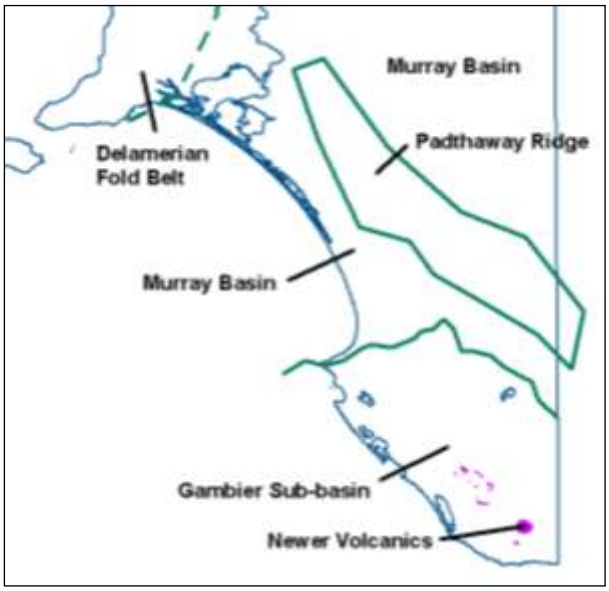

Rudman & Epp (1983) modelled the transient effect of a magma body being emplaced in the crust beneath the east rift zone of the Kilauea volcano in Hawaii. This serves as a useful analogue for the possible thermal impact of the emplacement of narrow magmatic columns beneath the volcanic centres in southeast South Australia. Their modelling showed that the lateral extent of the thermal anomaly due to the body increased over time, but that the vertical effect of transient heat emplacement remained relatively constant in comparison (figure 14).

Figure 13: Location of the NVP within the study area. The Gambier Sub-basin is the westernmost element of the Otway Basin. The easternmost volcanic centres are Mounts Gambier (north) and Schank (south), and are thought to be the youngest volcanoes in the NVP at 4,500–5,000 years of age.

While the model of Rudman & Epp has a much shorter time frame (125 years) than the NVP, several general observations that can be drawn from their work. Both lateral and vertical geothermal gradients change over time in response to the emplacement of a magma body, but the effects might not be obvious from a single borehole directly above the intrusion. In Rudman & Epp's model, the thermal effect of the intrusion is negligible at depths shallower than 1 km, even after 125 years. To detect transient effects on vertical heat flow one would need a well over 1,000 m deep. Alternatively, transient effects might be apparent from any relative thermal anomalies coincident with the known volcanic vents. All anomalies that have been observed can be explained by steady state mechanisms. The principle of 'Occam's Razor' (the simplest model that explains the data should be selected) therefore argues against transient thermal effects to explain the observed heat flow in the area.

The lack of a heat flow anomaly associated with the hot spot volcanism in the study area is not unusual. Stein and Von Herzen (2007) examined heat flow estimates from five different locations of hot spot volcanism globally and found that there is a distinct lack of high heat flow anomalies associated with them. They concluded that the upwelling plume that causes

the volcanic activity must have a relatively small thermal perturbation signature. Anomalies found in those studies were not greater than 10-15 mW/m^2.

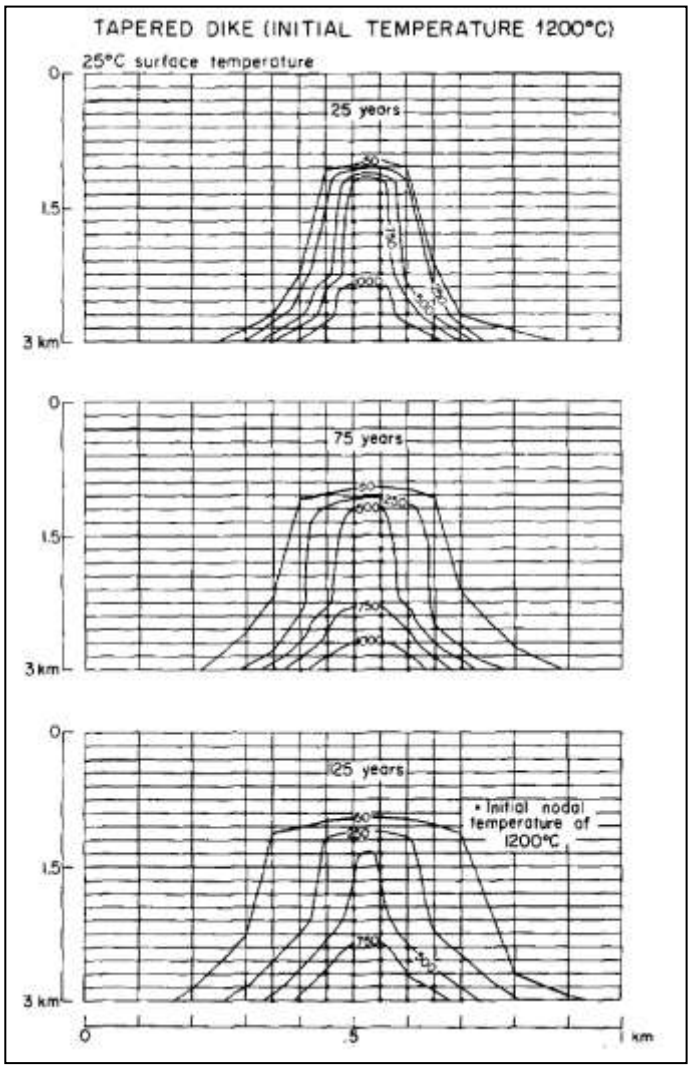

Figure 14: 2D modelling by Redman & Epp (1983). A transient heat producing body in the form of a tapered dyke 1.0 km wide is emplaced at 3.0 km depth. Regional conductivity is 2.5 W/mK and diffusivity is 1.0 X 10^{-6} m^2/s. Surface temperature is 25°C and a heat flux of 100 mW/m^2 is fixed for the lower surface. Transient temperatures were computed in time steps of one year. Predicted isotherms are presented for 25, 75, and 125 years after emplacement of the dyke.

7.4 Another application of modelling heat-producing bodies: IOCG-U mineral exploration

This section investigates the effects on surface heat flow of a large heat producing body hosted within a country rock with moderate heat production, lying beneath 500 m of flat-lying sedimentary cover that produces minimal heat (Figure 15). This model approximates the exploration target of many mineral explorers in the South Australian Stuart Shelf Olympic Domain region, where Neoproterozoic sediments overlie Mesoproterozoic and Palaeoproterozoic basement rocks. The target for the explorers is Iron Oxide-Copper-Gold-Uranium (IOCG-U) mineralisation, and the problem many explorers face is that deep holes through the cover rocks may be 'technical successes'—meaning they hit rocks of the right age and type—but with little or no IOCG-U mineralisation.

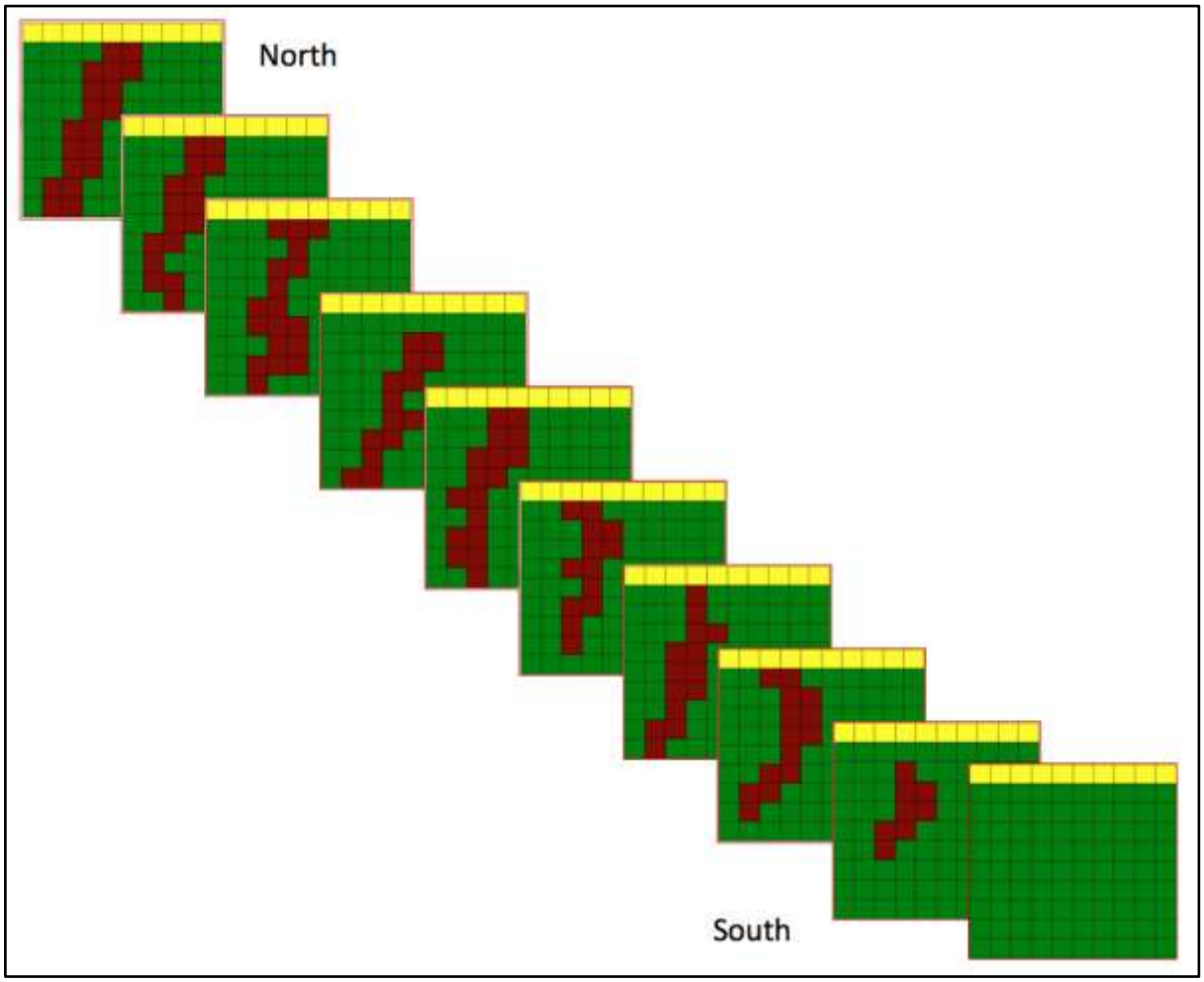

Figure 15: Stacked cross sections in the IOCG-U model. Each section is 5000 m x 5000 m, with each section 500 m apart. Yellow = cover sequence; 500 m thick, conductivity 3.5 W/mK, heat production 0.5 µW/m^3. Green = Host rock modelled as Hiltaba Granite; conductivity 3 W/mK, heat production 4 µW/m^3. Brown = IOCG-U ore body; conductivity 5 W/mK, heat production 30 µW/m^3. Basal heat flow to the model is uniform at 70 mW/m^2.

The results of steady state heat flow modelling using HeatSeek (Figure 16) show that an IOCG-U ore body buried under 500 m of cover could generate a surface heat flow anomaly

up to 35 mW/m^2 directly above it, with a detectable anomaly of 10 mW/m^2 as far as 2 km laterally away.

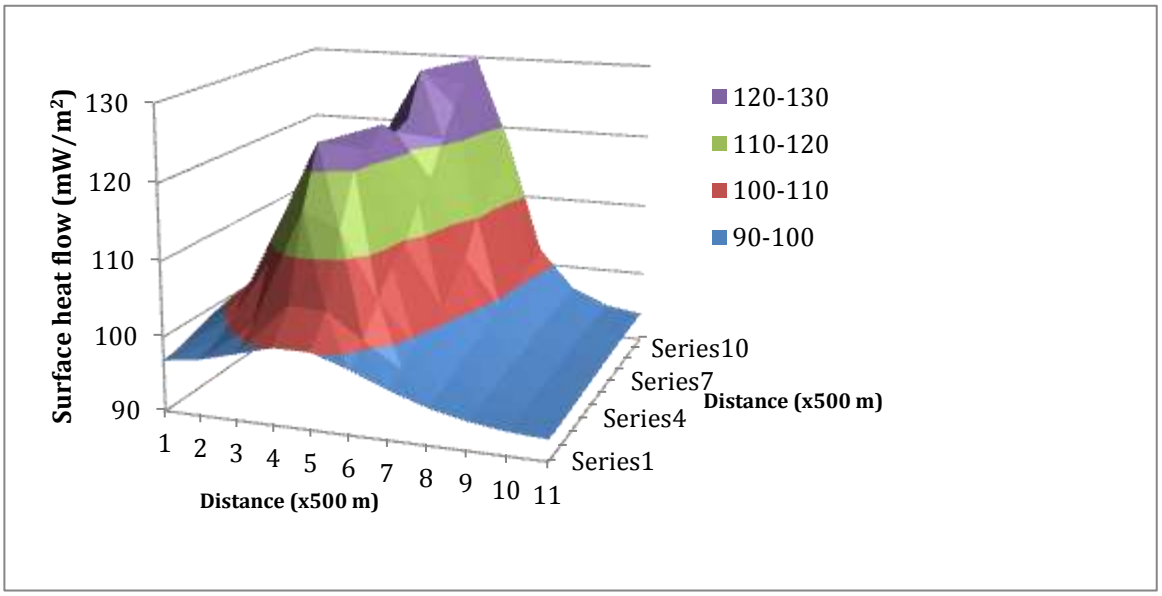

Figure 16: Predicted surface heat flow from the 3D model of the buried IOCG-U ore body in Figure 15. The maximum surface heat flow anomaly is 25 mW/m^2 greater than the background surface heat flow.

At smaller scale, Matthews & Beardsmore (2006; see Chapter 3) graphically demonstrated the effect on surface heat flow of a buried anomalous heat producing body. They showed that a heat producing body buried 250 m below the surface could have an observable effect on surface heat flow about 500 m either side of the body (Figure 17). The amplitude of the predicted surface heat flow anomaly is proportional to the magnitude of the buried heat source, and the wavelength of the anomaly relates to the depth of burial of the heat producing body. This is analogous to a surface gravity anomaly due to a buried dense body.

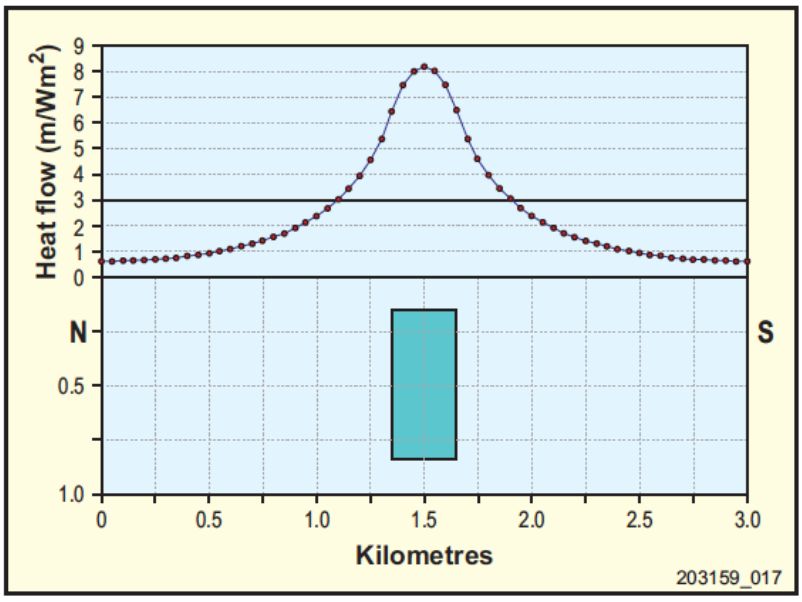

This modelling demonstrates that buried IOCG orebodies will create localised heat flow anomalies, and that measuring heat flow over prospects for such systems could assist explorers with drill targeting.

Figure 17: The localised effect on surface heat flow from a buried heat producing body of dimensions as shown and heat production of 60 µW/m^3 (from Matthews & Beardsmore 2006).

References

Beardsmore, G. R. & Cull, J. P., 2001, Crustal heat flow; a guide to measurement and modelling: Cambridge University Press p.324.

Jensen-Schmidt, B., Cockshell, C. D., & Boult, P. J., 2001, Chapter 5, Structural & tectonic setting. In: Boult, P.J. and Hibburt, J.E. (Eds), The petroleum geology of South Australia, Vol. 1: Otway Basin. 2nd edn. South Australia. Department of Primary Industries and Resources. Petroleum Geology of South Australia Series, Vol. 1, ch. 5.

Jorand, C., Krassay, A. & Hall, L. (2010) Otway Basin Hot Sedimentary Aquifers & SEEBASE Project Report to PIRSA-GA-DPI Vic.

Graeber, F. M., Houseman, G. A., Greenhalgh & S. A., 2002, Regional teleseismic tomography and the western Lachlan Oregon and the Newer volcanic province, Southeast Australia, Geophysical Journal International, 149 (2), p. 249-266.

Matthews, C. G., & Beardsmore, G. R., 2006, Heat flow: a uranium exploration and modelling tool? MESA Journal 41, p.12–14. Department of Primary Industries and Resources South Australia, Adelaide.

Mildren, S., Sandiford, M., 1995, A heat refraction mechanism for Low-P metamorphism in the northern Flinders Ranges, South Australia, Australian Journal of Earth Sciences, 42, 241-247.

Bullard, E. C., Maxwell, A. E., Revelle, R., 1956, Heat Flow through the Deep Sea Floor, Advances in Geophysics, 3, 153-181

Carslaw, H. S., and Jaeger, J. C., 1959, Conduction of Heat in Solids, Oxford Univ. Press, London, 510 pp.

Lee T. C., Henyey, T. L., 1974, Heat flow refraction across dissimilar media. Geophys. J. R. Astron. Soc., 39, 319-333.

Rudman, A. J. and Epp, D., 1983, Conduction models of the temperature distribution in the East Rift Zone of Kilauea Volcano; Journal of Volcanology and Geothermal Research, 16, p 189-204.

Sandiford, M., Frederiksen, S. & Braun, J., 2003, The long-term thermal consequences of rifting; implications for basin reactivation, Basin Research, 15 (1), p. 23-43.

Sheard, M. J. & Nicholls, I. A., 1989, 'Mount Gambier sub-province' in Johnson, R. W., Knutson, J. Taylor, S. R., (eds), Intraplate volcanism in eastern Australia and New Zealand, Cambridge, England, Cambridge University press, p 142.

Stein, C. A. & Von Herzen, R. P., 2007, Potential effects of hydrothermal circulation and magmatism on heatflow at hotspot swells, The Geological Society of America, Special paper 430, 2007.

Turner, S. P., Foden, J. D., and Morrison, R., 1992, Derivation of A-type magma by fractionation of basaltic magma and an example from the Padthaway Ridge, South Australia, Lithos 28, p. 151–179.
van Otterloo, HJ., 2011, Newer Volcanics Map (2011), https://vhub.org/resources/845

Appendix 1 – heat production data from selected Delamerian granites. U-Th-K geochemistry data from Turner et al (1992). Heat production data calculated using equations from Beardsmore & Cull (2001).

Name	Age (Ma)	Granite Type	U (ppm)	Th (ppm)	K (wt%)	A (μWm^{-3})
Marcollat Granite 1	485	A-type	2.2	24	5.32	**3.09**
Marcollat Granite 2	485	A-type	3.5	26	5.27	**3.6**
Marcollat Granite 3	485	A-type	3	22	5.21	**3.15**
Marcollat Granite 4	485	A-type	2.3	19	4.44	**2.63**
Marcollat Granite 5	485	A-type	3.6	20	4.37	**3.07**
Basins Microgranite 1	485	A-type	8.6	38	4.84	**5.91**
Basins Microgranite 2	485	A-type	8.9	43	4.77	**6.36**
Christmas Microgranite 1	485	A-type	16	55	4.32	**9.25**
Christmas Microgranite 2	485	A-type	10	42	4.66	**6.59**
Willalooka Granite 1	485	A-type	4.5	29	5.17	**4.1**
Willalooka Granite 2	485	A-type	4.5	30	5.02	**4.16**
Willalooka Granite 3	485	A-type	3.3	34	4.96	**4.1**
Willalooka Granite 4	485	A-type	8	38	4.67	**5.72**
Seismograph Granite	485	A-type	7.3	36	4.79	**5.38**
Gip Gip Granite	485	A-type	3.1	14	2.85	**2.29**
Kongal Granite 1	485	A-type	9.1	52	6.2	**7.27**
Kongal Granite 2	485	A-type	3.2	18	7.28	**3.18**
Kongal Granite 3	485	A-type	8.6	52	4.71	**6.94**
Kongal Granite 4	485	A-type	6.4	47	4.36	**5.89**
Tolmers Granite	485	A-type	16	45	5.11	**8.61**
Cold & Wet Granite	485	A-type	23	44	5.22	**10.57**
Coonalpyn Granite	485	A-type	14	54	5.13	**8.7**
Coonalpyn Gabbro	485		2.6	34	0.5	**3.34**
Gip Gip Rhyodacite	485		2	12	0.3	**1.5**
Bin Bin Rhyolite	485		3.9	17	9.84	**3.63**
Didicoolum Rhyolite	485		5.6	28	2.85	**4.05**
Papineau Rhyolite	485		3.4	14	3.22	**2.42**
Mt Monster Rhyolite 1	485		5.5	34	5.52	**4.81**
Mt Monster Rhyolite 2	485		5.1	27	5.1	**4.12**
Anabama Tonalite 1	505	I-type	2.6	10.2	2.02	**1.76**
Anabama Tonalite 2	505	I-type	4.1	11.5	2.31	**2.33**
Tanunda Granite	505	I-type	2	17	2.99	**2.22**
Reedy Creek Granodiorite	505	I-type	4.3	3	2	**1.72**
Reedy Creek Granite	505	I-type	6.1	29.5	4.38	**4.52**
Monarto Granite	505	I-type	0.3	29.8	3.39	**2.73**
Pt Elliott Granite	505	I-type	2.6	28.8	5.63	**3.61**
Vivonne Bay Granite 1	504	S-type	2.4	11	4.04	**2.02**
Vivonne Bay Granite 3	504	S-type	4.4	14.7	3.3	**2.79**
Vivonne Bay Granodiorite	504	S-type	6.4	16.9	3.5	**3.55**
Vivonne Bay Garnet Leucogranite	504	S-type	1.8	2.3	5.13	**1.34**
Stun Sail Boom River Granite 1	504	S-type	2.7	15.3	3.01	**2.3**
Stun Sail Boom River Granite 2	504	S-type	1.9	13.6	3.94	**2.06**
Stun Sail Boom River Granite 3	504	S-type	3.5	33	4.94	**4.1**
Stun Sail Boom River Monzogranite	504	S-type	4.7	17.9	5.58	**3.4**
Cape Younghusband Granite	505	S-type	2.2	32.3	4.01	**3.55**
Cape Willoughby Granite	509	S-type	6.4	16.2	4.23	**3.6**

Chapter 8

Conclusion

The work published in this thesis adds 64 new surface heat flow estimates to the Australian continent. The values all fall within the so-named South Australian Heat Flow Anomaly (SAHFA; Neumann et al 2000), and provide data coverage at a high spatial resolution.

This thesis attempted to address the following questions:

- Is the SAHFA, as shown in Cull (1982) and defined by Neumann et al (2000), a zone of blanket or even dominant high heat flow?
- What is the true nature of the SAHFA when considered on a 10km lateral scale?
- What are the possible reasons for the surface heat flow pattern in southeastern South Australia?

The first conclusion is that the answer to the first question is that the SAHFA is a region where anomalously high heat flow values are interspersed with low values.

Furthermore, the pattern of surface heat flow estimates suggests there is significant lateral variation in surface heat flow over lateral scales of tens of kilometres.

Knowledge of the geology of the study areas, and data collection, allowed conclusions to be drawn on the reasons for the surface heat flow pattern observed. In the Torrens Hinge Zone at Parachilna the anomalously high surface heat flow is likely due to the presence in the basement of U-Th-K rich rocks of the eastern Gawler Craton Olympic Domain. In the southern Murray Basin and western Otway Basin there is high variability in surface heat flow values, with a clear zone of anomalously high heat flow observed in the Padthaway Ridge area, known to have high heat producing granites in the basement.

Modelling of the western Otway Basin heat flow based on known geological features shows a strong correlation between modelled and observed values.

Importantly, no significant heat flow anomalies were observed around the volcanoes of the Newer Volcanics Province (NVP).

Because surface heat flow distribution relates directly to the distribution of heat producing elements (HPEs), this potential field could be used to explore for heat producing orebodies. Modelling presented in Chapter 7 shows the size of surface heat flow anomaly that could be expected above an iron oxide copper gold uranium (IOCGU) orebody.

Indeed as presented in Chapter 5, hot rocks, themselves heated by high concentrations of HPEs, have been discovered using exploration based on heat flow.

Each of the papers presented in this thesis (Chapters 3-6) represents a significant contribution to the scientific understanding of the SAHFA and the Central Australian Heat Flow Province (CAHFP).

Chapter 3 demonstrates that surface heat flow measurements, largely ignored by mineral explorers, could be a useful tool for finding iron oxide copper gold (IOCG) orebodies concealed under barren younger cover rocks. Basic modelling in that paper and in Chapter 7 showed that heat flow could be a determining factor when explorers assess the value of their prospects and whether to abandon them. Furthermore, heat flow could be a tool used before deep drilling for IOCG targets occurs, aiding explorers with their deep drill targetting.

Chapters 4, 5 and 6 contribute a total of 64 new surface heat flow estimates to the existing data set of Australian heat flow. Given that there were less than 30 estimates in total across South Australia before this research commenced, this in itself represents a significant contribution to science, tripling the total number of data points that existed before.

Chapters 4 and 6 are essentially companion papers that map surface heat flow to high spatial resolution in two adjacent study areas covering the southern Murray Basin, across the Padthaway Ridge and into the western Otway Basin. This vast region contained just one previous surface heat flow estimate. As discussed in Chapter 2, the region has a complex geological history, and understanding the tectonothermal evolution of eastern Australia is greatly aided by understanding the spatial distribution or surface heat flow. Chapter 1 outlines the importance of this heat flow data to science, society (e.g. to better understand the hazards associated with volcanism and seismic activity), and the energy industry (e.g. petroleum systems and geothermal exploration).

Chapter 5 makes two important contributions to science and society. Firstly, like the southeast South Australia study area, the large region known as the Torrens Hinge Zone contained just one previous surface heat flow estimate. The study area is in a longitudinal zone that sits between the Eastern Gawler Craton Olympic Domain and the Adelaide Geosyncline-Curnamona Craton, and the six new surface heat flow estimates provided data coverage in an area where there was none before. Secondly, the paper showed how testing a scientific hypothesis can bring a discovery from first principles of a new geothermal province where none had looked before. The hypothesis was that there would be both high heat flow and sufficient thermal insulation to induce high geothermal gradients in the Parachilna area. A structured test of this hypothesis, involving purpose-drilled heat flow exploration wells on a grid pattern over a prospect, revealed the Parachilna Geothermal Play, and the first stored heat geothermal resource defined in Australia.

Chapter 7 uses simple modelling incorporating known regional geology to examine the factors that have influenced the distribution of surface heat flow in the study areas. It first discusses the factors that may influence heat flow such as anomalous basement heat production, lateral thermal conductivity contrast, variable reduced heat flow and transient effects due to recent volcanism, then shows the results of simple modelling. Chapter 7 contributes to the scientific understanding of the surface heat flow of the

southeastern South Australia study area because it shows simple and plausible explanations for the observed surface heat flow distributions. It also adds to the modelling that has been previous published in Chapters 3 and 6. Because all of the Chapters deal with areas within the SA Heat Flow Anomaly, all components of the thesis contribute to the scientific understanding of it. The thesis has addressed each of the three questions that it set out to address.